The Application of Advanced Hydrodynamic Analyses
in Ship Design

by

Casey John Moton

B.S. Naval Architecture, U.S. Naval Academy, 1991

Submitted to the Departments of Ocean Engineering and Mechanical Engineering
in partial fulfillment of the requirements for the degrees of

Naval Engineer

and

Master of Science in Mechanical Engineering

at the

MASSACHUSETTS INSTITUTE OF TECHNOLOGY

June 1998

The Application of Advanced Hydrodynamic Analyses

in Ship Design

by

Casey John Moton

Submitted to the Departments of Ocean Engineering and Mechanical Engineering
on May 8, 1998, in partial fulfillment of the requirements for the degrees of
Naval Engineer
and
Master of Science in Mechanical Engineering

Abstract

Recent advances in computational hydrodynamics offer the opportunity to incorporate more accurate analyses earlier in the ship design process. In particular, significant work has been conducted towards the prediction of nonlinear wave-induced motions and loads in the time domain. Seakeeping analysis has traditionally been incorporated late in the design process, using parametrics and two-dimensional linear strip theory methods in the frequency domain. Model testing, due to its relative expense, is incorporated even later in the process. As a result, seakeeping performance is often evaluated after, rather than during, each stage of ship design. Serious problems, particularly in structural loading, may not be discovered until late in the process.

This research investigates the applicability of nonlinear time domain predictions to ship design. A method for incorporating time domain analyses of motions and loads in early design is proposed. Several hulls are tested in the frequency and time domains in moderate to severe seas. The first set of hulls are mathematically defined, derived from the well-known Wigley Seakeeping Hull, with variations in flare, tumblehome, and waterline entrance both above and below the calm waterline. A Very Large Crude Carrier, representative of many commercial hulls, is also analyzed.

The nonlinear motions and loads differ substantially from linear predictions, especially in critical operating conditions. The nonlinear methods also predict significant variations in performance due to flare and tumblehome, which are not adequately observed with linear theory. Despite increased preparation complexity and computation times, and requirements for validation, time domain methods should be incorporated in early design. Detailed analyses of hull concepts may then be conducted much sooner, reducing the economic and schedule impact of any necessary changes.

Thesis Supervisor: Dick K. P. Yue
Title: Professor of Hydrodynamics and Ocean Engineering

Acknowledgments

Professionally, this research could not have been completed without the instruction and encouragement of my thesis advisor, Professor Dick K.P. Yue, who forced me to relearn the scientific method. I would also like to thank Professor Ahmed Ghoniem, of the Department of Mechanical Engineering, for sacrificing his time to act as my second thesis reader.

The assistance of the entire Ship Technology Division of Science Applications International Corporation (SAIC) was vital to the conduct of this research. In particular, I would like to thank Dr. Woei-Min Lin and Mr. Ken Weems for their invaluable support in understanding, preparing, and operating the LAMP code.

Finally, I would like to thank all of the family and friends who assumed that I had merely dropped off the face of the Earth. In particular, I include my parents, who still say "Yes, you can" every time I say "No, I can't." Most of all I would like to thank my wife, Jill, and my son, Daniel. Jill took care of Daniel and everything else in my life while I studied. And Daniel, now you get your Daddy back.

Contents

List of Figures

List of Tables

Nomenclature

ABS	American Bureau of Shipping
A_{WA}	Waterplane Area, Aft of Midships
B	Molded Beam
BL	Mathematical Hull Baseline
BM_L	Longitudinal Metacentric Radius
C_B	Block Coefficient
CDF	Cumulative Distribution Function
CFD	Computational Fluid Dynamics
CG	Center of Gravity
C_I	Waterplane Inertia Coefficient, $= BM_L \nabla / BL^3$
C_{VPA}	Vertical Prismatic Coefficient, Aft of Midships
C_{VPF}	Vertical Prismatic Coefficient, Forward of Midships
D	Molded Depth
DDG	Guided Missile Destroyer
DOD	Department of Defense
DWL	Design Waterline
FFG	Guided Missile Frigate
FFT	Fast Fourier Transform
FP	Forward Perpendicular
Fr	Froude Number, $V/\sqrt{gLBP}$
g	Gravitational Acceleration
$H_{\frac{1}{3}}$	Significant Wave Height
H_w	Wave Height

i	ith harmonic (1,2,3,...), 0 = mean response, $calm$ = calm water steady state value
KG	Height of Center of Gravity above the Keel
k_{xx}	Mass Transverse Radius of Gyration
k_{yy}	Mass Longitudinal Radius of Gyration
L	Length (LWL unless otherwise specified)
LAMP	Large Amplitude Motions Program
LBP	Length Between Perpendiculars
LCB	Longitudinal Center of Buoyancy
LCF	Longitudinal Center of Flotation
LCG	Longitudinal Center of Gravity
LMPRES	LAMP Pressure Post-Processor
LOA	Length Overall
L_w	Wave Length
LWL	Length of the Waterline
MSF	Mixed Source Formulation
MSI	Motion Sickness Indicator
NTU	National Taiwan University
OI	Operating Index
POSSE	Program of Ship Salvage Engineering
$\hat{R}_1$	McCreight Rank
RAO	Response Amplitude Operator
RMS	Root Mean Square
ROE	Response Operating Envelope
s	Sample Standard Deviation
SA	Single Amplitude
SAIC	Science Applications International Corporation
SHCP	Ship Hull Characteristics Program
SIG	Significant One-Third Response
SMP	Ship Motions Program

SOE	Seakeeping Operating Envelope
SPI	Seakeeping Performance Index
SPI-1	Mission Effectiveness Index
SPI-2	Transit Time Index
SS	Sea State
STA	Ship Station
T	Molded Draft
T_0	Modal Wave Period
V	Ship Velocity
Vx	Mathematical Hull Variant x
$VBMx$	Total Vertical Bending Moment at Station x
$VBMx_i$	Vertical Bending Moment at Station x, ith harmonic
VLCC	Very Large Crude Carrier
$VSFx$	Total Vertical Shear Force at Station x
$VSFx_i$	Vertical Shear Force at Station x, ith harmonic
$\bar{x}$	Sample Mean
Z_i	Heave Response, ith harmonic
Δ	Displacement
ζ	Wave Amplitude
Φ	Total Disturbance Potential
Φ_I	Incident Wave Potential
Φ_T	Total Velocity Potential
κ_3	Skew
κ_4	Kurtosis
μ	Population Mean
σ	Population Standard Deviation ($\sigma^2 =$ Variance)
θ_i	Pitch Response, ith harmonic
ω	Absolute Wave Frequency
ω_e	Wave to Ship Encounter Frequency
∇	Volumetric Displacement

Chapter 1

Introduction

Hydrodynamics is a critical part of the ship system design process, directly or indirectly impacting nearly every other engineering aspect. Hydrodynamic design areas include ship resistance, propulsor design, seakeeping, maneuvering, and the dynamic impacts on hydrostatic stability. However, properly incorporating hydrodynamics in ship design is one of the most difficult tasks confronting the engineer. The fluid-ship interaction is an extremely complicated one and difficult to accurately predict. As a result, designers often rely on empirically based parametric data or simplified calculation methods during the early stages of design. As the design progresses, experimental model tests are often used to confirm the hydrodynamic characteristics of the hull. Because model testing involves the production of physical scale models and the use of large laboratory facilities, experiments can be quite costly. The high expense can force delay of model tests until late in the design process, and accurate hydrodynamic predictions transition from design to merely analysis tools. Any changes required in the ship hull form at this stage are likely to be far more expensive than if the deficiencies were predicted earlier.

The widespread availability of powerful high speed computers offers the opportunity to include accurate hydrodynamic analyses much earlier in the ship design process. Recently researchers have made significant efforts towards accurately predicting fluid flow around ships and appendages. Advances in numerically solving both inviscid potential flow fields and viscous laminar and turbulent flows using high

performance computers are now beginning to fill the design gap between early design methods and experimental studies. Computer methods are available for predicting ship resistance, propulsor performance, details of viscous flows around ships and submarines, and seakeeping.

Seakeeping, particularly, is a critical area of ship design. VADM R.E. Adamson, Jr., U.S. Navy, operationally defined seakeeping in 1975, while Commander, Naval Surface Forces Atlantic [1]: "Seakeeping, as it pertains to the U.S. Navy, is the ability of our ships to go to sea, and successfully and safely execute their mission despite adverse environmental factors." This definition of seakeeping is not merely naval – commercial ships too must execute their economic mission in harsh environments, although particularly severe seas may be avoided, which may not be possible in military scenarios. Technically, seakeeping involves the prediction of ship motions and structural loads which are induced by the hull's encounter with water waves. No matter the ship's mission, seakeeping will have an important impact on the ability to perform that mission. Seakeeping is arguably the most critical of all hydrodynamic sub-disciplines due to its impact on ship survivability, particularly in heavy to severe seas. This research concentrates on the seakeeping sub-discipline because of the severe risks to ships in dangerous seas.

Very early stage ship seakeeping design has traditionally relied on empirically-based parametric estimates of ship motion and load response amplitudes. For naval destroyer type hulls, designers often use ranking systems developed separately by Bales [2] and McCreight [3]. Each of these researchers statistically regressed key seakeeping response amplitudes as functions of ship underwater geometry. The same parameters of a new ship hull can be used to relatively compare predicted seakeeping performance as a single index value. These method are discussed further in Chapter 2. Other researchers, notably Loukakis and Chryssostomidis, have developed series for early prediction of ship seakeeping [4]. These series can be used in a similar fashion as the well-known resistance prediction method, the Taylor Standard Series. The Loukakis and Chryssostomidis series predicts motions and loads of ships with cruiser sterns as a function of beam to draft ratio (B/T), length to beam ratio (L/B), and

block coefficient (C_B).

For the next stage of seakeeping design, the use of linear strip theory predictions for motion and loads in the frequency domain is now widely accepted among naval architects as an early stage design tool. Salvesen, Tuck, and Faltinsen developed strip theory into a viable design calculation method for ships [5]. Their effort led to the current frequency domain calculation programs. Two of the most prominent of these are the U.S. Navy's Ship Motions Program and the MIT RAO5D code. Frequency domain programs can quickly calculate ship responses at a large number of speeds, headings, and wave conditions, and are thus ideal for early design, where a large number of hull alternatives may require analysis.

There are limits to the usefulness of parametric and frequency domain prediction methods in seakeeping design. Most parametric methods, including those of Bales and McCreight, are based on characteristics of the mean underwater hull form. Geometry factors above the calm waterline, such as flare or tumblehome, do not influence a ship's performance rank. Only a limited number of geometric parameters are used to predict performance. Some methods, such as the cruiser stern series use only length, beam, draft, and volumetric displacement as inputs. Additionally, if any hull or environmental characteristics fall outside the range of tested conditions, the extrapolated results may be questionable. Linear frequency domain codes also function on the assumption that ship responses to encountered waves may be linearly superposed to yield the total response. Again, only the mean underwater hull form is considered. Significant variations in above water geometry will affect the prediction accuracy. Additionally, the frequency domain programs linearize by assuming small wave and motion amplitudes. Sea states or ship characteristics which result in large amplitude motions or loads violate the conditions of this linearization. The linear predictions will break down in cases where seakeeping performance is most critical - where large amplitude responses seriously degrade ship performance or even threaten survival.

To overcome these problems, towing tank tests are traditionally performed later in design to predict vertical motions (heave and pitch) and loads in head seas, and possibly horizontal motions (especially roll) in oblique seas. As mentioned above,

these experimental tests are expensive. Again, changes in hull form at the stage of tank tests are more costly and have a larger effect on the rest of the ship design.

To overcome these difficulties, the prediction of wave-induced motions and loads in the time domain has been the primary goal of many of the recent computer advances in ship hydrodynamics. Efforts have ranged from nonlinear time domain implementation of strip theory, such as discussed by Burton, et al. [6], to the solution of the nonlinear three-dimensional problem. One example of the latter is the Large Amplitude Motions Program (LAMP) developed by the Ship Technology Division of Science Applications International Corporation (SAIC). The theory and some results of the LAMP code have been presented in several papers [7, 8, 9, 10]. A brief review of the theory and formulations of LAMP is given in 2.

With the availability of such time domain prediction methods, the obvious question to any ship designer should be: "How do I use them?" This research explores that question. A possible design progression which incorporates parametric, frequency domain, and time domain methods is proposed. Two types of hulls are considered. The first type consists of a series of six mathematically defined hull forms, based on the well-known Wigley seakeeping hull. While primary dimensions of the ship (L, B, T, and C_B) are fixed, two parameters important to seakeeping – flare angle and waterline entrance angle – are varied both above and below the mean waterline. Two hulls are different from the baseline Wigley hull only above the waterline – one with flare, and the other with tumblehome. These hulls are particularly interesting in that parametric and linear methods predict exactly the same performance as the baseline. A commercial Very Large Crude Carrier (VLCC) hull is also examined.

Each hull is analyzed in the frequency domain with SMP, and in the time domain with the different implementations of LAMP. All hulls were tested in irregular seas in the frequency and time domains. Regular wave runs to determine Response Amplitude Operators (RAO's) were also conducted in the time domain. The results of the different calculation methods are compared. Finally, recommendations are made for the use of time domain codes in seakeeping design, discussing both the results of this research and several other applications not examined explicitly here.

Chapter 2

Design Method

Incorporation of seakeeping in the ship design process requires the selection of reasonable performance criteria, which typically consist of a series of motion and structural load limits. The ship's ability to meet these performance criteria is then analyzed in sea states corresponding to the expected operating environment of the vessel. Chapter 2 discusses the selected performance criteria and operating environments for both the mathematical and commercial hulls and the prediction tools selected for comparison. Finally, a proposed method for incorporating time domain predictions in the design procedure is presented.

2.1 Performance Criteria

2.1.1 Motion Limits

The first step in measuring the seakeeping performance of a ship is the establishment of motion (and load) limits, beyond which occurs degradation of one or more aspects of the total ship system. These criteria apply in any sea state, ship speed, or heading with respect to the waves. Motion criteria can generally be grouped into two categories: primary and derived. Primary criteria include the basic ship motions – surge, sway, heave, roll, pitch, and yaw – and their velocities and accelerations. Motions at a point other than the ship center of gravity (CG) are also considered primary criteria

as they are fully defined by the six basic motions. Derived criteria can actually be more critical in their degradation of the ship's mission. These criteria include relative motions at a point, defined as the difference between the amplitude of the vertical point motions (displacement, velocity, or acceleration) and the wave motion (again, displacement, velocity, or acceleration) at that point. Several other derived responses are themselves functions of relative motion, including deck submergence (wetness), emergence (such as at the propeller), and slamming. Slamming occurs when the ship emerges out the water at a point, and reenters the water above a threshold relative velocity. A motion sickness indicator (MSI) is also available to estimate the likely percentage of sea sickness among the crew. Excellent descriptions of the motion limits are available in Lewis, 1989 [11] and Bhattacharyya, 1978 [12].

Appropriate naval motion limits for design have been well defined by Comstock, et al., 1980 [13], and recommended as a U.S. Navy (USN) design standard [14]. Motion criteria are established for each warfare mission of naval ships, e.g. anti-air warfare, anti-submarine warfare, and aviation operations. For purposes of this study, the recommended criteria for transit operations are used to define ship requirements. These criteria are summarized in Table 2.1 on the facing pagea.

For transit missions, the deck wetness and slamming limits define conditions where damage to the ship hull or deck equipment could occur. The roll, pitch, and acceleration criteria define conditions where the ability of ship's personnel to function effectively would be degraded. The acceleration conditions typically are applied at the vessel's bridge – station[1] 3 is used as a conservative typical position. USN standards for ship-equipment interface also define the level of dynamic forces which all shipboard equipment must be designed to encounter [17]. For the mathematical hull, the personnel-related acceleration limits are exceeded before the equipment interface standards, therefore only the personnel standards are considered.

Commercial ship criteria are less well-defined than naval criteria. However, Aertssen, et al. (1968, 1972) studied the the seakeeping performance of several commercial ships and proposed appropriate design criteria [15, 16]. These criteria are prescribed for

---

[1]A longitudinal hull station numbering system of 0 to 20 is used throughout this document.

Criteria	Naval Monohull (Transit)
Roll (°)	8.0
Pitch (°)	3.0
Vert. Accel. (g) STA3	0.4
Lat. Accel. (g) STA3	0.2
Slam Freq. STA3	20/hr.
Dk. Wetness STA0	30/hr.
Note: **Significant 1/3 Single Amplitudes**	

a. Naval Transit Criteria [14, 13]

Criteria	Bulk Carrier (Transit)
Vert. Accel. (g) STA3	0.5
Slam Accel. (g) STA3	0.2
Slam Freq. STA3	3/100
Dk. Wetness STA0	5/100
Prop. Emergence STA20	25/100
Note: **RMS Single Amplitudes**	

b. Commercial Transit Criteria [15, 16, 11, p.143]

Table 2.1: Selected Seakeeping Criteria for Naval and Commercial Hulls

typical vessels in *Principles of Naval Architecture* [11, p. 143]. The Aertssen criteria for bulk carriers are applied to the VLCC hull in this research, and are summarized in Table 2.1b. Note that the selected naval criteria are defined as the average of the highest one-third response amplitudes ("Significant Single Amplitude (SIG SA)"). The commercial criteria are the root mean square response amplitudes (RMS SA).

2.1.2 Structural Load Limits

Motion criteria are relatively easy to define since they typically correspond to an observable response, e.g. motion of the ship, or wetness of the foredeck. Structural load limits, however, are more difficult to quantify since the stresses of the ship are not immediately discernible until failure occurs, unless strain measuring devices

are installed for real time feedback to the ship's operators. In early ship design, initial scantling sizes are traditionally estimated based on projected vertical bending moments and shear stresses. These moments and stresses are calculated based on the ship's longitudinal buoyancy and weight distribution. Besides the still water condition, both naval and commercial criteria typically require the calculation of maximum design stresses which are expected to occur in both a severe hogging and severe sagging condition.

For USN ships, the hull is balanced on a trochoidal wave, with the length of the wave equal to the ship's length, $L_w = LBP$, and the height of the wave defined as $H_w = 1.1\sqrt{LBP[feet]}$. For the design hogging condition, the wave is centered on the ship with the crest at amidships. For the sagging condition, crests are positioned at the perpendiculars. After weight and buoyancy are balanced in each condition, the shear stresses and bending moments are calculated along the length of the ship. The resulting stresses are the design maximums for initial structural definition [18].

For commercial ships, various criteria typically apply, dependent upon the ship's classification society, flag nation standards, etc. A typical criteria is that used by the American Bureau of Shipping (ABS) [19]. These deterministic rules are semi-empirical functions of ship length, beam, and block coefficient which estimate additional shear stress and bending moment in sagging and hogging conditions.

Both the USN and ABS criteria are static and so often criticized for representing deterministic solutions to what is realistically a probabilistic problem. ABS is implementing probabilistic criteria through its Safehull software. Though still deterministic, the Navy static wave balance is supplemented by the additional inclusion of stresses due to wave slap, water on deck, and other secondary loads. Dynamic stresses due to ship motion are included with guidelines such as the DOD-STD-1399, discussed above.

There are several other categories of structural loads that must be considered during design. Besides the vertical shear stresses and bending moments, both horizontal and torsional loads should be considered as primary hull girder loads. Severe local loads can also occur due to wave hydrostatic and hydrodynamic pressure. Slamming

Sea State Number	Significant Wave Height (m) Range	Significant Wave Height (m) Mean	Percentage Probability of Sea State	Modal Wave Period (sec) Range	Modal Wave Period (sec) Most Probable
0 - 1	0 - 0.1	0.05	0	—	—
2	0.1 - 0.5	0.3	5.7	3 - 15	7
3	0.5 - 1.25	0.88	19.7	5 - 15.5	8
4	1.25 - 2.5	1.88	28.3	6 - 16	9
5	2.5 - 4	3.25	19.5	7 - 16.5	10
6	4 - 6	5	17.5	9 - 17	12
7	6 - 9	7.5	7.6	10 - 18	14
8	9 - 14	11.5	1.7	13 - 19	17
>8	>14	>14	0.1	18 - 24	20

Table 2.2: U.S. Navy Sea State Standards [14]

can create severe local loads and ship whipping responses. Finally, the fluctuations of stresses due to these load factors are an important consideration in fatigue prevention.

Many of these additional loads are not currently predicted well. Such calculations are one potential benefit of nonlinear time domain methods and are discussed briefly in Section 7. However, as a reference load limit during this research, the USN static wave balance is applied to the mathematical hulls, and the ABS limit to the VLCC hull. The structural limit calculations are further discussed in Sections 3.1.4 and 3.2.1.

2.1.3 Operating Environment

Seakeeping performance is dependent on the ship hull, the ship's operating profile (speeds and headings, discussed in Section 2.1.4), and the sea environment. The sea conditions are typically defined by sea state, representing expected wave heights, wave modal periods, and wind speeds. Table 2.2 represents standard sea conditions in the winter North Atlantic, and is recommended for design by the U.S. Navy [14]. Expected wind conditions are not included, since none of the selected motion or load criteria are explicitly wind dependent. Performance criteria for aviation operations are strongly wind dependent. Comstock, et al., performed a thorough study of the

seakeeping characteristics of naval aviation-capable ships using wind criteria in 1982 [20].

For this research, sea states 4 (moderate) through 8 (severe) are considered. A Bretschneider two-parameter spectrum is used to define each sea state based on the most probably significant wave heights and modal periods, so that:

$$S(\omega) = 486.0 \cdot H_{\frac{1}{3}}^2 T_0^{-4} \omega^{-5} e^{-1948.18 \cdot T_0^{-4} \omega^{-4}}$$

Only long-crested unidirectional seas are considered in the seakeeping assessments.

2.1.4   Seakeeping Measures of Performance

Once the ship's motion and load limits are established, and the operating environment defined, the ship's seakeeping performance is evaluated at each desired condition. Two well-established methods for quantifying overall seakeeping performance are the Mission Effectiveness Index (SPI-1) and the Transit Time Index (SPI-2) [11].

Mission Effectiveness Index (SPI-1)

The SPI-1 is the percentage of time that a ship in a given condition can perform its military or commercial mission, given a projected operating environment. Performance of a mission assumes that no motion or load limits are exceeded. SPI-1 is calculated in the following manner:

1. Calculate the ship's motions and loads in each sea state of interest, over all possible speeds and headings with respect to the waves. For each motion, the data are often presented in a speed polar format, such as in Figure 2-1 on the next page. Here, the significant one-third pitch amplitude in sea state 6 for the mathematical baseline of this study (Wigley Seakeeping Hull) is contour plotted, as calculated by the frequency domain program SMP. The radial axis is ship's speed in knots. The angular axis is heading with respect to the waves. For each motion, the appropriate limits are overlaid. In Figure 2-1, response contours above the pitch limit of 3° are dashed. If all speeds and headings are
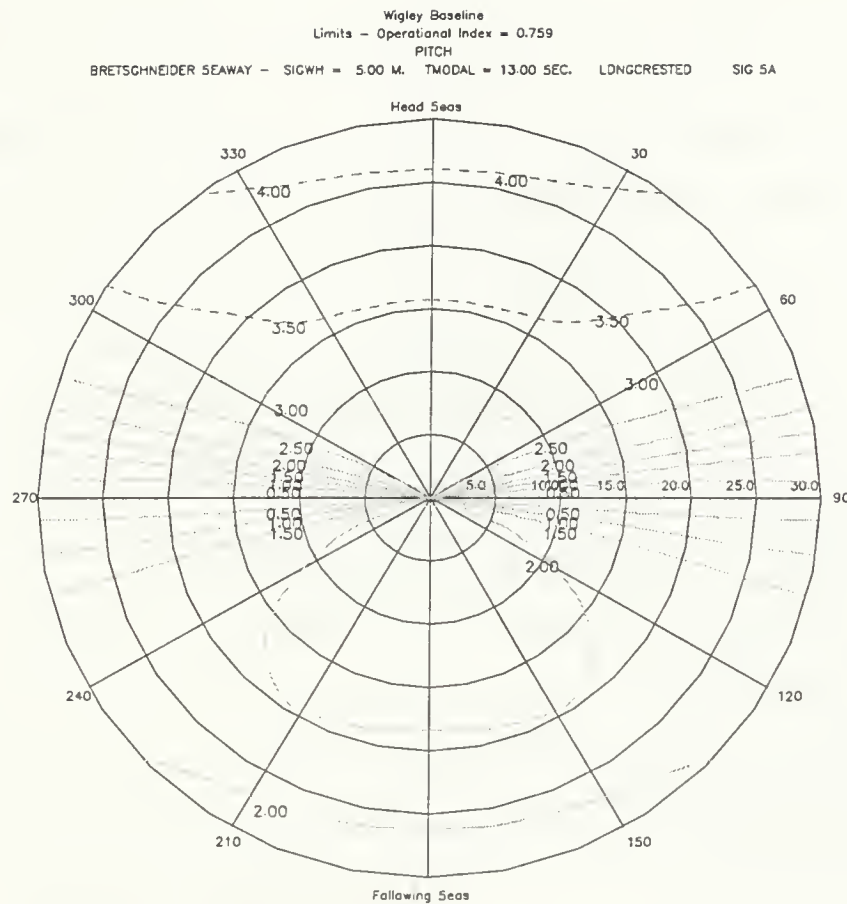
28

Figure 2-1: Speed Polar Plot, Mathematical Baseline, Pitch (SS6)

weighted equally, the Response Operating Envelope (ROE) for pitch in this case is 0.759. The ROE indicates that the Wigley Baseline does not exceed pitch limits in SS6 at 75.9% of all possible speeds and headings.

2. For each mission, all of the applicable ROE's are overlaid for each sea state. Again for SS6, the naval transit limits defined in Section 2.1.1 are overlaid against ship response and plotted in Figure 2-2 on the following page. Dotted areas indicate speeds and headings where one or more of the transit motion limits are exceeded. The Seakeeping Operating Envelope for each mission in each sea state is the intersection of all the applicable ROE's. The SS6 Transit SOE is only 23.7%, limited primarily by roll in addition to pitch. One of the primary strengths of the SPI-1 method is that each speed-heading combination can be weighted by its probability of occurrence in the ship's expected operating profile. The Operating Index (OI) for the mission is then the SOE weighted
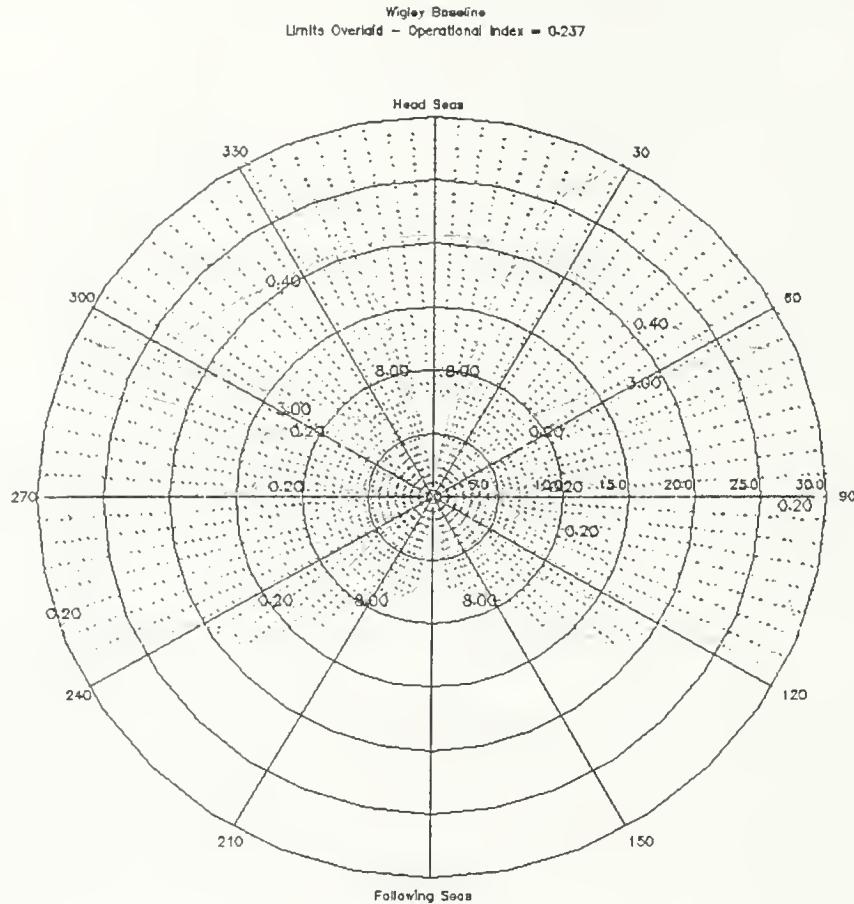
29

Figure 2-2: Speed Polar Plot, Mathematical Baseline, Naval Transit Mission (SS6)

by the speed-heading probabilities. In this example, however, all speeds and headings are weighted equally, and the OI equals the SOE. Mathematically, for the transit mission,

$$OI_i = \sum_{Speed} \sum_{Heading} SOE \cdot w_j$$

where w_j is the probability of each speed-heading.

3. Next, the OI for each mission area in each sea state is weighted by the probability of that sea state, yielding a total mission OI. The mission OI's are then weighted by the mission importance to yield SPI-1, or:

$$SPI = \sum_{Missions}^{i} m_i \sum_{SS}^{j} OI_i \cdot p_j$$

where m_i is the mission weighting, and p_j is the sea state probability, defined in Table 2.2 on page 27.

For military ships, SPI-1 is particularly well suited for seakeeping comparison because both the speed-heading operating profile and the mission importance can be included. Frequency domain programs, like SMP, are particularly well suited for the calculation of SPI-1, due to their calculation speed. All speed-heading combinations can be quickly calculated.

Transit Time Index (SPI-2)

The transit time index, or SPI-2, is defined as the amount of time a given distance would take to travel in calm water, divided by the amount of time the same trip would take in the actual sea environment. Alternatively, the expected speed fraction is used, which is the ratio of actual maximum speed to calm water maximum speed for a given transit route [11]. SPI-2 is often used for commercial ship analysis, where port-to-port transit time is the primary concern. When analyzing transit missions for naval ships, SPI-2 is also applicable.

Unlike SPI-1, SPI-2 considers both involuntary and voluntary speed losses. Involuntary speed losses are caused by added resistance in waves and loss of propulsor efficiency due to the sea environment and wave-induced motions. Voluntary speed losses are considered under the assumption that the ship's operators would change either speed or heading if any motion limits were exceeded at their current speed and heading. For military ships particularly, this assumption would not always be true – depending on the tactical situation, the ship may need to perform a mission at any speed or heading, even if performance is degraded by motions or loads. For moderate to high speed ships, the involuntary speed losses are typically small compared to the voluntary speed losses, and are often neglected.

To calculate SPI-2, SOE diagrams for the transit mission in each sea state are prepared as above. For each heading in each sea state, the maximum speed at which transit is possible without voluntary speed reduction is recorded. Finally, the maximum speed is weighted by the ship heading probability with respect to the waves for each sea state. The weighted average maximum speed for each sea state is then weighted by the probability of occurrence for each sea state, and summed to yield the

average expected speed. This speed is divided by the ship's maximum speed, yielding the expected speed fraction. This method applies if the minimum distance route is taken, regardless of possible routing around bad weather. If that assumption is not true, the transit time fraction should be used.

For purposes of this research, only the transit missions of the mathematical (naval criteria) hulls and the VLCC are considered. Thus, SPI-2 is an appropriate measure of seakeeping performance. Additionally, only head seas are considered (discussed in Section 2.3.2), so that the expected speed fraction is calculated for head seas. Hereafter, SPI refers to SPI-2, unless otherwise specified.

2.2 Prediction Tools

With the motion and load criteria defined, and the head-seas only SPI selected as the performance index for frequency and time domain calculations, the different prediction methods in the study are now considered.

2.2.1 Parametric

Empirical or semi-empirical parametric prediction methods are often the first sea-keeping evaluation tool used in the ship design process. By definition, parametric tools use the known characteristics of similar ships to interpolate for the unknown seakeeping performance of the current ship.

Two of the most common parametric methods in naval monohull seakeeping design are those proposed by Bales in 1980 [2] and by McCreight in 1984 [3]. Bales considered the head seas seakeeping performance of twenty destroyer-type hulls over a range of operating speeds in various sea states. He developed a performance index (the Bales Index) which is a function of eight responses: heave, heave acceleration, pitch, relative motion at the bow, absolute vertical acceleration at the bow, absolute vertical displacement at the stern, relative motion at the stern, and a slamming co-efficient measured at Station 3. The performance of each ship was then regressed as a function of several key hull geometry parameters, including: waterplane area coef-

32

ficients forward and aft of amidships (C_{WF} and C_{WA}), draft-to-length ratio (T/L), vertical prismatic coefficient forward and aft of amidships (C_{VPF} and C_{VPA}), and cut-up ratio (c/L). Cut-up (c) is the distance from the ship's forward perpendicular to the point where the keel begins to rise above the baseline towards the stern. Displacement was not explicitly considered, as all tested ships had full scale displacements of about 4300 metric tons. A ship's final index score is calculated based on its geometric properties, and can then be adjusted for its displacement.

McCreight expanded on this method in 1984. While considering the same list of important seakeeping responses, he tested twenty-five hulls in addition to the original Bales series, extending the applicable range of hull parameters. Regression of seakeeping performance was attempted for several additional hull parameters, including volumetric displacement (∇). Additionally, cut-up ratio was eliminated as a parameter. The resulting regression equation for the McCreight Index is:

$$\hat{R}_1 = a_0 + a_1 BM_L \nabla + a_2 C_{VPF} + a_3 C_{VPA} + a_4 C_I + a_5 L + a_6 T/B$$

$$+ a_7 A_{WA}/\nabla^{2/3} + a_8 (LCB - LCF)\nabla + a_9 (L/2 - LCB)/\nabla^{1/3} + a_{10} L^2/BT$$

where: $\hat{R}_1$ is the McCreight Rank, BM_L is longitudinal metacentric radius, A_{WA} is waterplane area aft of amidships, LCB is longitudinal center of buoyancy, LCF is longitudinal center of flotation, and C_I is a waterplane inertial coefficient, equal to $BM_L \nabla/BL^3$. The regression coefficients, a_i, are available in [3]. The McCreight Rank calculation is performed for each of the mathematically defined hull forms in Chapter 4.

Parametric methods such as the Bales or McCreight ranks, or series such as the Loukakis and Chryssostomidis seakeeping study [4], are very useful for extremely early design in selecting primary hull dimensions which generally will improve seakeeping. However, like linear methods, the above water hull is not considered, and any other variations from the hulls of the empirical database reduce their usefulness in design.

2.2.2 Frequency Domain: SMP

After parametric methods, the next step in seakeeping design is typically the use of linear frequency domain methods based on two-dimensional (2-D) strip theory. Their usefulness has already been demonstrated through the rapid preparation of speed polar plots such as those in Section 2.1.4. The frequency domain program used to predict motions and loads for the mathematical hulls and VLCC in this study is the U.S. Navy standard, Ship Motions Program, 1995 version[2] (SMP95).

Linearized strip theory programs, such as SMP and the MIT RAO5D program, were developed based on the calculation methods of Salvesen, Tuck, and Faltinsen [5]. Strip theory methods, though extremely useful for early design, suffer from the failure of the linear assumption for certain hulls and sea conditions. 2-D strip theory requires that the ship length be much greater than both the beam and the draft, so that end effects are not important in the potential flow solution. The SMP user's manual warns that prediction accuracy is degraded when $L/B < 5$ [21]. Additionally, linearization requires that the properties of the hull sections and waterplanes throughout the range of motion be well represented by the calm water values. Hull geometry above the calm waterline, including flare or tumblehome, does not affect the solution. The linearization assumption thus requires that ship motions be limited to small amplitudes. SMP again specifically warns that prediction accuracy degrades for wave heights greater than ship's draft,.

Finally, the linear frequency domain method assumes that the ship's response to a system of waves (such as irregular seas) is simply the sum of the responses to each individual wave, through superposition. Only the first order response is considered. For vertical motions or loads like heave and pitch, this assumption is often valid as long as motion amplitudes remain small. For lateral motions or loads, such as roll, however, the linear assumption is typically not valid. SMP applies a weakly nonlinear correction to model hull and appendage lift viscous damping based on the

---

[2]SMP95 was used for regular and irregular wave predictions for the mathematical hulls, and irregular seas prediction for the VLCC. VLCC regular waves predictions were actually performed first chronologically, using SMP91. Load RAO's were not calculated for the VLCC due to a known error in the SMP91 loads algorithm, which was corrected in SMP95.

significant roll amplitude. During irregular seas calculations, an iterative procedure for roll response is implemented.

As long as the assumptions of the the linearized 2-D solution are valid, programs like SMP are extremely rapid, useful tools. The recommended design procedure outlined in Section 2.3 uses linear frequency domain programs to narrow down the conditions which warrant nonlinear time domain analysis. Using regular wave analysis, the linear prediction of zero higher order response is also examined in Chapter 6.

2.2.3   Time Domain: LAMP

The Large Amplitude Motions Program (LAMP), developed by the Ship Technology Division of Science Applications International Corporation (SAIC), was used to perform all time domain calculations for this study. LAMP is representative of current computational fluid dynamics (CFD) codes for the prediction of nonlinear ship motions and loads in the time domain. A brief review of the LAMP methodology provided here is similar to the description found in Shin, et al. (1997) [9]. More detailed descriptions of the LAMP theory are available in the LAMP User's Manual, and in Lin and Yue (1990) [22, 7].

LAMP computes a time domain solution for a general three-dimensional body floating on a free surface. Six degree-of-freedom motions are permitted. In the most advanced formulation, the complete hydrodynamic, hydrostatic, and Froude-Krylov potential solution is calculated at each time step on the ship's instantaneous underwater hull form. Note that this is a major difference from linear methods, where only the mean underwater body is considered. The wave pressure forces are combined with any external forces to solve the equations of motion at each time step. The hull pressure forces may also be used to calculate hull bending and torsional moments and shear forces. Due to the complexity of applying the fully nonlinear body boundary condition, several different formulations have been developed. These formulations, along with SMP, are compared in Table 2.3 on the following page.

LAMP-1 provides a fully linear implementation of the 3-D time domain method.

SMP	2-D Linear Hydrodynamics (Strip Theory)
	Linear Hydrostatic Restoring and Froude-Krylov Wave Forces
	Frequency Domain
LAMP-1	Free Surface Boundary Condition on Mean Water Surface
	3-D Linear Hydrodynamics
	Linear Hydrostatic Restoring and Froude-Krylov Wave Forces
LAMP-2	Free Surface Boundary Condition on Mean Water Surface
	3-D Linear Hydrodynamics
	Nonlinear Hydrostatic Restoring and Froude-Krylov Wave Forces
LAMP-4	Free Surface Boundary Condition on Incident Water Surface
	3-D Nonlinear Hydrodynamics
	Nonlinear Hydrostatic Restoring and Froude-Krylov Wave Forces

Table 2.3: LAMP and SMP Formulation Comparison

The computations are much less intensive, but the results still suffer from the disadvantages inherent with the mean body boundary condition. However, the limitations of 2-D methods do not apply. Additionally, simply switching to the time domain eliminates the requirement for the linear superposition assumption required by frequency domain methods. For large-amplitude responses, this difference should be quite significant. LAMP-4 is the fully nonlinear implementation, solving the underwater potential solution on the instantaneous hull surface. However, LAMP-4 is far more computationally intensive than LAMP-1. LAMP-2 is an approximate nonlinear method which retains many of the advantages of both LAMP-1 and LAMP-4. In this formulation, the hydrodynamic potential is still solved on the mean underwater body, but the hydrostatic and Froude-Krylov wave forces are applied to the instantaneous underwater body. In head seas and vertical motions, where these forces typically dominate, LAMP-2 may be very useful.

The mathematical implementation of the LAMP method is discussed briefly below. The fluid motions are described by a velocity potential

$$\Phi_T(\vec{x}, t) = \Phi_I(\vec{x}, t) + \Phi(\vec{x}, t)$$

where Φ_I is the incident wave potential and Φ is the total disturbance potential due

36

to the presence of the ship. $\vec{x}$ is a position vector and t is time. The velocity potential must satisfy Laplace's equation,

$$\nabla^2 \Phi = 0$$

.

The disturbance potential solution must satisfy the free surface and body boundary conditions, along with a radiation condition. The free surface boundary condition is linearized in all three formulations, such that

$$\frac{\partial^2 \Phi}{\partial t^2} + g\frac{\partial \Phi}{\partial z} = 0 \qquad \text{on} \qquad S_f(t), t > 0$$

where g is gravitational acceleration. The body boundary condition is next applied on the instantaneous underwater body for LAMP-4 and the mean underwater body for LAMP-1 and LAMP-2,

$$\frac{\partial \Phi}{\partial \vec{n}} = \vec{V}_n - \frac{\partial \Phi_I}{\partial \vec{n}} \qquad \text{on} \qquad S_b(t), t > 0$$

where n is a unit normal vector to the body out of the fluid and V_n is the instantaneous body velocity in the normal direction. Obviously, $S_b(t)$ is constant for LAMP-1 and 2. Next, the radiation conditions require that the disturbance velocity potential goes to zero at infinity, S_∞,

$$\Phi = \frac{\partial \Phi}{\partial t} \to 0 \qquad \text{on} \qquad S_\infty, t > 0$$

Finally, the initial conditions require a zero disturbance potential on the free surface at $t = 0$,

$$\Phi = \frac{\partial \Phi}{\partial t} = 0 \qquad \text{on} \qquad S_f(t), t = 0$$

Two methods have been included in LAMP to solve for the potential function, $\Phi(t)$ at each time step. The first uses a transient free-surface Green function $(G^0 + G^f)$, with homogeneous singularities placed on the hull surface only. This formulation, along with the boundary conditions is graphically summarized in Figure 2-3a, from
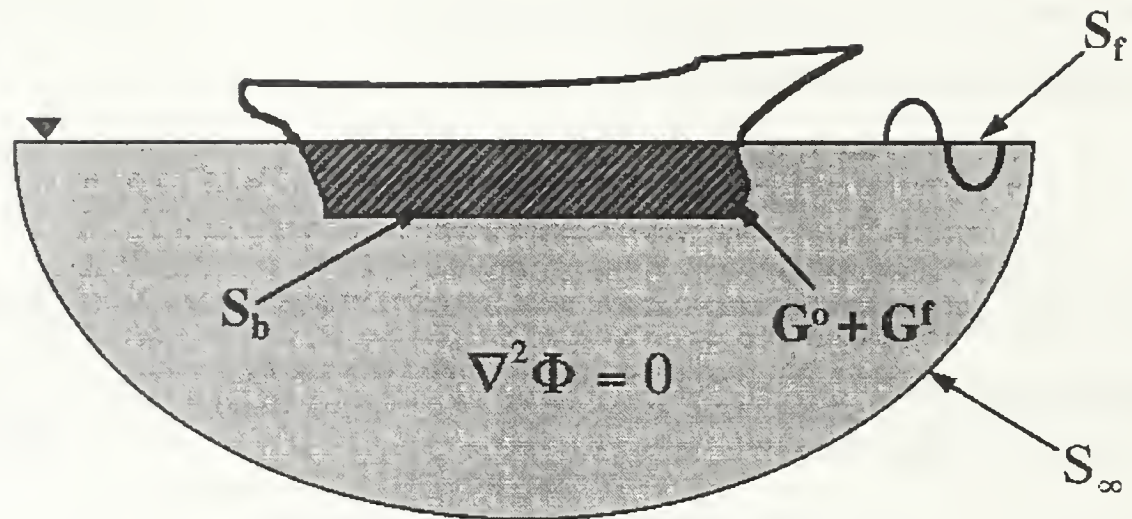
a. Transient Green Function Formulation
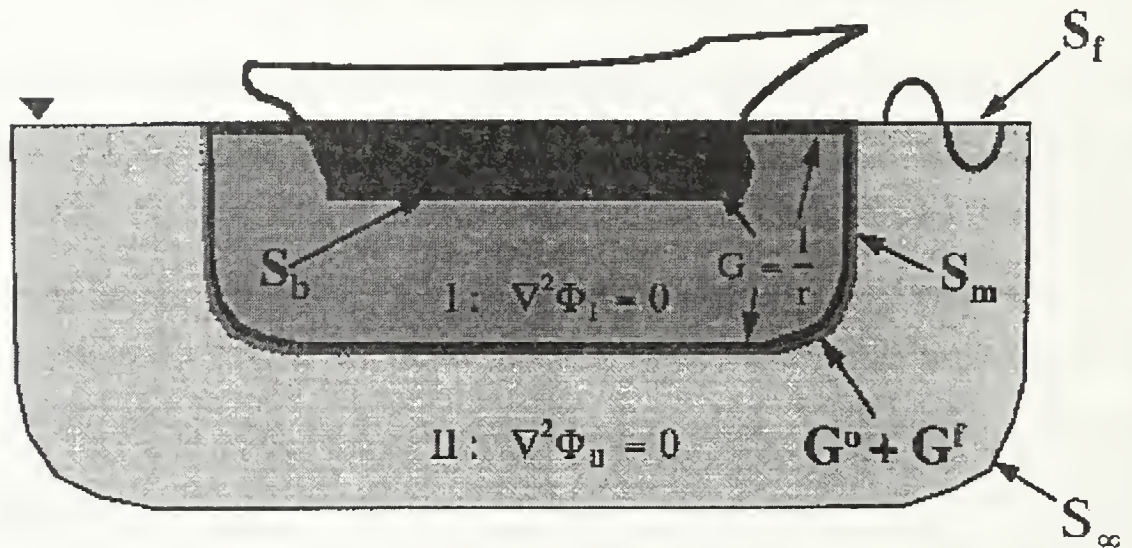
b. Mixed Source Formulation

Figure 2-3: LAMP Formulations [22]

the LAMP User's Manual. A mixed source formulation (MSF), recently developed, is summarized in Figure 2-3b. In this method, the fluid is split into two domains (I and II). The MSF distributes simple Rankine sources (G) on the hull, local free surface, and a matching surface, S_m, between the two fluid domains. A transient Green function is applied on the matching surface. Both SAIC testing and the author's experience with both the VLCC and mathematical hulls in large-amplitude motion cases indicate that the MSF is more robust, particularly with non-wall-sided hull geometries [23]. Consequently, the mixed source formulation was used in all LAMP runs.

38

LAMP provides the user with several other options affecting the time domain solution method. For the MSF, two options for the inner boundary of the free surface panelization are available. For both methods, the hull matching surface is used as the outer edge of the free surface panelization. In the first method, the actual hull waterline is used as the inner boundary of the free surface, yielding a "body-fitted" free surface grid. In the second, a shifted and scaled copy of the matching surface is used as the inner boundary, resulting in minimized gaps between the hull and free surface grid. For all LAMP runs, the body-fitted method was used. However, some LAMP-4 runs were attempted unsuccessfully with the gapped method. This is discussed in Section 5.2.3.

Two methods are also available for cutting the panelization of the hull at the mean waterline. In the default method, component cutting, the intersection of the mean or incident free surface is calculated at each station. The underwater station is then resplined with the same number of points at each time step. The alternate method, master geometry cutting, does not respline stations under the free surface. Submerged panels are maintained, and panels at the waterline are trimmed off. The component cutting method was used for all LAMP-1 and LAMP-2 runs, which use the mean underwater body regardless. Because the hulls were tested in cases likely to have large-amplitude motions, the master geometry cutting method was used in most LAMP-4 cases. Some VLCC cases, with less severe motions than the smaller mathematical hulls, used component cutting in LAMP-4. The comparison is briefly discussed in Section 6.3.

Calculation of the pressure from the potential flow solution can also be linearized by dropping the nonlinear second order term in Bernoulli's equation, $\frac{1}{2}|\vec{\nabla}\Phi|^2$. The pressure linearization speeds up calculation, particularly for LAMP-4, and generally results in negligible differences for head seas cases. The linearized method was used for all cases, after consultation with SAIC.

Finally, for all head seas cases, the hull was fixed in all directions except heave and pitch, which is also a normal experimental setup. Additional details of the LAMP setup for each hull are included in Sections 3.1.5 and 3.2.2.

2.3 Time Domain Methods in Design

Because of the increased computation time required for 3-D time domain runs, apply-
ing them in the same manner as current frequency domain programs is not feasible.
In fact, to test a transversely symmetric hull from zero to thirty knots (five knot
increments), in head to following seas (15° increments) would take ninety-one runs
per sea state. In this section, two alternative methods of incorporating time domain
runs in design are proposed. The first is to use time domain codes (hereafter, LAMP)
to verify the frequency domain (hereafter, SMP) predictions for the SPI. The second
is to use LAMP as a simulated experimental testing facility.

2.3.1 Seakeeping Performance Index Verification

Once SMP is used to calculate either SPI-1 or SPI-2 for a hull, LAMP can be used
to verify the critical points in each ROE or SOE. These critical points are the speeds
and headings where either motions or loads first exceed the threshold. For example,
referring again to Figure 2-1 on page 29, the pitch ROE of the mathematical baseline
in SS6, LAMP could be used only at the speeds and headings where the pitch limit
of 3° is exceeded. Assuming 15° heading increments, the hull would be tested at
000, 015, 030, 045, and 060, for a total of only five runs. The speed at each heading
would initially be the SMP predicted crossover speed. Using an appropriate iteration
scheme, only a few additional runs at each heading should be required to define the
ROE.

To reduce the number of required runs even further, LAMP may be used to verify
the SOE, where all motion and load limits for a single mission are overlaid, as in
Figure 2-2 on page 30. To verify the SS6 Transit Mission SOE, LAMP tests would
be conducted at: (1) 000 to verify pitch limit crossover, (2) 180 to verify 30 knots
is feasible, and (3) 120, 135, 150, and 165 to verify roll limit (8°) crossover. A total
of six initial runs would be necessary, with follow-on runs for iteration to the actual
limit crossover speeds.

Testing Application of SPI Verification Method For this study, a modified SPI (transit speed limit) for head seas only is calculated for the mathematical hulls and the VLCC. This reduces the number of required LAMP runs even further, since only the threshold speed at 000 need be verified. Using SMP, the head seas SPI is calculated for each hull in sea states 4 through 8, based on the transit motion limits defined in Section 2.1.1. Of course, mission limits and the ship's operating guidelines may also include load limits. The results of the SMP SPI calculations are included in Section 4.2.1 on page 74. The decision of which operating conditions to test with LAMP is also discussed. Because the use of LAMP as a simulated experimental facility is more scientifically interesting, most of the time domain runs were completed for that procedure. Only a few examples of ROE and SOE verification were completed.

2.3.2 Simulation of Experimental Facilities

Another major use of codes like LAMP will be as simulated experimental facilities, such as tow tanks. Because of the relative expense associated with constructing models for seakeeping tests and performing the tests in a suitable facility, experiments are currently conducted late in the ship design process, if at all. Comparisons of alternative concept hulls would be completed with existing 2-D linear codes like SMP. If the hulls differ in a way that is not considered in SMP, as with above water changes, the linear predictions may be inadequate. LAMP may be used to perform seakeeping analyses earlier in design, reducing the number of required model tests.

In the case where hulls being considered are similar to those for which the time domain code is validated, design perturbations may be investigated earlier with more accurate methods than SMP. Model tests may be substantially reduced, and perhaps even reserved for simulation of critical conditions later in design, where the survivability of the hull in severe seas is under examination. However, if the proposed hulls are a significant departure from previous computational tests, model tests on a single baseline may be conducted early in the design. The experimental results may then be used to validate the LAMP predictions and, working with the code authors, to

improve the computational prediction method. Once the code is validated for the new hulls, perturbations to the baseline may be considered without the need for additional model construction. Model tests may finally be included to once again validate the final hull's computational results. The use of the computational tool will not likely eliminate model testing for validation, but should substantially reduce the required tests, allowing the application of accurate seakeeping predictions during design, not just for analysis of the final hull.

Using LAMP in this manner should reduce design budgets. Assuming that the initial overhead of LAMP tests and model tests are comparable (which may be a conservative estimate in favor of model testing), the ability to continue use of LAMP on modified hulls with minor changes to panelization and hull setup should save research and development money.

Additional substantial costs may be eliminated when hull girder load testing is considered. Constructing and testing a model to accurately measure vertical, horizontal, and torsional deflections is significantly more expensive than motions only testing. Yet these measurements are essential for thorough structural design and proper design of load-sensitive equipment. In LAMP, these loads are easily calculated once the ship's projected weight distribution has been modeled. And since dynamic loads are functions of the weight distribution, motions, and wave pressure forces, load predictions should be accurate if motion predictions are adequately validated. Transient events such as slamming-induced whipping loads may also be considered in design. Precise predictions of instantaneous pressure along the hull are also available from the time domain fluid potential solution. These pressures may be used as input for time domain structural and/or acoustic finite element methods. Such measurements are extremely difficult to obtain experimentally.

Testing Application of Experimental Simulation Method In this research, the majority of the LAMP tests are devoted to application of the experimental simulation method. As proposed in this section, SMP is used to narrow down the number of required LAMP test runs. Two approaches for the use of LAMP as a test facility

are then applied. In the first method, LAMP is used to simulate irregular seas runs of about fifteen minutes real time each. Motion and load amplitudes are then calculated directly from the LAMP time domain predictions. In the second method, LAMP is used as a regular wave test facility. For heave, pitch, and vertical loads, the amplitudes of the first and any higher harmonics are calculated from the regular seas time domain predictions. These harmonics are then used as a form of Response Amplitude Operator (RAO) to predict responses in irregular seas. As mentioned previously, the testing included only head seas. Although much work needs to be done assessing the oblique seas design capabilities of LAMP, time restrictions limited this study to head seas, and vertical motions and loads. However, this is appropriate to an analysis of 3-D time domain code utility in early design, since head seas are often the most severe encountered by a ship, and are typically the subject of experimental tests. Table 2.4 on the next page lists the ship responses which are measured with both SMP and LAMP. This list includes the motions defining the naval and commercial transit limits, and those motions considered by the Bales and McCreight parametric indices. Vertical shear, which typically reaches absolute maxima at the hull quarter points, and vertical bending moment at amidships are compared for the loads.

Heave[†]
Pitch[†]
Heave Acceleration
Vertical Acceleration at Station 0
Vertical Acceleration at Station 3
Vertical Displacement at Station 20
Relative Motion at Station 0
Relative Motion at Station 3
Relative Velocity at Station 3
Relative Motion at Station 20
Deck Wetness at Station 0
Slamming at Station 3
Propeller Emmersion at Station 20
Vertical Shear Force at Station 5[†] [*]
Vertical Shear Force at Station 15[†] [*]
Vertical Bending Moment at Station 10[†]
[†]Only these responses are calculated in regular waves.
[*] Measured at Sta. 4 & 16 for VLCC, point of static hog maxima.

Table 2.4: Measured Responses in LAMP and SMP

Chapter 3

Hull Geometries

3.1 Mathematically Defined Hulls

3.1.1 Motivation

The primary test hulls for this research are a group of six mathematically generated surfaces, derived from the well-known Wigley Seakeeping Hull (hereafter, the Wigley Hull). The Wigley Hull is an extremely simple hull with zero flare along its length. The hull is fore-and-aft symmetric, with offsets becoming zero at the perpendiculars. There is no flat of bottom, and both the stem and stern are vertical. The mathematical definition can be applied to any desired length, beam, and draft. The formulation of the Wigley Hull is fully described in Section 3.1.3. The hull is the baseline for this study, and a plot of the geometry (applied to the study dimensions) is shown in Figure 3-3a, in Section 3.1.4. The baseline has varying depth, which is also discussed in that section.

This hull has proven extremely popular for hydrodynamic research both because of its simplicity and because the hull definition may be included analytically in the governing equations of motion. But why include such a hull in current numerical seakeeping studies, when high power computers are available? The primary reason is again that the hull's simplicity makes it an excellent tool for early code validation. However, though such a hull form is extremely useful for 2-D linear predictions of

seakeeping motions, it is inadequate for proper testing of 3-D nonlinear codes.

The alternative is to create a hull which maintains the simplicity of the original Wigley Hull, but which is useful for comparative studies using LAMP and SMP. The hulls designed for this study meet this goal. These mathematically defined hulls were accomplished through the superposition of additional hull forms with the original Wigley Seakeeping Hull components. The use of such hull forms allows the variation of certain hull geometrical parameters which are considered significant in their effect on both seakeeping and other hydrodynamic characteristics, such as resistance. Additional advantages and disadvantages of such hull forms include:

- With proper variation of mathematical components, desired hull characteristics may be easily achieved, without possibly inconsistent modifications of offset or B-Spline definitions.

- Simple hull shape eliminates many hull characteristics which might reduce the applicability of the research. Specifically, fore-and-aft symmetry removes effect of stern shape as a variable. However, some of these simplifications may simultaneously reduce the realism of the tests.

- Significant research has previously been conducted on Wigley type hulls, for example, Gerritsma (1988), Journée (1992), and Adegeest (1994) [24, 25, 26].

- Mathematical definition allows rapid generation of panelized hulls.

Section 3.1.2 further describes the selection of which parameters were to be held constant or varied for each hull. The mathematical hulls are to act as the "naval-like" hulls in this study, although the final choice of hull particulars certainly does not preclude commercial applicability.

3.1.2 Constant and Varied Hull Parameters

Before commencing the design of the mathematical hull forms, the possible combinations of hull parameters which would be used to specify the hull shape were examined. Priorities in proper selection of the parameters were:

1. Select standard hull parameters generally used by naval architects in describing hull shape characteristics.

2. Vary items which are accepted as having a significant impact on the hydrodynamic characteristics of ships.

3. Vary items which would realistically be possible to alter in the early design stages of a ship hull.

4. Hold constant parameters which would potentially be constrained by the specifications of a design, such as length, beam, draft, and displacement.

5. Limit geometry variation to isolate changes in hydrodynamic performance to a small number of variables.

6. Vary parameters to develop a hull form which includes characteristics that do not affect linear seakeeping calculations (especially above waterline hull form.)

7. Vary the proper number of parameters to constrain the hull selection uniquely without preventing a determinate solution. This is a function of the number of mathematical hull forms to be superimposed.

It is generally accepted that overall seakeeping performance may be improved by any one of several methods [11, 12]: increasing length to draft ratio (L/T), increasing the ratio $L^2/(BT)$, increasing the beam to draft ratio, B/T (which increases damping effects), and increasing length to volume ratio (L/∇). Besides these primary ratios, seakeeping may also be improved by altering the standard coefficients of form, especially by reducing block coefficient (C_B) or increasing waterplane coefficient (C_{WP}). It is also possible to alter longitudinal bending moment responses by varying the midships section coefficient (C_M).

While the above adjustments can in general improve seakeeping motions, it is possible to specifically improve pitch response by increasing waterplane area at the ends of the ship - and particularly the bow. Quantitatively, this requires increasing the waterplane moment of inertia coefficient, C_A. At the bow, which controls worst case

pitch response in head seas, waterplane area may be maximized by increasing both the flare angle (α) and/or the waterplane entrance angle (γ). These two angles are defined in Figure 3-1 on the facing page. Increasing flare forward will generally result in a more "V-shaped" hull form. Flare angle may usually be increased to 20-25°, and a reasonable hull form maintained [11]. In fact, U.S. Navy design recommendations, based on work conducted by Bales (1979), state that ships in this range of flare[1] have "superior wetness" performance [27, 28]. The flare for the first set of varied hulls was in fact set at 20°. Increasing entrance angle will also improve pitch response, but can have a drastic effect on ship resistance. These angles, and flare in particular, will to a great extent determine the hull shape near the bow. Proper flare can reduce pitch motions, green water on deck, and relative bow motions. Extreme flare can in turn create severe slamming loads.

Once the important hull parameters in seakeeping prediction were defined, the task of choosing which to vary and which to maintain constant was completed. Because of their significant impact on hydrodynamic performance, flare and entrance angle were chosen as the primary parameters to be varied in generation of a test series. Length, beam, draft, and displacement are held constant. Hull depth, although not a factor in the mathematical definition, is constant for all variants. These restrictions simulate a realistic challenge in early design. Ship payload and performance requirements may drive the choice of main particulars, but the designer has some latitude in creating a hull form (e.g. in selection of flare and entrance) that meets these criteria.

3.1.3 Hull Component Definitions

With the selection of hull parameters to be varied or maintained constant, the actual task of mathematical definition is possible. Achieving reasonable mathematical hull forms proved quite challenging, and is completely documented in Moton (1996) [29]. A review of the process and the final definition method is included here. All hulls are defined with nondimensional coordinates, since the final dimensions were not chosen

---

[1]Measured at Station 3, 15%L aft of the FP.
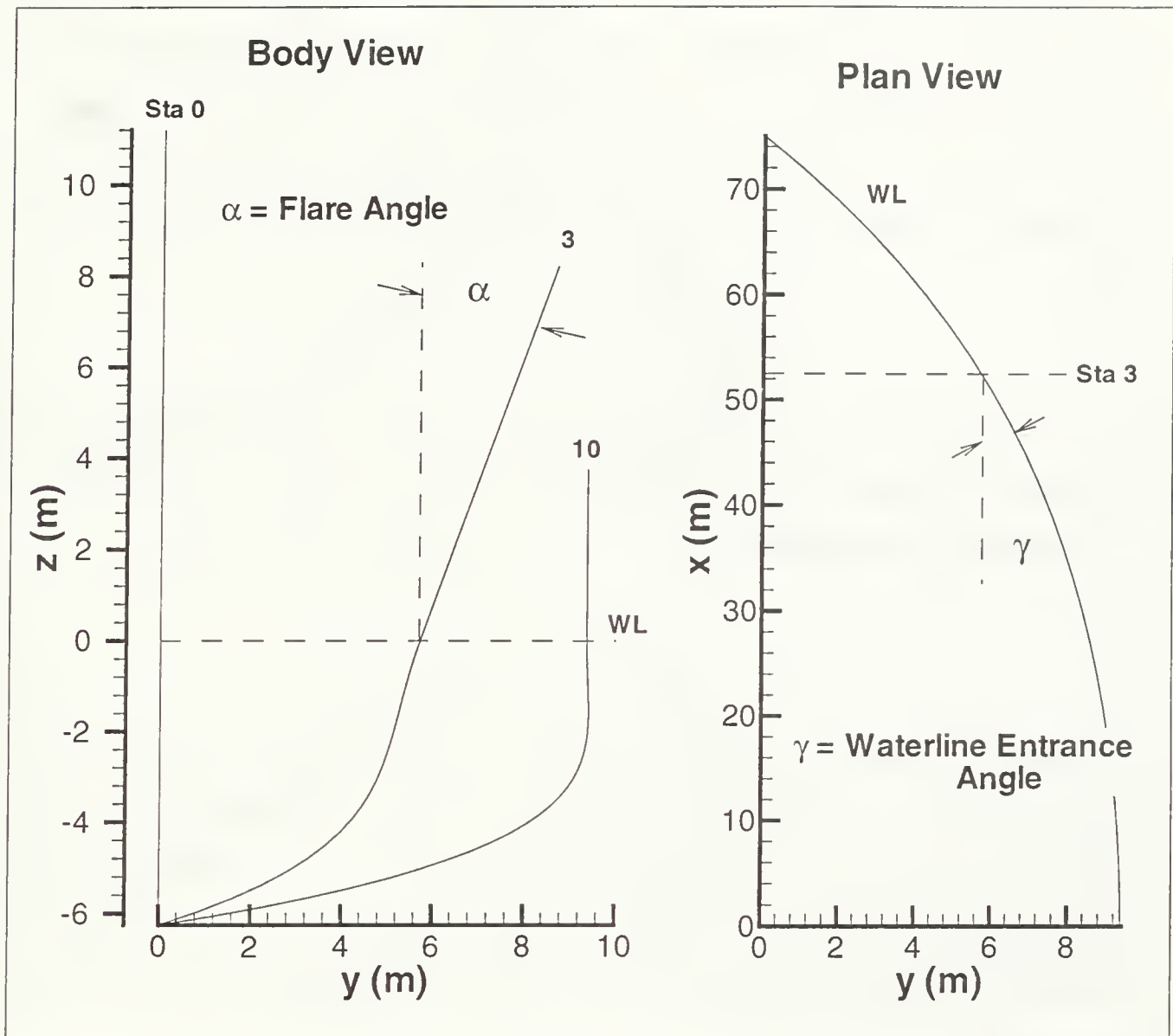
Figure 3-1: Flare and Entrance Angle Definitions (Variant 3 Lines)

until after the mathematical definition was created. These coordinates are:

$$\eta = 2x/L$$

$$\xi = 2y/B$$

$$\zeta = 1 + z/T$$

with $x = 0$ at amidships, and positive forward; $y = 0$ on the centerline and positive to port; and $z = 0$ at the design waterline and positive up.

49

The baseline hull is the Wigley Seakeeping Hull, introduced in Section 3.1.1. This hull is defined as the superposition of two hulls, the original Wigley Resistance hull (4th order in η, 2nd order in ζ), and an additional hull (2nd order in η, 4th order in ζ). The second hull was designed to raise the section coefficients by adding displacement and creating a sharper bilge radius. The definition equation for the Wigley resistance hull is:

$$\xi = \beta_1 \zeta (2 - \zeta)(1 - \eta^2)(1 + 0.2\eta^2)$$

β_i is a weighting factor for each hull, and is the parameter which is varied to achieve the desired hull forms. This hull is graphically displayed in Figure 3-2a[2]. The second hull component is defined as:

$$\xi = \beta_2 (1 - \zeta)^2 (2 - \zeta)\zeta(1 - \eta^2)$$

Each of these hulls was specifically defined to have zero slope (zero flare) at the design waterline. The hulls are both symmetric about amidships and the design waterline. Hull 2 was carefully selected by Wigley to provide a reasonable looking, full hull form when combined with hull 1 in exactly the same proportions ($\beta_1 = \beta_2$). Achieving a reasonable hull shape while varying these original proportions proved quite difficult.

Any surface to be added to the original two hulls would have to meet several boundary conditions, imposed by the necessity of having a viable ship hull form, which still maintained most of the basic useful characteristics of the original Wigley Hulls. These boundary conditions are:

- Zero offset at the forward and aft perpendiculars (mathematically, $\xi = 0$ for all ζ, $\eta = (1, -1)$)

- Zero offset at the baseline ($\xi = 0$ for all η, $\zeta = 0$).

- Symmetric about amidships ($\xi(\eta, \zeta) = \xi(-\eta, \zeta)$).

---

[2]These plots are displayed with hull particulars set to the final selected values: $L = 150$ m, $B = 18.75$ m, and $T = 6.25$ m, and $\beta_i = 1$ for ease of comparison. See Section 3.1.4
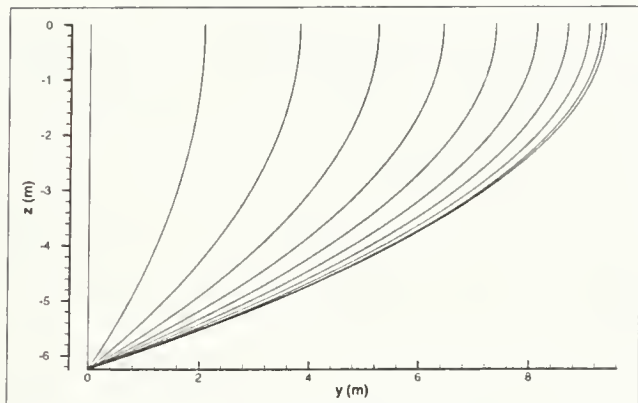
a. Wigley Resistance Hull
$$\xi = \zeta(2 - \zeta)(1 - \eta^2)(1 + 0.2\eta^2)$$
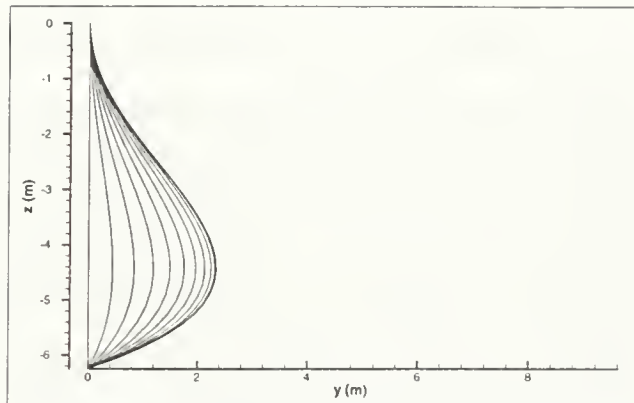
b. Wigley Seakeeping Hull Addition
$$\xi = (1 - \zeta)^2(2 - \zeta)\zeta(1 - \eta^2)$$
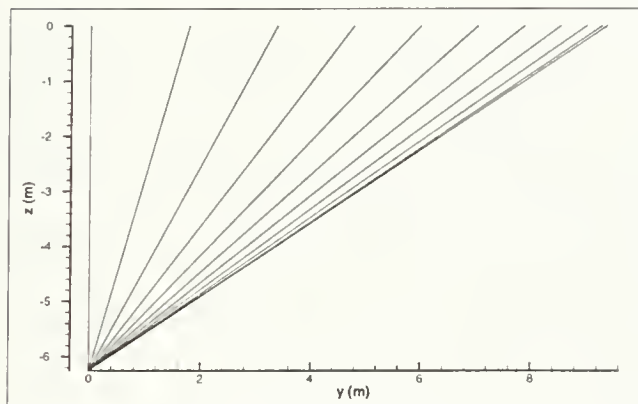
c. $\xi = (1 - \eta^2)\zeta$
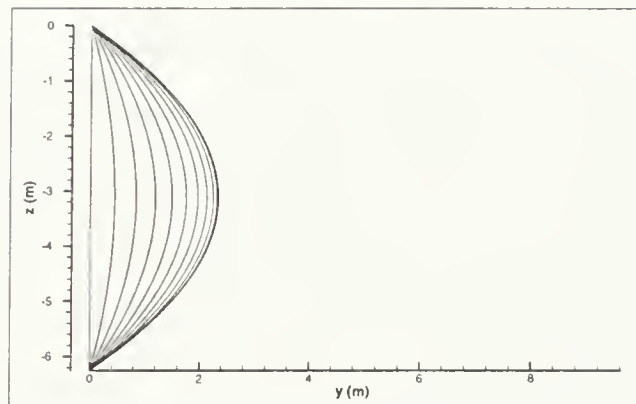
d. $\xi = (1 - \eta^2)\zeta(1 - \zeta)$
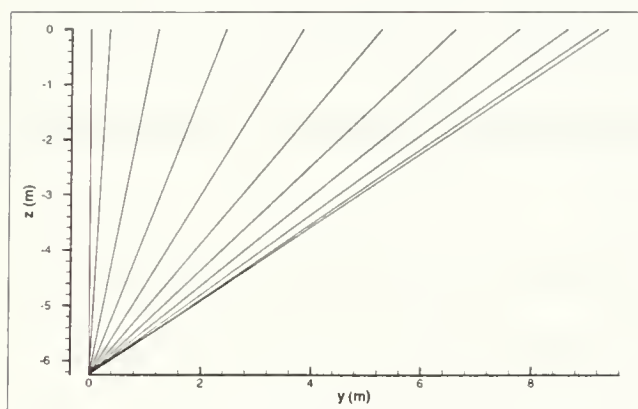
e. $\xi = (1 - \eta^2)^2\zeta$
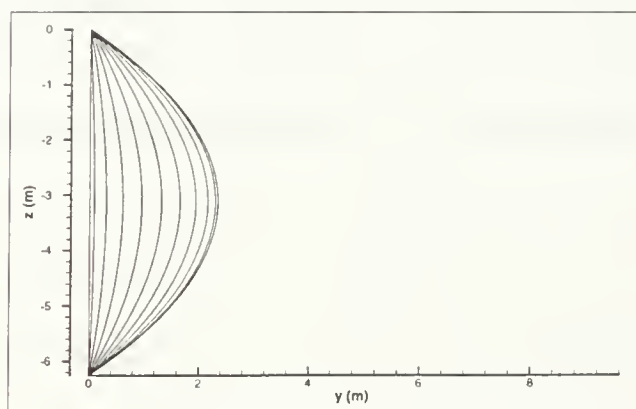
f. $\xi = (1 - \eta^2)^2\zeta(1 - \zeta)$

Figure 3-2: Mathematical Hull Individual Components (test hull dimensions, $\beta_i = 1$)

The fore-aft symmetry condition is not required in actual ship hull forms, but is an important aspect of the Wigley Hull. Maintaining such symmetry eliminates questions about the effect of afterbody shape on hydrodynamic performance.

The original two hulls include second and fourth order dependency on ζ, which resulted in zero flare at the design waterline. The initial strategy for adding additional hulls to the two Wigley components was to have the final hull form be a complete polynomial in ζ. The number of hulls is determined by the number of parameters to be held constant, so that a linear combination of hulls, with varied β_i coefficients, achieves the desired parameters. Since B, C_B (i.e., displacement), flare angle, and entrance angle are the set parameters, four total hulls are needed for a determinate solution[3]. Thus, at least two new mathematical hulls are required.

Recalling the hull boundary conditions, a careful analysis of possible hull forms with varied dependency on ζ was completed, examining the offsets and slopes at the baseline and the waterline. Only hulls with zero offset at the baseline were considered. A successive addition of these hull forms should hopefully result in achievement of the desired flare angles with a reasonable looking hull form. The first order dependency in ζ was added by using a linear hull, with second order dependency on η, such that:

$$\xi = \beta_3(1 - \eta^2)\zeta$$

which for the first time adds flare at the waterline, and contributes to the waterline beam. This hull shape is plotted in Figure 3-2c.

The second order in ζ hull was already present, as the Wigley Resistance Hull. The third order hull was chosen specifically to provide negative flare at the waterline. A proper combination of this hull with the first order hull should provide the desired flare. After examining several different forms of third order hulls with negative flare,

---

[3]B and C_B are required constant for all hulls; flare and entrance are varied for each hull, yielding four total parameters. L and T are also held constant, but because they are used to nondimensionalize the independent parameters ζ and η, they do not require additional equations.

the most suitable was selected:

$$\xi = \beta_4(1 - \eta^2)\zeta(1 - \zeta)$$

This hull is plotted in Figure 3-2d.

With only these four components, flare had to be increased simultaneously with entrance angle to achieve a feasible hull. However, only a very narrow range of entrance angles corresponding to each flare angle prevented a significant bulge beneath the waterline, due to the second component of the Wigley Seakeeping Hull. In addition, as flare and entrance were increased even slightly, the forebody became extremely full, causing a hollow between the bow and amidships.

To overcome the limitation in hull variation caused by this hollow, additional hulls were added to provide variation in η as well as ζ. As stated earlier, the original Wigley Seakeeping Hull had a 2nd order and a weak 4th order dependency on η. A complete set of polynomials is not possible in η because the hull must be fore and aft symmetric. In addition to this boundary condition, a new condition, that beam is maximum at amidships, was applied. This condition is necessary to prevent hollows in the waterlines. To meet these η boundary conditions, only even-ordered polynomials are feasible. The second order dependency in η is provided in all four components previously selected. The fourth order dependency was provided by adding two hulls, which are identical to components 2 and 3, but as functions of $(1 - \eta^2)^2$ vice $(1 - \eta^2)$, such that:

$$\xi = \beta_5(1 - \eta^2)^2\zeta$$

$$\xi = \beta_6(1 - \eta^2)^2\zeta(1 - \zeta)$$

which are plotted in Figures 3-2e and f, respectively.

The use of six hulls required specification of six constraints to achieve a determinate solution. The previous constraints of B, C_B, and flare and entrance angles at the DWL at 15% LBP aft were maintained. Two additional constraints were required. Flare angle at the DWL, at amidships, was specified as 0.0. This is a realistic value

53

and yielded very reasonable amidships shapes. The second constraint was picked to counteract the problem of longitudinal bulges developing between the forward perpendicular and the constrained entrance angle at 15% aft. Entrance angle was specified at 5% aft on the DWL. This angle was held constant for each specific entrance angle at 15% aft, so that waterlines remained fair.

These hull combinations work extremely well and allow large variations of flare and entrance angles, both independently and simultaneously. The next step in definition of the mathematical hulls is selection of the hull dimensions, flare angles, and waterline angles.

3.1.4   Characteristics

Primary Dimensions

The primary dimensions of the ship must be determined before the test matrix of flare and entrance angle variation is developed. As stated in the previous section, length, beam, draft, and block coefficient are held constant for all hulls. Rather than use nondimensional values, length is set to 150 m, which is very typical of current destroyer type hulls. Although LAMP can accept nondimensional geometries, and SMP can accept model scale inputs, dimensional values are used to provide a physical aspect appropriate for design. Additionally, the motion criteria, load limits, and sea state definitions may be maintained as defined.

With length defined, beam and draft are set to yield specified values of L/B and B/T. The goal is to create a hull form with dimensions that are feasible for both naval and commercial ship types. Based on typical hull geometries [30, p. 20], L/B is 8.0, yielding $B = 18.75$ m, and B/T is 3.0, yielding $T = 6.25$ m. Another goal of dimensional selection was to choose L/B and B/T to match a test case where tabulated experimental seakeeping data is available. However, the only such data available for a Wigley Seakeeping Hull was that published by Gerritsma (1988) and Journée (1992) [24, 25]. Unfortunately, their hulls had L/B equal to 5.0 and 10.0, both of which were considered too extreme for this study. Finally, displacement

(set as block coefficient) is maintained constant for each hull at $C_B = 0.5605$. This corresponds to the block coefficient of the baseline Wigley Seakeeping Hull.

The depth for all hulls is identical. Depth at the forward perpendicular is based on the minimum freeboard requirements recommended by Bales, which have been incorporated into U.S. Navy design standards for combatant ships [28, 27]. The minimum freeboard at the forward perpendicular is parametrically defined by:

$$FBD_0 = 10.5 + 0.045(LBP - 150) - 0.00002(LBP - 150)^2 - 0.20[(LBP/T) - 27.5]$$

where all quantities are in meters. The hull depth then initially decreases one meter per station as per the Bales recommendations. Following a splined transition to amidships, the depth for the aft half of the ship is constant at $D = LBP/15$. This is a parametric minimum to provide structural adequacy of the box girder, used in early naval surface combatant design [31]. U.S. Navy recommendations for minimum freeboard at the aft perpendicular are satisfied by this value.

Although seemingly minor, the choice of sufficient freeboard ensures that deck wetness does not dominate the SPI-2 calculations, particularly in moderate seas. Linear methods only require freeboard at the FP for the deck wetness calculation, however, nonlinear methods such as LAMP-2 and LAMP-4 require adequate definition of the above water hull along the entire length of the ship.

Flare and Entrance Angle Variation

The first four test hulls include the baseline (Wigley Seakeeping), and three variants. In the first variant, flare is increased, allowing the underwater hull to change. In the second variant, entrance angle is increased, again with subsequent underwater hull changes. In the third variant, both flare and entrance angle are increased. Using the hull dimensions and desired flare and entrance angles, a computer program was used to calculate the β_i weighting factors for each mathematical component. Each of the final hull geometrical constraints is the linear sum of that same parameter in each of the six mathematical components. As a result, a linear equation may be solved to

determine all β_i given any combination of desired hull characteristics.

Flare is varied first. The selected flare angle of 20° is within the maximum reasonable range and yields suitable hull forms. Entrance angle of the baseline Wigley with chosen dimensions is 11.9°. As with a real design, the optimum entrance angle is a trade-off between seakeeping improvement and ship resistance increase. However, the entrance angle increase between the Baseline and Variants 2 and 3 should be large enough to noticeably affect seakeeping. Saunders (1957) recommends that entrance slope be less than 19.47° to allow a traveling pressure-point surface wave pattern to form at the stem of the ship [32]. Entrance angles above this value can result in significant resistance increases. The entrance angle of Variants 2 & 3 is increased by approximately 5° to 17°. This increase is significant, yields reasonable hull shapes, but does not approach the 19.47° threshold.

The main particulars of the first four hulls (Baseline plus Variants 1-3) are included in Table 3.1 on page 59. Body plots of the hulls plus isometric views showing the LAMP input panelization (before resplining) are shown in Figures 3-3a, b, and c, and 3-4a.

The hulls look quite reasonable. Note that the increase of flare with block coefficient held constant resulted in more V-shaped hulls. When flare was increased without an increase in entrance angle, there is significant curvature change in the forebody, as in Variant 1. In Variant 3, both flare and entrance angle are increased, and the V-shape is more pronounced, but with less curvature change than in Variant 2. Additionally, Variant 2 does have a slight hollow just below the waterline, but only near amidships. Although undesirable, the hollow is very localized near the center of the ship, and should have a negligible effect on motion or load responses.

Variants 4 and 5 are particularly interesting hulls for testing. Both of these hulls are identical to the baseline under the design waterline. However, Variant 4 has flare matching Variant 1 and 3 above the waterline, although the transition is smoothed by splining. Variant 5 has a constant 10° of tumblehome (negative flare) above the waterline. Again the transition is smoothed at the waterline and near the perpendiculars. Tumblehome has been recently investigated in combatant hull design in an
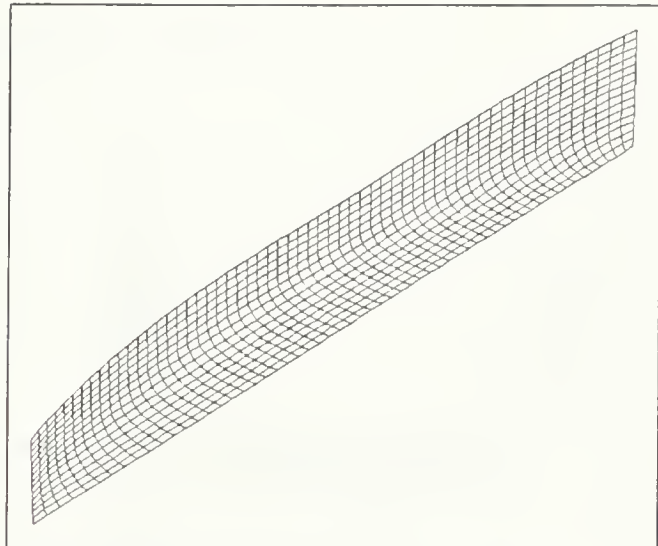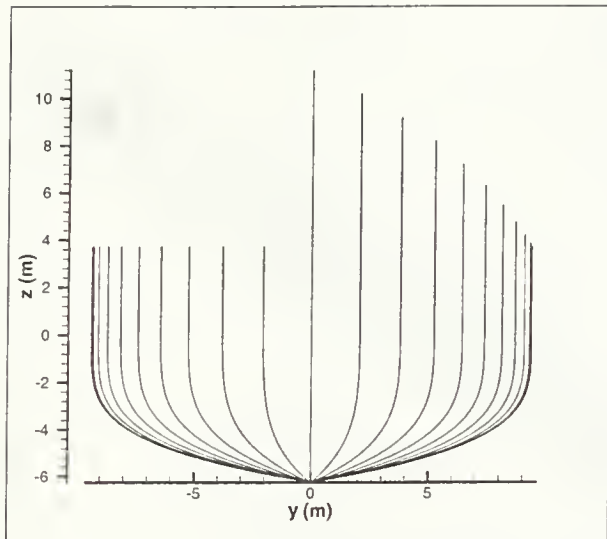
a. Baseline (Wigley Seakeeping Hull)
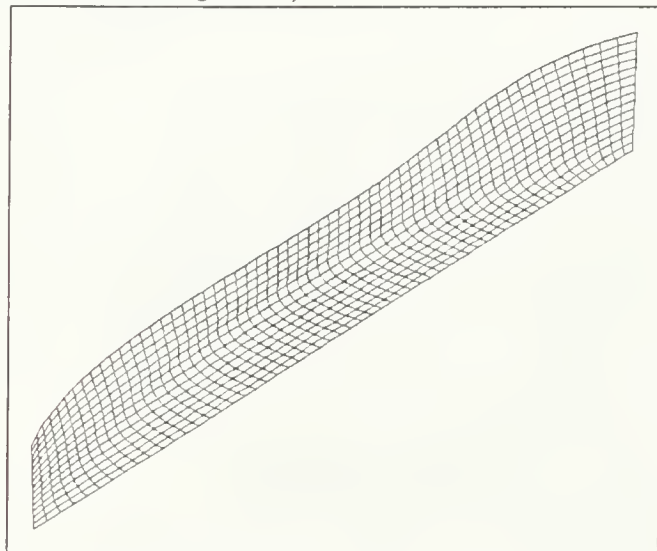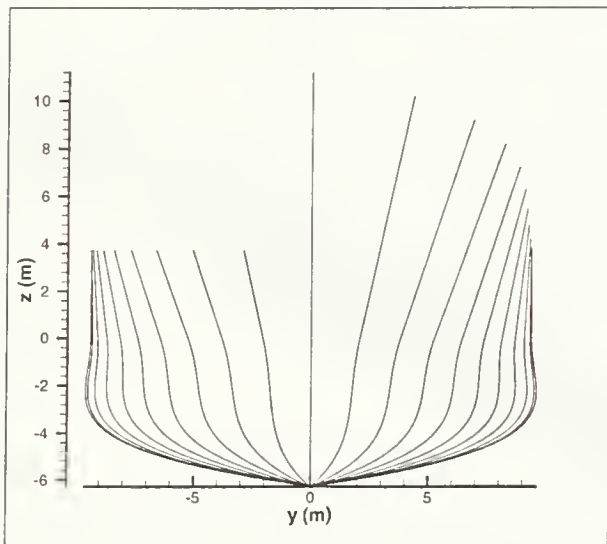
b. Variant 1 (Flare Angle Increase)
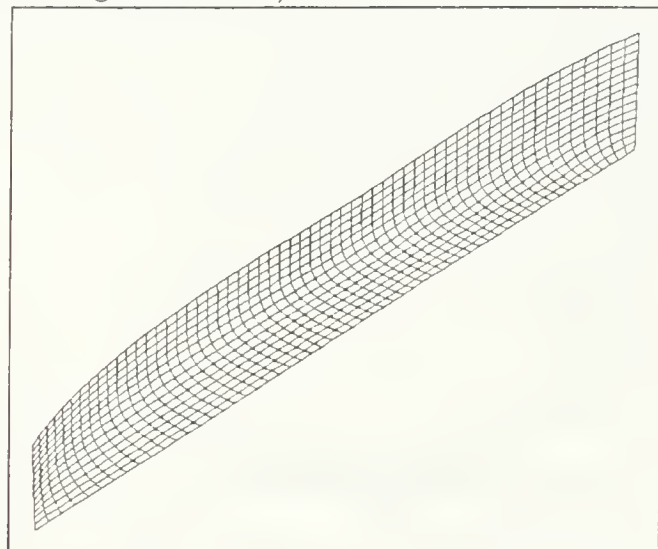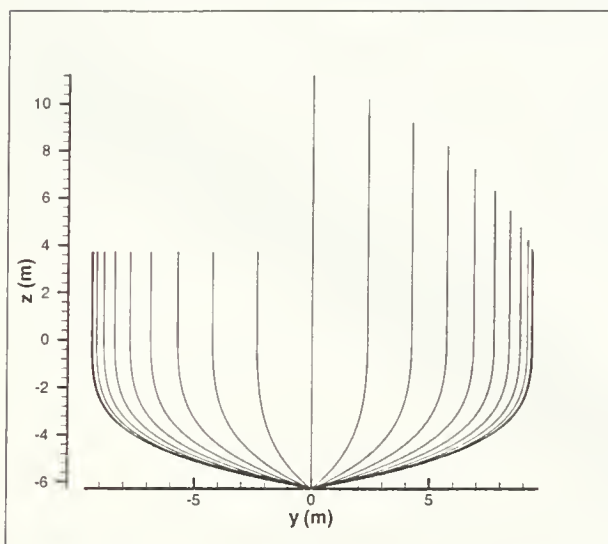
c. Variant 2 (Entrance Angle Increase)

Figure 3-3: Mathematical Hull Geometries (BL, V1, V2) —
Body Plots and Input Panelization (Az. 30°, El. -20°)

57
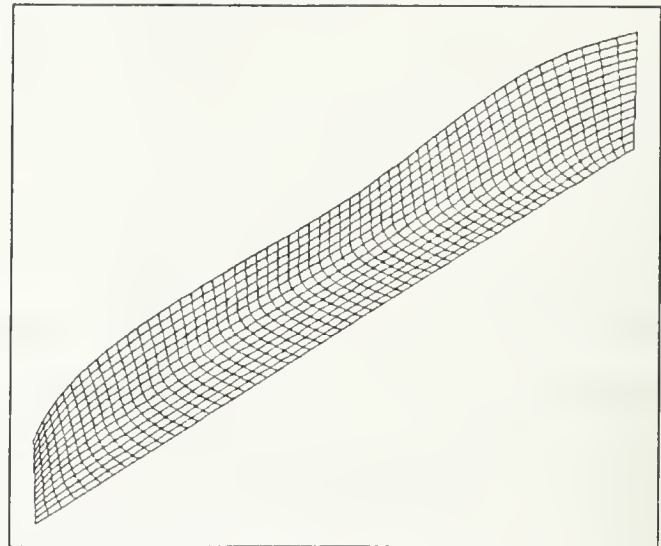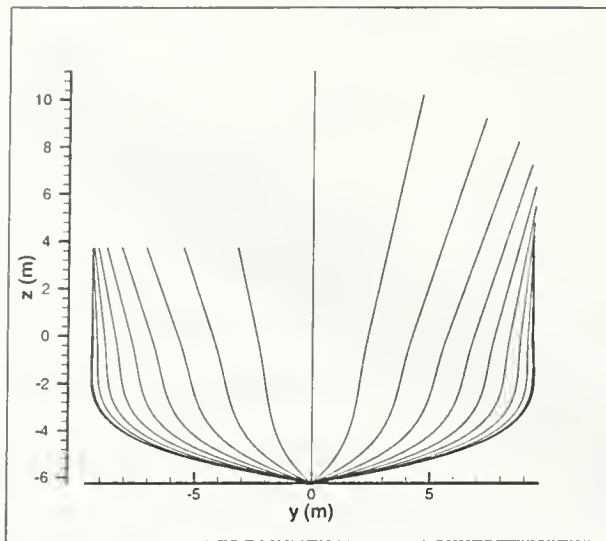
a. Variant 3 (Flare and Entrance Angle Increase)
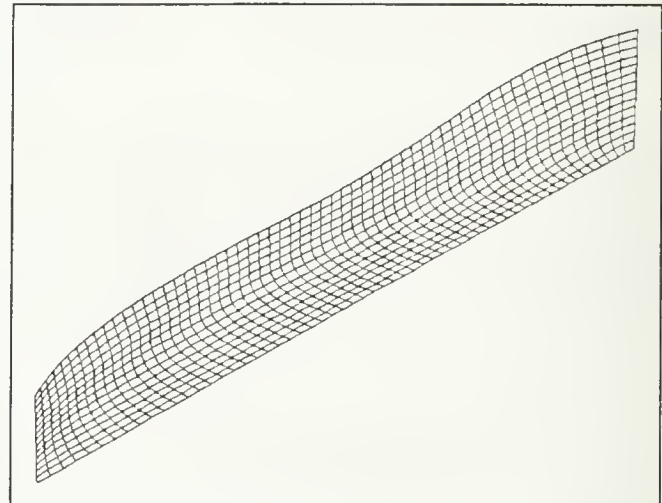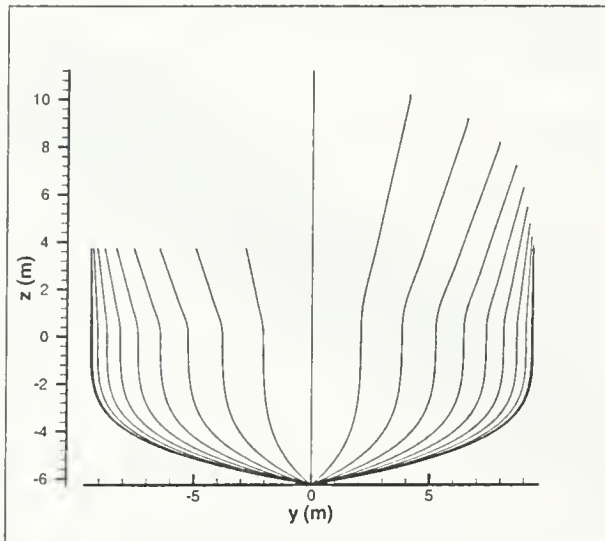
b. Variant 4 (Flare Above Waterline Only)
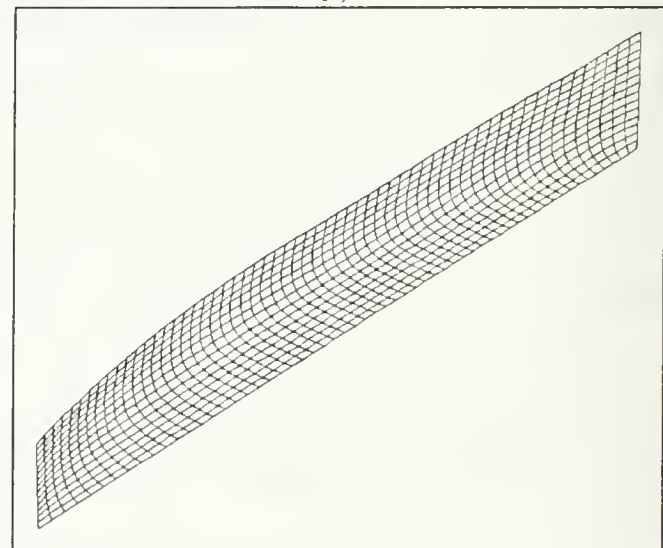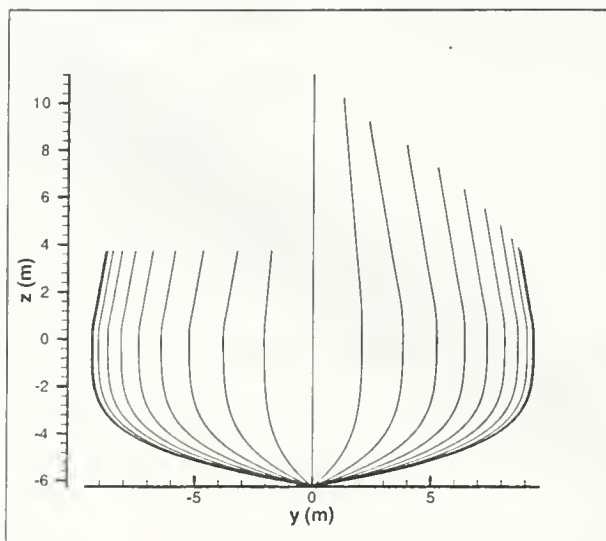
c. Variant 5 (Tumblehome Above Waterline Only)

Figure 3-4: Mathematical Hull Geometries (V3, V4, V5) —
Body Plots and Input Panelization (Az. 30°, El. -20°)

Parameter	Mathematical Hulls					
	BL	1	2	3	4	5
L (m)	150.0					
B (m)	18.75					
T (m)	6.25					
L/B	8.00					
B/T	3.00					
C_B	0.5605					
∇ (m³)	9853					
Δ (MT)	10099					
LCB/L	0.50					
LCF/L	0.50					
KG (m)	5.95					
k_{yy}, k_{zz}	$0.25 \cdot L$					
k_{xx}	$0.30 \cdot B$					
α Sta. 3 (°)	0.0	20.0	0.0	20.0	20.0[†]	-10.0[†]
γ Sta. 3 (°)	11.9	11.9	17.0	17.0	11.9	11.9
GM_T/B	0.100	0.095	0.114	0.113	0.100	0.100
GM_L/L	1.567	1.542	1.663	1.664	1.567	1.567

†: Flare for these hulls does not begin until just above DWL.

Table 3.1: Mathematical Hull Main Particulars

effort to reduce ship radar cross sections. The 10° slant angle is typical of such studies. These variants are shown in Figures 3-4b and c. Because these hulls are identical to the Baseline in underwater hull form, both parametric and linear methods (SMP and LAMP-1) would predict identical responses. However, nonlinear methods (LAMP-2 and LAMP-4) should predict a difference. With these two variants, a total of six mathematical hulls are defined for testing.

Weight Distribution and Static Loading

Weight requirements for seakeeping analysis are a function of the desired results. For motions, all that is required is the displacement, position of the center of gravity (CG), and mass moments of inertia about CG. The mass moments of inertia are typically expressed using the radius of gyration. For the mathematical hulls, the longitudinal center of gravity (LCG) is at amidships, resulting in even trim. Transverse center of

gravity (TCG) is on the centerline, for zero heel. Vertical center of gravity above the keel (KG) is set to yield a ratio of transverse metacentric height to beam (GM_T/B) of 0.1 for the Baseline – a typical value. KG is then maintained constant for all other variants, at 5.95 m. GM_T/B then changes due to small variations in waterplane inertia for each variant. Maintaining KG constant vice GM_T/B for all variants is appropriate given the proposed design scenario, where the entire weight distribution is fixed. Both the pitch and yaw gyradii are set to $0.25 \cdot L$, a typical design value. Likewise, roll gyradii are $0.30 \cdot B$. Both yaw and roll gyradii, however, will not effect head seas results.

If vertical load predictions are desired, a longitudinal weight distribution is required. The U. S. Navy's Program of Ship Salvage Engineering (POSSE) was used to develop this distribution. POSSE is used by the Navy Supervisor of Salvaging and Diving to perform stability and structural analyses of both commercial and naval vessels in the intact, damaged, and grounded conditions. It includes the capability to rapidly develop typical weight distributions for various ship types, so is useful for parametric estimation.

In keeping with the use of the mathematical hulls as "naval-like" variants, the weight distribution for the DDG-51 *Arleigh Burke* Class destroyer is used as a parent. POSSE scaled this distribution to match the input displacement and LCG for the mathematical hulls. The Ship Hull Characteristics Program (SHCP) was then used to calculate the static shear forces and bending moments, based on the POSSE-generated weight distribution, and the hull offsets. Buoyancy curves were generated for three standard loading conditions, which are typical during design: still water, hogging, and sagging. For the hogging and sagging conditions, the wave used had $L_w = LBP$ and $H_w = 1.1\sqrt{LBP[feet]}$ with the crest at amidships or the ends of the ship, respectively. This formulation is commonly used by the Navy for design estimates of maximum shear forces and bending moments [18].

With the weight and buoyancy curves, SHCP calculated the vertical shear forces and bending moments for each afloat condition. Because the ship had a natural hogging condition in still water, the worst case shear forces and bending moments

occurred in the hogging wave condition. For consistency among variants, the calculated Baseline hull's shear forces at the forward and aft quarter points (Sta. 5 and 15), and the bending moment at midships (Sta. 10), are used as the reference load limits. The differences between the worst case static hog loads and the calm water values are shown in Table 3.2. These values are plotted in subsequent vertical shear force (VSF) and bending moment (VBM) response analyses.

Parameter	Static	Hog	|Hog-Static|
VSF Station 5 (kN)	149.83	1084.37	934.54
VSF Station 15 (kN)	-325.86	-1262.42	936.56
VBM Station 10 (kN-m)	15227.7	57720.7	42493.0

Table 3.2: Mathematical Baseline Static Load Limits

3.1.5 Computational Tool Setup

SMP

Only the mean underwater portion of each hull is modeled since 2-D strip theory does not take above water geometry into effect. Twenty-one stations, with ten offsets per station in equal girth segments, are used for the SMP hull definition. No appendages were modeled. The weight distribution closely approximated that developed by POSSE, since SMP only allows weight positions at the same longitudinal positions of the offset input.

LAMP

LAMP-1 and 2 were set up in the following manner for both irregular wave and regular wave tests. In most cases, the default or recommended values as per the LAMP User's Manual were applied for consistency. LAMP Version 2.8.5 was used for all mathematical hull tests.

All mathematical hull runs were completed with the mixed source formulation (MSF) of LAMP. A body-fitted free-surface (see Section 2.2.3) was used. The match-

ing surface extended 215 m ($= 1.43L$), 35 m ($= 1.87B$), and 25 m ($= 4.00T$) in the longitudinal, transverse, and vertical directions, respectively, around the hull. The number of panels on the matching surface was 21, 6, and 11 panels in the longitudinal, transverse, and vertical directions respectively. SAIC provided significant consultation in ensuring the mixed-source formulation was properly set up for all LAMP runs.

LAMP includes the ability to respline input geometry. The input panelizations (shown in the right columns of Figures 3-3 and 3-4) are excessively dense for the actual potential field calculation. For all LAMP-1 and 2 runs, the underwater geometry was resplined to 10 waterline points and 40 station points, resulting in 351 panels per side.[4] SAIC has performed several panelization sensitivity studies using the Wigley Hull, and this number of panels should exceed the sensitivity level, at the cost of a somewhat slower than necessary computation time. In LAMP-1 and 2, which solve the potential flow problem with the linear body boundary condition, the underwater resplining occurs only at the beginning of the test run. Figures 3-5a and b show the Baseline hull after resplining. The geometry of the matching surface is also shown in grey-shade. Additional comments on the LAMP-4 test runs are included in Section 5.2.

For all cases, the ship was fixed in surge, sway, roll, and yaw, and free in heave and pitch. A time step of approximately 0.156 seconds (0.04 nondimensional[5]) was used, as per the LAMP manual recommendation [22]. Each irregular seas run lasted 6000 time steps, for about 15.6 minutes worth of real time data. Each regular wave run lasted 1400 time steps for 219 seconds of data. In all cases, this was sufficient for any initial transients to become negligibly small.

---

[4]Because only head seas were tested, the flow field is transversely symmetric, and only half the hull need be panelized.

[5]Time is nondimensionalized by $\sqrt{L/g}$.
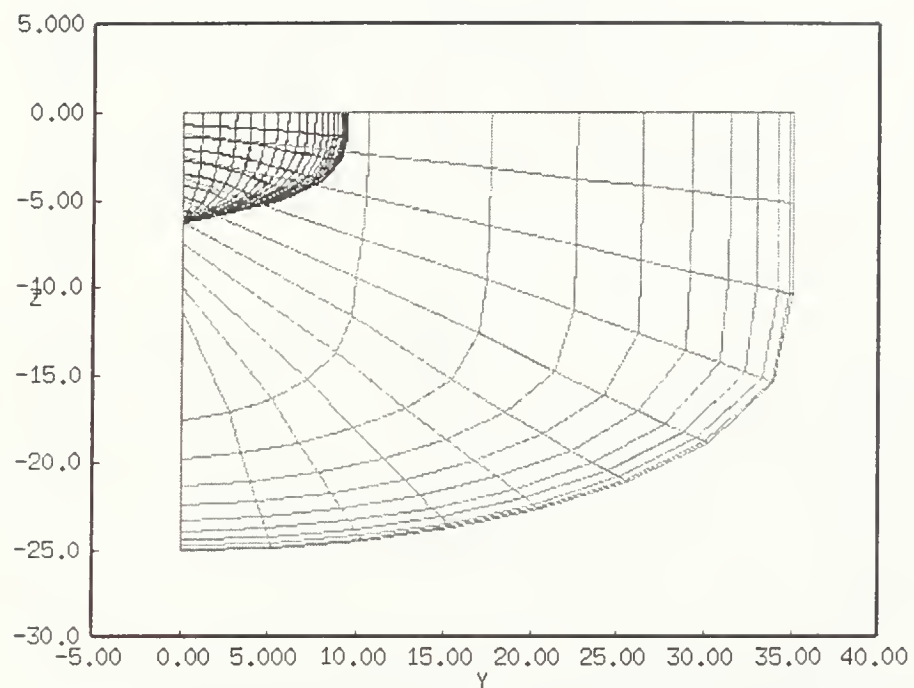
a. Body View (solid: hull, grey: matching surface)
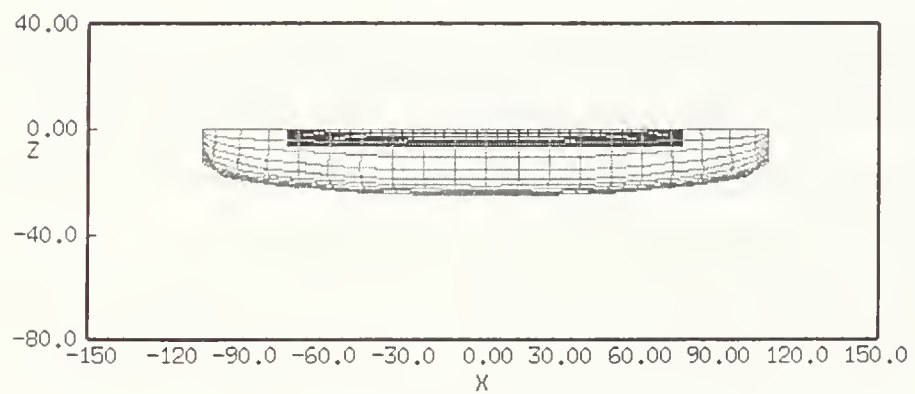
b. Profile View

Figure 3-5: Mathematical Hull LAMP-1/2 Output Geometry

63
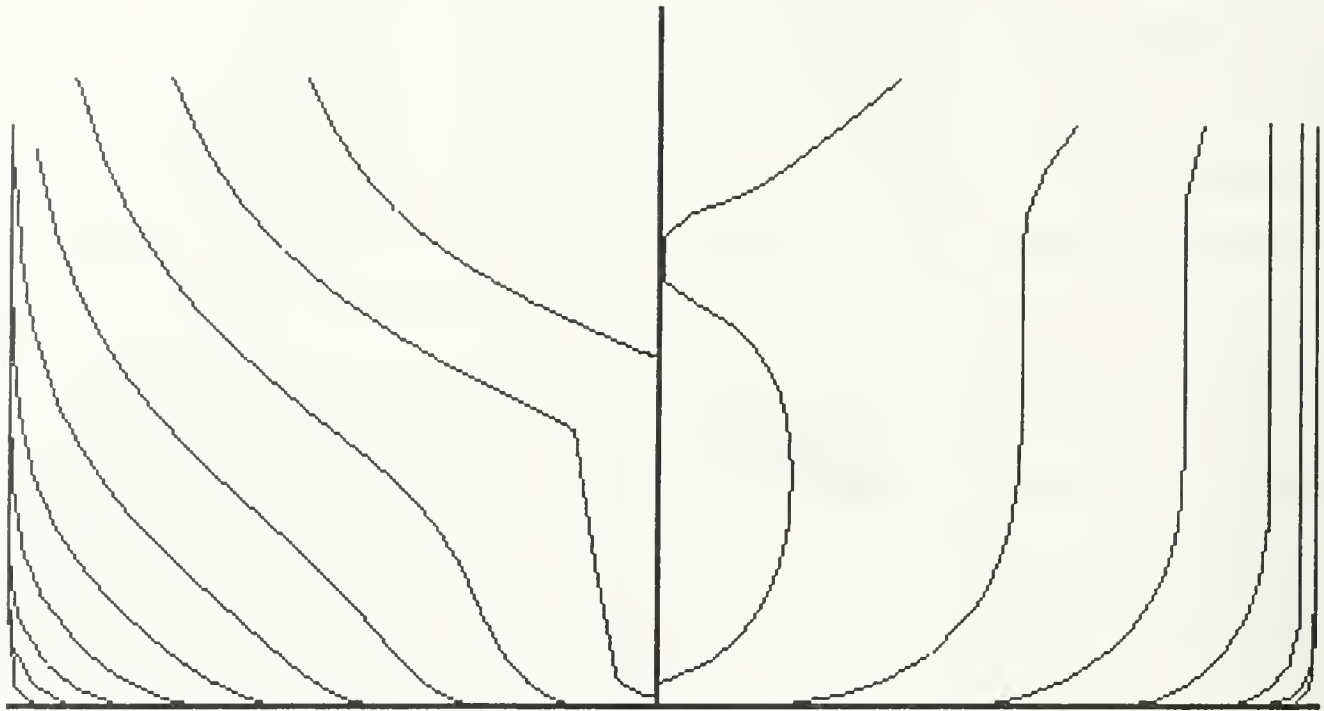
Figure 3-6: VLCC Body Plot

3.2 Very Large Crude Carrier Hull

Besides the mathematical hull series, one additional hull was examined using both SMP and LAMP. This hull form is a 260,000 deadweight tonnage oil tanker (VLCC: Very Large Crude Carrier) developed by the National Taiwan University (NTU) Department of Naval Architecture and Ocean Engineering.

Although this hull form is representative of modern oil tanker designs, there are aspects of its hull geometry which made it an excellent case study for advanced seakeeping analysis. These hull form aspects are discussed further in Section 3.2.2.

3.2.1 Characteristics

NTU provided the hull offsets and major characteristics of the VLCC. A body plan of the hull is shown in Figure 3.2.1. Main parameters of the ship are listed in Table 3.2.1 on the facing page. As with the mathematical hulls, the VLCC required panelization and generation of weight curve data for load predictions.

LOA	329.00 M
LBP	315.00 M
B	58.00 M
D	28.70 M
T	19.50 M
Δ	296939.6 MT
KG	20.50 M
k_{yy}	0.25 LOA
k_{xx}	0.30 B

Table 3.3: VLCC Hull Main Parameters

Weight Distribution and Static Loading

Since NTU did not specify a weight distribution, a typical commercial ship weight curve was developed based on the overall displacement and center of gravity of the VLCC. The POSSE program was again used to generate a weight distribution curve based on the hull offsets, service speed (15.5 knots), stern type (transom), and number of screws (assumed 1).

POSSE was also used to estimate the static shear force and bending moment curves. As with the mathematical hulls, the hogging condition stresses are the most severe for the VLCC. The maximum shear forces occurred at Stations 4 and 16 and the maximum bending moment at Station 10, amidships. As a result of this analysis, vertical shear forces (VSF) in waves were calculated at stations 4 and 16, and vertical bending moments (VBM) at station 10.

After determining the expected locations of maximum shear and bending stresses, an alternative method was used to calculate load limits. As discussed in Section 2.1.2, the ABS deterministic criteria are applied to the VLCC to develop shear force and bending moment dynamic design limits. The ABS rules do not provide calm water loads, but only maximum dynamic loads, equivalent to the "|Hog - Static|" values for the mathematical hulls. These limits are shown in Table 3.4 on the next page. These limits are plotted in the VLCC irregular seas results as reference values.

Parameter	Dynamic Design Limit
VSF Station 4 (kN)	82490
VSF Station 16 (kN)	9527630
VBM Station 10 (kN-m)	75891

Table 3.4: VLCC Static Load Limits

3.2.2 Computational Tool Setup

Panelization

The first step of preparing the hull for testing with LAMP is proper panelization. There were several characteristics of the VLCC hull which made it quite difficult to panelize successfully. This fact alone makes the VLCC an interesting follow-up to the mathematical hulls. The first panelization problem was the bulbous bow. The bulb was defined as a separate surface initially, and then attached to the main hull surface component. The stern of the ship also proved an extremely difficult panelization challenge from a CFD standpoint.

Unlike the mathematical hull, the panelization of the VLCC could not be developed automatically. The offsets were initially converted into a coarse panelization file which was then manipulated using I3G/Virgo Version 4.80 (a CFD panelization tool developed by the Wright Laboratory Flight Dynamics Directorate.) These offsets were regridded using equal waterline spacing and full cosine station spacing for the LAMP input files. The body consisted of three components - the main hull, the bulb, and the bow overhang. The bow overhang is required for LAMP2/4 runs only.

Two panelizations were tested in LAMP. Each panelization was created by using LAMP to respline the input panelization as directed by the control file. The panelizations were completed with the help of SAIC programmers, primarily due to difficulties in modeling the VLCC stern and bow bulb geometry. The first panelization was used in the majority of the LAMP-1 & 2 runs and is shown in Figure 3-7b. This is the input geometry resplined with 11 equally spaced waterlines and 21 stations with full hyperbolic tangent spacing (denser at both ends: shortest panel length was

66
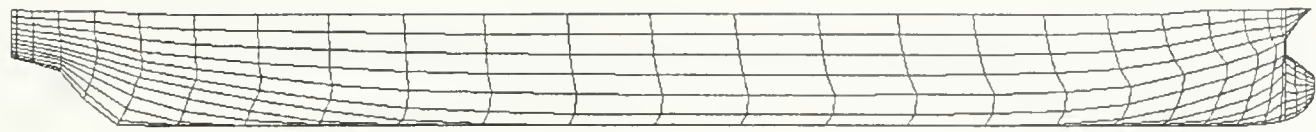
a. Input panelization
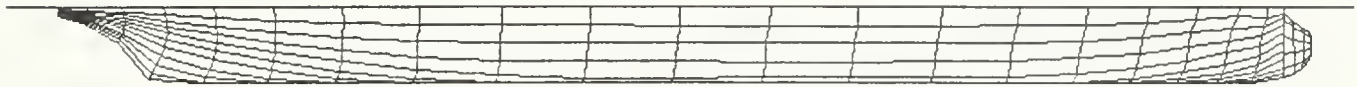
b. LAMP-1/2 trimmed and resplined panelization #1

c. LAMP-1/2 trimmed and resplined panelization #2

Figure 3-7: VLCC LAMP Panelization

0.025 times the total waterline length) on the main hull. Hyperbolic tangent spacing worked well in improving the stern panelization.

This initial panelization was adequate for LAMP-1/2 runs, but failed when LAMP-4 runs were attempted. LAMP-4 was first set to respline each hull station under the instantaneous free surface (component cutting, see Section 2.2.3) to ensure adequate panelization. However, the intersection between the main hull and the bulb surfaces caused a problem when LAMP attempted to piece the body and the MSF matching surface into consistent contours for generation of the free surface grid. SAIC examined the surfaces and assisted by combining the bulb, bow overhang, and forward 20% of the hull into one surface, which was attached to the remainder of the hull. This input panelization resplined more smoothly than the first panelization. LAMP was used to respline this input geometry with the bow component having 7 stations, with 1/2 hyperbolic tangent spacing (denser at forward end: shortest panel length fraction 0.075). The aft section of the hull was resplined to 18 stations, with full hyperbolic tangent spacing (shortest panel length fraction 0.040). The resulting panelization is shown in Figure 3-7c for LAMP-1/2. This panelization is then resplined at each time step for LAMP-4.

SMP

For SMP, the VLCC hull was modeled like the mathematical hulls, with 21 stations and ten offsets per station. No appendages were modeled, although the bulb and stern skeg offsets were included in the hull geometry.

Chronologically, the VLCC regular wave tests actually occurred before the mathematical hull tests and the VLCC irregular wave tests. At the time of the regular wave calculations, the author only had access to the 1991 version of SMP. Vertical load RAO's were to be calculated, but the author subsequently discovered that SMP91 has a known error in its loads calculation algorithms. As a result, regular wave load predictions were not available from SMP. However, the 1995 version of SMP, which was used for irregular seas tests, correctly calculates loads.

For calculation of the SPI, the maximum VLCC speed is assumed to be 25 knots. However, regular and irregular wave responses were extracted for only one speed, 15.5 knots (service speed) in head seas.

LAMP

LAMP-1/2 was set up in the following manner for the VLCC tests. LAMP Version 2.8.5 was used for all runs.

Initially, LAMP was run using the transient Green function formulation for calculation of the flow potential field. However, the stern shape of the VLCC resulted in numerical instability with this method. LAMP was then switched to the MSF which successfully handled the ship geometry. Like the mathematical hulls, the matching surface extended 450 m ($= 1.43L$), 100 m ($= 1.72B$), and 70 m ($= 3.6T$) in the longitudinal, transverse, and vertical directions, respectively, around the hull. The number of panels on the matching surface was 21, 6, and 11 panels in the longitudinal, transverse, and vertical directions respectively. Again, SAIC provided significant help in ensuring the mixed-source formulation was properly set up for all LAMP runs. An example of the mixed-source formulation LAMP panelization is included as Figure 3-8 on the facing page. The view shows the panelization for both the free surface and
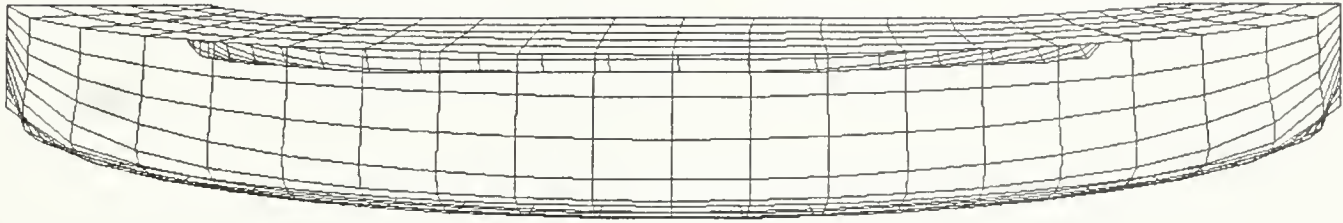
Figure 3-8: VLCC LAMP Mixed Source Panelization from 90° azimuth and 10° up elevation

the matching surface around the hull panelization.

For all cases, the ship was fixed in surge, sway, roll, and yaw, and free in heave and pitch. A time step of 0.227 seconds (0.04 nondimensional) was used. 1000 time steps were selected for all regular seas runs, resulting in 227 seconds of data for each test - in all cases sufficient for initial transients to become negligibly small. For irregular seas runs, 4000 time steps were calculated, resulting in 15.1 minutes of real time data per run.

Both regular and irregular wave tests were conducted at 15.5 knots only (ship service speed), in head seas using LAMP-1 and 2. LAMP-4 was used for several regular waves tests, which are discussed in Section 6.3. Additionally LAMP-1 and 2 were used to test the ship at steady speed with no waves to calculate the mean responses at 15.5 knots in calm water.

Chapter 4

Parametric and Frequency Domain Methods

The first steps in the proposed seakeeping design method are basically equivalent to the early design procedures currently in use for both naval and commercial vessels. The differences are in the way the methods are used to cue the next level of testing – in this case LAMP-1. The objective is to demonstrate both of the methods for incorporating time domain predictions in design, discussed in Section 2.3. First the parametric McCreight method is applied to the mathematical hulls only, since this index is limited to destroyer-type forms. Then, SMP is used for frequency domain testing of both the mathematical hulls and the VLCC. Finally, the application of the results of the tests for time domain cuing are discussed.

4.1   Parametric Evaluation of Mathematical Hulls

The McCreight method, which calculates a comparative index based on several parameters describing the underwater geometry (see page 33), is applied to the mathematical BL, Variant 1 (V1), Variant 2 (V2), and Variant 3 (V3). Variants 4 (V4) and 5 (V5) receive the same ranks as the BL, since all three ships have the same underwater hull form. The calculated McCreight ranks are shown in Table 4.1 on the next page, along with additional reference scores. These reference ships include the U.S. Navy's

71

Hull	Score
BL	10.524
V1 (Flare+)	10.524
V2 (Entrance+)	13.674
V3 (Flare & Entrance+)	13.674
V4 (AW Flare+)	10.524
V5 (AW Tumblehome)	10.524
Additional Ships (for Reference)	
FFG-7 (USN Frigate)	5.955
DDG-51 (USN Destroyer)	14.327
McCreight Hulls 29/22 (4300MT)	19.154/-1.847
McCreight Hulls 29/22 (5800MT)	26.023/1.993
McCreight Hulls 29/22 (7300MT)	32.343/5.473
McCreight Hulls 29/22 (8800MT)	38.261/8.703
Notes: 1. FFG-7 – L 124.4m, B 13.8m, T 4.8m, Δ 4031MT	
2. DDG-51 – L 142.0m, B 17.9m, T 6.2m, Δ 8430MT	
3. McCreight Hull 29 is top performer – Base L 138.6m, B 17.3m, T 4.3m.	
4. McCreight Hull 22 is bottom performer – Base L 117.5m, B 14.2m, T 4.8m.	
5. McCreight Hulls responses are geometrically scaled for each Δ.	

Table 4.1: McCreight Ranks of Mathematical Hulls

Oliver Hazard Perry frigates (FFG-7 class) and *Arleigh Burke* destroyers (DDG-51 class). Also included are the best and worst performers of the ships in the McCreight database, with their results scaled (by McCreight) for several displacements.

The McCreight parametrics indicate a negligible difference in performance between the BL and V1, despite the addition of flare both above and below the waterline. Changes in waterplane area and inertia between the two hulls are insignificant, and all other McCreight geometrical parameters are unchanged. Both V2 and V3 should perform markedly better than the other variants in both linear and nonlinear tests. The increase of entrance angle is favorable for seakeeping. Waterplane area and inertia both increase. The vertical prismatic coefficient also increases, indicating that the new hull sections are more U, rather than V, shaped. The effect on resistance, however, should be unfavorable. No difference between the BL, V4, and V5 is predicted, since these hulls are identical below the mean waterline. However, their significant variations above the waterline should be a factor in LAMP-2 and 4 tests.

Regression Term	Tested Range	BL	V1	V2	V3
a_3: C_{VPA}	0.45657 to 0.69651	0.80860	0.80860	0.77843	0.77843
a_4: $C_I = \frac{BM_L \nabla}{BL^3}$	0.036905 to 0.052757	0.036151	0.036151	OK	OK
a_7: $A_{WA}/\nabla^{2/3}$	2.6691 to 4.6232	2.1210	2.1210	2.2032	2.2032
a_8: $(LCB - LCF)\nabla$	-9355.3 to -87181	0.0000	0.000	0.0000	0.0000

Table 4.2: Out-of-Range Geometry Factors for McCreight Index

As compared to the reference ships, the mathematical variants (L 150m, B 18.75m, T 6.25m, and Δ 10,099MT) are poor performers. The primary cause is the hull longitudinal symmetry, which results in a zero score for the index equation a_8 term ($a_8(LCB - LCF)\nabla$) and the a_9 term ($a_9(L/2 - LCB)/\nabla^{1/3}$). The a_8 term ($a_8 = 9.18775 \cdot 10^{-5}$) improves the ship score when LCB is aft of LCF. The a_9 term ($a_8 = -6.03225$) improves the score when LCB is aft of midships.[1] Despite this poor performance, the ships are suitable for comparative purposes, and the symmetry precludes stern shape as a additional influence in the study.

The parametric method is quite useful for its intended purpose - the selection of main hull dimensions and form coefficients. However, like any engineering method, it should not be used by designers unless familiar with the calculation procedure. Any hull deviations which are not included in the parametric regression, such as above water changes, will not result in a different ranking.

Hull parameters which are outside the index range require extrapolation, which is not recommended. The mathematical hulls included several terms which required extrapolation; these are noted in Table 4.2. All of these deviations can again be attributed to the fore and aft symmetry, which is unusual, particularly since most current destroyers have transom sterns. However, comparisons between these hulls are valid, and demonstrate the limits of parametric indices.

While the McCreight parametric method may be very useful for selection of hull dimensions, the examination of specific motion and loads responses requires an analyses with a physics-based model. Such analysis will typically begin with 2-D linear

---

[1] Again, see McCreight (1984) for further details on the regression equation, including geometry range, regression coefficients, and database scores [3].

frequency domain programs, such as SMP.

4.2   Frequency Domain Results

SMP was used to test the mathematical hulls (BL, V1, V2, and V3) and the VLCC in sea states 4, 5, 6, 7, and 8. For the mathematical hulls, the entire range of speeds and headings are discussed, before the head seas case is specifically analyzed. For the VLCC, only head seas results are discussed.

4.2.1   Mathematical Hulls

The results of the SMP irregular seas tests are shown in Figure 4-1 on the next page for the BL/V4/V5 hulls. These polar plots indicate the SOE[2] for the naval transit mission, according to the limit criteria defined in Table 2.1 on page 25. The shaded areas indicate where one or more motion limits are exceeded. The contour boundaries are labeled by the limit value of the exceeded response.

The mathematical hulls perform quite poorly in roll (limit 8°), with the OI already reduced to 63.9% in SS4. Roll is the only limiter however, until SS6. The SS6 envelope is limited by roll, lateral and vertical accelerations, and pitch. Excluding following seas, seakeeping is unsatisfactory except for a small area straight into the waves at speeds less than 8 knots. Roll continues to dominate, indicating that the Wigley type hulls, even at moderate L/B ratios, are not suitable for oblique seas tests. In SS7, the OI degrades further, and both slamming and deck wetness occur in head seas. Transit is now not possible in head seas without exceeding motion limits. In SS8, with particularly severe wave conditions, the OI is 0.00%. Although not shown, the V2 and V3 hulls perform better, but are also poor in high sea states.

The analysis of the SMP results for all speeds and headings in the polar plot format is quite practical, and very useful in the design process. However, the SPI defined

---

[2]which equals the OI in this case, since all speed-heading combinations are weighted equally.

74
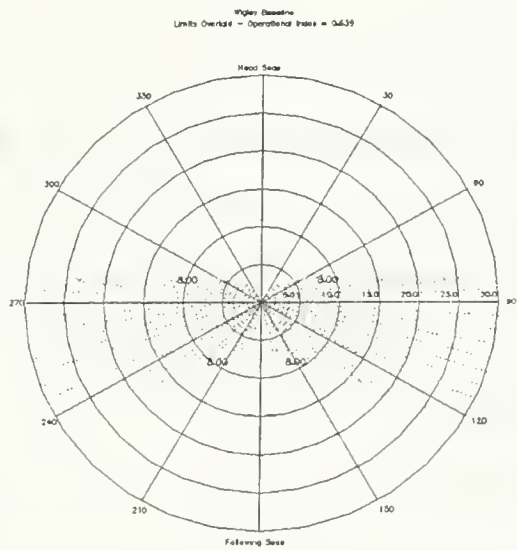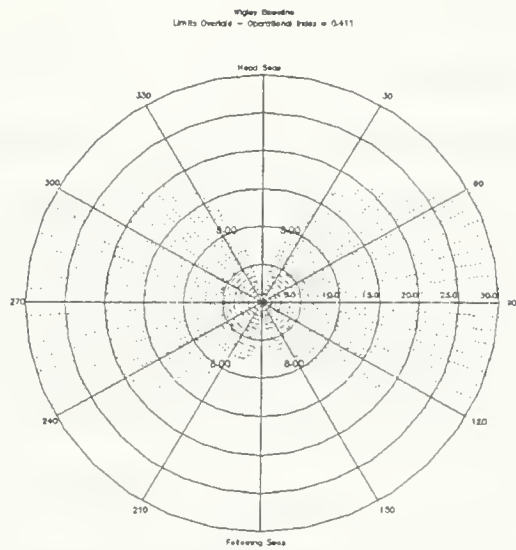
a. Sea State 4

b. Sea State 5
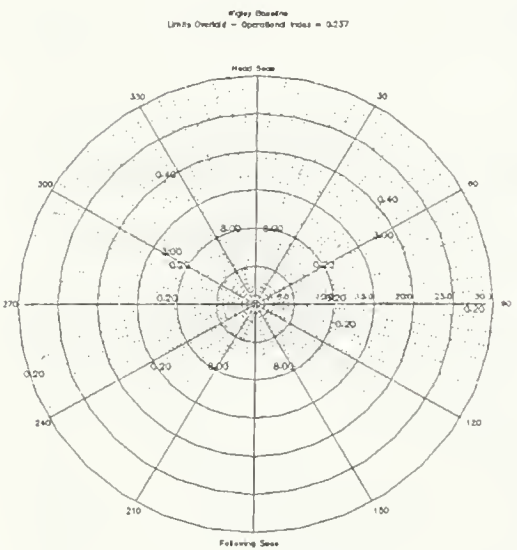
c. Sea State 6
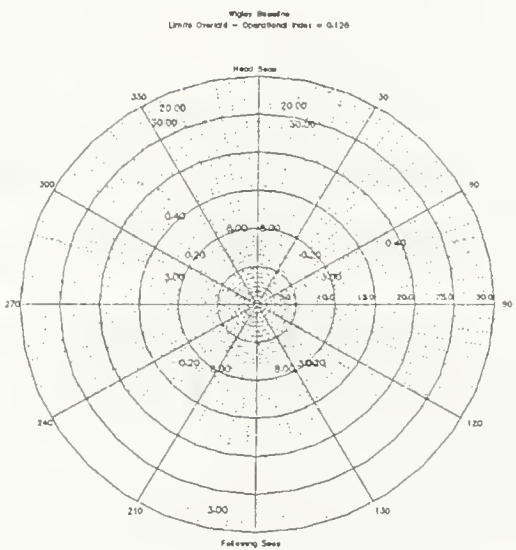
d. Sea State 7
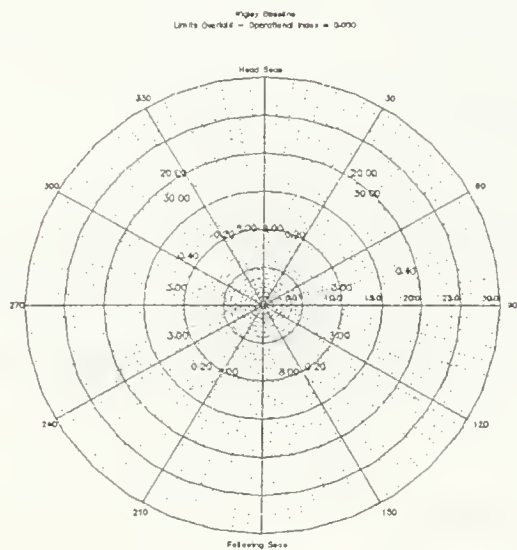
e. Sea State 8

Figure 4-1: Transit Seakeeping Operating Envelopes – Hulls BL/V4/V5 (SMP)

for this study is limited to vertical motions and loads in head seas only. Responses for the mathematical hulls were extracted for head seas to determine the head seas transit speed, which is the motion measure of effectiveness discussed in Section 2.1.4. These maximum transit speeds are included for each limit criteria, at each sea state, in Table 4.3 on the next page. The most limiting criteria for each sea state are shown in Table 4.4 on page 78.

Conclusions from the SPI calculations include:

- Pitch is the limiting factor for all hulls in all sea states. Assuming that the pitch limit is disregarded, all hulls could transit at 11.8 to 13.1 knots even in SS8. Note that performance in roll and lateral accelerations do not affect the head seas results.

- The increase of flare alone in V1 does not have a significant effect on the SPI, although pitch is slightly worse and all other criteria slightly better.

- As with the parametric predictions, SMP clearly indicates that V2 and V3 are the best performers. Combining a flare increase with entrance angle increase (V3) improves performance most. However, at the highest sea states, pitch dominates, so that the total SPI change between hulls is quite small.

- In moderate sea states (SS4 and SS5), all of the hulls can achieve maximum speed in head seas. North Atlantic seas should be no worse than SS5 about 73.2% of the time (see Table 2.2 on page 27).

The small change in SPI between the worst performer (V1, SPI=0.7793) and the best performer (V3, SPI=0.7962), because of the dominance of the pitch limit, suggests one of the dangers with simplifying seakeeping performance measurement to a single indicator. V2 and V3 perform measurably better than BL and V1 in all criteria except pitch, even in severe seas. In particular, V2 and V3 do not surpass the slamming limit until SS8, and can travel about four knots faster than the BL in SS7 before deck wetness exceeds the limit. Unlike pitch and vertical acceleration (which primarily degrade mission performance), slamming can endanger the hull with

76

Criteria	Sea State				
	4	5	6	7	8
Pitch ≤3.0°	30.0	30.0	8.2	0.0	0.0
Vert. Acc STA3 ≤0.4g	30.0	30.0	19.2	14.4	11.8
Slams per hour ≤20	30.0	30.0	30.0	23.4	18.0
Deck Wetness per hour ≤30	30.0	30.0	30.0	20.7	14.2

a. Hulls BL/V4/V5

Criteria	Sea State				
	4	5	6	7	8
Pitch ≤3.0°	30.0	30.0	8.1	0.0	0.0
Vert. Acc STA3 ≤0.4g	30.0	30.0	19.8	14.6	11.9
Slams per hour ≤20	30.0	30.0	30.0	23.9	18.3
Deck Wetness per hour ≤30	30.0	30.0	30.0	21.0	14.2

b. Hull V1

Criteria	Sea State				
	4	5	6	7	8
Pitch ≤3.0°	30.0	30.0	10.5	0.0	0.0
Vert. Acc STA3 ≤0.4g	30.0	30.0	21.1	15.6	12.8
Slams per hour ≤20	30.0	30.0	30.0	30.0	20.0
Deck Wetness per hour ≤30	30.0	30.0	30.0	24.1	15.8

c. Hull V2

Criteria	Sea State				
	4	5	6	7	8
Pitch ≤3.0°	30.0	30.0	11.0	0.0	0.0
Vert. Acc STA3 ≤0.4g	30.0	30.0	22.2	16.1	13.1
Slams per hour ≤20	30.0	30.0	30.0	30.0	20.8
Deck Wetness per hour ≤30	30.0	30.0	30.0	25.0	16.2

d. Hull V3

Table 4.3: Mathematical Hull Naval Criteria Limiting Speeds (SMP)

Hull	Method	Sea State					SPI
		4	5	6	7	8	
BL	SMP	30.0	30.0	8.2	0.0	0.0	23.40
		—	—	P	P	P	(0.7798)
V1 (Flare +)	SMP	30.0	30.0	8.1	0.0	0.0	23.38
		—	—	P	P	P	(0.7793)
V2 (Ent +)	SMP	30.0	30.0	10.5	0.0	0.0	23.80
		—	—	—	P	P	(0.7933)
V3 (Flare & Ent +)	SMP	30.0	30.0	11.0	0.0	0.0	23.89
		—	—	P	P	P	(0.7962)
V4 (AW Flare +)	SMP	30.0	30.0	8.2	0.0	0.0	23.40
		—	—	P	P	P	(0.7798)
V5 (AW Tumblehome)	SMP	30.0	30.0	8.2	0.0	0.0	23.40
		—	—	P	P	P	(0.7798)
Criteria: VA3 – Vert. Acceleration STA3 (0.4g); S – Slamming (20 ph)							
DW – Deck Wetness (30 ph); P – Pitch (3.0°)							

Table 4.4: SPI (Naval Criteria) of Mathematical Hulls

severe whipping loads. Wetness can be a severe hazard both to topside equipment and personnel. Improvements in these responses are important, especially in naval ships, where performance of a mission, even in a degraded capacity, may be expected in higher sea states. Beyond mission effectiveness, ship and crew survivability is the ultimate goal in severe seas.

Further analysis of the SMP predictions (beyond the SPI measure) is best performed with graphical plots. The SMP predictions for the responses listed in Table 2.4 on page 44 are plotted for all speeds in head seas in Chapter 5, on Figures 5-1 through 5-16, beginning on page 98, with the LAMP predictions.

In particular, loads, which were not explicitly included in the transit limits, are plotted in Figures 5-3 on page 104 through 5-5 on page 110. The horizontal dashed lines indicate the designated limits, based on the USN static wave balance criteria, and summarized in Table 3.2 on page 61. SMP predicts that the vertical shear force at Station5 (VSF5) is not surpassed until approximately 23 knots at SS7, and 18 knots at SS8. Vertical Bending Moment (VBM10) limits are not reached until about 26 knots in SS7, and 19 knots in SS8. The VSF15 limits should never be exceeded.

These load threshold speeds are the determining factors in several LAMP runs (see Section 4.2.3).

4.2.2 VLCC 26

SMP was also used to predict motions and loads at all headings in speeds up to 25 knots. The 15.5 knot service speed was specifically examined. Although polar plots were not generated, the SPI (maximum transit speed in head seas), was calculated, based on the motion commercial criteria in Table 2.1 on page 25. The VLCC performed extremely well in all speeds, because of its large displacement. SMP predicts that the ship is able to achieve 25 knots in all sea states up to SS7. At SS7 and 8, the deck wetness criteria is exceeded at zero speed, resulting in a 0.0 overall SPI for those conditions. However, no other motion criteria are ever exceeded. While excellent for the operators of the VLCC, the SPI verification method for the commercial limits using time domain codes would be rather boring, with test cases only at SS7 and 8, 0 knots. Accordingly, time domain methods for the VLCC are used only in the experimental simulation mode, for both regular and irregular waves.

The VLCC irregular wave predictions are plotted in Section 5, Figures 5-17 through 5-32, beginning on page 126. Load predictions are shown for VSF4 in Figure 5-19 on page 132, VBM10 in Figure 5-20 on page 135, and VSF15 in Figure 5-21 on page 138. SMP load predictions are not available in SS7 and 8, since the resulting values exceeded the code's output format specifications. The limit lines are those calculated with the ABS criteria, and summarized in Table 3.4 on page 66. In no case do the loads even approach the ABS criteria, again making for a relatively uninteresting problem.

Although the VLCC tests do not pose an interesting problem for time domain testing, this confirms an obvious, yet important, conclusion. Displacement is the ultimate seakeeping enhancer, and very large ships with conventional hull forms may not warrant time domain or experimental research. However, this may be a premature conclusion until the VLCC time domain results are presented.

79

4.2.3 Transition to the Time Domain

The power of 2-D codes like SMP is in their computing speed. Regular waves responses for each hull, at all speeds and headings, were generated in just a few minutes on a typical PC. Applying the regular wave results to irregular sea conditions requires even less time. The rapid generation of results makes SMP a very powerful early design tool. However, the use of 2-D linear theory does have disadvantages. The SMP predictions for the mathematical BL, V4, and V5 are identical since the underwater hull geometry is not varied. Differences in actual performance should occur for these ships, particularly in large amplitude motions cases.

However, while comparing the performance of the variants is interesting, the primary goal is to use the SMP predictions to narrow the scope of any computational time domain tests or model experiments. As discussed in Section 2.3, two such methods are proposed. The first uses SMP-determined measures of effectiveness to cue LAMP runs. These runs can be used to verify the SMP limiting speeds. The second method uses SMP to identify sea states (irregular waves), individual wave frequencies (regular waves), speeds, and headings for time domain analyses. The more advanced (and expensive) time domain tests may then be limited to only those cases where the assumptions of 2-D linear theory are violated.

Section 5 summarizes the tests completed to demonstrate both of these methods for the mathematical hulls. Based on the SMP results, the LAMP testing for the SPI verification method includes:

- Confirmation of Limiting Speeds in Sea States 5, 6, and 7:

    - Sea State 5 at 30 knots, to confirm all motions are within limits.

    - Sea State 6 at pitch limiting speeds for each hull.

    - Sea State 7 at 0 knots, to confirm pitch limit is surpassed even at zero speed.

- Given that pitch limits are exceeded, examination of other motions and loads are included:

- Sea State 7 at 14.5 knots, for all hulls. This is approximately the point where the hulls first begin to exceed the Vertical Acceleration at Station 3 limit.

- Sea State 7 at 23 knots, for all hulls. This is the speed where VSF5 begins to exceed the design limit calculated from the USN wave balance criteria. VBM10 begins to exceed the criteria at slightly higher speeds.

- Sea State 8 at 18 knots, approximately where all ships begin to exceed the VSF5 limit and nearly exceed the VBM10 limit.

The SS7 23 knot and SS8 18 knot runs, although realistically unlikely since the pitch and acceleration limits are well exceeded, do occur before the slamming limit is passed. From the author's experience as a deck officer on a U.S. Navy cruiser, pitch, acceleration, and wetness limits are often exceeded in rough weather. However, when the ship begins to slam, speed is almost always reduced, except when transit time is mission critical.

Incorporation of SPI verification in an actual design procedure would probably require many additional test runs to determine the actual transit speeds, using all versions of LAMP, and possibly model tests. While useful for design, completing this sequence would likely not prove very interesting from a scientific aspect. Therefore, these runs are completed (in some cases, attempted) in LAMP-1 only, and no iteration is conducted. Additional runs in other sea states and speeds are completed with LAMP-1, 2, and 4. The testing procedure is discussed in Section 5.1.3.

For the VLCC, discussed above, the irregular waves testing will include only the service speed, 15.5 knots, in head seas, at sea states 4 through 8. For both the mathematical hulls and the VLCC, a regular wave testing method is also demonstrated. This method is further discussed in Chapter 6.

Chapter 5

Time Domain Methods: Irregular Waves

Two methods are proposed for obtaining response predictions in sea states using the time domain. Both methods are similar to commonly used techniques in experimental seakeeping tests. First, the hulls are run through irregular wave systems at each desired speed and sea state, and the responses directly measured. This method is discussed in this chapter. In the second method, regular wave tests are used to define the ship response (amplitudes and phases) for a given speed. These predictions are then converted to the frequency domain to calculate responses in specific sea conditions. This method is presented in the next chapter.

The primary goal of this analysis is to examine the differences between the 2-D frequency domain predictions and the 3-D time domain predictions. In particular, the design utility of each of these methods is assessed for the various hulls, in a wide range of sea conditions and speeds. The question of which method matches physical reality is an issue which can not be fully assessed, since neither experimental nor full scale data are available for the mathematical hulls or the VLCC. However, hypotheses are presented which discuss the question of physical accuracy.

5.1 Irregular Waves Methods in Design

5.1.1 Introduction

With linear frequency domain methods, response predictions in irregular seas are possible only after response amplitude operators (RAO's) have been calculated in regular waves. RAO's must be calculated separately for each speed and heading with respect to the waves (wave encounter conditions). For vertical motions and loads, these RAO's are typically assumed to vary linearly with wave height. To calculate responses in irregular seas, the principle of linear superposition is used, and the ship responses to each wave in the spectrum are simply summed to yield the total response. In design, this is typically accomplished through the use of wave and response spectra. Any expected sea condition may be defined by an appropriate wave energy spectrum, $S_\zeta(\omega)$. For these tests, the Bretschneider spectrum is used, as discussed in Section 2.1.3. The energy spectrum is then converted to a function of ship-to-wave encountered frequency, rather than absolute frequency $(S_\zeta(\omega) \to S_\zeta(\omega_e))$. The wave encounter spectrum, which is directly proportional to the squares of the component wave amplitudes at each frequency, is then multiplied by the square of the RAO function (in units of response amplitude per unit wave amplitude). The result is the response energy spectrum, $S_z(\omega_e)$:

$$S_\zeta(\omega_e) \cdot |RAO(\omega_e)|^2 = S_z(\omega_e)$$

The properties of the response spectrum, including area (the variance of the response), and spectral moments, are then used to statistically calculate appropriate measures of response amplitude. Such measures include the RMS value (used for VLCC analysis) and the average of the one-third highest responses, or Significant amplitude (used for mathematical hull analysis). For extreme responses, the Significant 1/10th, 1/100th, or higher amplitudes may be calculated. An important limit to the current application of such statistical methods to response spectra is the assumption that the instantaneous response values follow a Gaussian, or normal, probability

density function. Likewise, the peak amplitudes are assumed to be satisfactorily described by a Rayleigh probability distribution. If these assumptions do not apply, valid conclusions may still be drawn by comparing response spectral areas and moments, but the calculation of statistical response predictions is more difficult. This problem is further discussed below.

5.1.2   Options for Time Domain Analysis

Time domain methods offer the capability to directly simulate actual ship responses, without the limitations of tow tank length, where numerous runs are required to obtain the same quantity of data. However, simply simulating ship responses, while scientifically interesting, is not as valuable for the engineering design process. A goal of time domain simulation should be the generation of the same seakeeping measures of performance that are calculated with current frequency domain methods. Such results enhance the utility of time domain codes in the earlier stages of design.

Once a time domain run in irregular waves is complete, two options for post-processing the data are possible. In the first method, the entire data run (or a suitably chosen window) is converted to the frequency domain with the use of Fourier Transform techniques, such as the Fast Fourier Transform (FFT). The same statistical methods used in frequency domain codes predictions may then be employed. Response spectral moments and areas may be calculated for comparison. For design purposes, RMS or Significant response amplitudes may also be determined. However, unless a suitable probability density function is known, statistical methods may be suspect. The assumption of a Gaussian distribution for ship responses is examined again in Section 6.4.1 on page 201 for the mathematical hulls.

The other method for processing is straight forward cataloging of each peak[1] in the time domain data. The RMS or Significant response amplitudes may then be directly calculated as per their definitions. For example, the response peaks are recorded and sorted by absolute (maxima and minima) magnitude, the highest one-third peaks

---

[1]A *peak* is defined as a maximum response value between an upcrossing and a downcrossing of the mean response, or, likewise, a minimum between a downcrossing and upcrossing.

separated, and then simply averaged to produce the Significant amplitude. Whether or not responses calculated in this manner may be assumed statistically valid for the actual ship response in the given sea state is dependent on sample size. "What is a large enough sample size?" is a difficult question, and is a function of ship geometry, sea conditions, speed and heading, and even the desired response. Extensive tests using varied sample sizes would be necessary to answer the question, and are not within the scope of this study.

The "cataloging peaks" method is used for all irregular seas LAMP runs. Concerns about assuming a Gaussian distribution for response values to determine Significant amplitudes precluded application of the FFT method. The Gaussian assumption would most likely be invalid in the same conditions where the use of the LAMP code is critical. A thorough comparison of the results from both methods would be useful, but is a future goal.

5.1.3   LAMP Test Plan

Initial LAMP runs were chosen to demonstrate both the SPI verification and experimental simulation methods. The first choices for SPI verification are discussed in Section 4.2.3. A complete summary of attempted or completed LAMP runs is shown for the mathematical hulls in Table 5.1 on the next page, and for the VLCC in Table 5.2.

In addition to the mathematical hull runs for SPI verification, additional runs were desired in each sea state at a low and high speed. These runs are necessary to assess the impact of hull form, speed, and sea state on predicted responses. Chronologically, all SPI verification runs were performed before the additional runs, so that the conclusions from the former could be used to narrow the scope of the latter. Although the run results are more fully described in Section 5.2, a summary of the decisions for the scope of LAMP testing is included here:

- The LAMP-1 SPI results sufficed to demonstrate the SPI verification method; all LAMP-2 runs were designed for comparative analysis.

Conditions	BL	V1	V2	V3	V4	V5
SS4, 10 kts (Fr 0.134) [†]	1,2	1,2	1,2	1,2	2	2
SS4, 20 kts (Fr 0.268) [†]	1,2	1,2	1,2	1,2	2	2
SS5, 10 kts [†]	1,2	1,2	1,2	1,2	2	2
SS5, 20 kts [†]	1,2	1,2	1,2	1,2	2	2
SS5, 30 kts (Fr 0.402) [‡]	1	1	1	1		
SS6, 8.1 kts (Fr 0.109)		1				
SS6, 8.2 kts (Fr 0.110)	1					
SS6, 10 kts [†]	1,2	1,2			2,4	2
SS6, 10.5 kts (Fr 0.141) [†]			1			
SS6, 11 kts (Fr 0.148)[†]				1		
SS6, 20 kts [†]	1,2	1,2	1,2	1,2	2,4[‡]	2
SS7, 0 kts (Fr 0.000)	1	1	1	1		
SS7, 14.5 kts (Fr 0.194)	1,2	1,2			2	2
SS7, 20 kts	1,2	1,2			2,4[‡]	2
SS7, 23 kts (Fr 0.308) [‡]	1	1				
SS8, 18 kts (Fr 0.241)	1,2,4[‡]	1,2,4[‡]			2,4[‡]	2,4[‡]
Notes: "1","2", and "4" refer to LAMP run type.						
All runs in head seas.						
†: Run(s) unstable late; majority of data usable.						
‡: Run(s) failed; no data used.						

Table 5.1: Mathematical Hulls LAMP Irregular Seas Run Summary

Conditions	VLCC Runs
SS4, 15.5 kts (Fr 0.143) [‡]	1,2
SS5, 15.5 kts [†]	1,2
SS6, 15.5 kts	1,2
SS7, 15.5 kts	1,2
SS8, 15.5 kts	1,2
Notes: "1" and "2" refer to LAMP run type.	
All runs in head seas.	
†: Run(s) unstable late; majority of data usable.	
‡: Run(s) failed; no data used.	

Table 5.2: VLCC LAMP Irregular Seas Run Summary

- Low speed runs (10 knots) and high speed runs (20 knots) were used in sea states 4, 5, and 6. In SS6, the SPI pitch limit verification runs doubled as the LAMP-1 low speed runs. The 14.5 knot runs in SS7 doubled as low speed runs.

- Difficulty in running LAMP at high speeds required cancellation of the 30 knot runs in SS5 and the 23 knot runs in SS7, both intended for SPI verification. 20 knot runs in SS7 were successful.

- Results at SS 4-7 were sufficient to draw conclusions about the effect of speed on the differences between LAMP and SMP. The 18 knot run in SS8, chosen to examine the VSF5 and VBM10 threshold speeds, was the only run in this sea state.

- LAMP-1 and 2 runs in moderate sea states (4, 5, and 6) clearly indicated that V2 and V3 are superior in seakeeping performance, as predicted by both the McCreight and SMP methods. Runs in severe seas concentrated on the BL, V1, V4, and V5.

- LAMP-4 runs, which require significantly more computational time than LAMP-1 or 2, were first attempted in the most severe condition (SS8 at 18 knots), but were not successful. Additional runs in SS7 and SS6 at 20 knots also failed. The only successful LAMP-4 irregular seas run was for V4 in SS6 at low speed. V4 was selected for special analysis because LAMP-2 predicted a noticeable change in performance from the BL, which the linear methods (SMP and LAMP-1) could not predict.

No SPI verification runs were conducted for the VLCC. The response at service speed only (15.5 knots) was examined with LAMP-1 and 2 in sea states 4-8, although the SS4 run was not successful. Because the VLCC responses, discussed fully in Section 5.3, did not significantly change in LAMP-2 from the LAMP-1 values, no LAMP-4 runs were warranted. Several regular waves runs were completed with LAMP-4, however.

The LAMP setup has been thoroughly discussed in Sections 2.2.3, 3.1.5, and 3.2.2.

5.2   Mathematical Hull Predictions

All LAMP runs which were successfully completed[2] were post-processed to calculate
the Significant responses by cataloging all peaks. The results for all SMP and LAMP-
1/2 tests are presented in Figures 5-1 through 5-16, beginning on page 98. The
primary motions (heave and pitch) and vertical loads are plotted in a larger scale; all
secondary motions are more compactly presented.

5.2.1   SMP Results and SPI Verification Tests

The SMP tests have also been discussed in Section 4.2.1. In addition to those com-
ments on SPI verification, the following conclusions are evident from the SMP irreg-
ular seas predictions:

- Vertical Motions: The BL is worst performer. V1 is slightly better at higher
  speeds. V2 and V3 are noticeably improved, with V3 the best performer, espe-
  cially at higher speeds. Added flare seems to improve heave response as speed
  increases.

- Vertical Loads: The BL is the best performer, except for VSF15 in low to
  moderate speeds at high sea states. V1 performs worse in all conditions, except
  in VSF15. Entrance angle increase, in V2 and V3, markedly increases loads,
  with the effect increasing with speed and sea state. Again the only exception is
  VSF15 at high speeds, where V3 performs best.

Following the SMP irregular seas tests, LAMP-1 runs were conducted to demon-
strate the SPI verification method, based on the discussion in Section 4.2.3. These
tests indicate the following:

- For pitch at SS6 from 8 to 11 knots, all hulls exceed the motion limit (3°),
  whereas SMP predicts the threshold is just crossed. Additional LAMP-1 runs

---

[2]As indicated in Table 5.1 on page 87, several cases slowly developed numerical instabilities late
into the runs. In all such cases, the data were conservatively truncated, resulting in 10 vice 15
minutes of real time data. LAMP recommendations for truncating data at the beginning of the run
(typically less than 130 time steps in the conditions tested) were applied.

would be required to confirm the actual threshold speed. Another alternative is to use the SS6 high speed run, and estimate threshold speed assuming a similar trend with increasing speed as predicted by SMP. Note that at SS6 (10kt), the differences between LAMP-1 and 2 runs are negligible.

- Trends in SS7 and SS8 for both VSF5 and VBM10 indicate that the threshold speeds predicted by SMP are conservative. Both LAMP-1 and 2 indicate the limits will not be surpassed until above 20 knots in SS8. Actual transit at that speed would be extremely unlikely.

- Both LAMP-1 and LAMP-2 predict that the Vertical Acceleration at Station 3 limit will be surpassed in SS7 before the SMP predicted speed.

- For the discrete event criteria (wetness and slamming), valid conclusions are not possible. This problem seriously hinders SPI verification with time domain codes, and is discussed both below and in Section 5.4.

These results are sufficient to demonstrate that SPI verification using time domain methods is a viable procedure for incorporating them into design. Using SMP to reduce the required LAMP runs works very well. The biggest difficulty is the ineffective use of time domain codes to predict the probabilities of discrete events, especially since such responses are common in both naval and commercial seakeeping criteria.

The remainder of the LAMP irregular seas analysis is devoted to examination of the effects of hull form, speed, and sea conditions on predictions.

5.2.2 Trends in Irregular Waves Predictions

A detailed list of conclusions from the mathematical hull irregular seas predictions follows. A summary of the most important conclusions is included in Section 5.4.

- For heave and associated derived motions, including heave acceleration. (charts begin p. 98):

– Time domain responses are higher than SMP predictions in all sea states. The differences increase as both speed and sea state increase. In the SS7 0kt case, heave matches SMP predictions.

– Differences between LAMP-1 and 2 are small until SS6 20kt. At this speed, and all SS7 and 8 runs, LAMP-2 predicts higher responses.

– LAMP-1 and 2 both predict superior performance of V2 and V3. Differences are small in SS4 and 5. In SS6 high speed run, LAMP-2 begins to predict increased heave over LAMP-1.

– LAMP-1 predicts negligible differences between BL and V1, as did SMP. In LAMP-2, the addition of flare, in both V1 and V4, improve performance over BL. Tumblehome, in V5, degrades heave slightly.

• For pitch and associated derived motions (p. 101):

– Time domain predictions are higher than SMP in all test conditions, although relative trends are similar. As with heave, the differences increase with speed and sea state, although not as markedly. SS7 0kt case matches SMP predictions.

– As with heave, differences between LAMP-1 and LAMP-2 are small until 20kt at SS6. Above this condition, LAMP-2 actually predicts lower pitch values.

– LAMP-1 and 2 both predict superior performance of V2 and V3. Again, differences between LAMP methods are generally minor.

– Flare slightly degrades performance of V1 and V4, as predicted by LAMP-2, particularly as speed increases. This result is contrary to both LAMP-1 and SMP, which predict better pitch with addition of flare. V5 has slightly lower pitch, at higher speeds and sea states, than BL.

– Overall, the differences in pitch seem less sensitive to hull variations and calculation method than heave.

- VSF5, VBM10, and VSF15 follow very similar trends, and are discussed simultaneously:

  - Both LAMP-1 and LAMP-2 underpredict SMP in all conditions for VSF5 and VBM10. The difference in minor in SS4, but increases with speed and sea state, dramatically for LAMP-2. Even in the SS7 0kt case, LAMP still underpredicts SMP. For VSF15, LAMP overpredicts SMP, but is otherwise very similar in behavior to VSF5 and VBM10.

  - Differences between LAMP methods are minor at SS4 and 5. Beginning with the low speed runs at SS6, LAMP-2 responses become significantly lower than LAMP-1 predictions, especially in high speed cases.

  - LAMP-1 predicts slightly worse responses for V2 and V3. The difference is more apparent in LAMP-2, but not as clear as predicted by SMP.

  - LAMP-2 predicts the best performance for V5, but only slightly better than BL. Flare sharply increases loads, particularly at higher speeds and sea states.

  - VSF15 predictions in LAMP are similar to VSF5 and VBM10 in the trends observed for individual hull performance. However, the results are less sensitive to speed and sea state, showing almost no major variation between LAMP-1 and 2 until the SS7 high speed runs.

- Additional comments for the other derived responses include:

  - Vertical Acceleration at the Bow (Stations 0 and 3): These responses follow the same trends as pitch, although they are also a function of heave. Unlike pitch, however, both LAMP-1 and 2 predict higher responses in all conditions. The difference between LAMP methods increases markedly, and at high speeds and sea states, LAMP-2 is actually close to SMP.

  - Relative Motions at the Bow (Stations 0 and 3): Differences between LAMP methods are quite small for all conditions at STA0. Similar trends are noted for STA3, although the SS8 test differences are larger. Relative

92

Velocity at STA3 is also similar. V2 and V3 are best performers, but only noticeably in high speed cases.

- Motions at the Stern (Station 20): Both vertical and relative displacement have similar trends, as expected. LAMP-2 begins to predict much lower responses than LAMP-1, most noticeably in the SS7 and 8 high speed runs. Hull variations are small, but tumblehome slightly improves performance, and flare is worse, as with pitch.

- Deck Wetness and Slamming: Drawing trends from the LAMP predictions for discrete events is quite difficult. Variations with hull form are not consistent, other than that LAMP-2 predicts different responses for the flared hulls. For these two criteria, LAMP generally follows the SMP predictions, however. The problem with discrete event predictions is discussed fully in Section 5.4.

- Propeller Emmersion: The LAMP predictions are so widely scattered that they are unusable. Part of the problem is due to the discrete event difficulty discussed above. However, since stern motions are fairly benign, these responses should at least follow reasonable trends.

Only one run was successfully completed in LAMP-4 (this problem is further discussed below) at 10 knots in SS6 for the V4 hull. Although the variations between LAMP-1 and 2 were typically not significant until the SS6 high speed run (20 knots), the data for the 10 knot run are displayed in Table 5.3 on the next page.

Drawing engineering conclusions from only one data run is unwise, but in this case, with minimal differences between LAMP-1 and 2, the 10 knot run is interesting. LAMP-4 predicts a drop of a few percent in heave, VSF5, and VBM10. Smaller response decreases are noted in pitch and VSF15. It is possible that the improvements in pitch and loads predicted by LAMP2 in this case are further validated by LAMP-4. At higher speeds and sea states, LAMP-2 predicted that flare degraded pitch and load response. Unfortunately, it was not possible to confirm this behavior with LAMP-4.

Method	Significant Single Amplitude Responses				
	Heave (m)	Pitch (°)	VSF5 (kN)	VBM10 (kN-m)	VSF15 (kN)
SMP	1.392	3.137	4626	187590	2232
LAMP-1	1.518 (9.1%)	3.367 (7.3%)	4003 (-13.5%)	167867 (-10.5%)	3122 (39.9%)
LAMP-2	1.523 (9.4%)	3.342 (6.5%)	4059 (-12.3%)	169187 (-9.8%)	3157 (41.4%)
LAMP-4	1.465 (5.2%)	3.301 (5.2%)	4287 (-7.3%)	176359 (-6.0%)	3113 (39.5%)
Note: Percent differences are with respect to SMP predictions.					

Table 5.3: V4 Prediction Comparison, Irregular Seas (SS6, 10 kts)

5.2.3 Difficulties with LAMP Irregular Seas Tests

LAMP Setup and Numerical Instability

As noted in Table 5.1 on page 87, several of the irregular seas cases developed numerical instabilities late in the runs, requiring approximately five minutes of real time data to be discarded (a conservative amount). These cases included all runs in sea states 4 and 5, and runs at 10 knots or above in sea state 6. In each case, the numerical instabilities caused gradual increases in responses, which were not severe enough to fail the run, but were quite noticeable. The instabilities were first prominent in the VSF5 and VBM10 loads and pitch motions. Eventually, heave motions also went unstable.

While the time scope of the research did not allow detailed investigation of the reason for the instabilities, the author suspects that reducing the time step might solve the problems. The time step for all runs was purposefully set to the default recommended by the LAMP manual, which is nondimensionalized by $\sqrt{L/g}$. As with all LAMP parameters, the default or recommended values were used where possible, since the assessment of design utility must not only consider the quality of the results, but also the ease of program use. The unstable runs occurred in the lower sea states, which have the lowest modal periods, and hence the highest wave frequencies. In SS6, the 8.1 and 8.2 knot runs were fully stable, but instabilities developed as low as 10

knots. There seems to be a correlation with increasing wave encounter frequencies. The failed high speed runs at 30 knots in SS5 and 23 knots in SS7 also follow this trend. As encounter frequency increases for a given hull form, the minimum time step to prevent instability should probably decrease. A worthwhile improvement to the time domain codes would be recommendations of time step based on formulation method, ship geometry, speed, and wave conditions.

In addition to the LAMP-1 and 2 instabilities, significant problems with LAMP-4 runs were experienced. The first LAMP-4 runs were attempted in SS8 at 18 knots, the most severe condition tested, on the assumption that this case would be the most useful for a fully nonlinear prediction. The runs initially employed component cutting of panels (LAMP parameter ICUTWL=0), in which each station is resplined with the same number of points below the instantaneous free surface at each time step. These runs failed quickly in the severe SS8 motions, due to numerical instabilities resulting from the repanelized geometry.

The next attempts employed master geometry cutting, where the panelization is carefully trimmed at each station below the free surface (ICUTWL=1). While lasting longer than the component cutting method, LAMP-4 still failed, due to an error in waterline generation. At each time step in LAMP-4, a single, closed-loop waterline is generated for the rotated and translated ship hull, which has been repanelized under the instantaneous free surface. This waterline is used in creation of the free and matching surfaces in the mixed source formulation. In cases of severe motions and/or poor hull panelization, the body waterline may be very difficult to determine. LAMP-4 runs were attempted using both the body-fitted and gapped free surface grid generation methods (LAMP IFSMIX parameter, see Section 2.2.3). However, the severe SS8 runs failed, even with the gapped free surface option. LAMP-4 runs using master geometry cutting and gapped free surfaces were also attempted at 20 knots in sea states 6 and 7, but failed. SAIC examined the test data, and determined that problems with the free surface calculations also caused those runs to fail.

The problems with these runs in no way suggest a problem with the calculation formulation used in the LAMP code. All of the failed runs could likely be solved

with appropriate changes to hull and matching surface panelization, time step size, and other LAMP parameters. Time limitations simply did not allow such a detailed study, and the runs which failed to provide any data were not critical to the report conclusions. In short, the problem is the author's. However, the problems experienced provide another valid conclusion. Computational fluid dynamics codes are typically difficult to implement, unless the user is very experienced with the formulations involved and the intricacies of hull and free surface panelization. The implications to their utility in the design process are discussed again in Chapter 7.

Weight Distribution

The definition of the weight distribution in the LAMP and SMP cases also caused some difficulties. The initial concern resulted from analyses of the SPI verification runs at sea states 6, 7, and 8. (Load plots for the mathematical hulls begin with VSF5, in Figure 5-3 on page 104, VBM10 in Figure 5-4 on page 107, and VSF15 in Figure 5-5 on page 110.) For both VSF5 and VBM10, the time domain predictions are well below the SMP responses. In VSF15, the opposite is true. The differences are considerable compared to motions. The load calculations and weight distributions in LAMP were rechecked in detail, and no discrepancies found.

In current versions of SMP, the ship's weight distribution must be entered as point masses at exactly the same stations where hull geometry is defined. Although this is a significant (and unnecessary) limitation, the weight curve developed for the mathematical hulls was minimally adjusted to meet the restriction (see page 3.1.4 for weight curve discussion). These changes did result in a minor imbalance between weight and volume, and LCG and LCB. LAMP allows entry of ship's weights as distributed loads centered at a point, however, for consistency with SMP, the weights were also entered as point masses. Maintaining consistency between the two methods is more important in this study than matching the generated weight distribution.

After the SPI verification tests, the LAMP still water loads were found to vary significantly from those calculated by the Ship Hull Characteristics Program (SHCP), where the weight distribution is defined as distributed masses along the ship length.

Specifically, SHCP predicted the calm water means for VSF5, VBM10, and VSF15 as 1470 kN, 1459384 kN-m, and -3197 kN, respectively, representing a hogging condition. LAMP, with the weight defined in point masses matching SMP, predicted -969 kN, 69490 kN-m, and -6879 kN – a significant difference. Investigation showed that the discrepancy was caused by the weight-buoyancy imbalance[3] resulting from point-mass definition. To test this theory, the weight distribution in LAMP was modified to more closely reflect the SHCP distribution. The new predicted means were 1612 kN, 123690 kN-m, and -4666 kN – much more realistic values for the hogging condition.

Several runs in irregular seas were completed with the new weight distribution. The calculated dynamic loads were actually more different from the SMP values than for the original LAMP distribution, but were quite close.

Despite the poor quality of the point-mass defined weight distribution, the remainder of the LAMP runs used the same setup to maintain complete consistency with the SMP distribution. In later runs at the lower sea states, the LAMP predictions approach those from SMP. Regular wave testing, in the next chapter, also examined the load responses. The important conclusion is, in fact, that dynamic loads are far more sensitive to increasing speed and sea state than motions.

---

[3]Note, the weight distributions in both LAMP and SMP do NOT affect motion calculations. The only weight data required for motions are CG, and the mass gyradii.
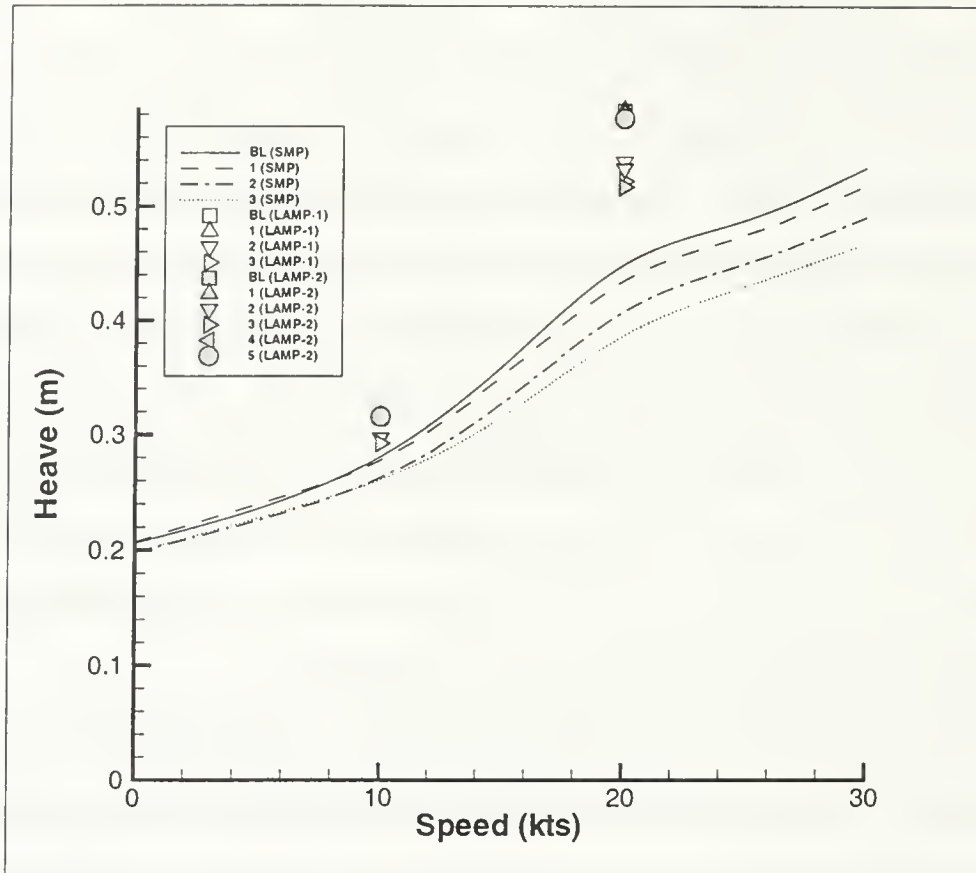
a. SS4
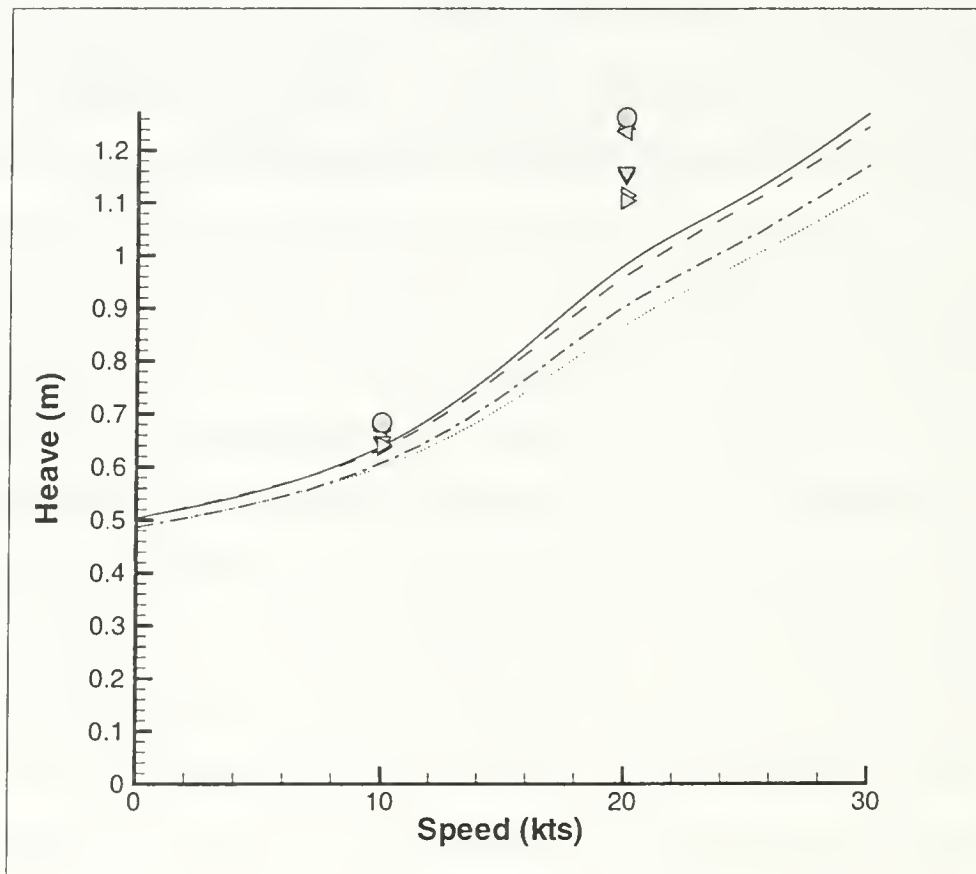
b. SS 5

Figure 5-1: Mathematical Hull Heave (SIG SA)
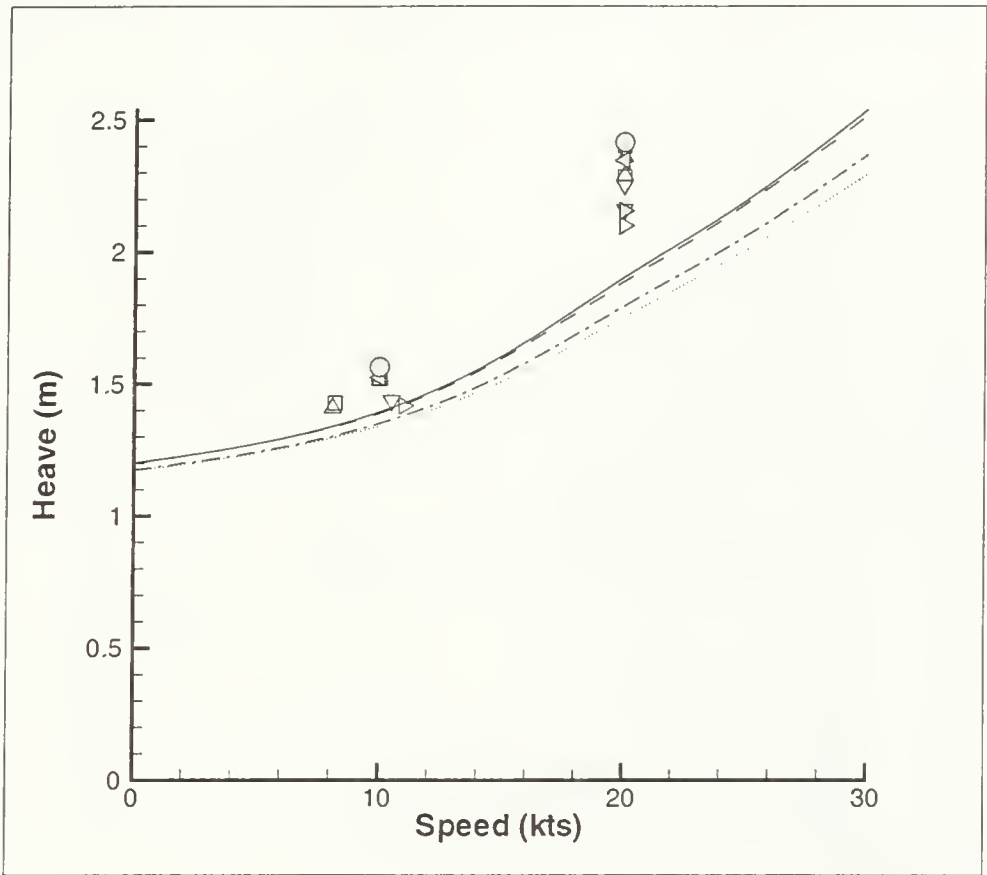
c. SS6
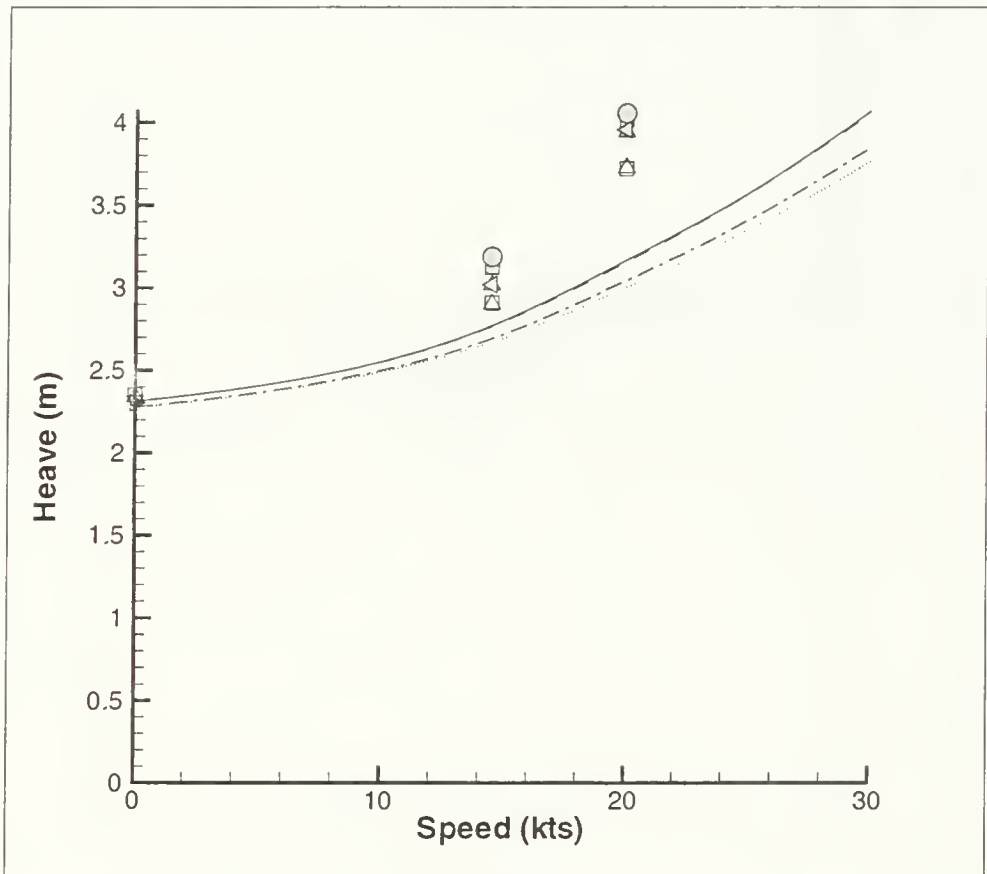
d. SS 7
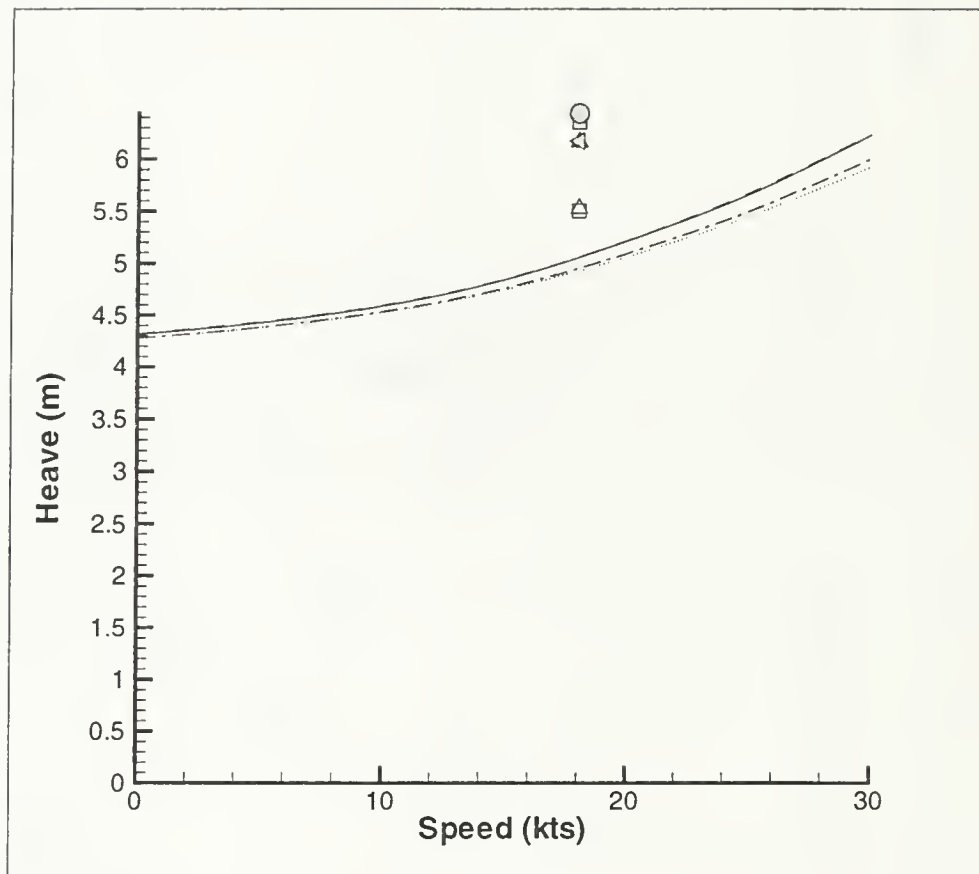
e. SS8
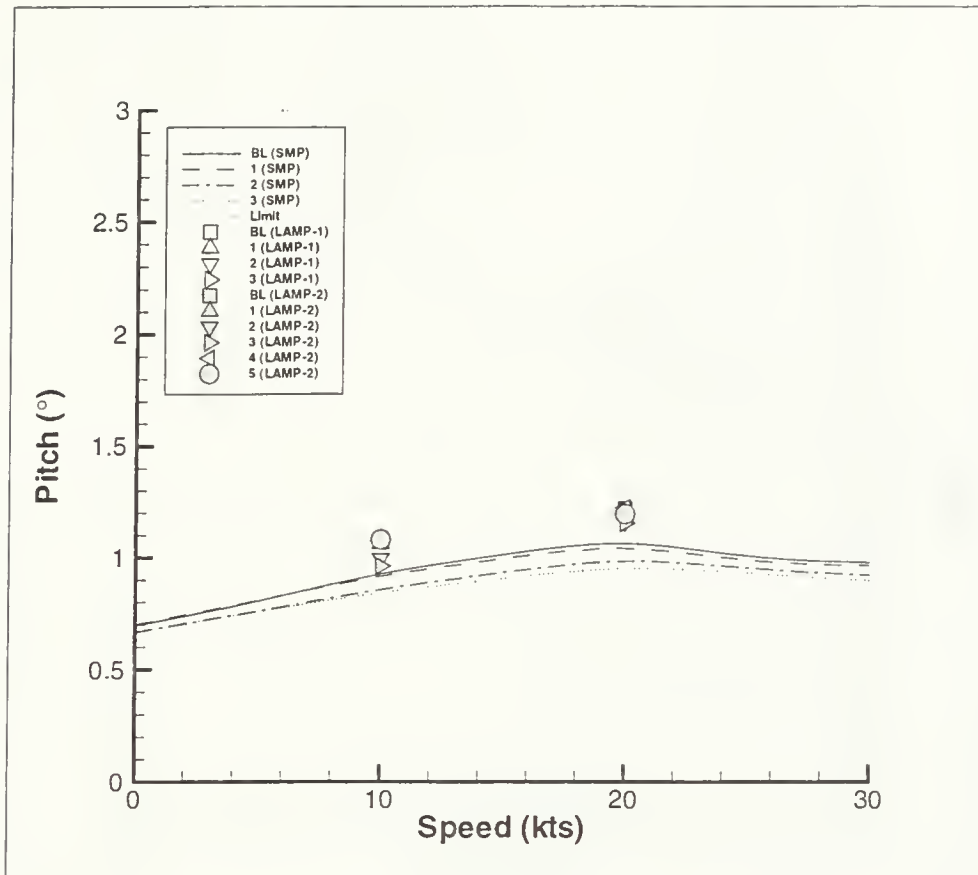
a. SS4
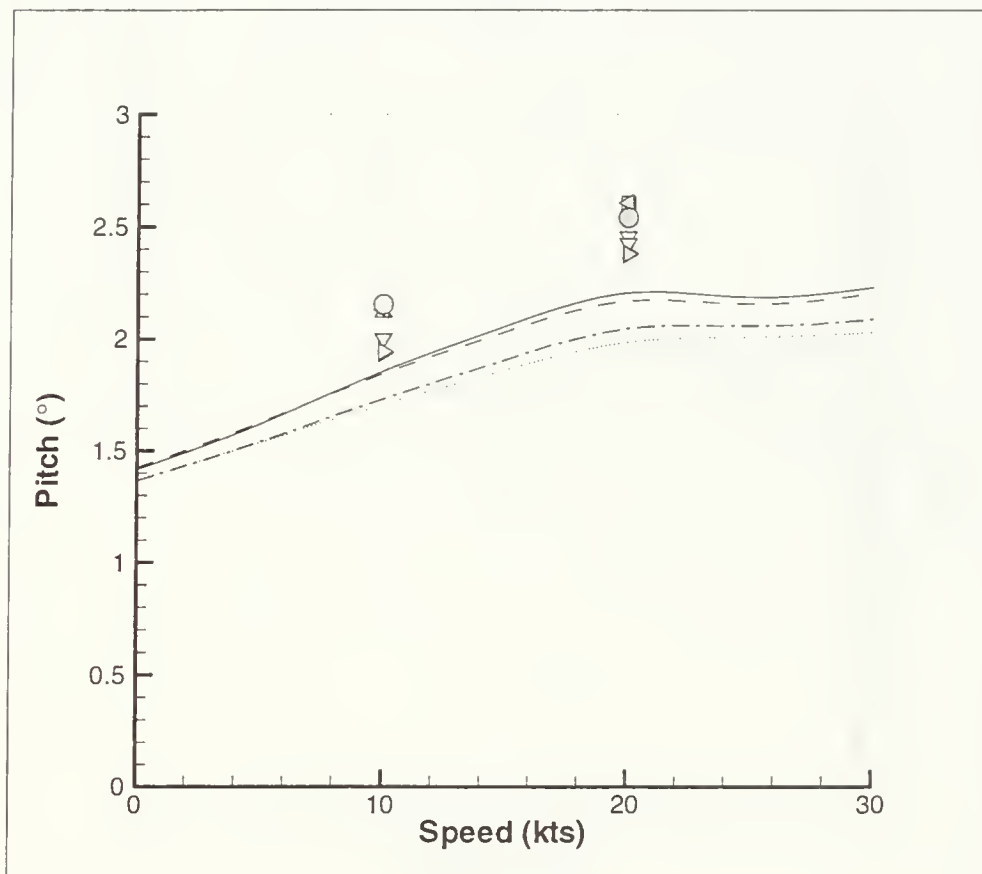
b. SS 5

Figure 5-2: Mathematical Hull Pitch (SIG SA), Limit $\equiv$ Naval Transit Limit

101

c. SS6

d. SS 7

102
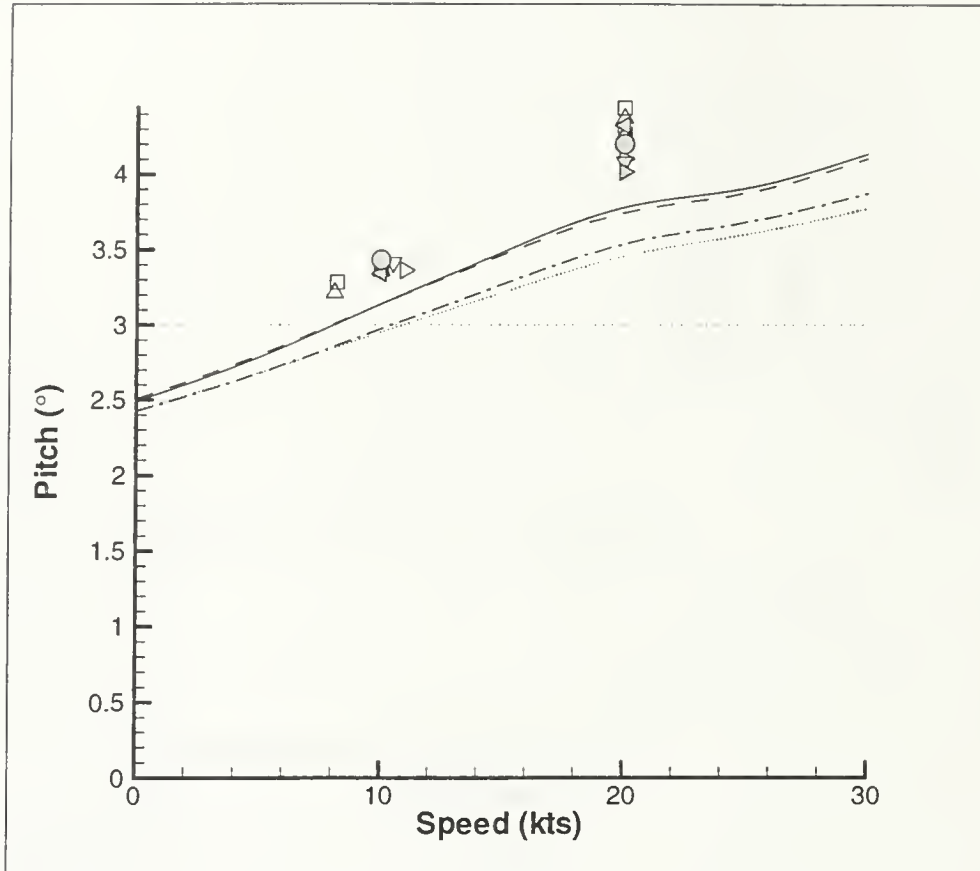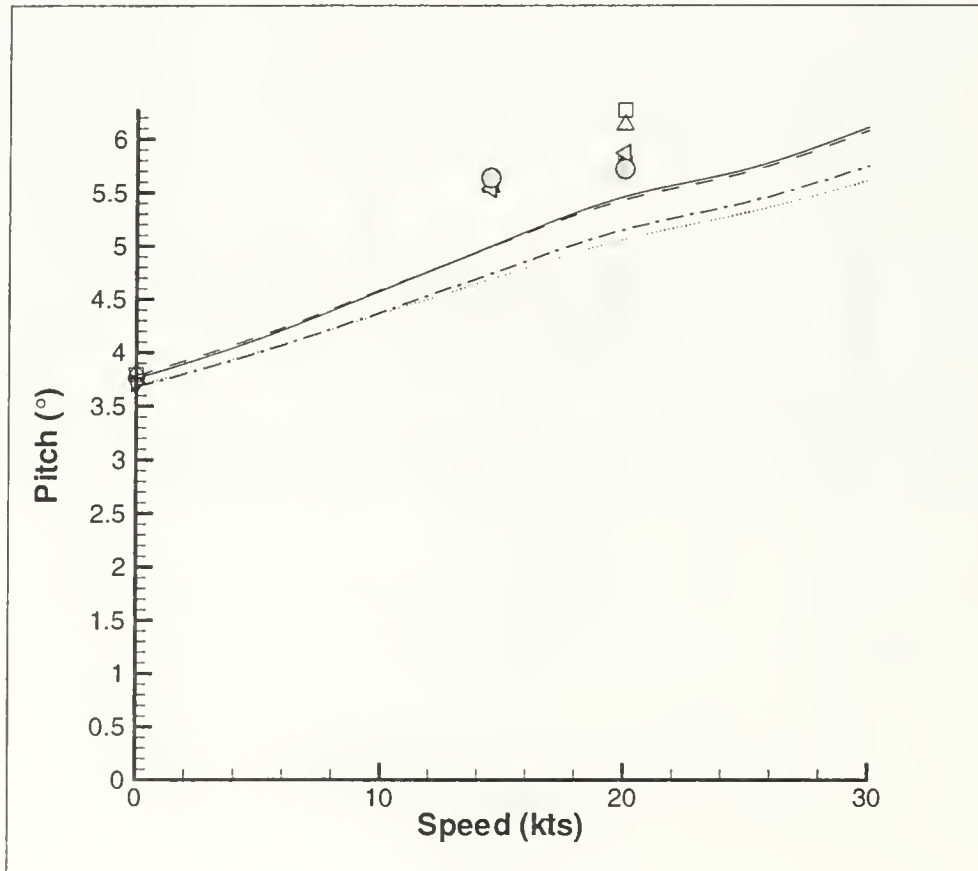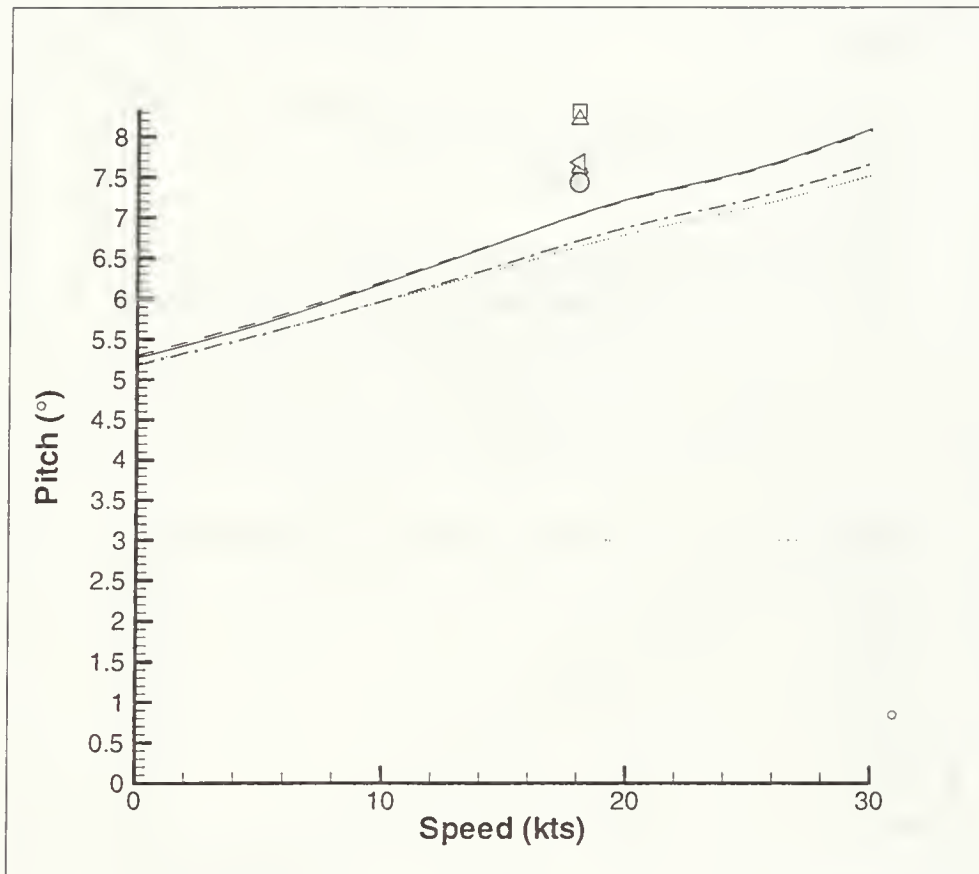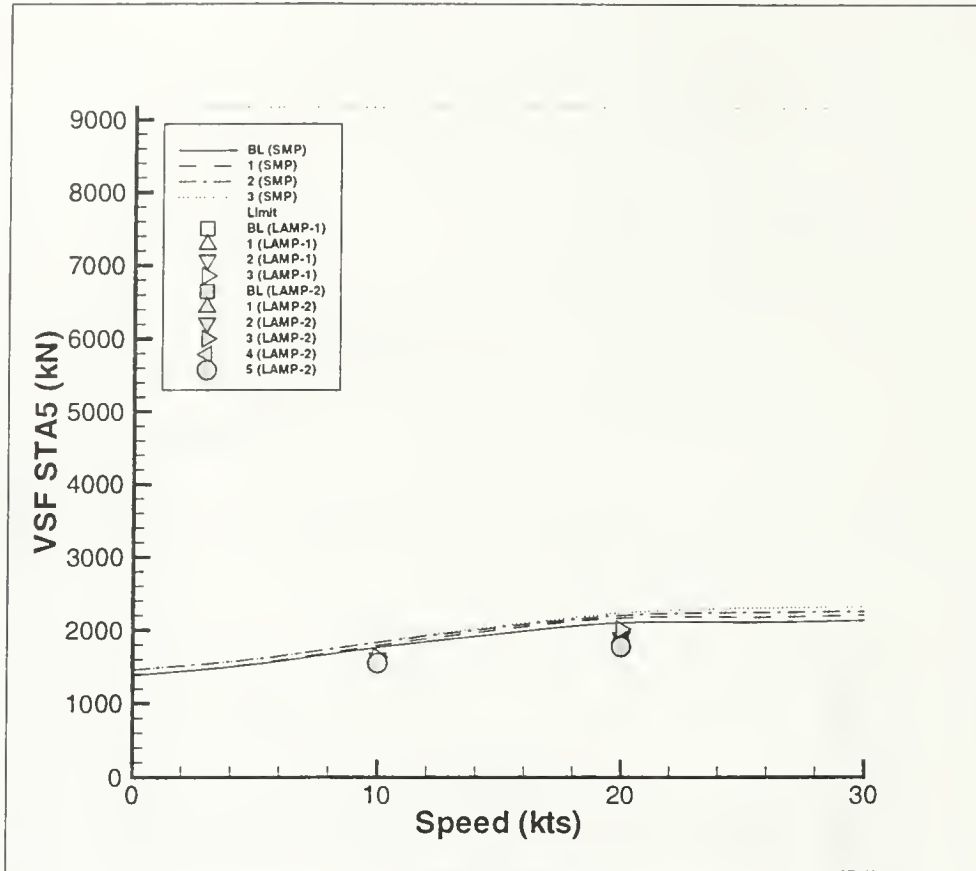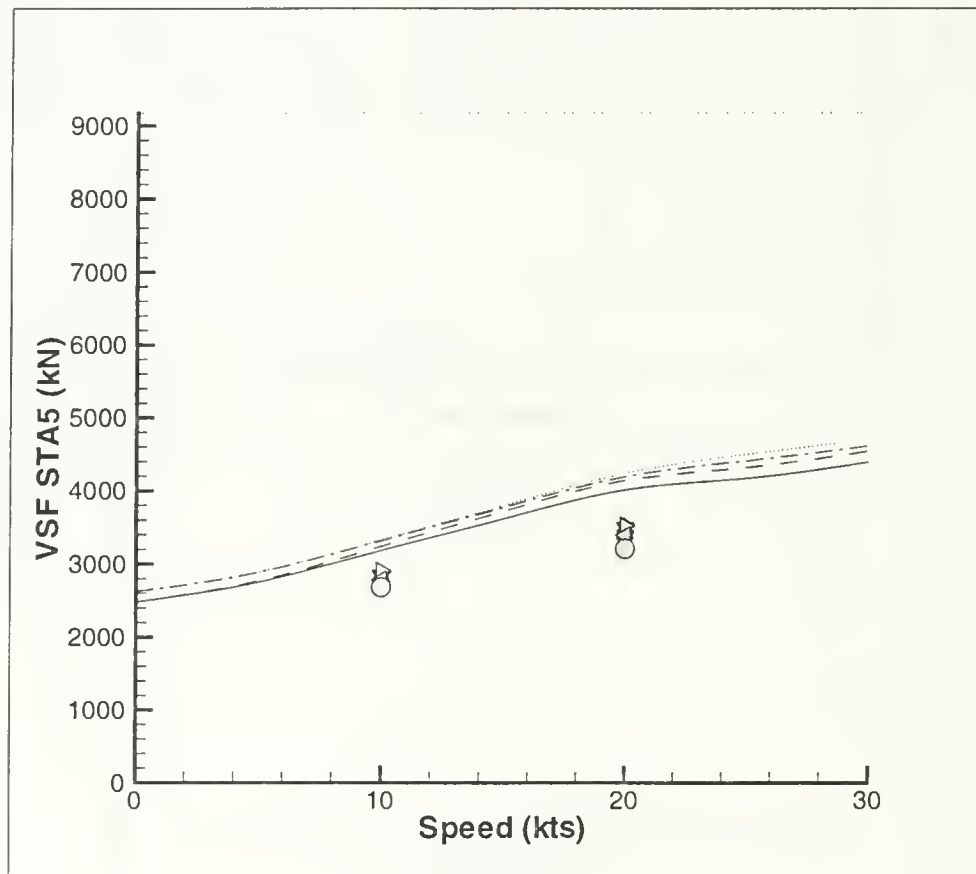
e. SS8

a. SS4

b. SS 5

Figure 5-3: Mathematical Hull Vertical Shear Force STA5 (SIG SA), Limit $\equiv$ Naval Design Limit

c. SS6

d. SS 7

105
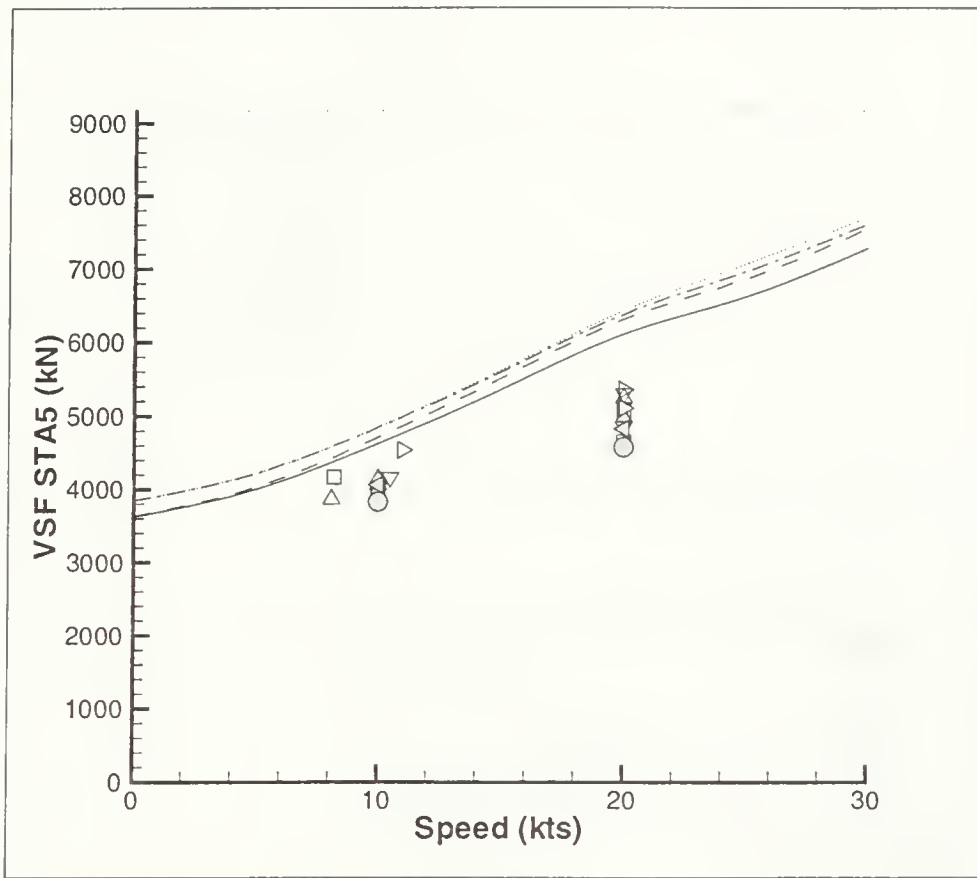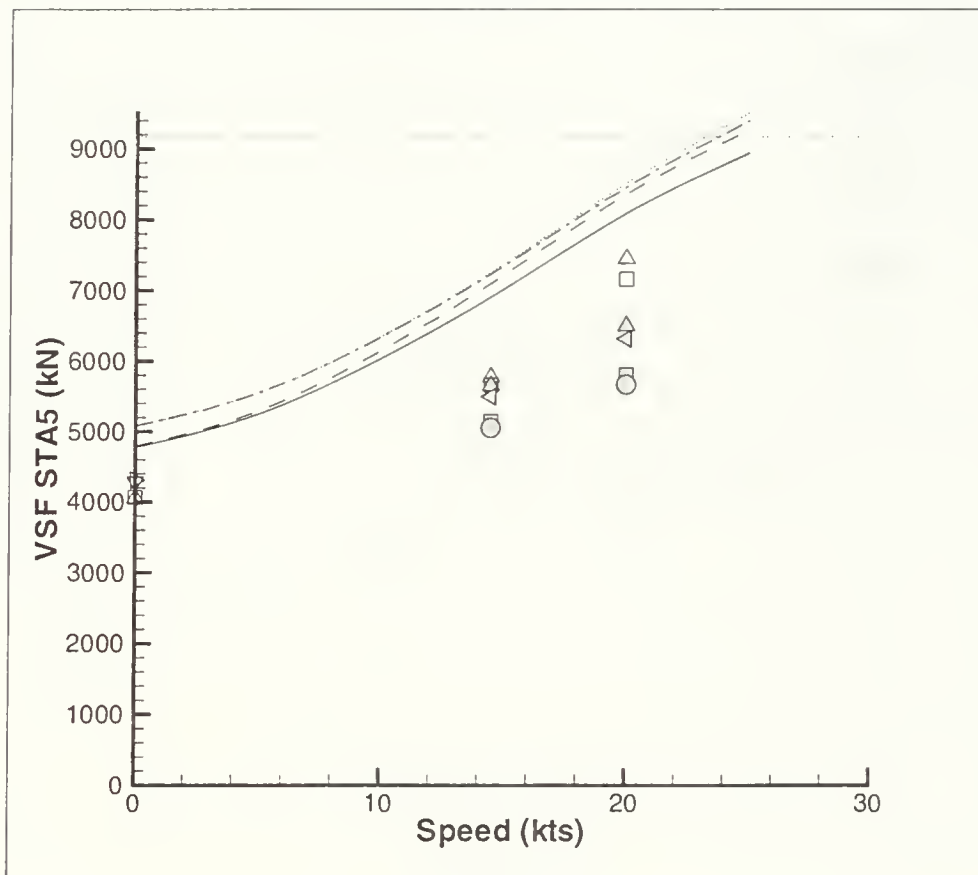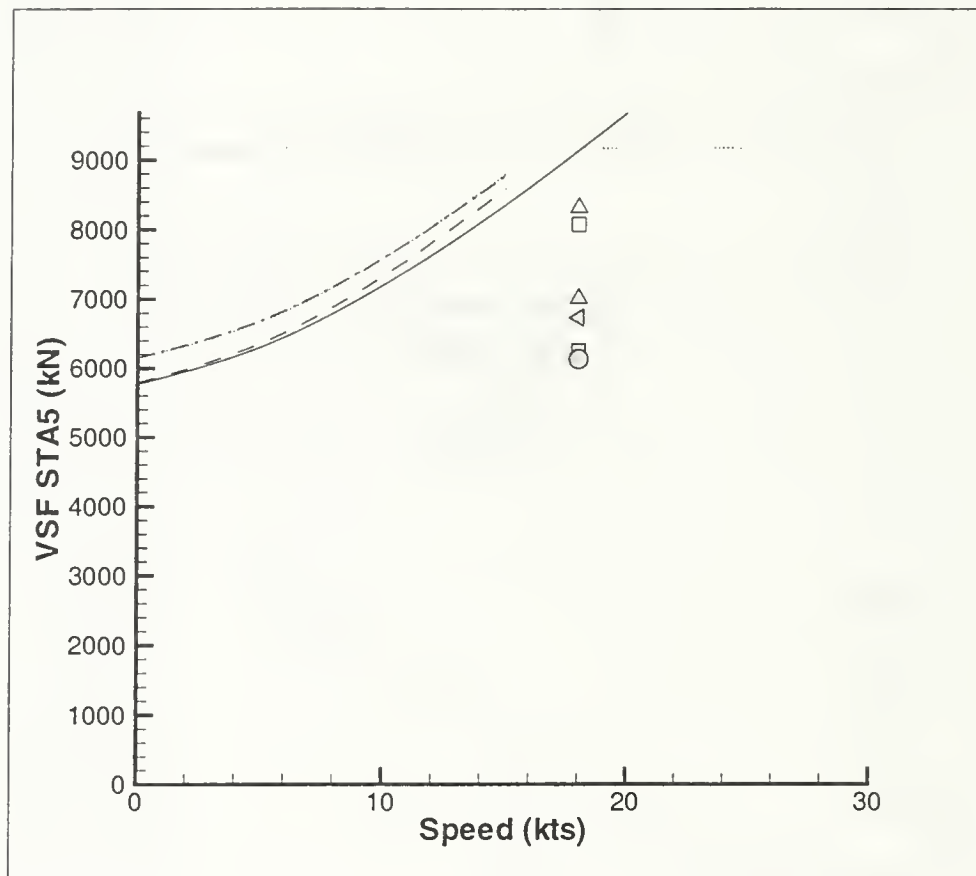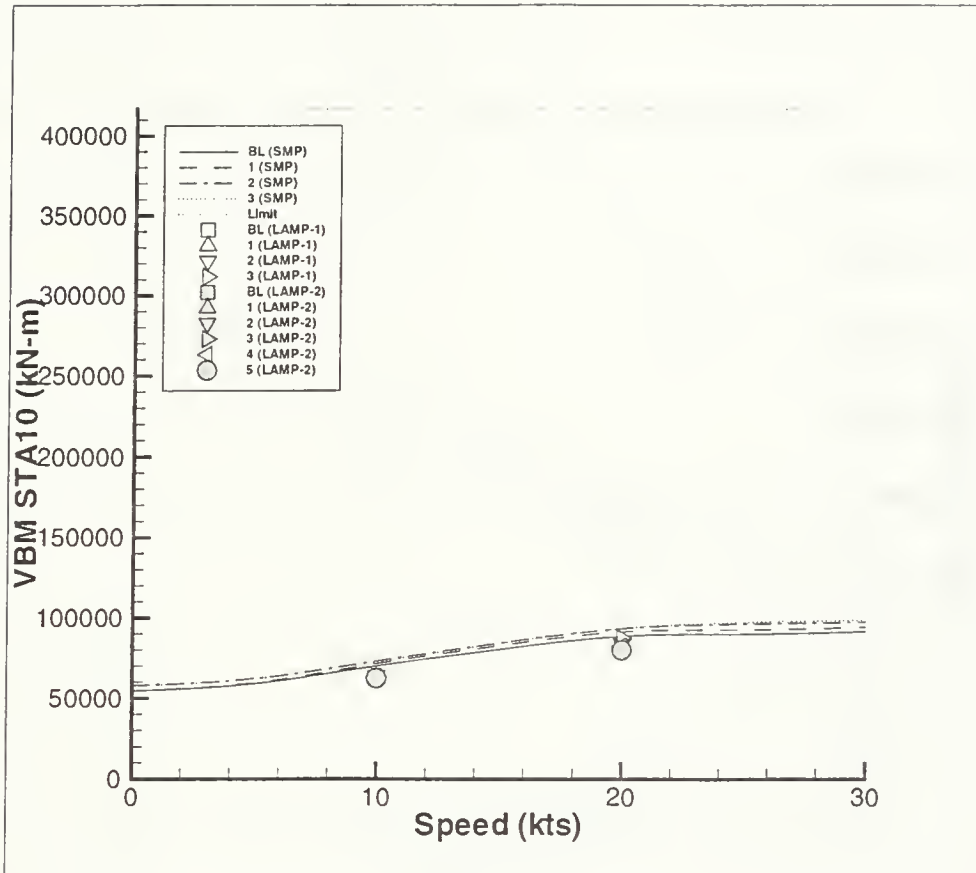
e. SS8

a. SS4

b. SS 5

Figure 5-4: Mathematical Hull Vertical Bending Moment STA10 (SIG SA), Limit ≡ Naval Design Limit
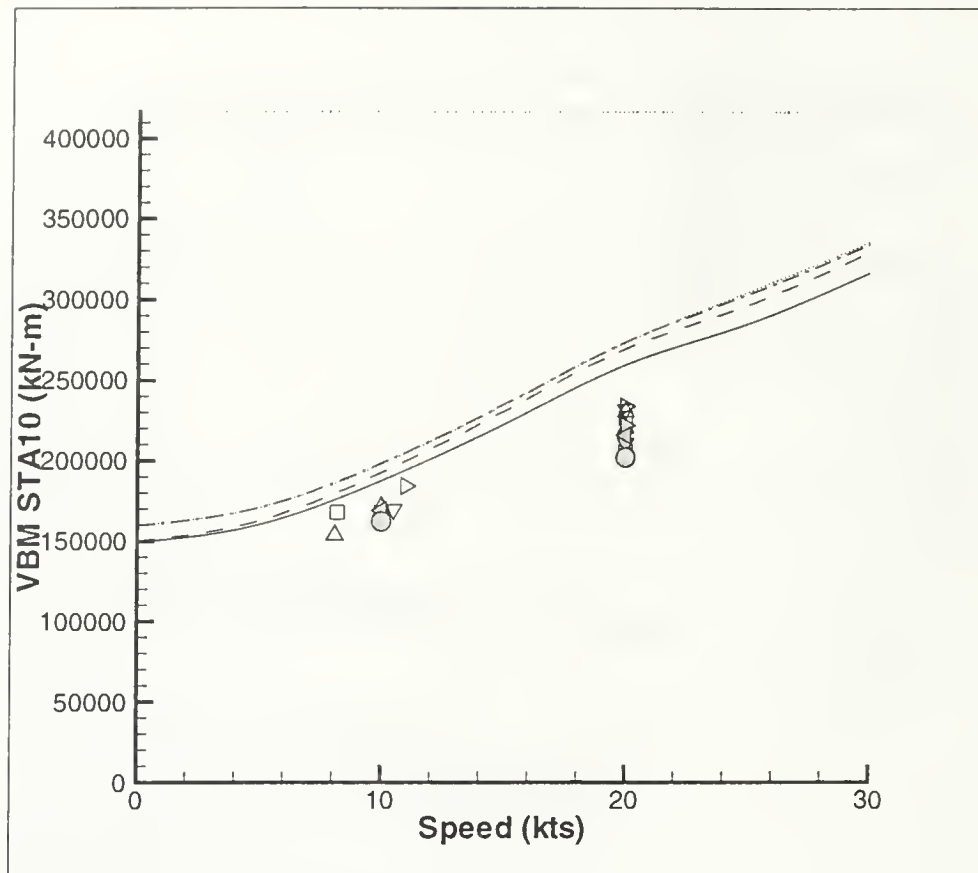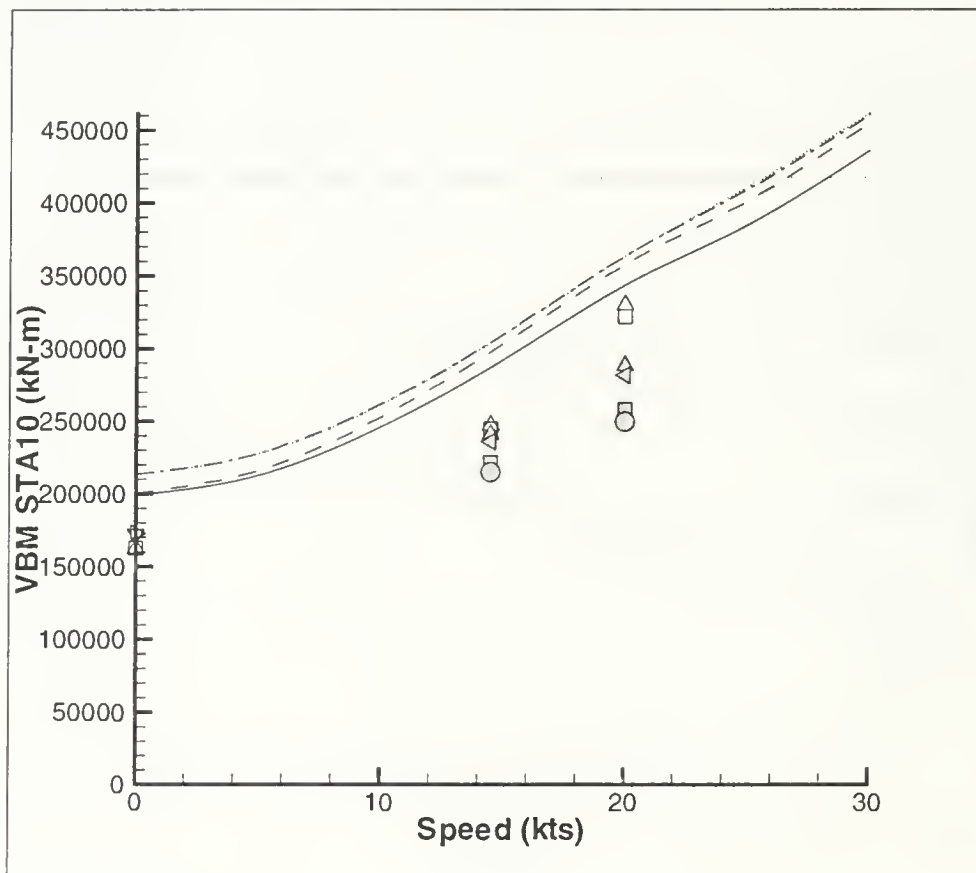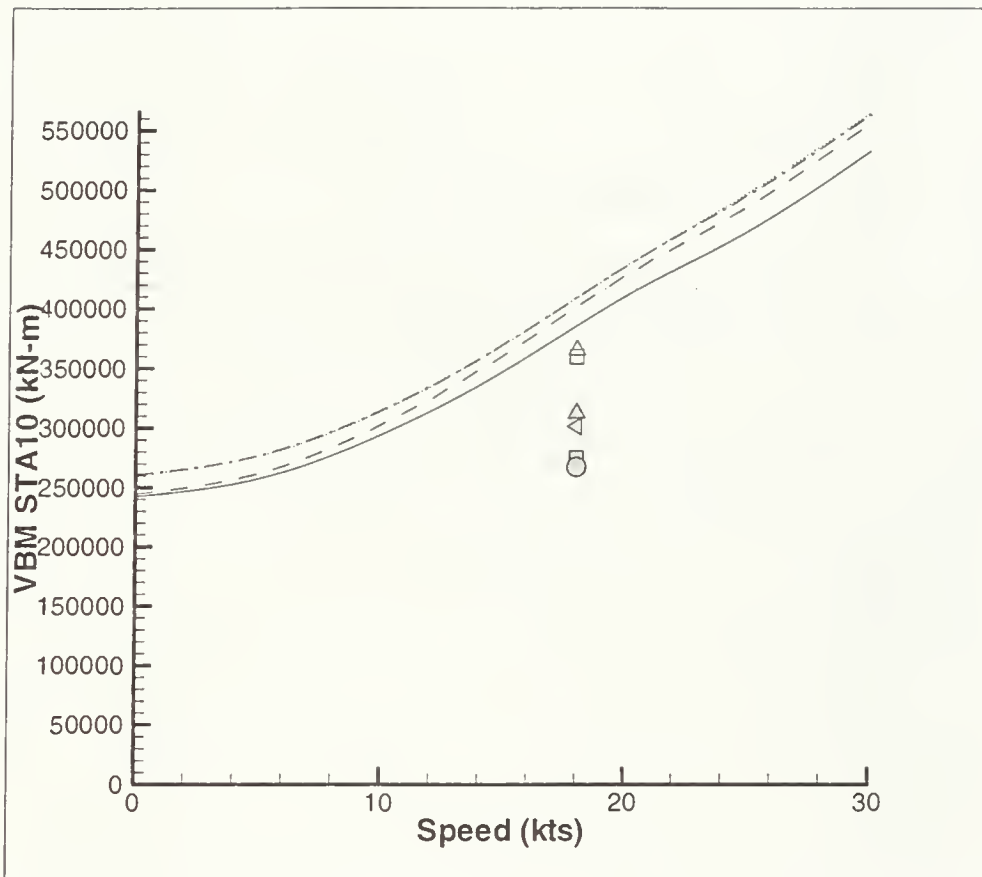
c. SS6

d. SS 7

e. SS8
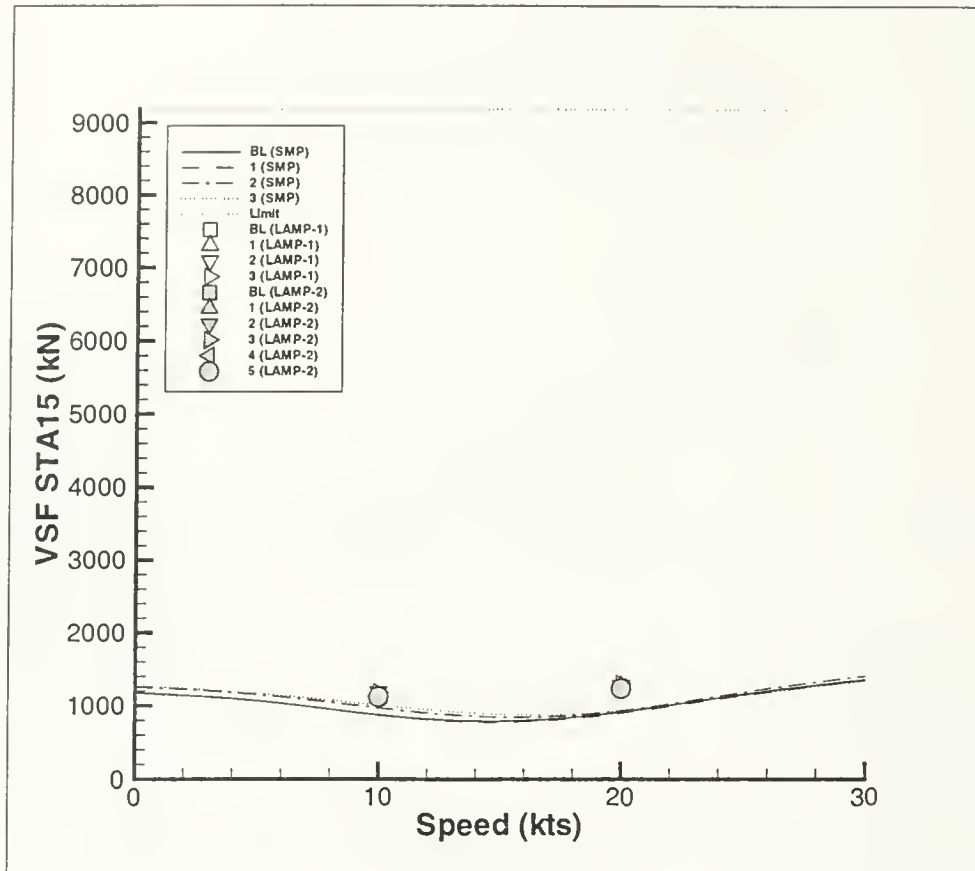
a. SS4
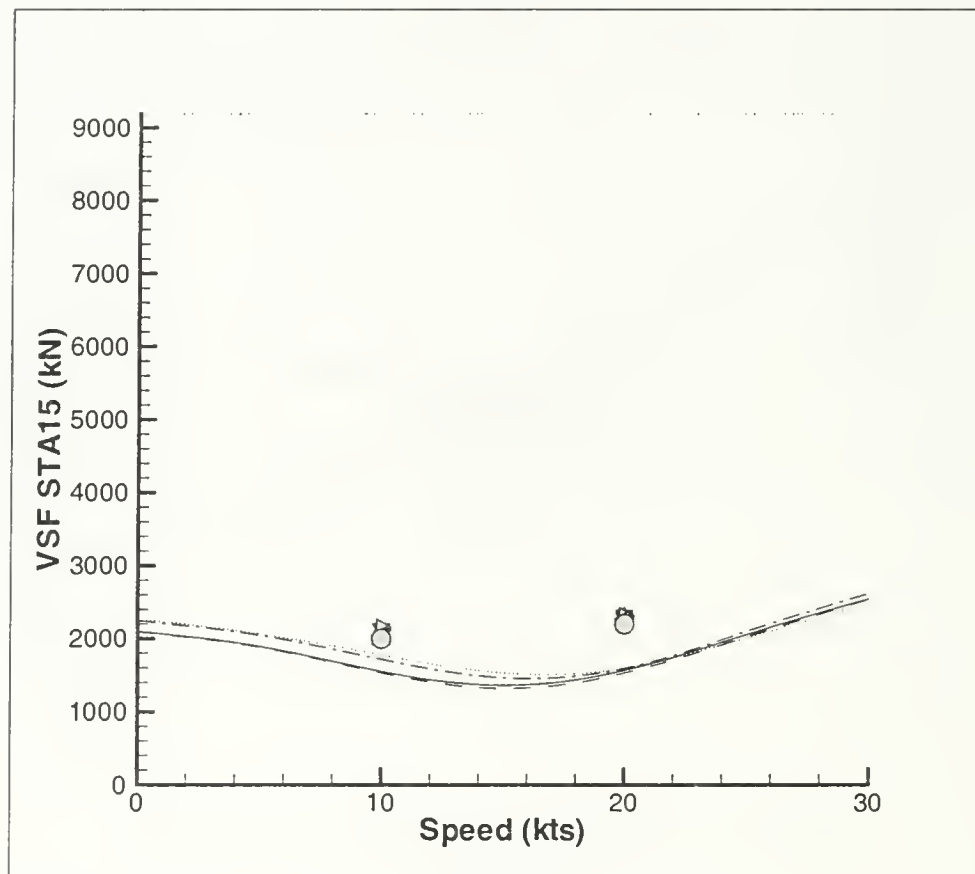
b. SS 5

Figure 5-5: Mathematical Hull Vertical Shear Force STA15 (SIG SA), Limit ≡ Naval Design Limit

110

c. SS6

d. SS 7

111
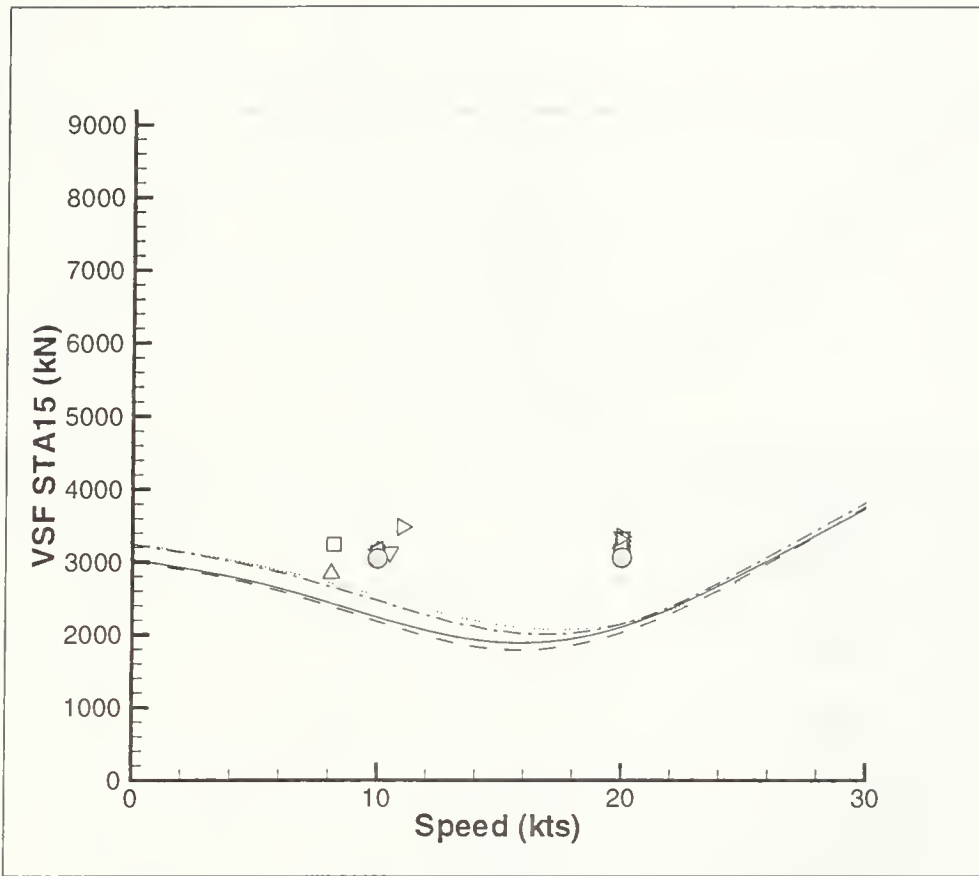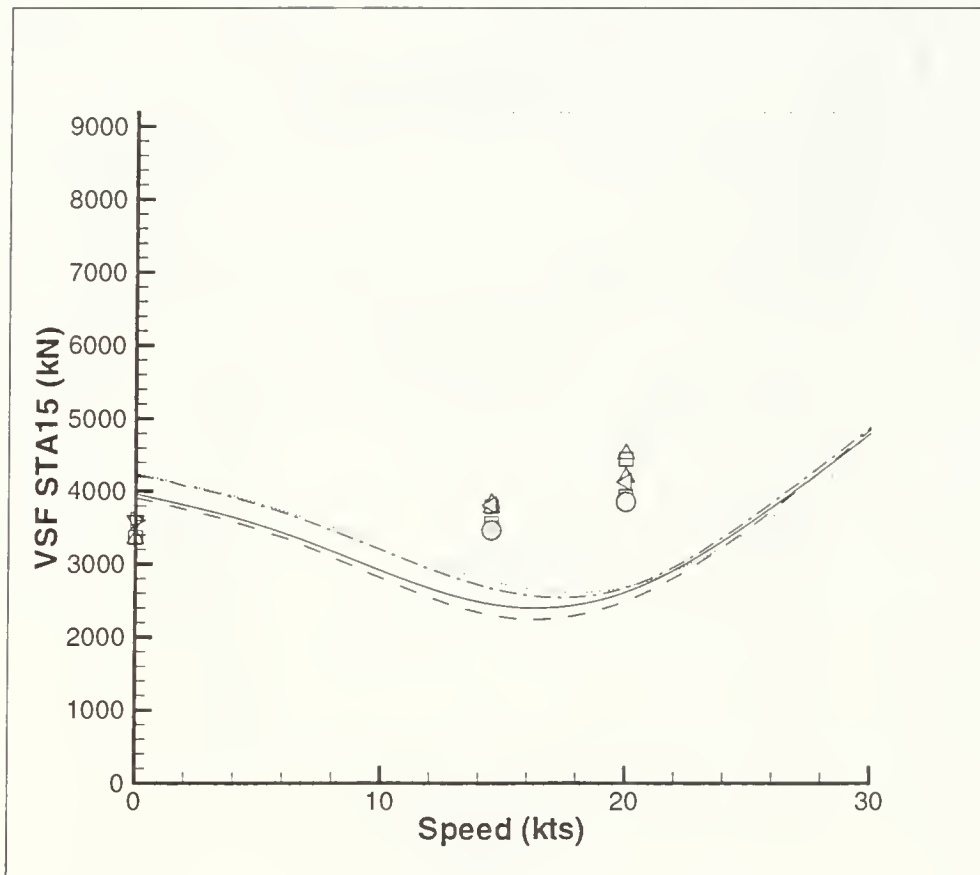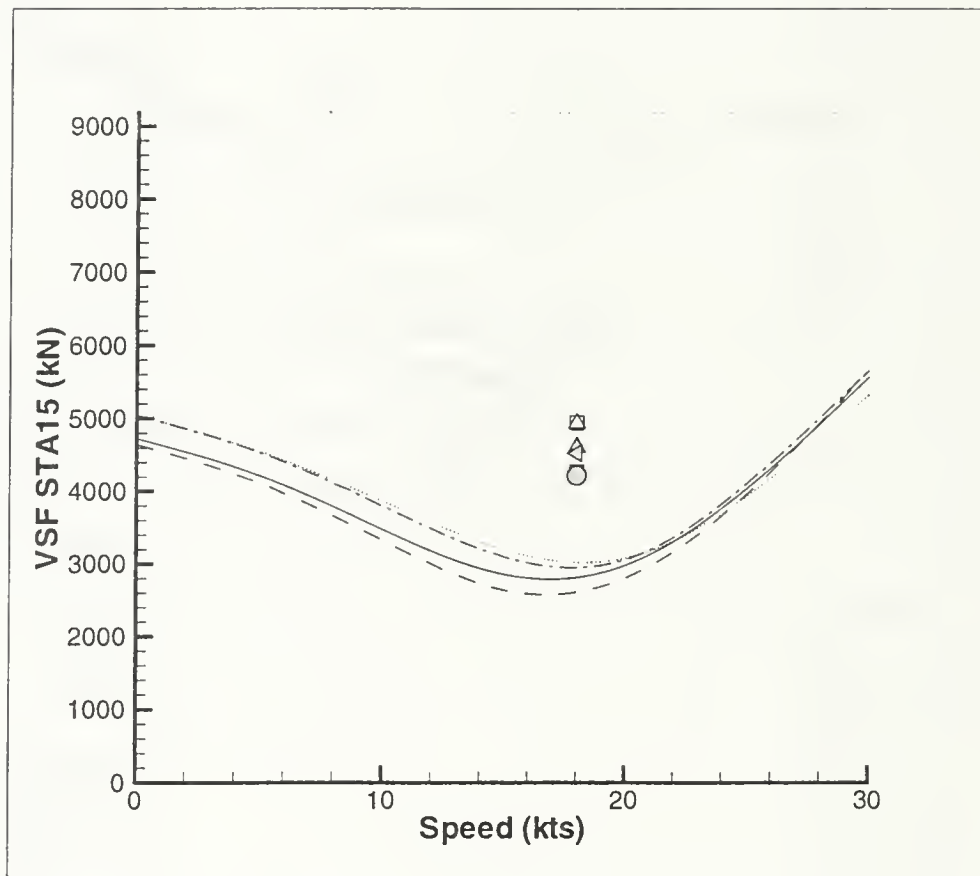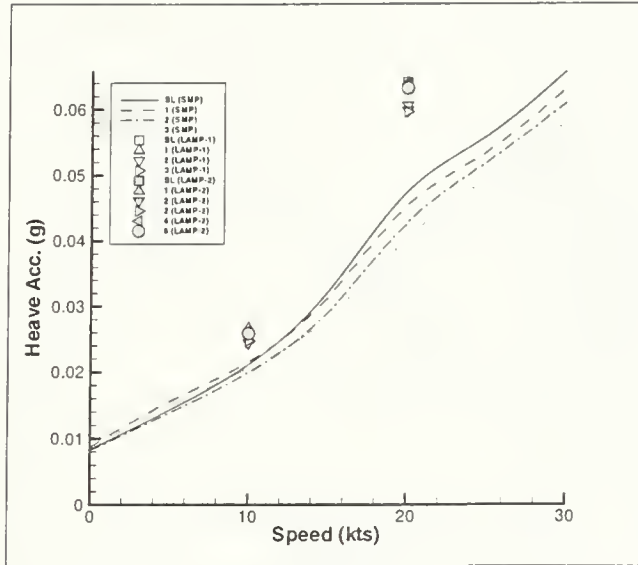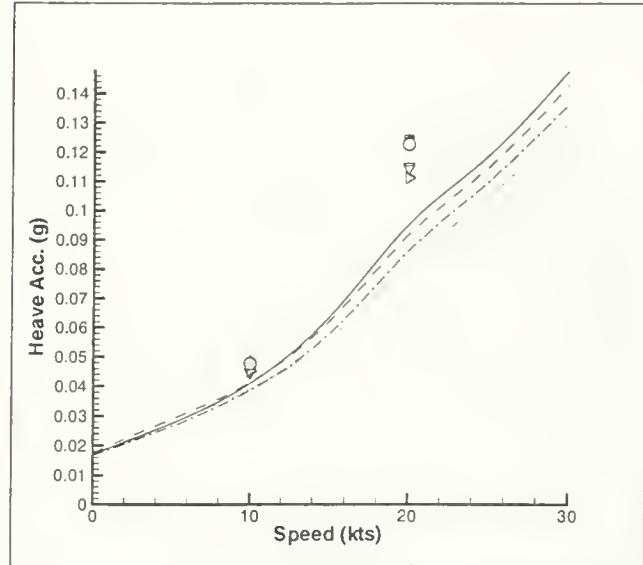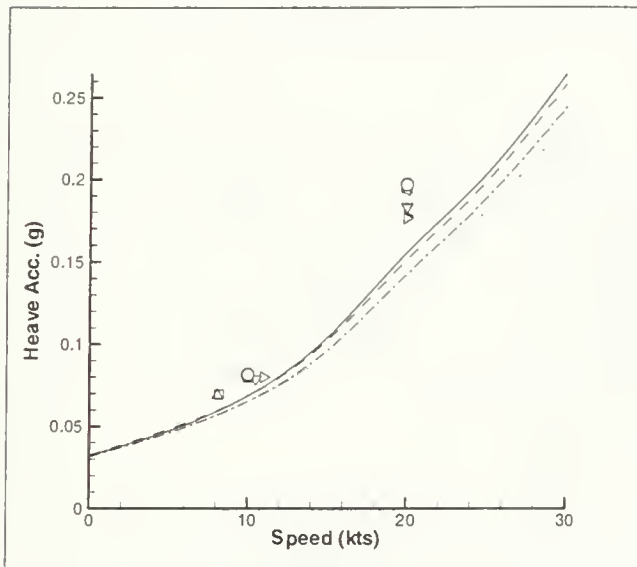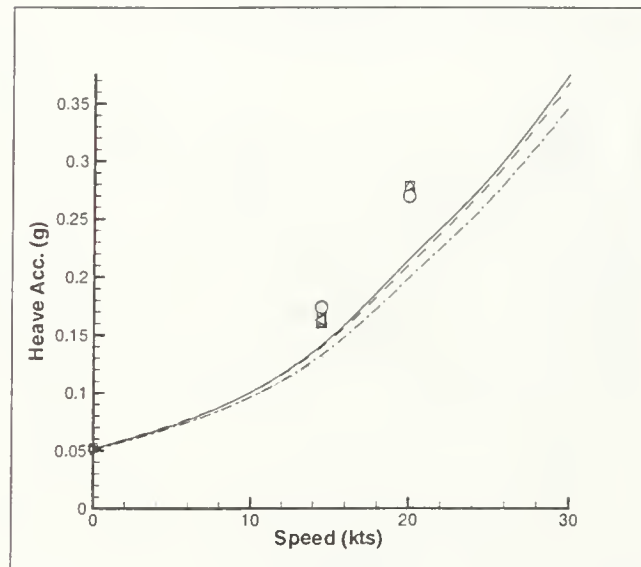
e. SS8
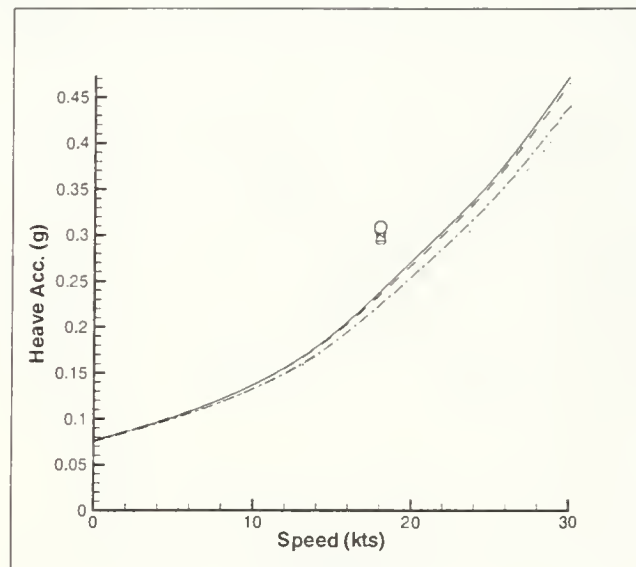
a. SS 4

b. SS 5

c. SS 6

d. SS 7

e. SS 8

Figure 5-6: Mathematical Hull Heave Acceleration (SIG SA)

113
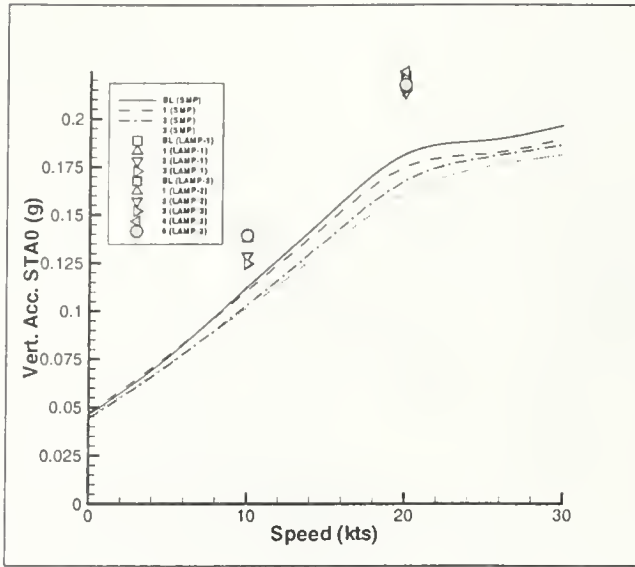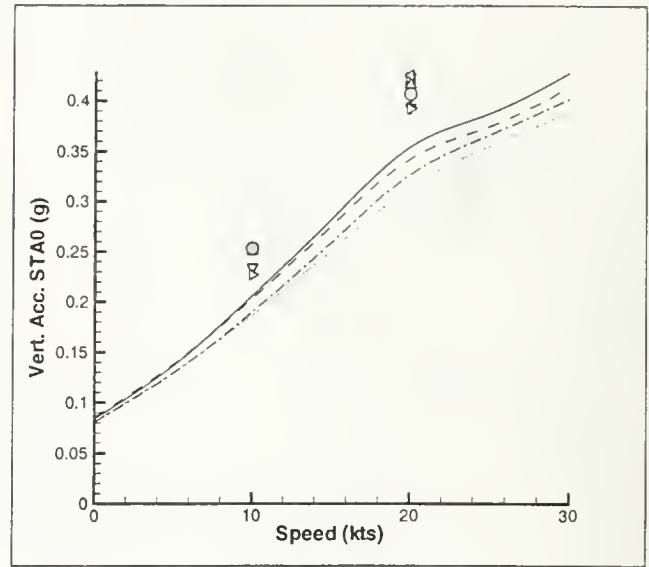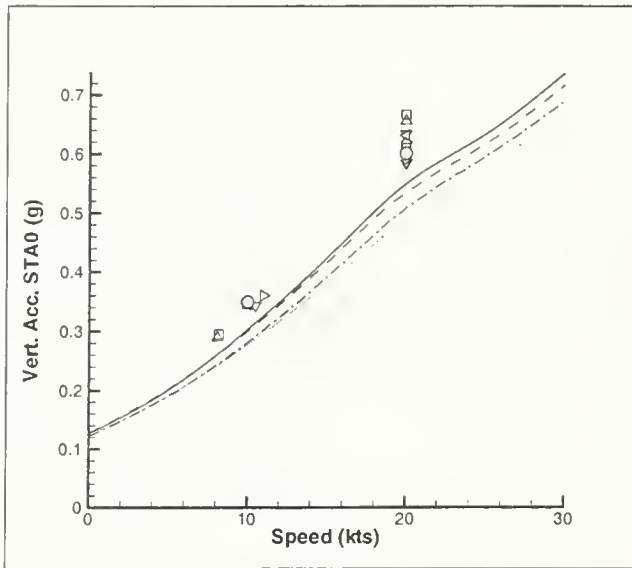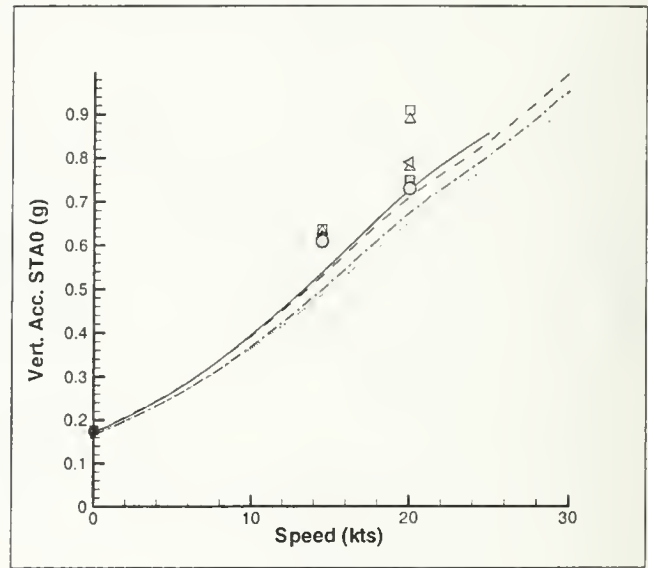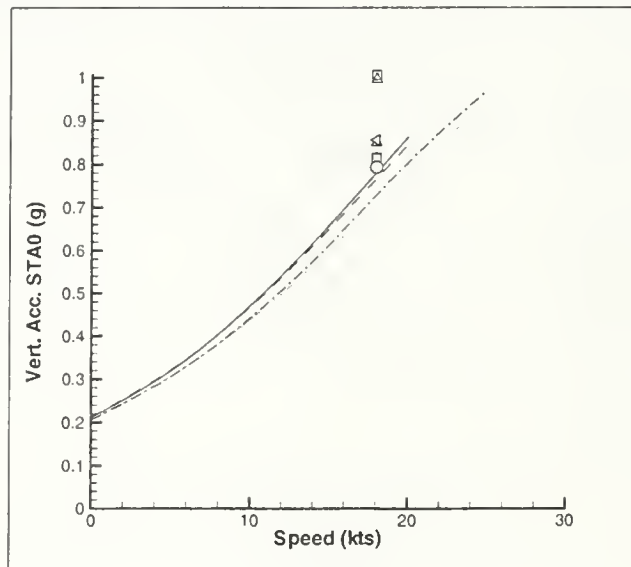
a. SS 4

b. SS 5

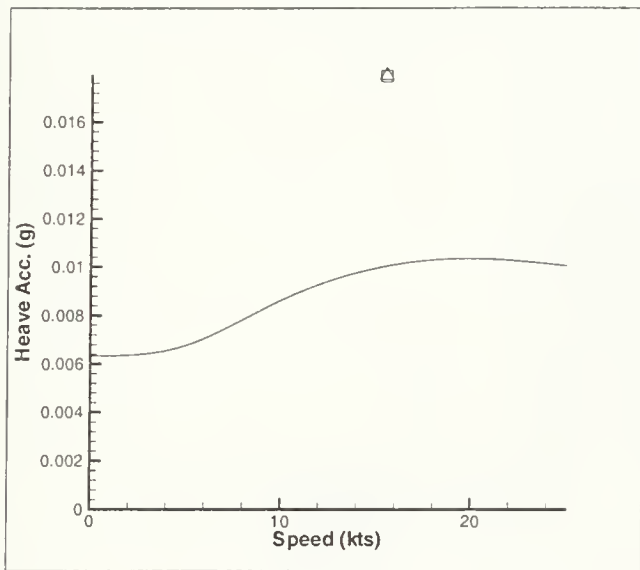c. SS 6

d. SS 7

e. SS 8

Figure 5-7: Mathematical Hull Vertical Acceleration STA0 (SIG SA)
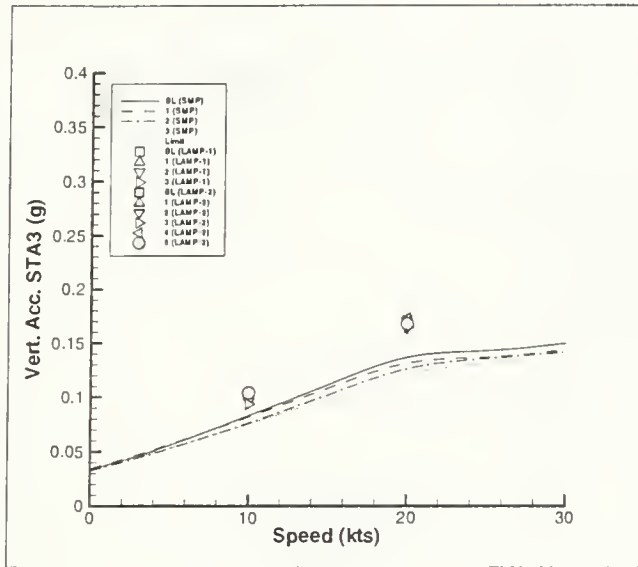
a. SS 4
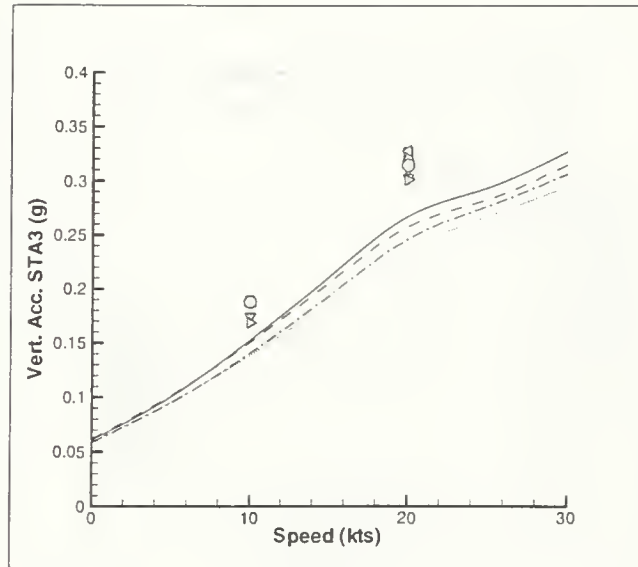
b. SS 5
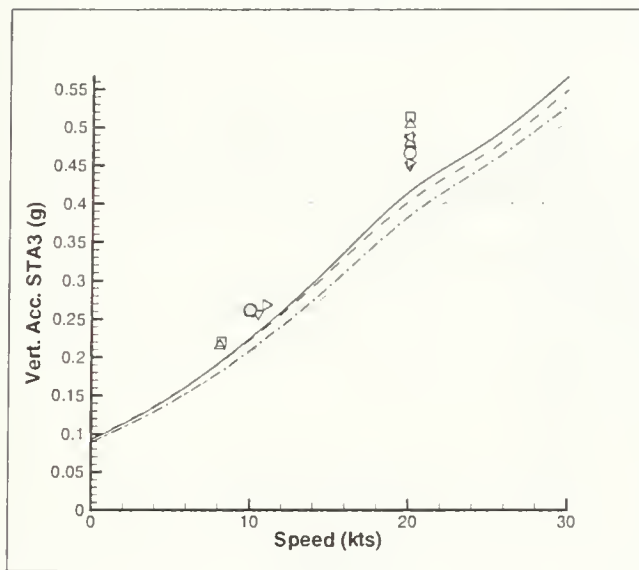
c. SS 6
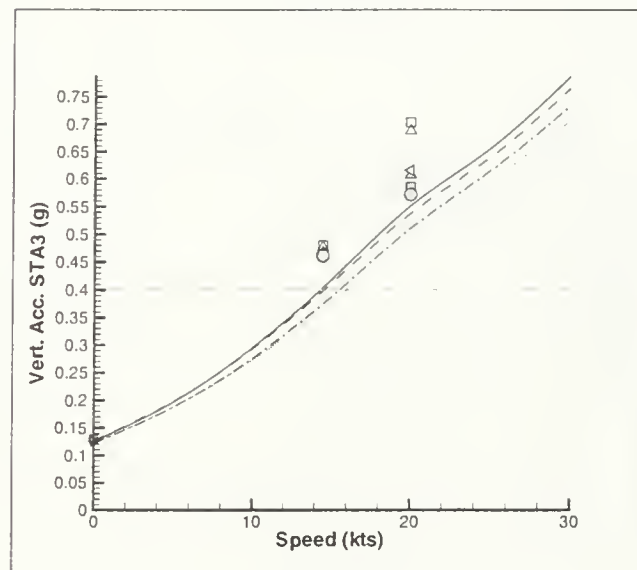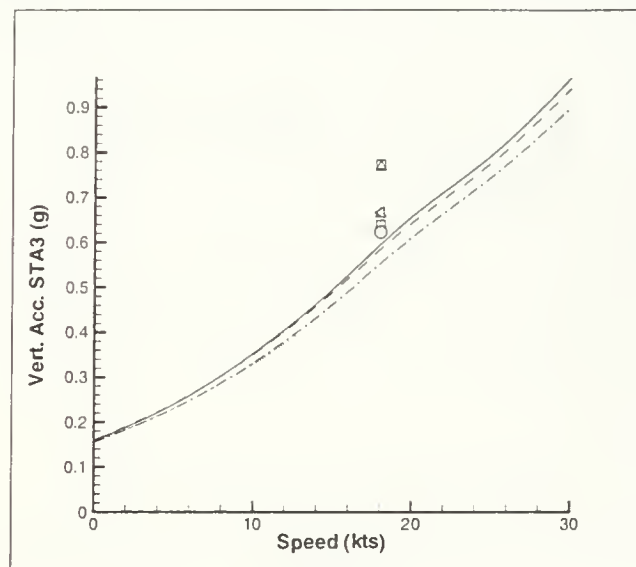
d. SS 7

e. SS 8

Figure 5-8: Mathematical Hull Vertical Acceleration STA3 (SIG SA), Limit ≡ Naval Transit Limit
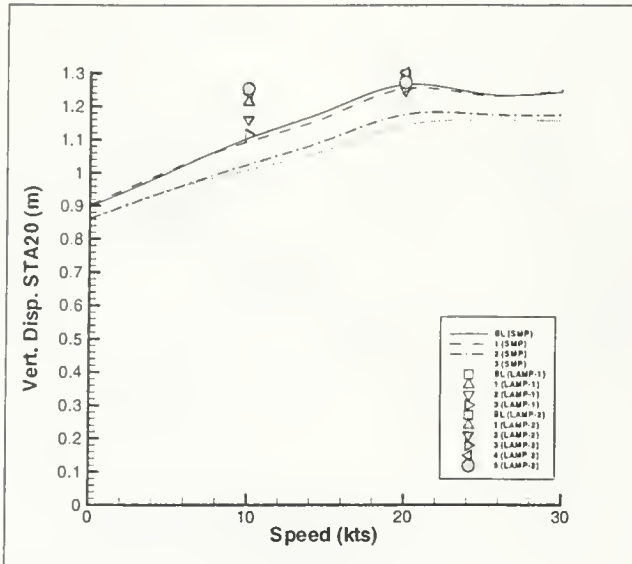
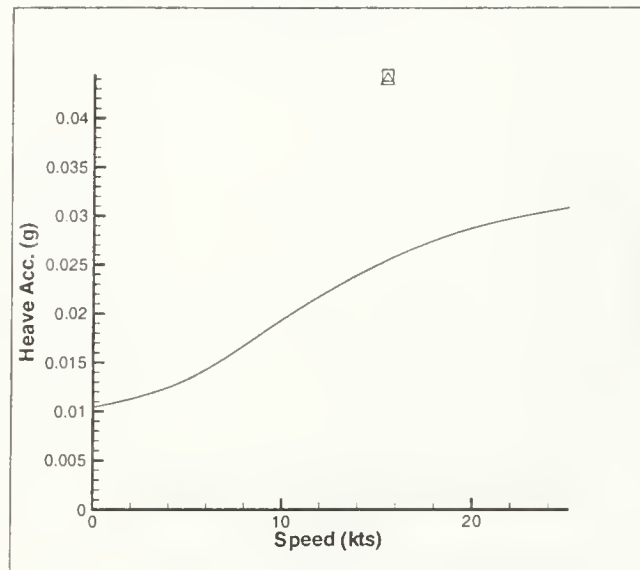a. SS 4
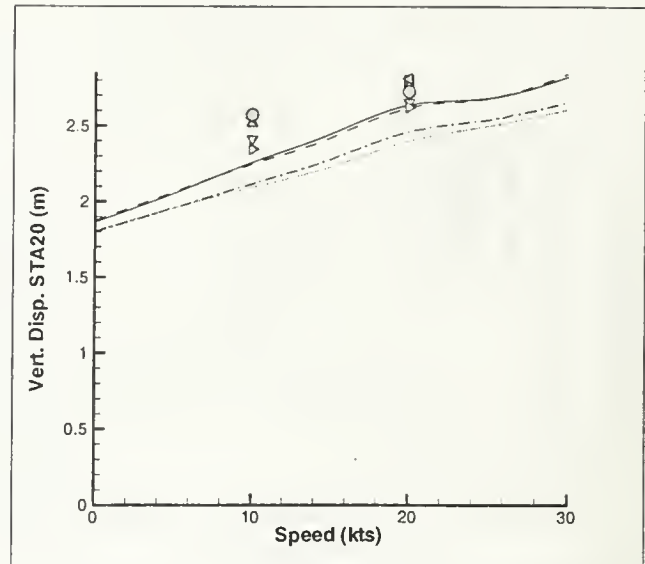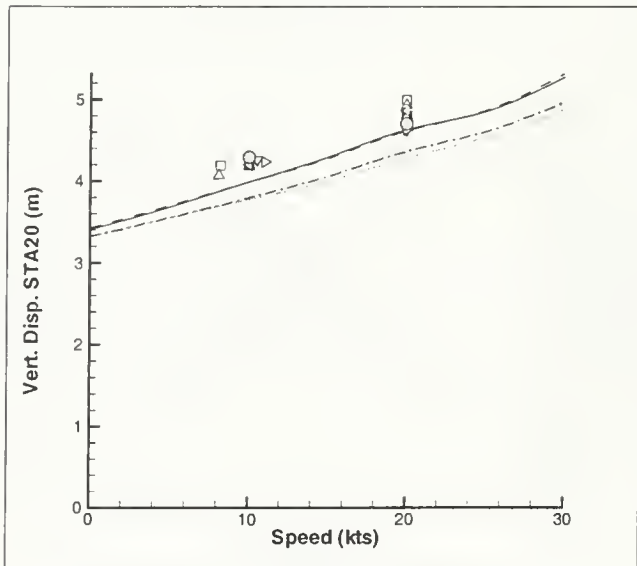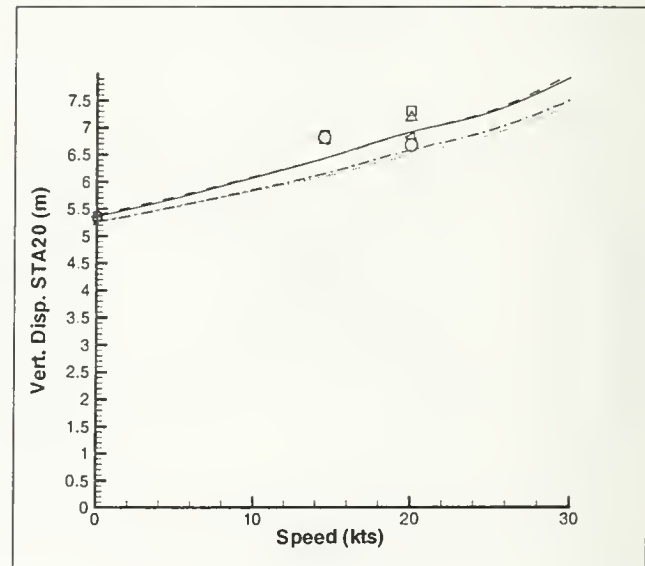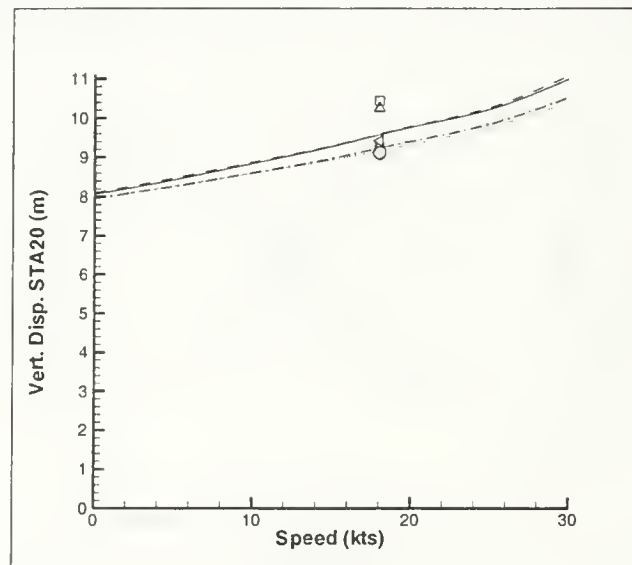
b. SS 5

c. SS 6

d. SS 7

e. SS 8

Figure 5-9: Mathematical Hull Vertical Displacement STA20 (SIG SA)
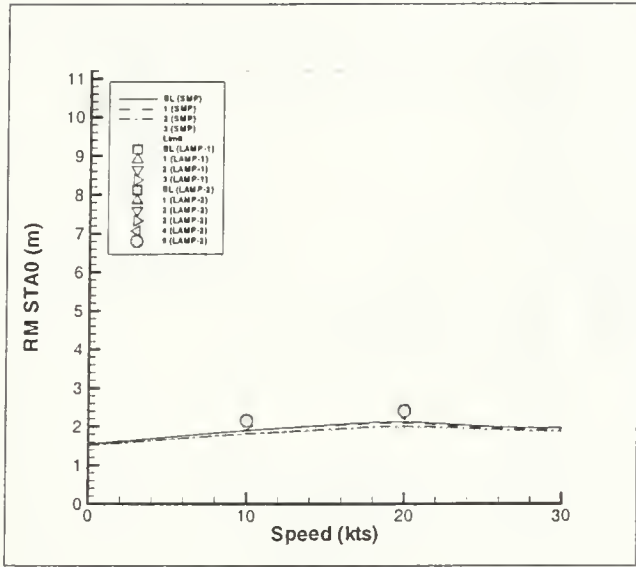
a. SS 4
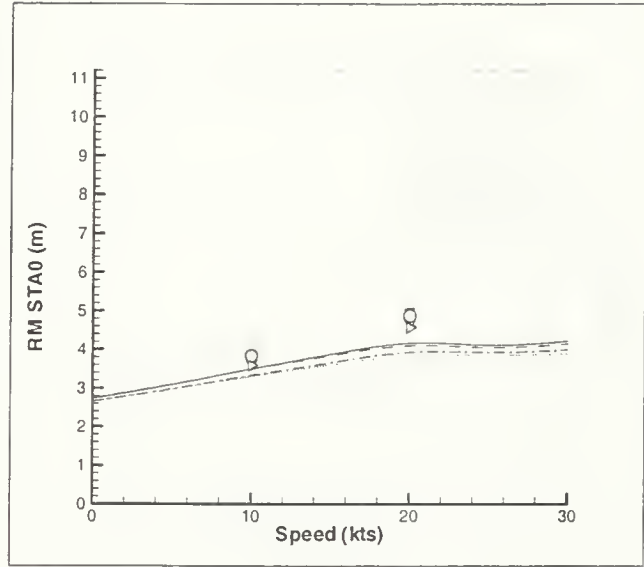
b. SS 5
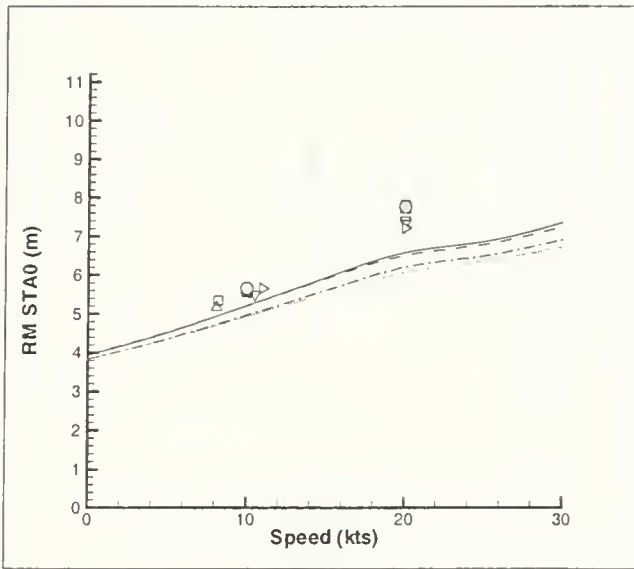
c. SS 6
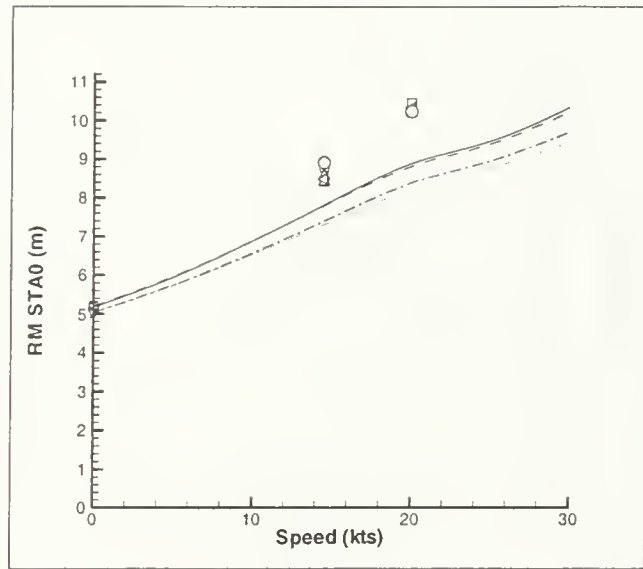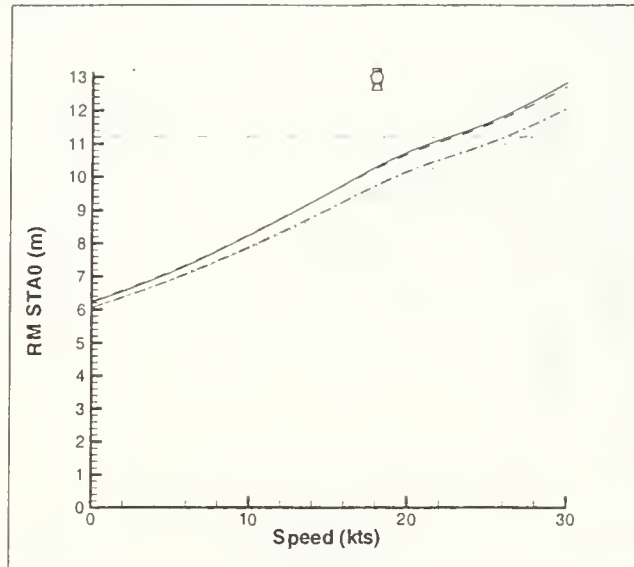
d. SS 7

e. SS 8

Figure 5-10: Mathematical Hull Relative Motion STA0 (SIG SA), Limit ≡ Freeboard (Deck Wetness Factor)
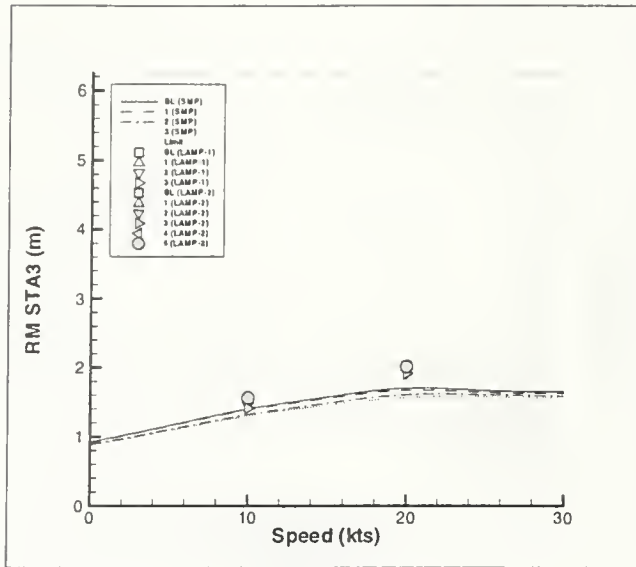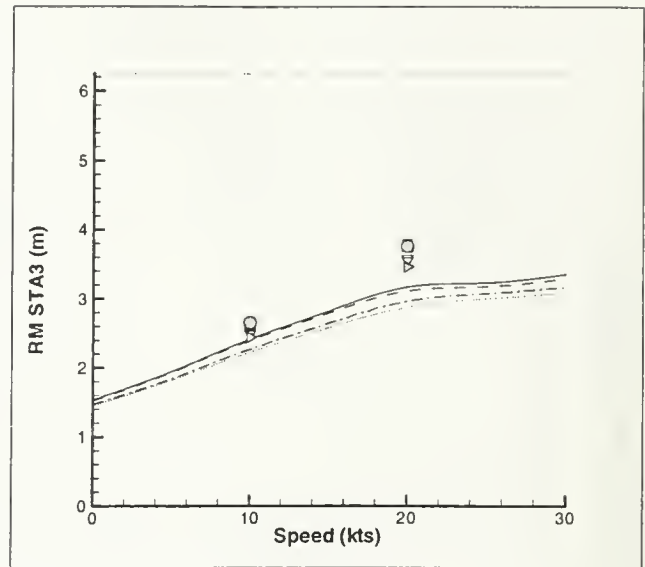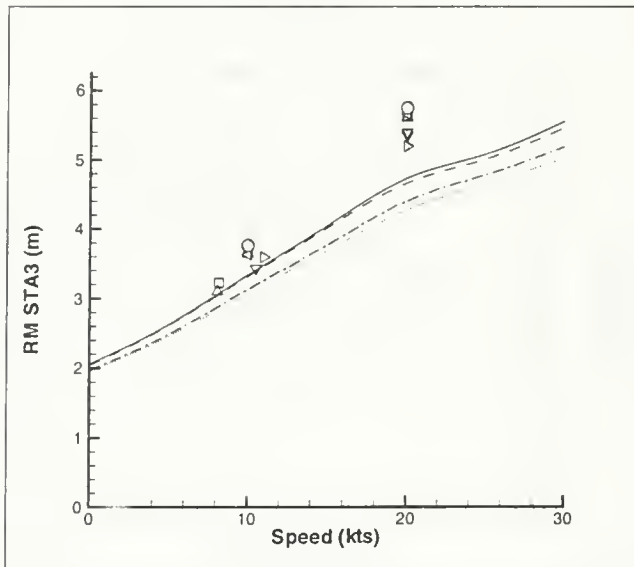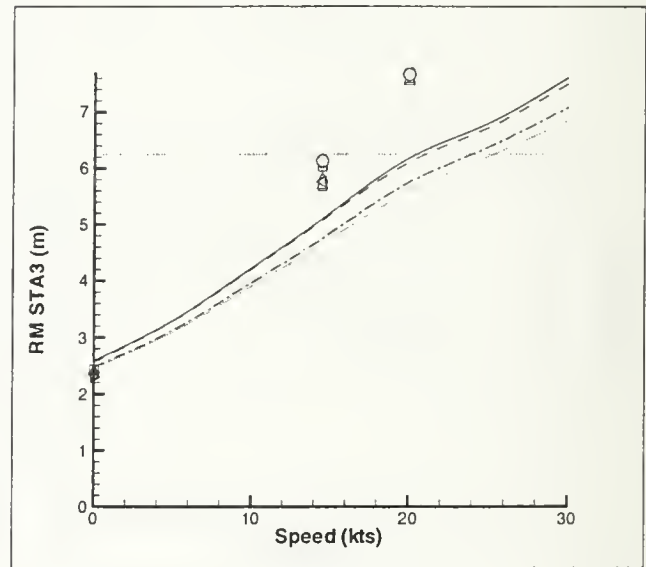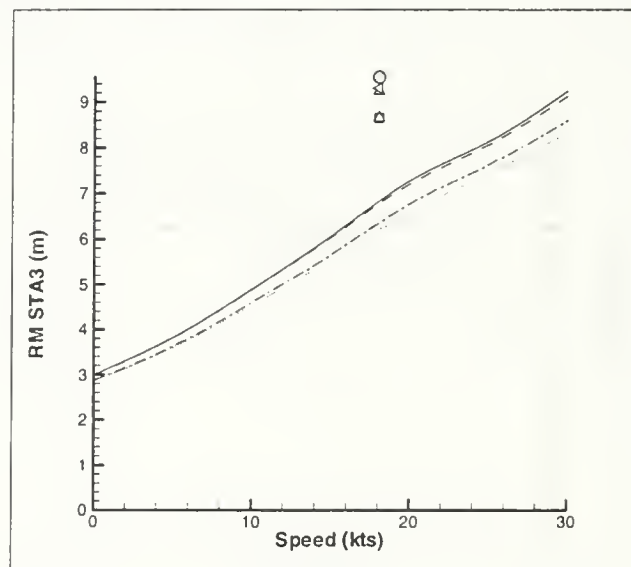
Figure 5-11: Mathematical Hull Relative Motion STA3 (SIG SA), Limit ≡ Keel Emergence (Slamming Factor)
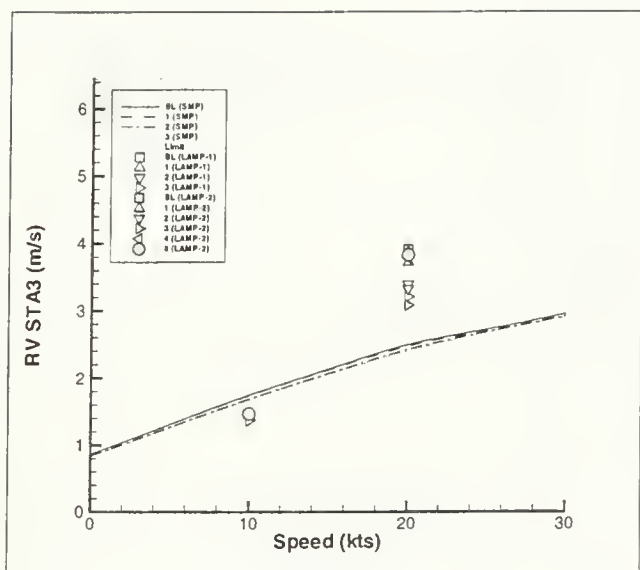
a. SS 4
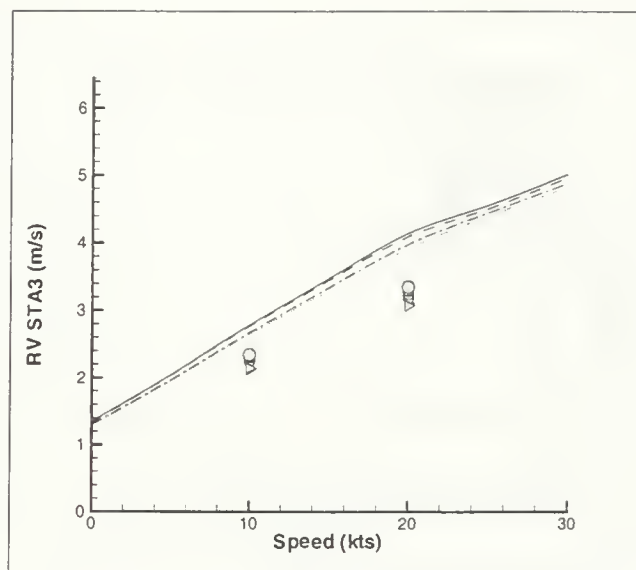
b. SS 5
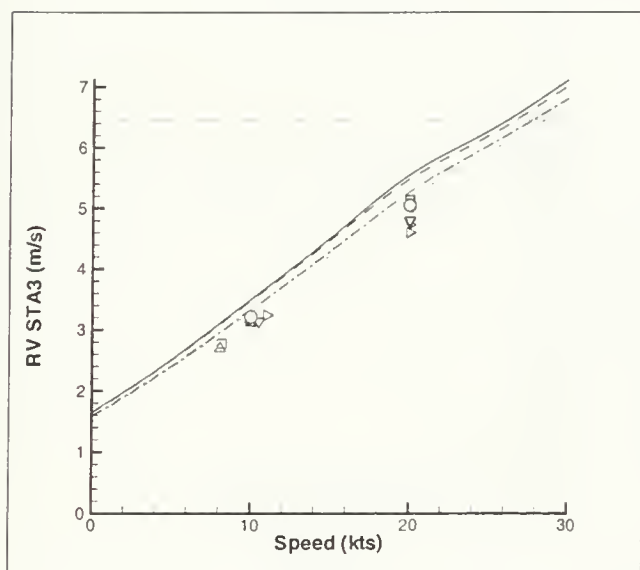
c. SS 6
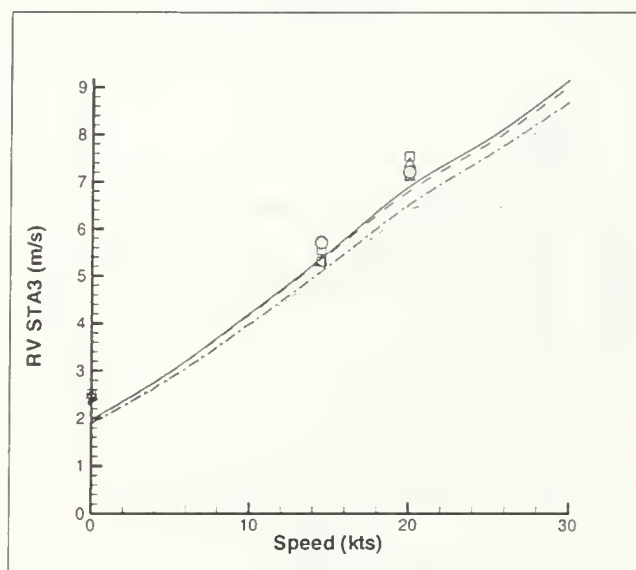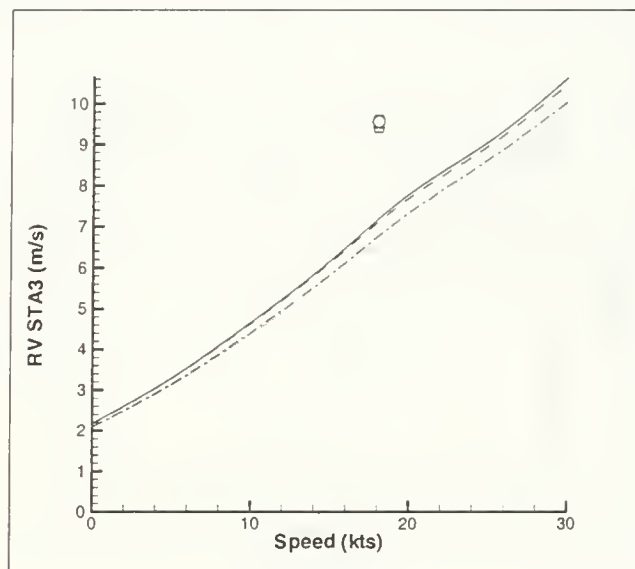
d. SS 7

e. SS 8

Figure 5-12: Mathematical Hull Relative Velocity STA3 (SIG SA), Limit ≡ Slamming Threshold Velocity

119
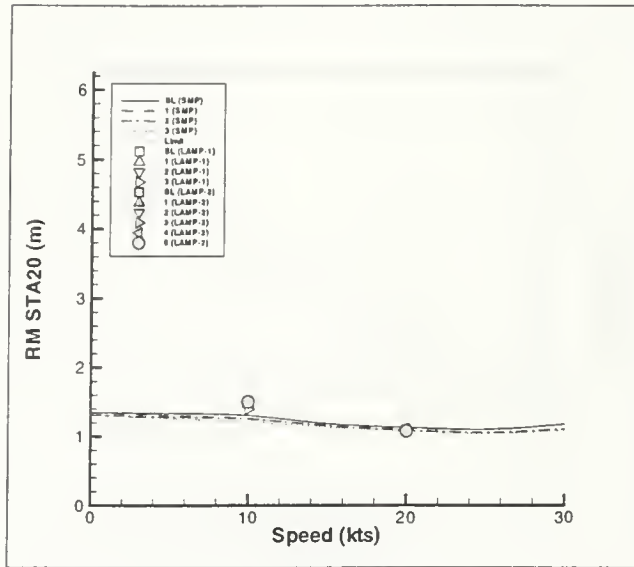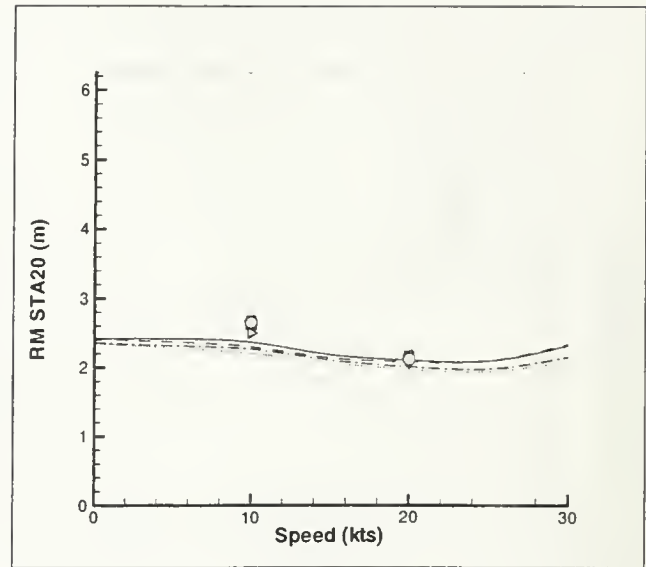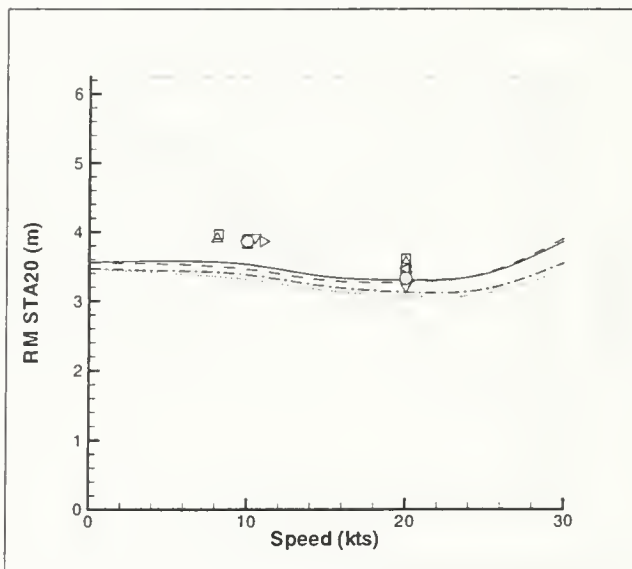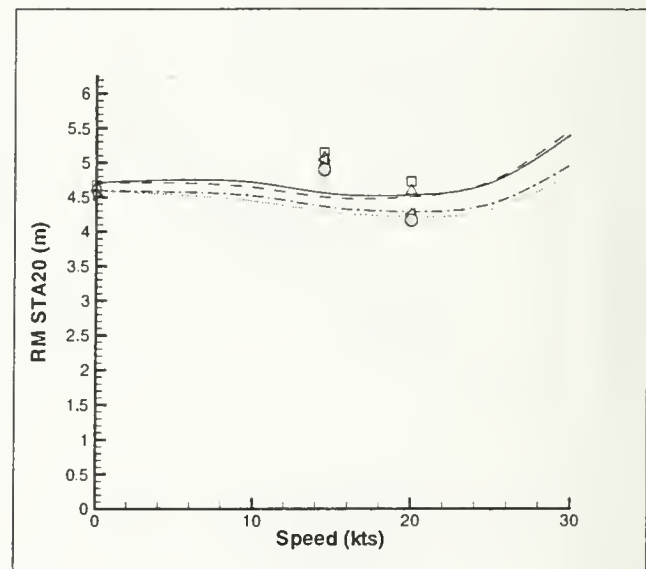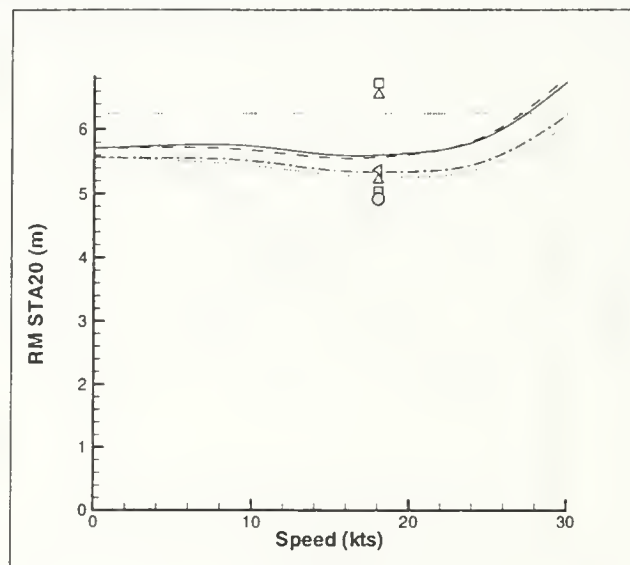
a. SS 4
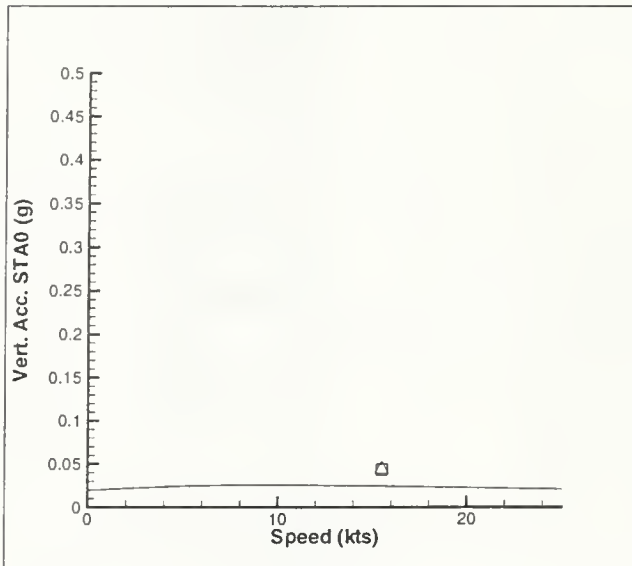
b. SS 5

c. SS 6

d. SS 7

e. SS 8

Figure 5-13: Mathematical Hull Relative Motion STA20 (SIG SA), Limit $\equiv$ Keel/Propeller Emmersion

120
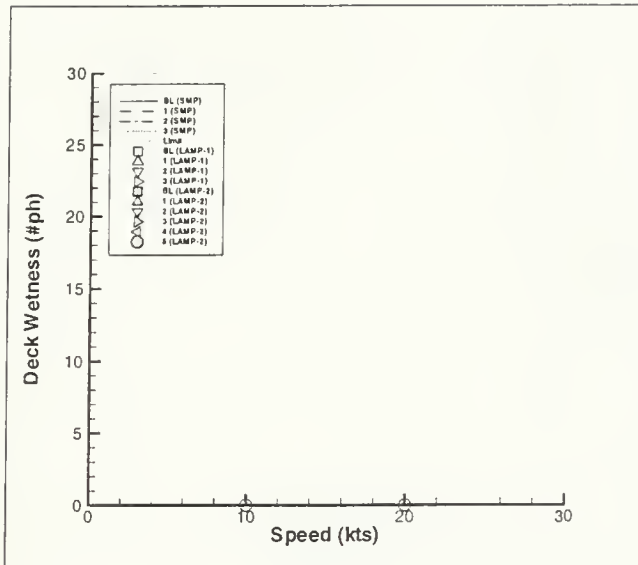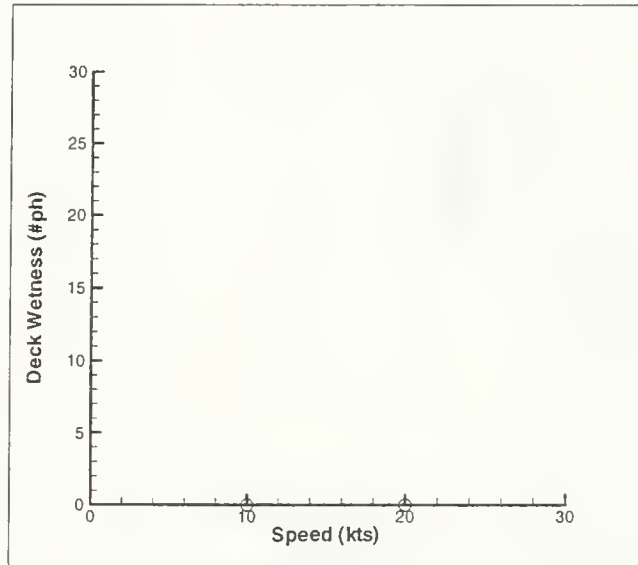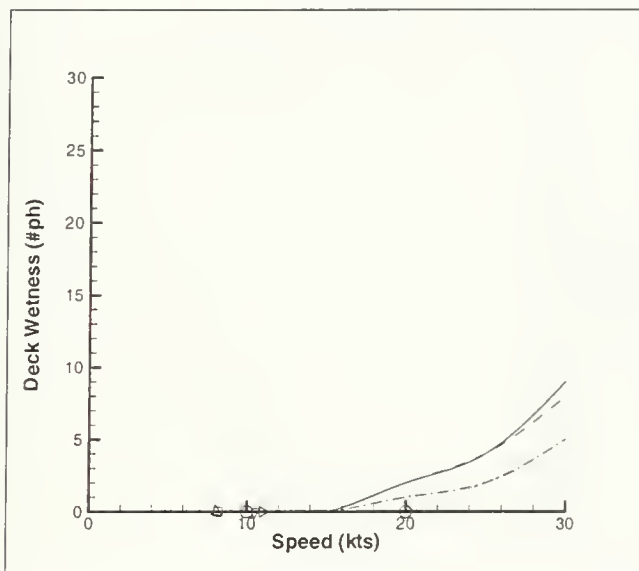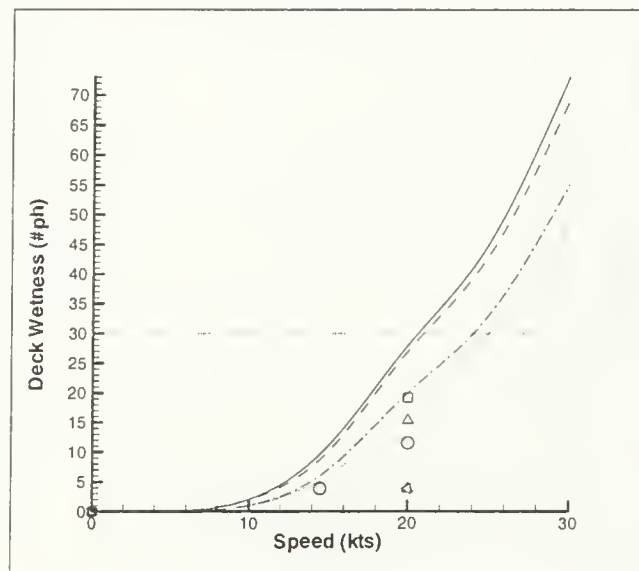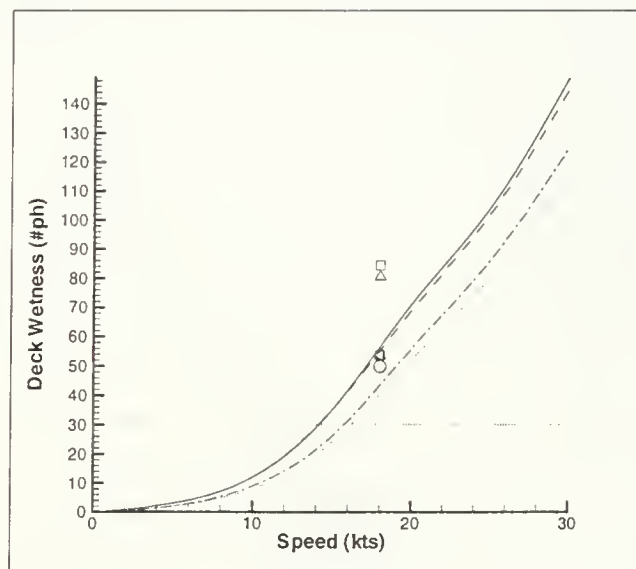
a. SS 4   b. SS 5

c. SS 6   d. SS 7

e. SS 8

Figure 5-14: Mathematical Hull Deck Wetness STA0 (SIG SA), Limit $\equiv$ Naval Transit Limit

121
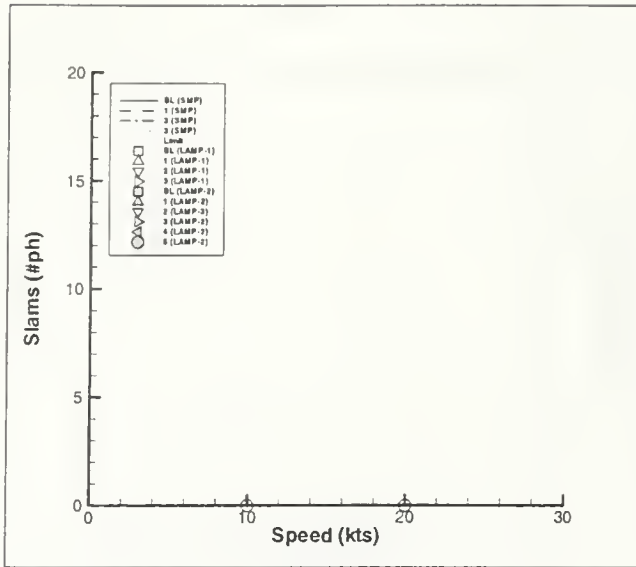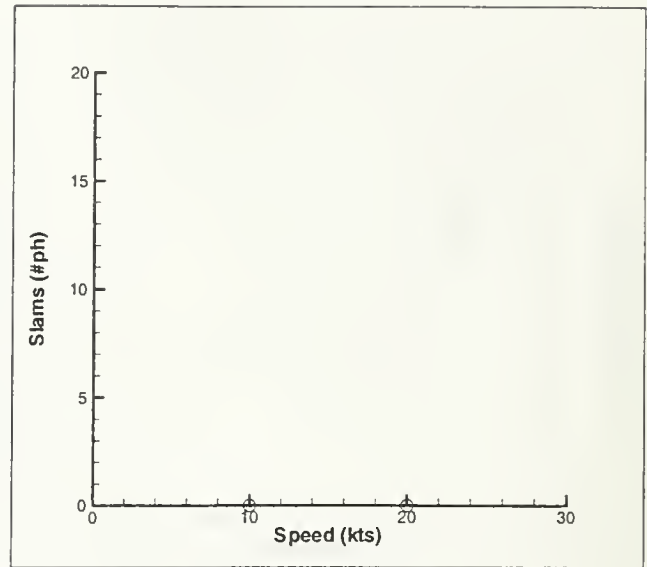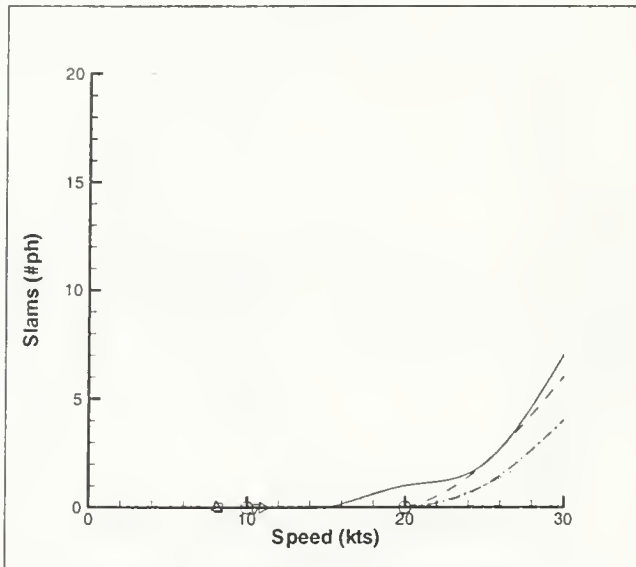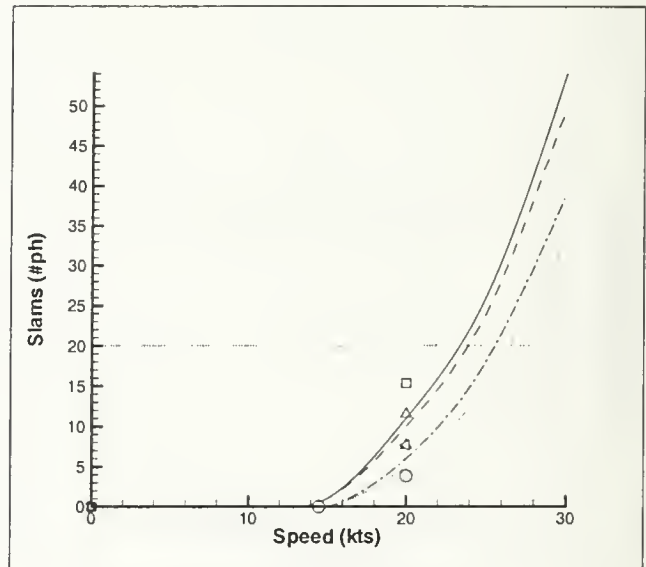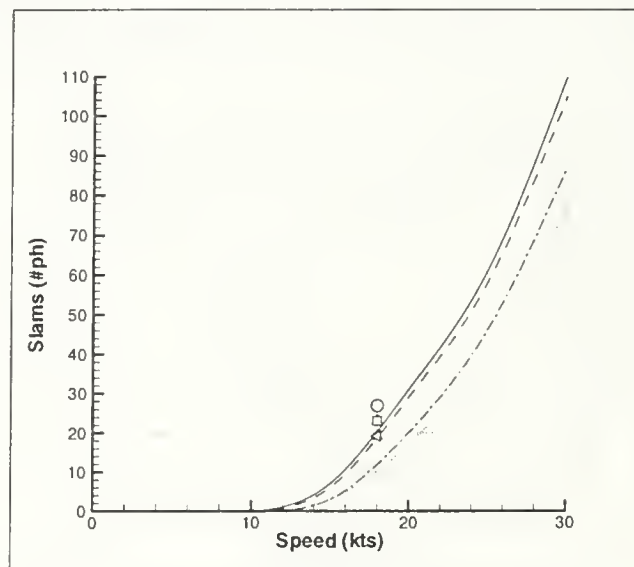
a. SS 4

b. SS 5

c. SS 6

d. SS 7

e. SS 8

Figure 5-15: Mathematical Hull Slamming STA3 (SIG SA), Limit ≡ Naval Transit Limit

122
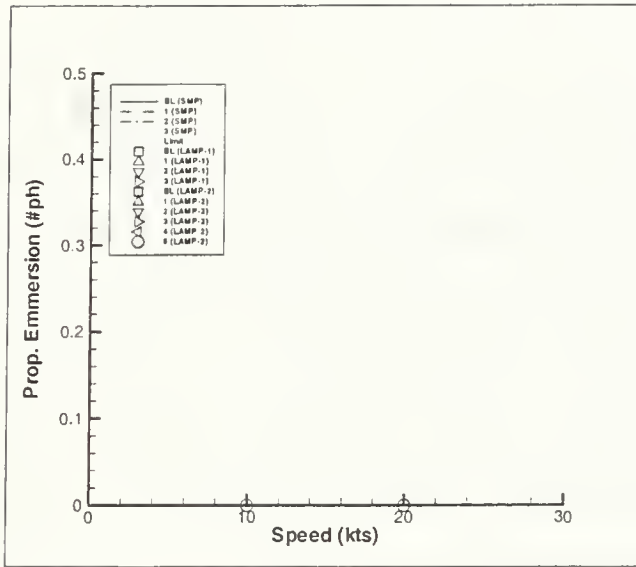
a. SS 4
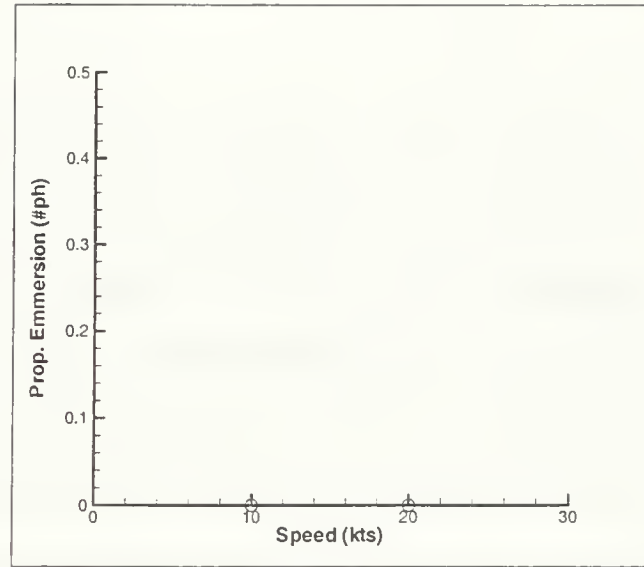
b. SS 5
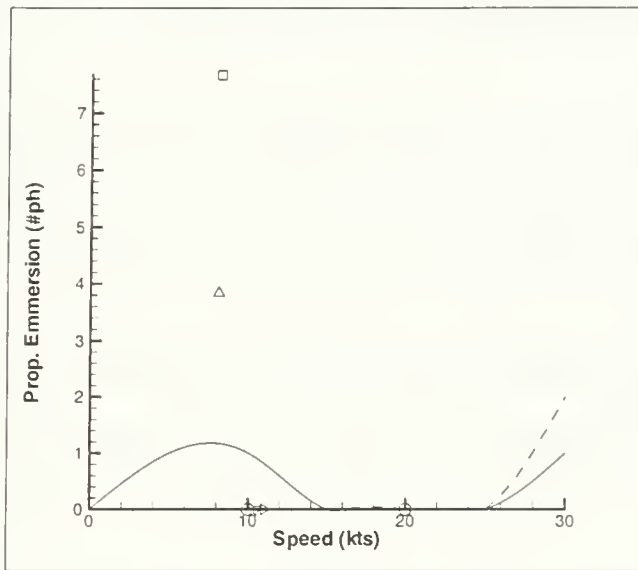
c. SS 6
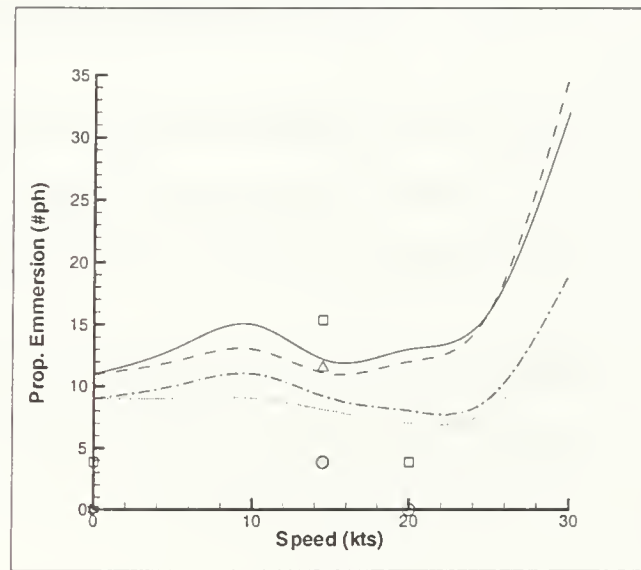
d. SS 7
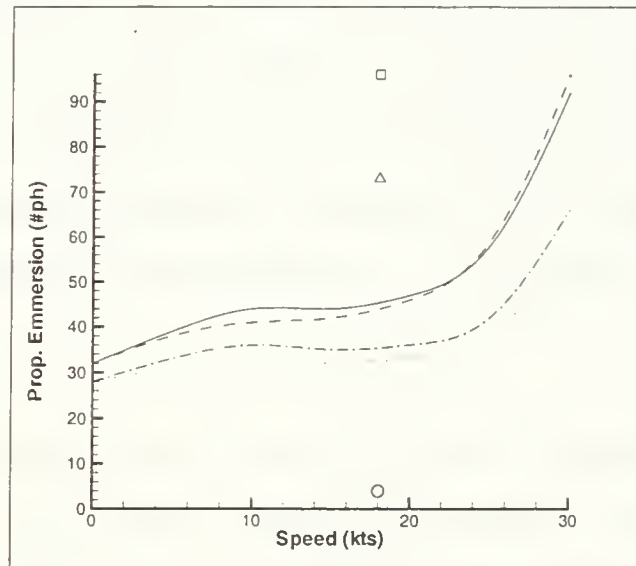
e. SS 8

Figure 5-16: Mathematical Hull Propeller Emmersion STA20 (SIG SA)

123

5.3 VLCC Predictions

All runs listed in Table 5.2 on page 87 were completed in LAMP-1 and LAMP-2. As with the mathematical hulls, runs in the smaller sea states (higher modal wave frequencies) were difficult. The SS5 run experienced similar problems with late instability, and the SS4 run became unstable so early that no data were extracted. As with the mathematical hulls, the use of the default time step for all conditions is the probable cause, and time step variation is needed. However, runs in SS5 and above provided sufficient data for a useful analysis. The SMP and LAMP irregular seas responses are plotted starting with Figure 5-17 on page 126.

The VLCC irregular seas responses suggest the following conclusions:

- Heave: The differences between LAMP-1 and 2 calculations are minor. However, both LAMP methods predict much larger heave responses – 60 to 100% higher. Heave motions are quite small until the severe sea states, 7 and 8.

- Pitch: Responses show similar trends to heave, with LAMP results 50 to 60% higher than SMP. LAMP-2 responses increase more rapidly than LAMP-1 responses, starting in SS6.

- Vertical Loads: LAMP overpredicts SMP, but less than for motions – approximately 20 to 40% for VSF4, 5 to 13% for VBM10, and 9 to 35% for VSF15. Comparisons are only valid for SS5 and 6, as LAMP SS4 runs were unsuccessful, and SMP SS7 and 8 values exceeded the output format specifications. Differences between LAMP-1 and 2 are negligible until SS8, where LAMP-2 predicts higher loads.

- Absolute and Relative Vertical Motions: Absolute vertical motions follow the same trends as heave and pitch motions. Relative motion trends are similar, although relative motion at STA0 increases more sharply with sea state than other responses. Relative velocity at STA3, a factor in slamming, is the only VLCC response in which LAMP predicts lower responses than SMP, until SS8.

Relative motion at the stern, STA20, has very small differences between LAMP and SMP, and very slow increase with sea state.

- Discrete Events: As with the mathematical hulls, using time domain methods to establish probabilities for events such as slamming, deck wetness, and propeller emmersion is difficult. LAMP predicts a higher incidence of deck wetness at SS7 and 8. Both LAMP and SMP predict no slamming events, even in SS8. As before, the propeller emmersion results have wide scatter in SS8, the only condition where they are predicted to occur.

As discussed earlier, no LAMP-4 runs were attempted, since the differences between LAMP-1 and 2 responses were quite small, even in sea state 8.
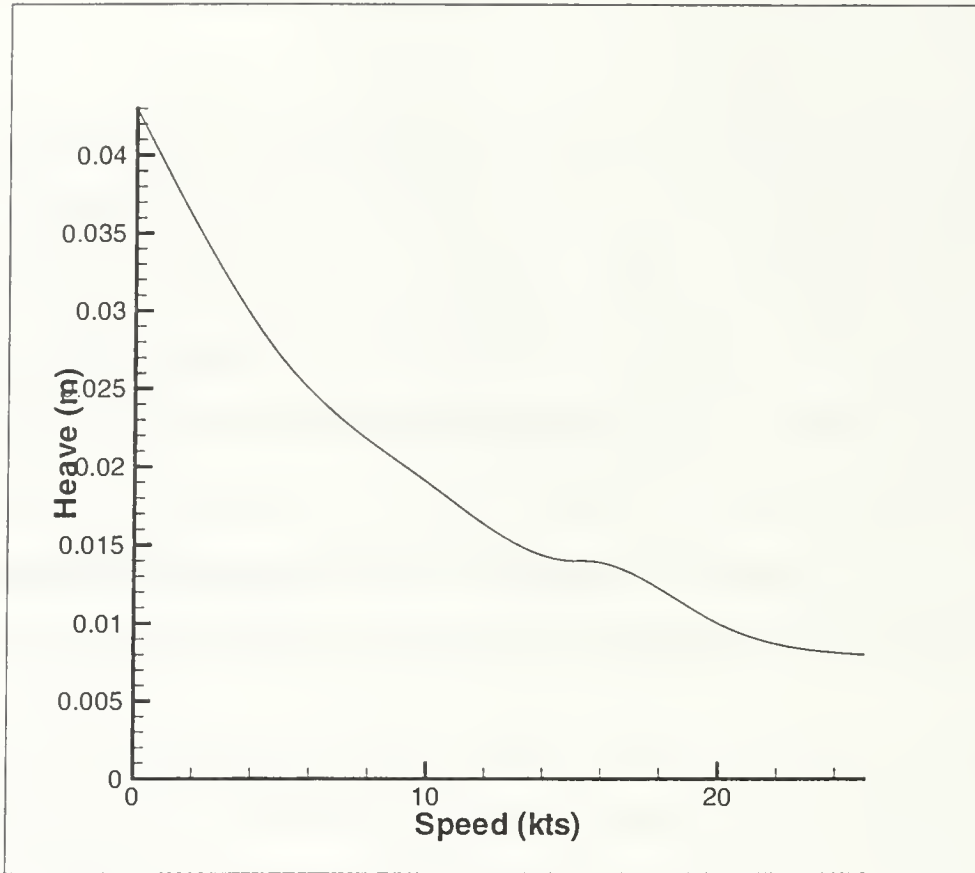
a. SS4
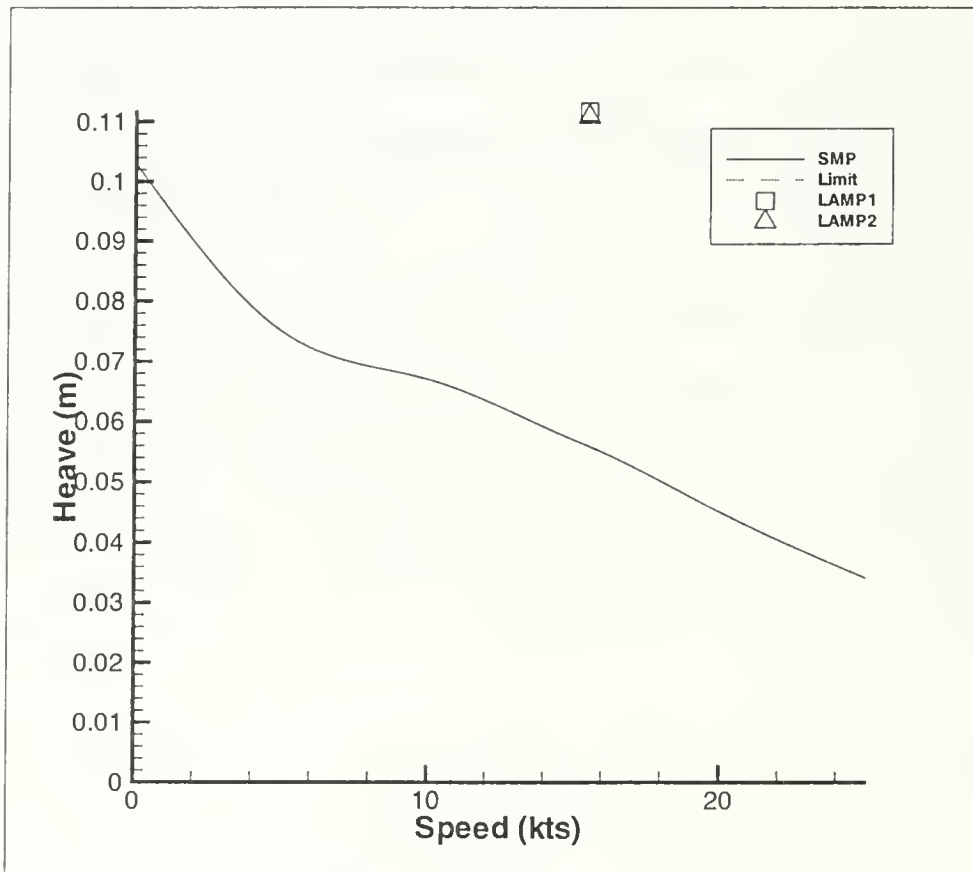
b. SS 5

Figure 5-17: VLCC Heave (RMS SA)
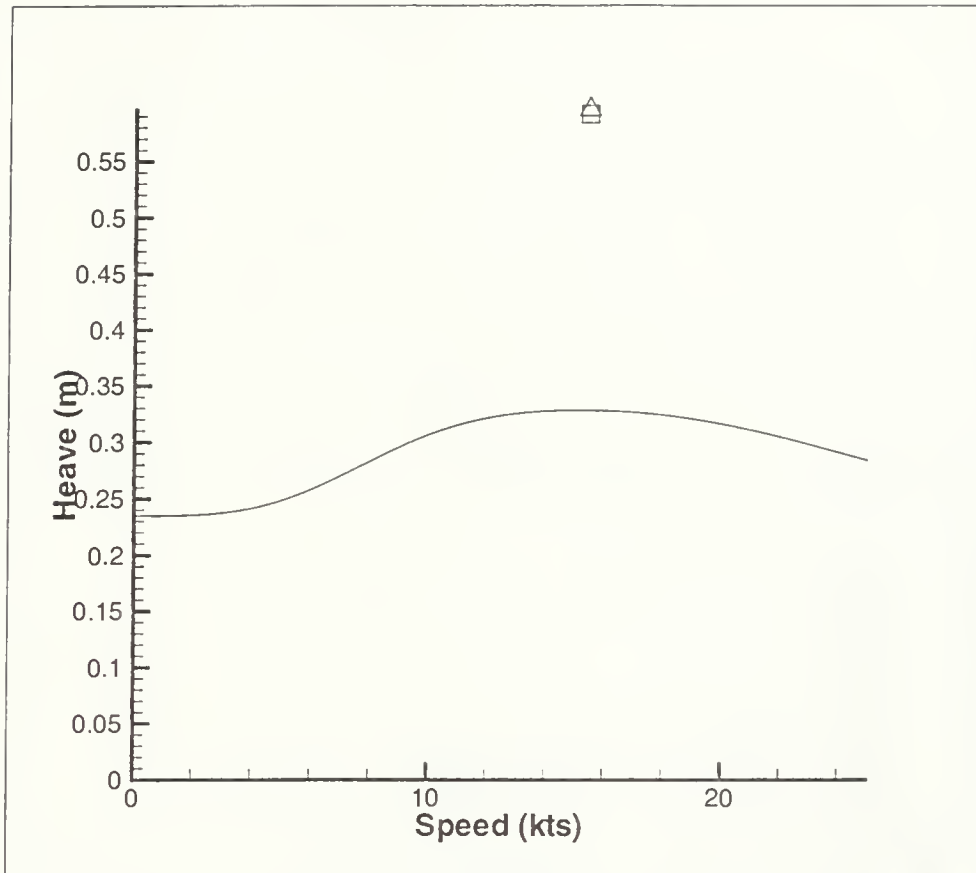
c. SS6
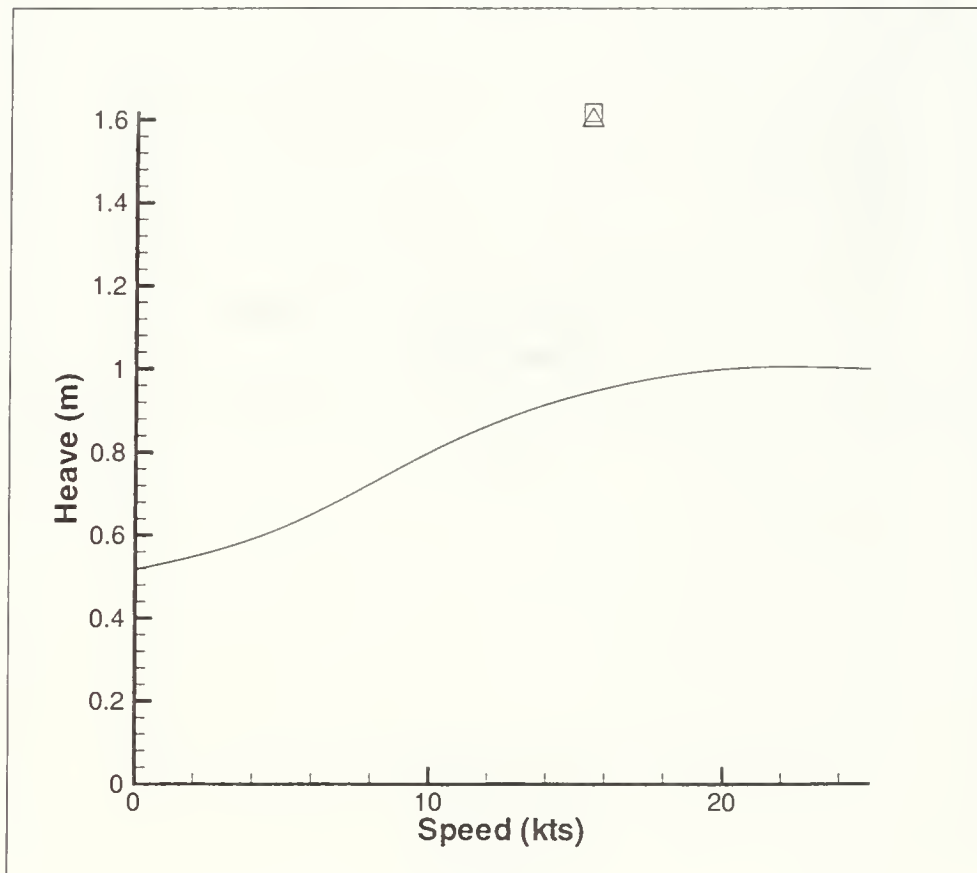
d. SS 7
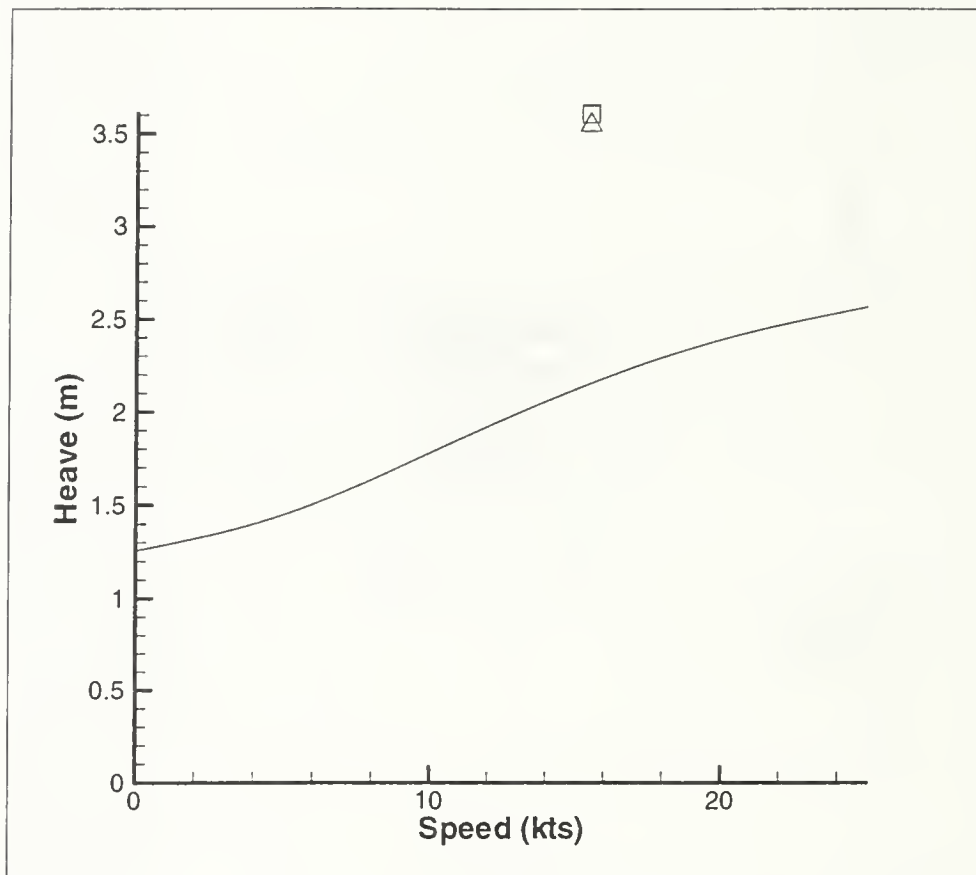
e. SS8
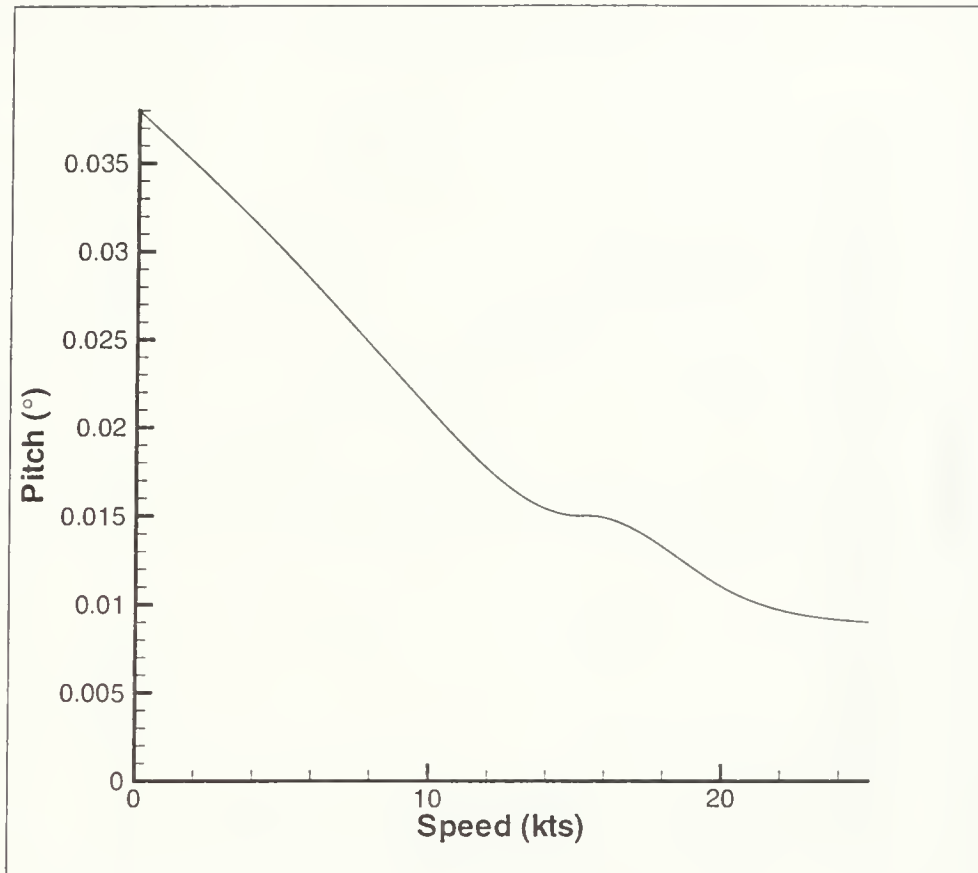
a. SS4
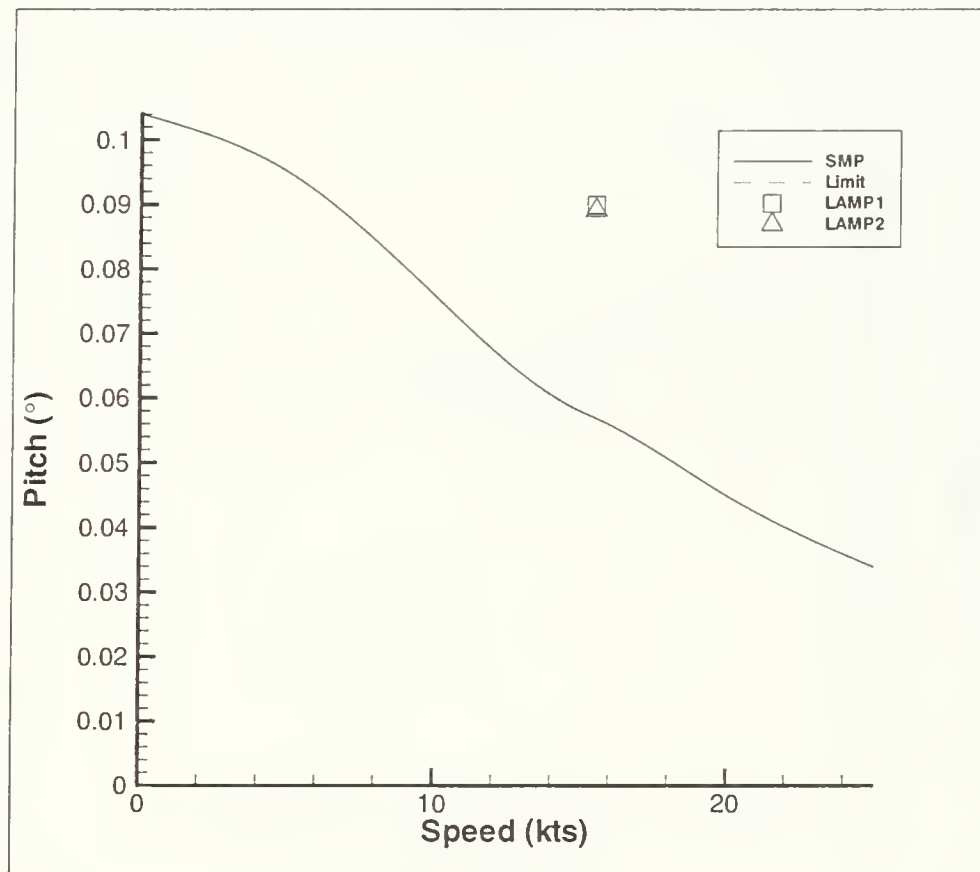
b. SS 5

Figure 5-18: VLCC Pitch (RMS SA)

129

c. SS6

d. SS 7

130

e. SS8

131
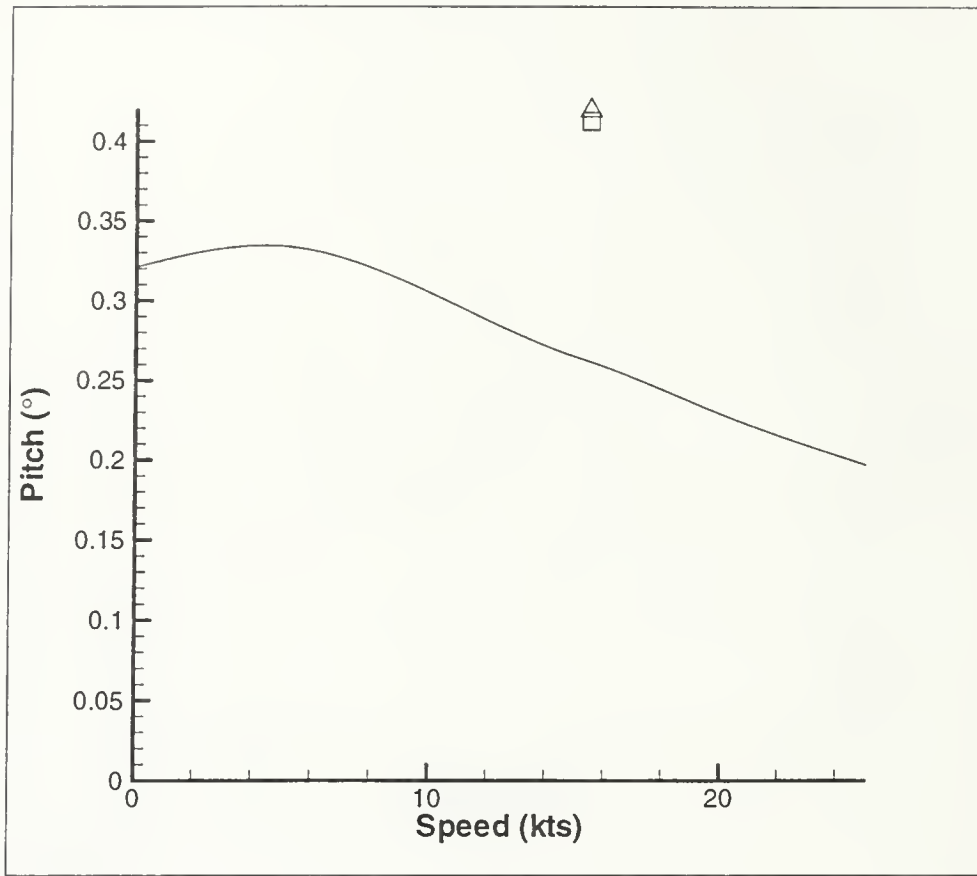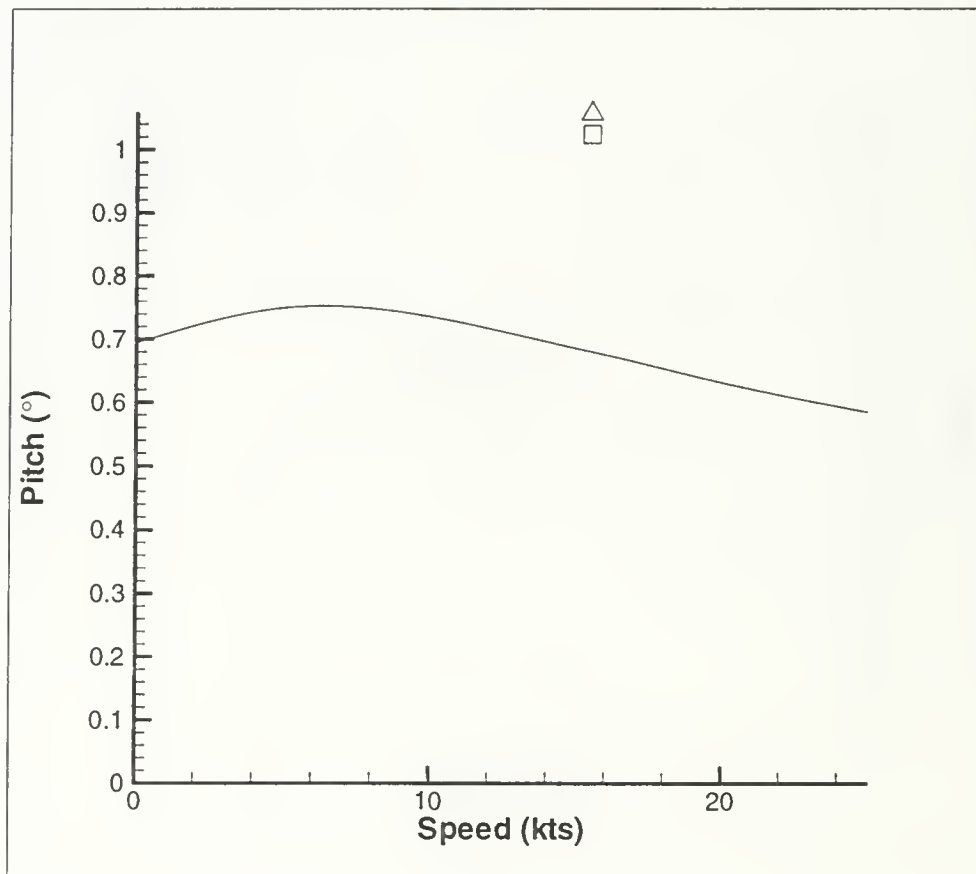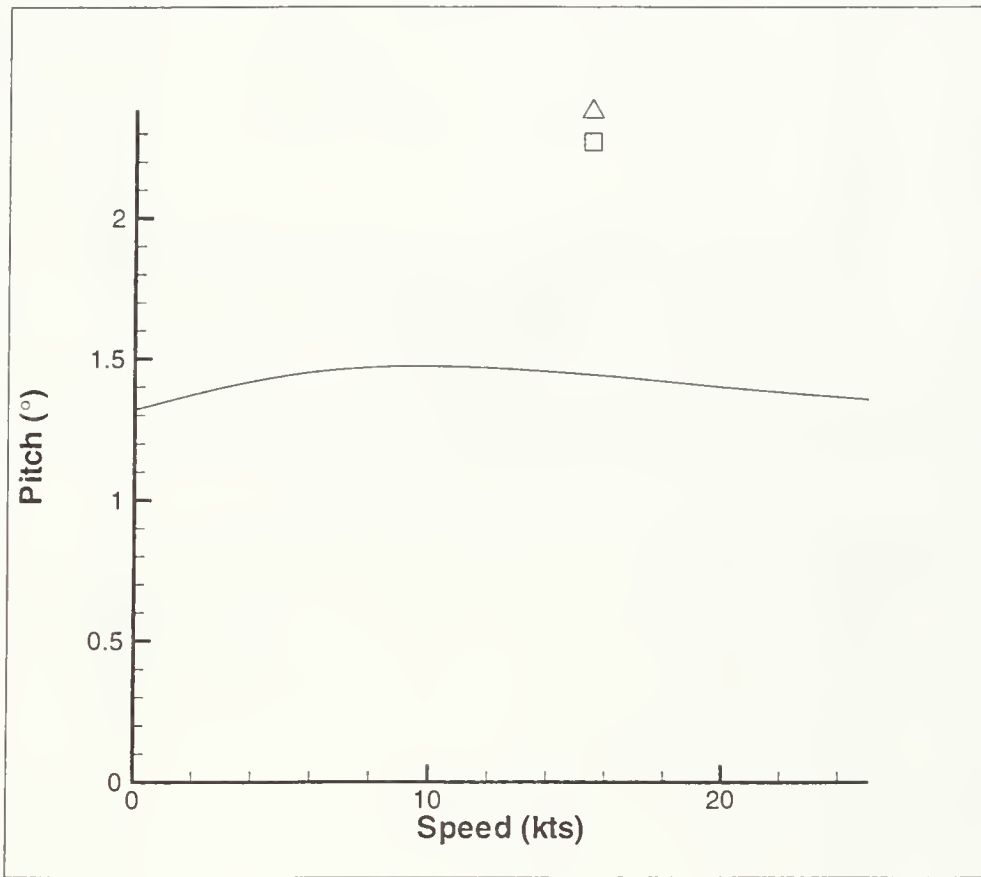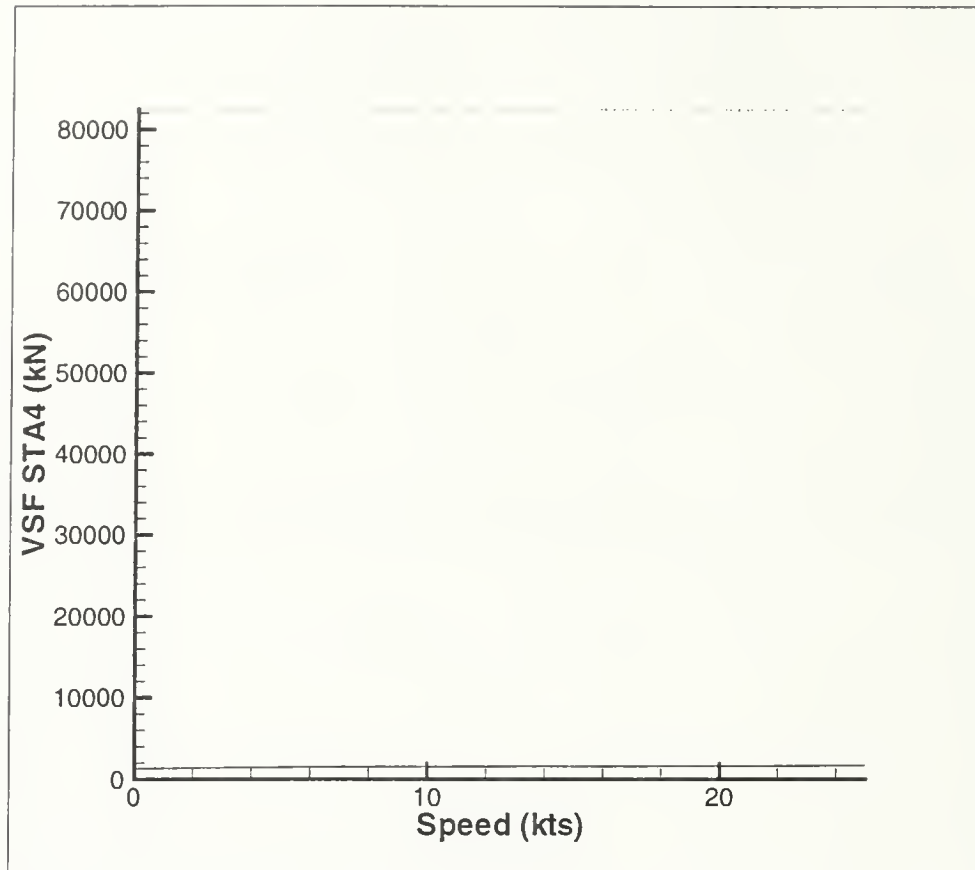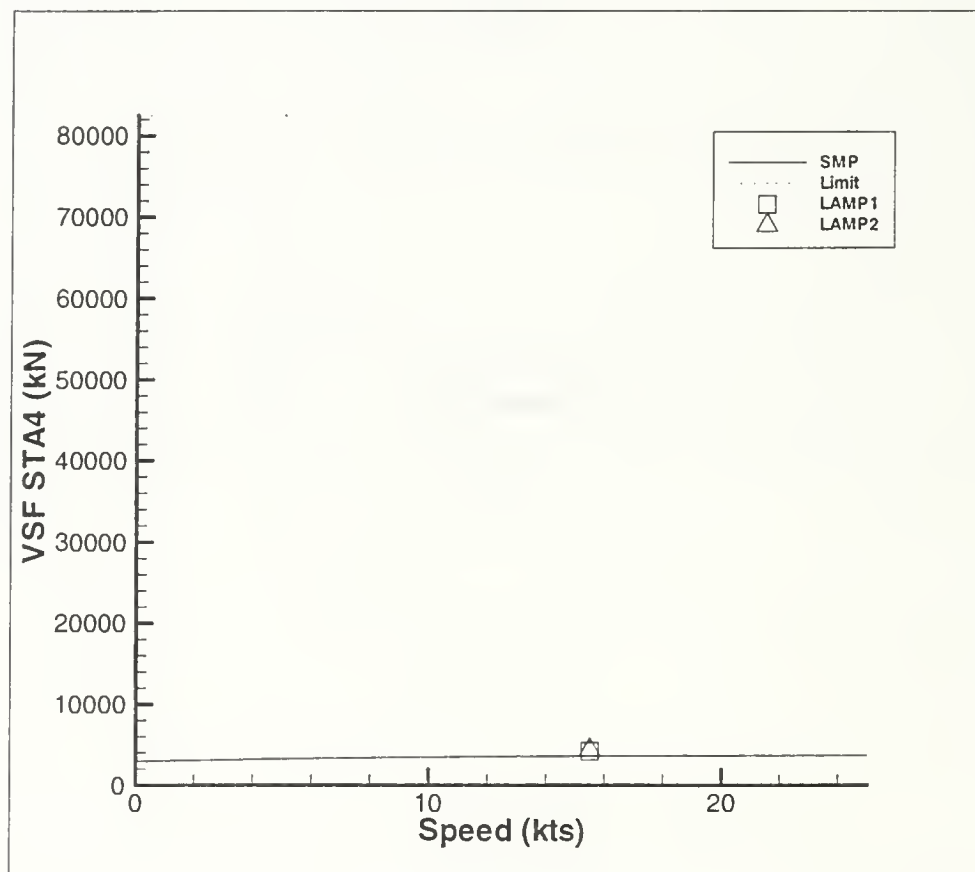
a. SS4

b. SS 5

Figure 5-19: VLCC Vertical Shear Force STA5 (RMS SA), Limit $\equiv$ ABS Design Value for Hog

c. SS6

d. SS 7

133

e. SS8

134
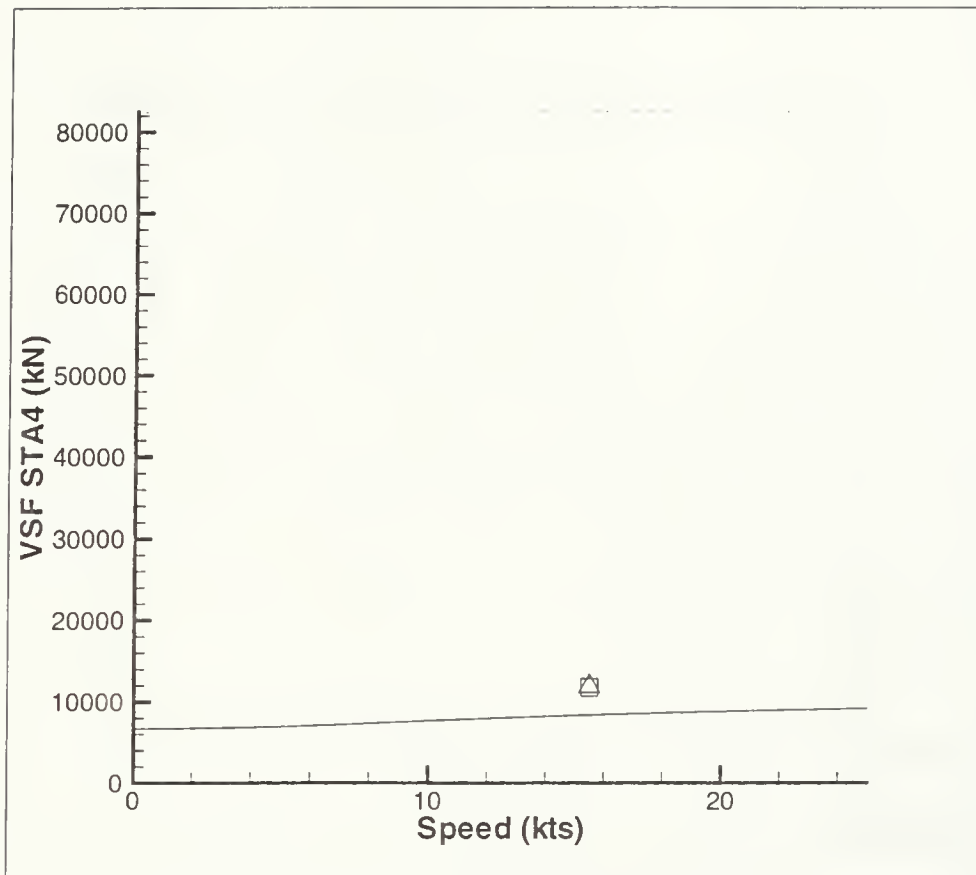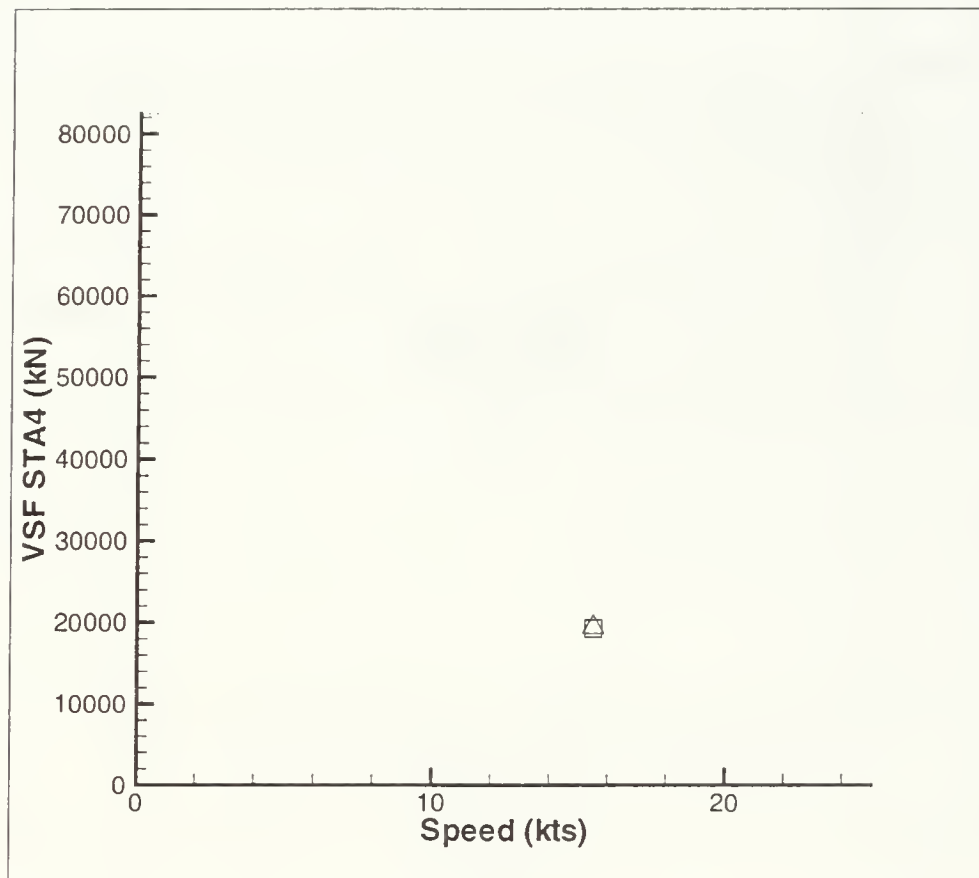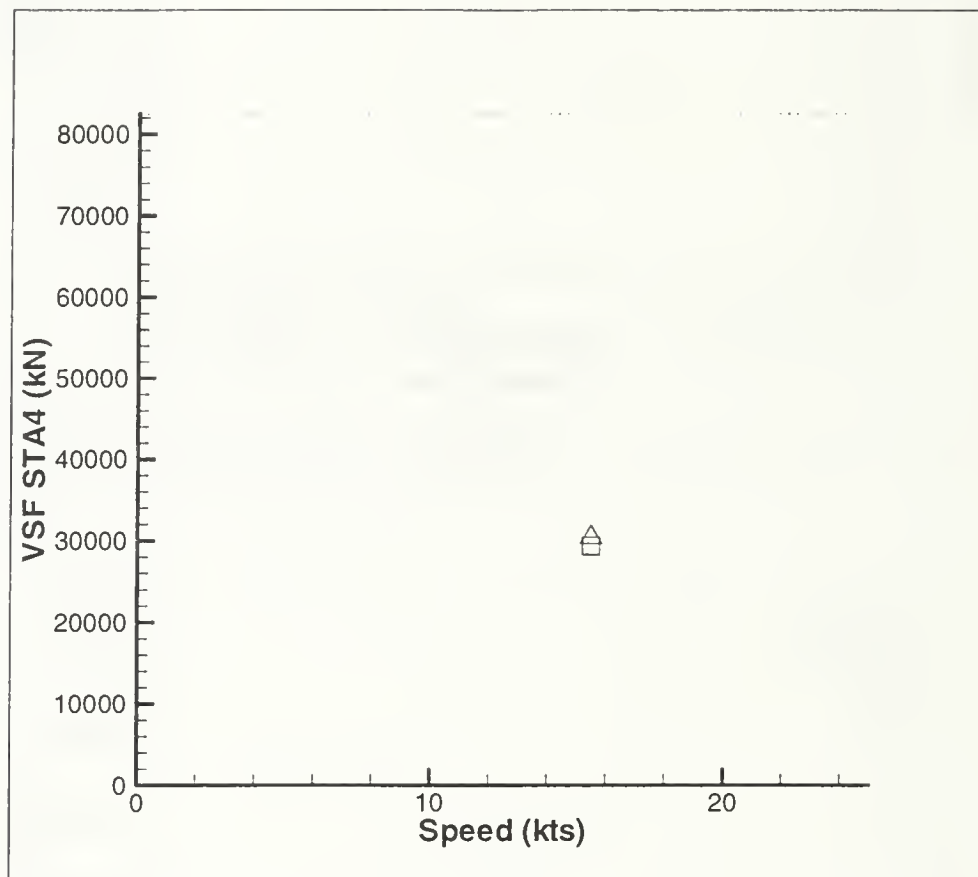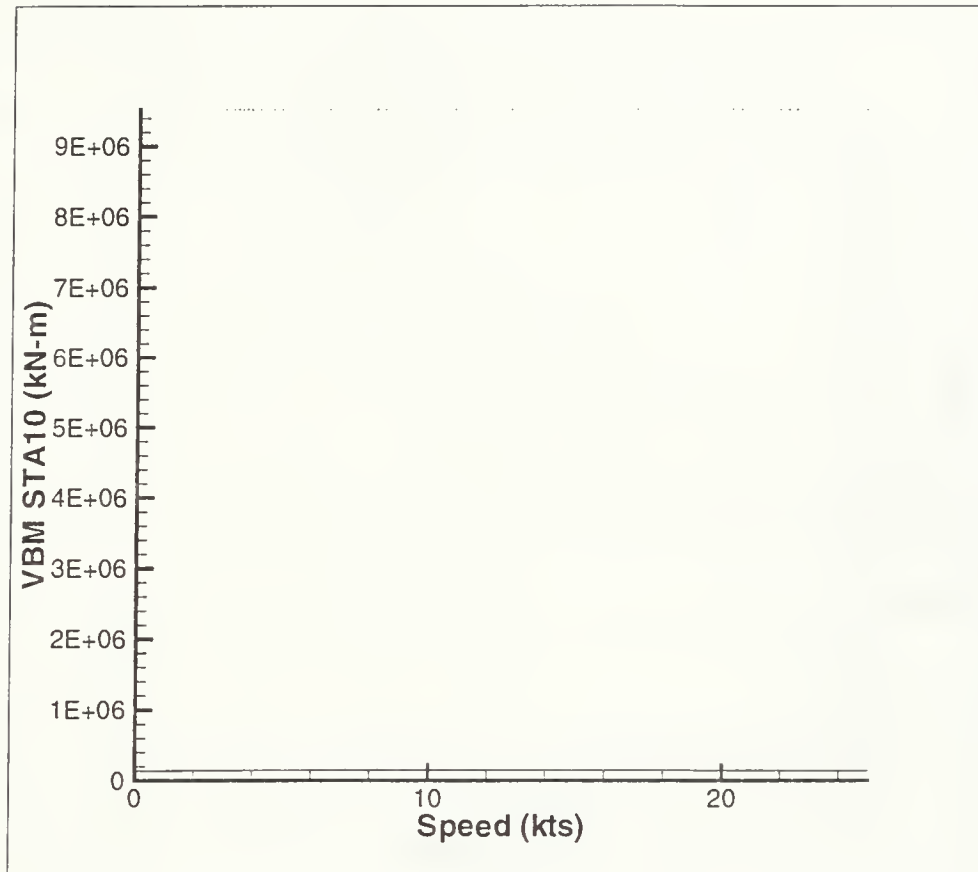
a. SS4

b. SS 5

Figure 5-20: VLCC Vertical Bending Moment STA10 (RMS SA), Limit ≡ ABS Design Value for Hog
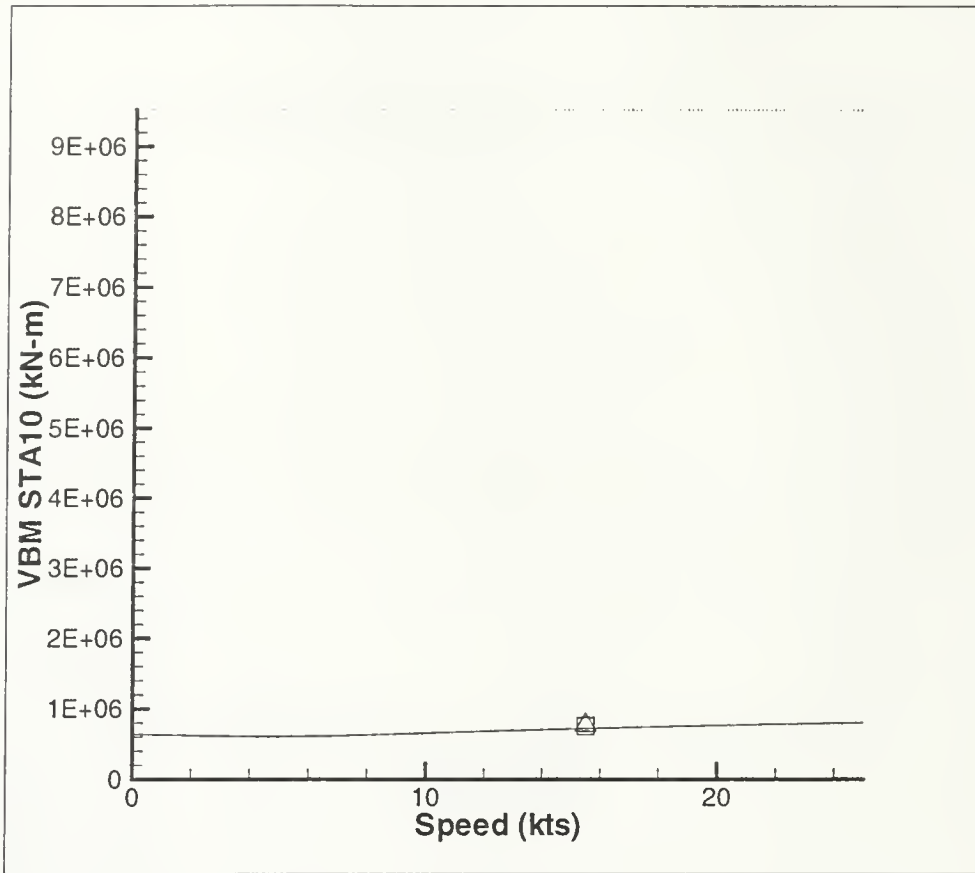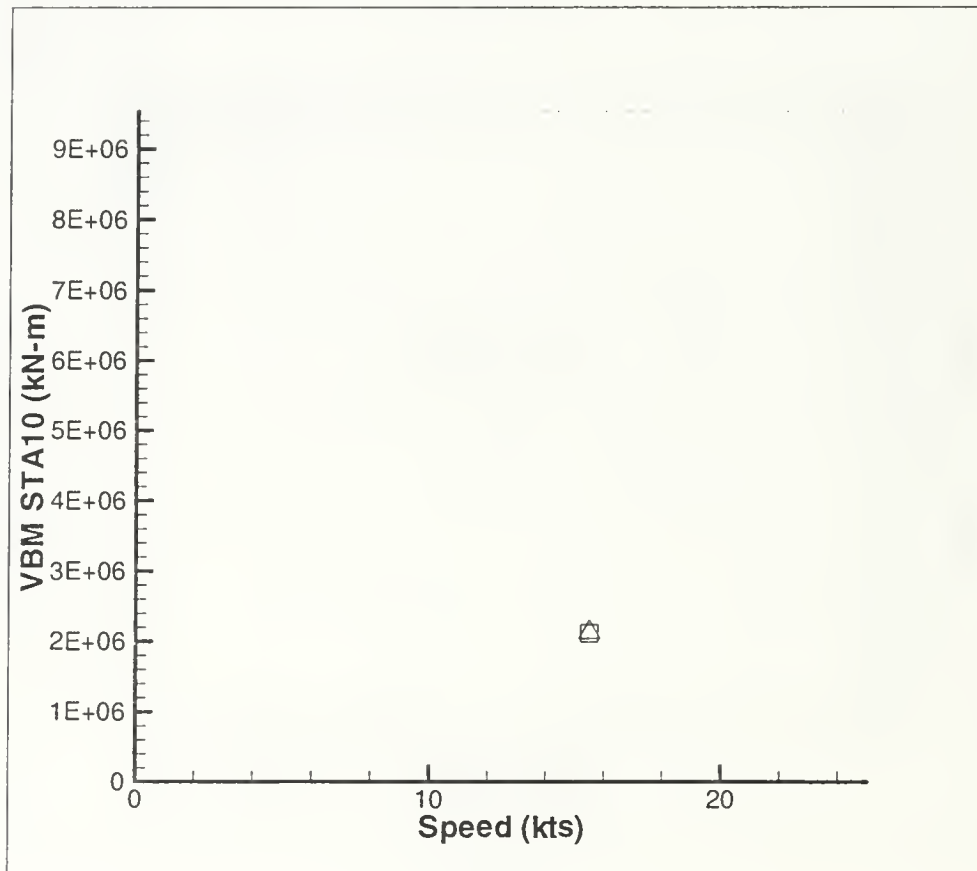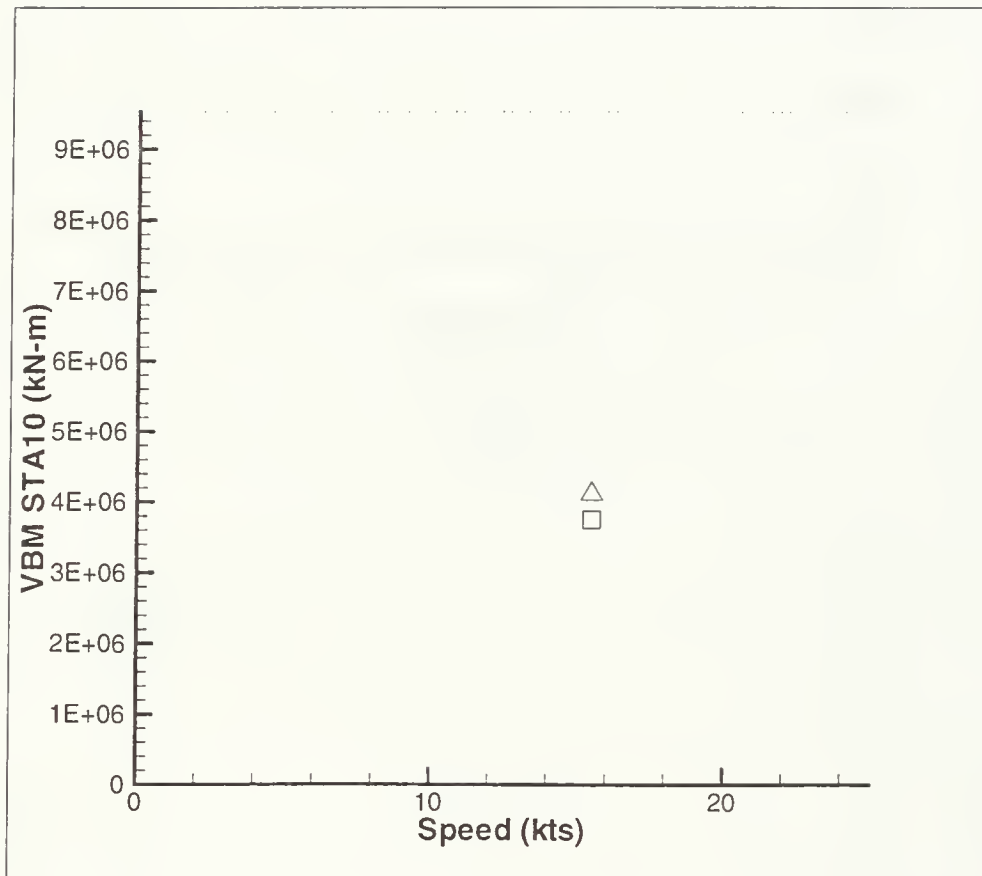
c. SS6

d. SS 7

e. SS8
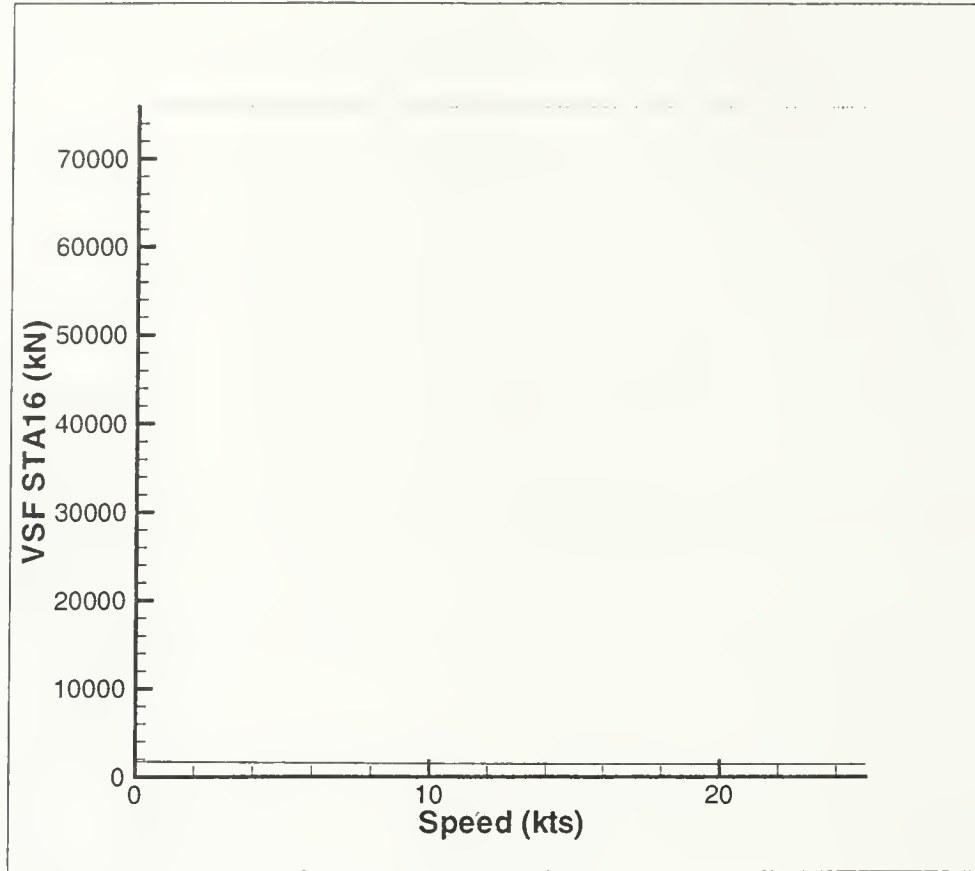
a. SS4
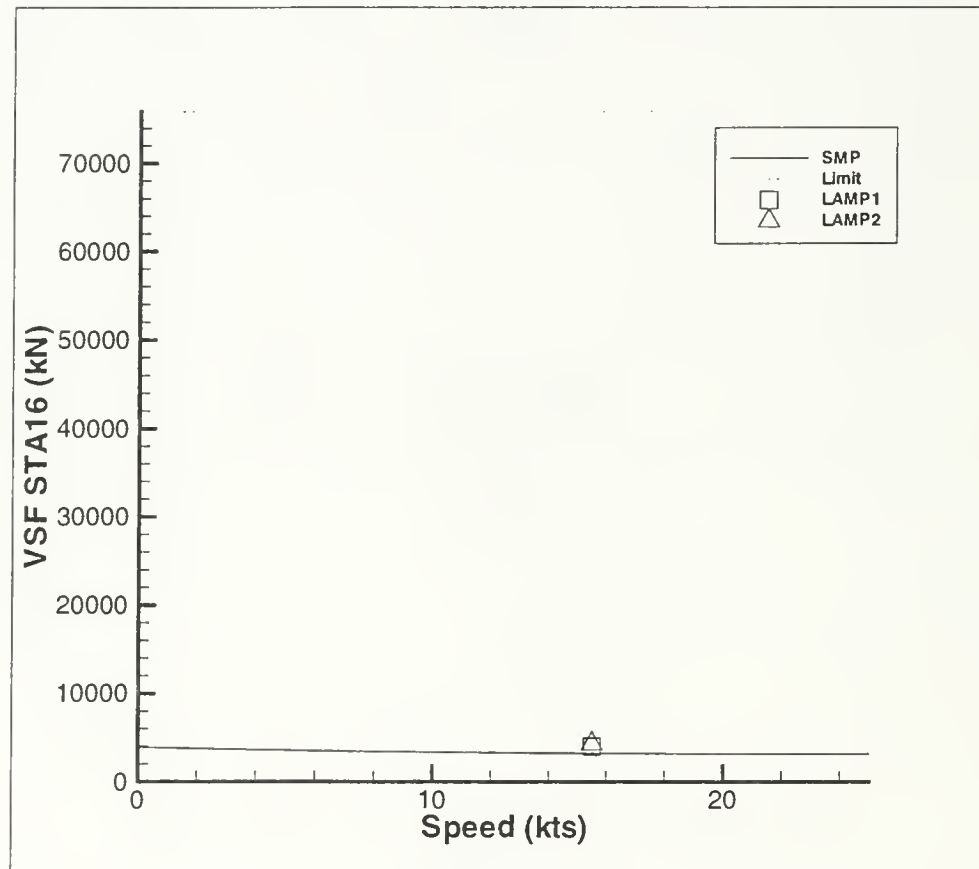
b. SS 5

Figure 5-21: VLCC Vertical Shear Force STA15 (RMS SA), Limit $\equiv$ ABS Design Value for Hog
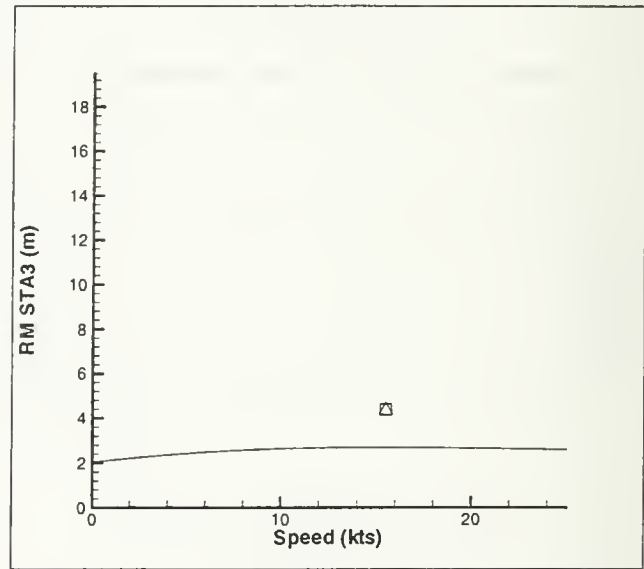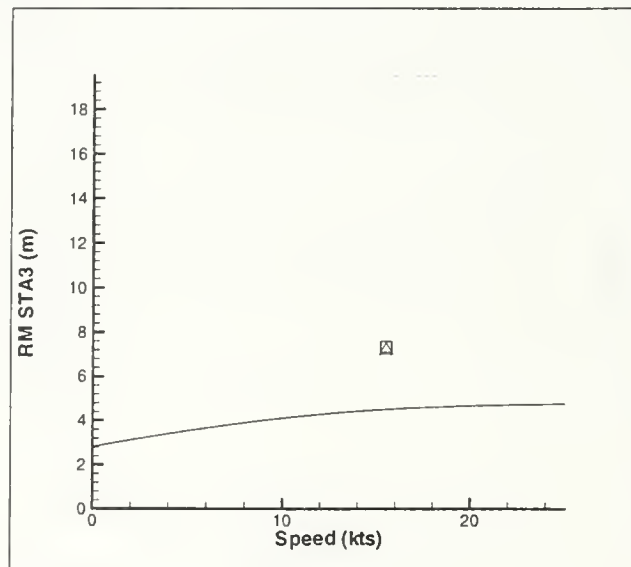
c. SS6

d. SS 7

139
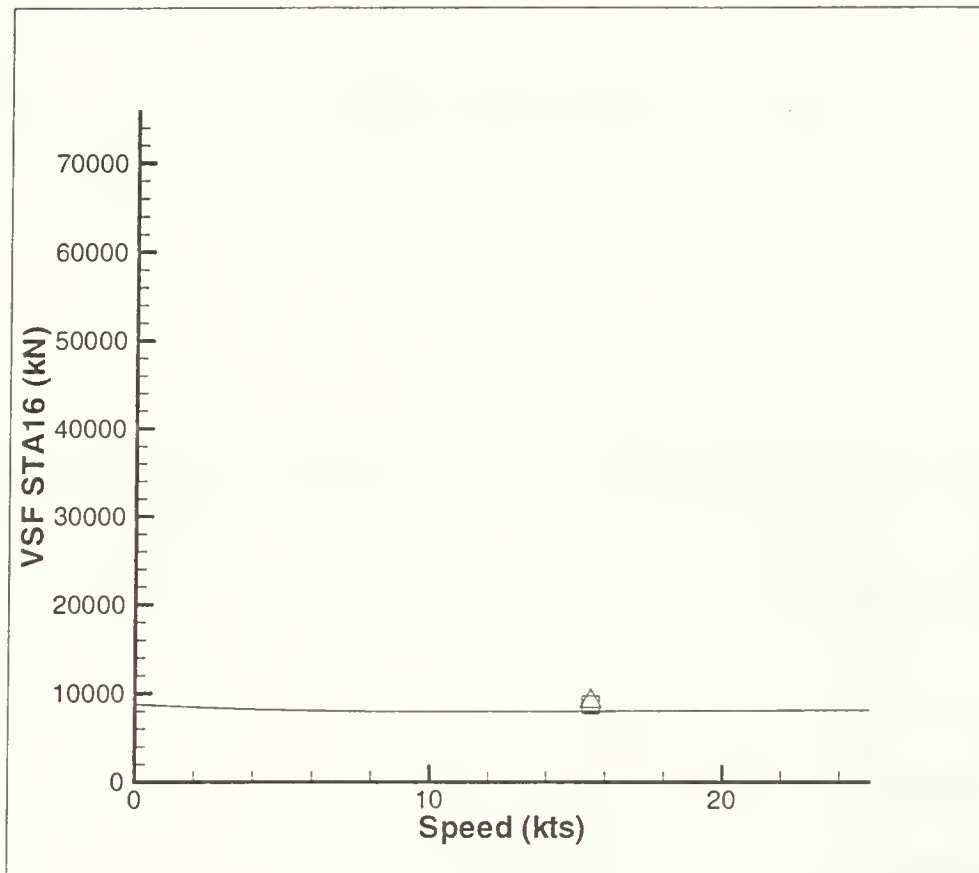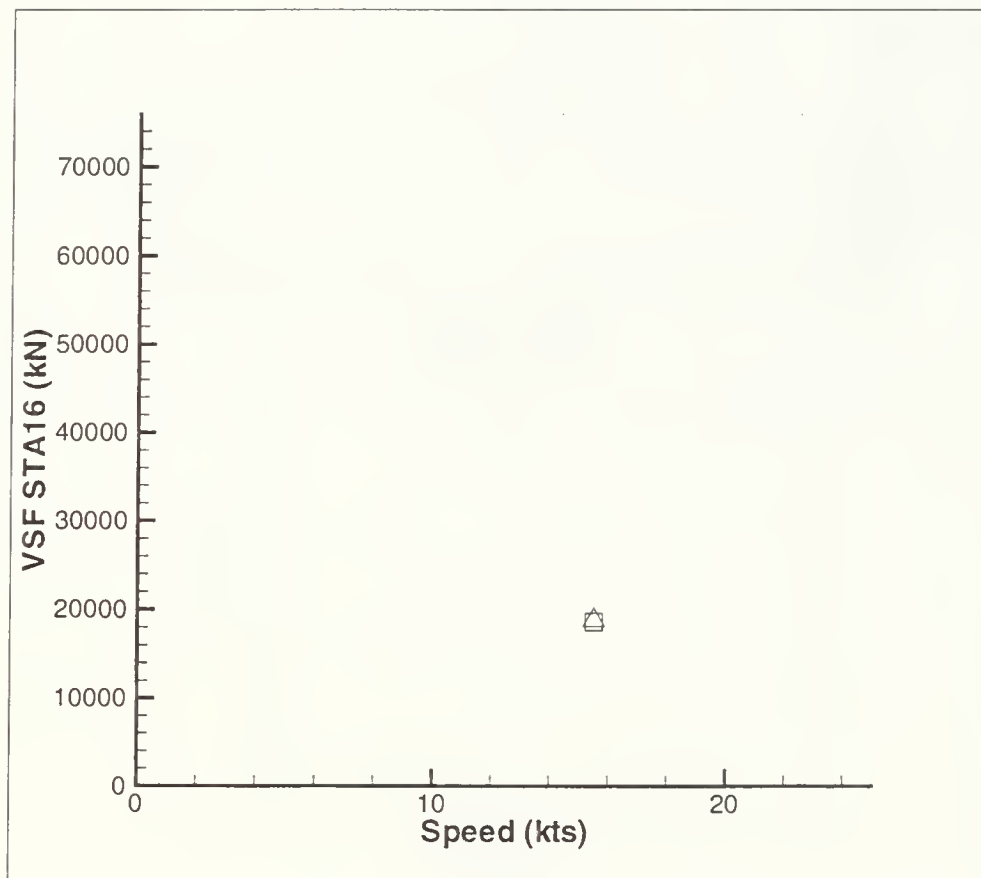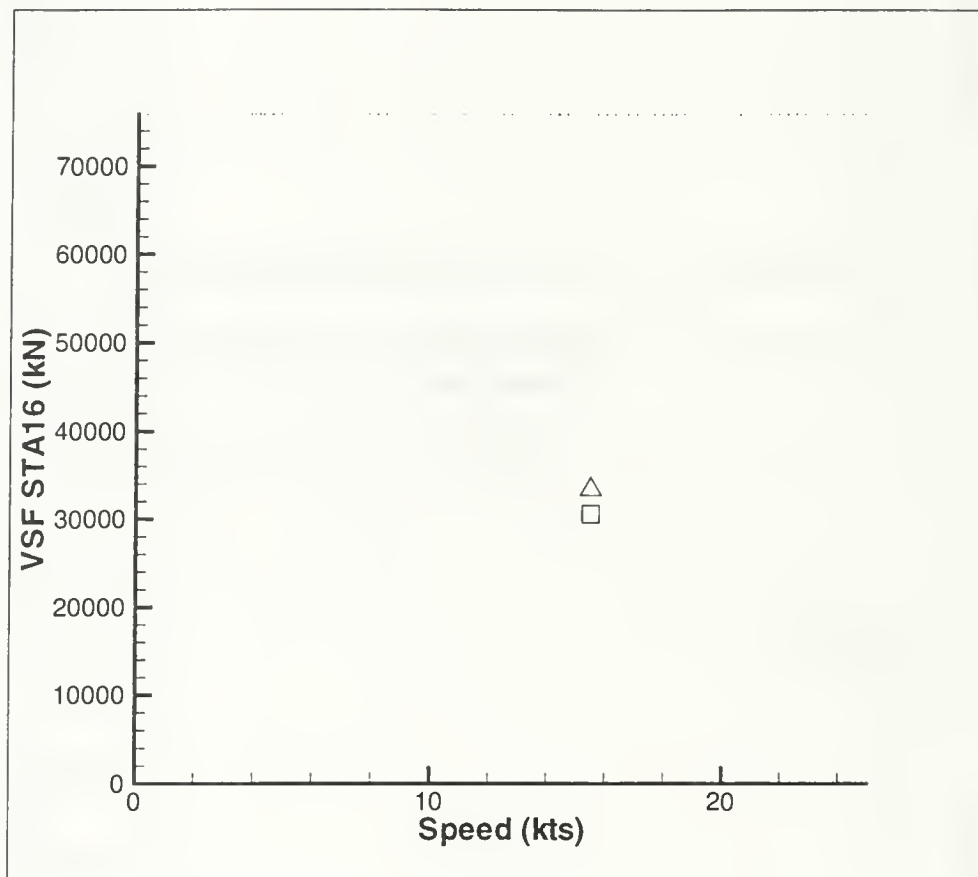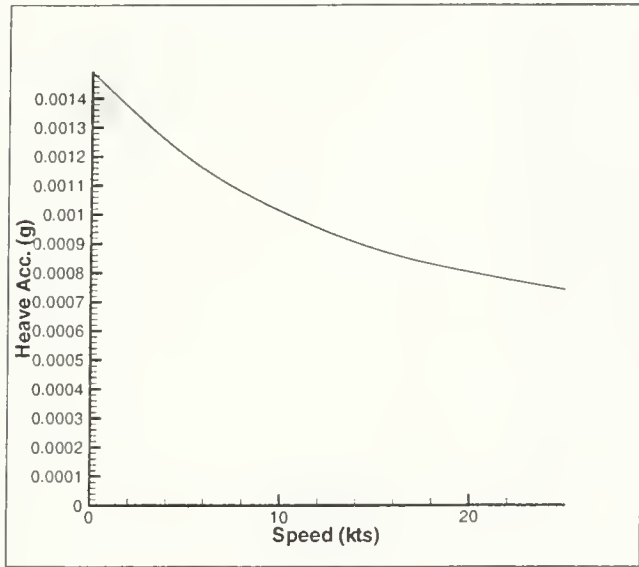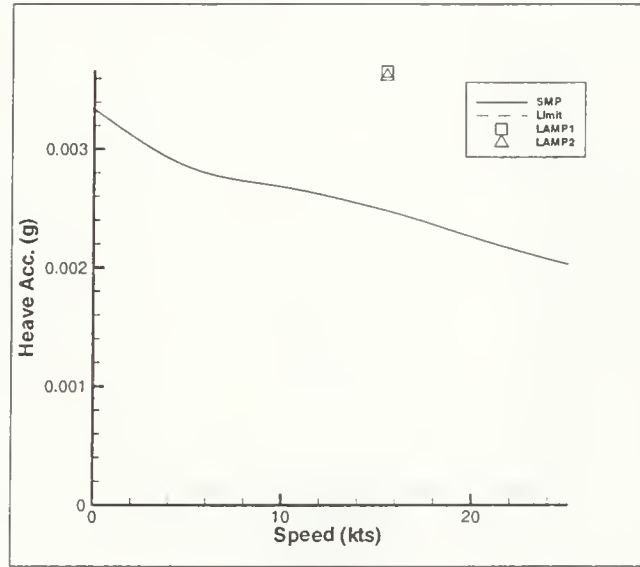
e. SS8
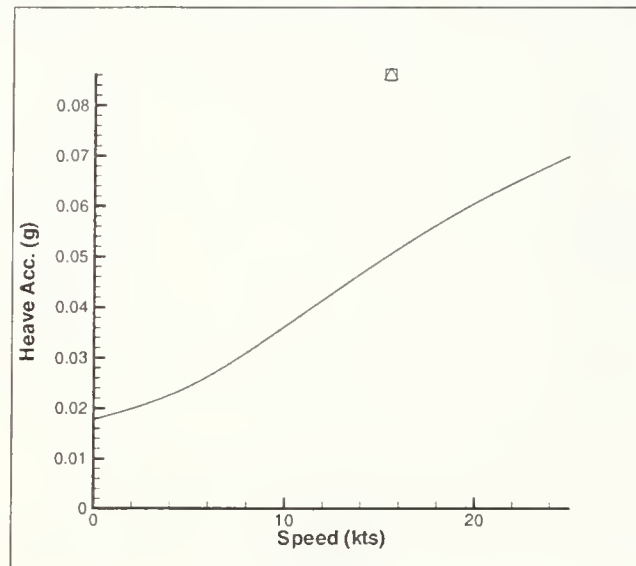
a. SS 4   b. SS 5

c. SS 6   d. SS 7

e. SS 8

Figure 5-22: VLCC Heave Acceleration (RMS SA)
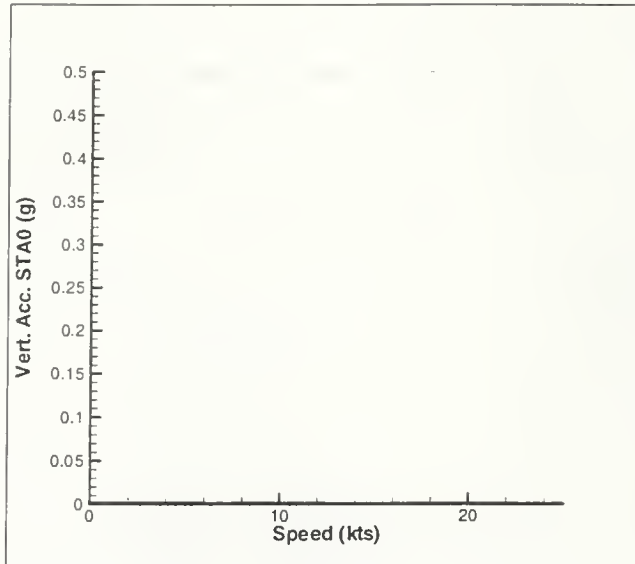
a. SS 4
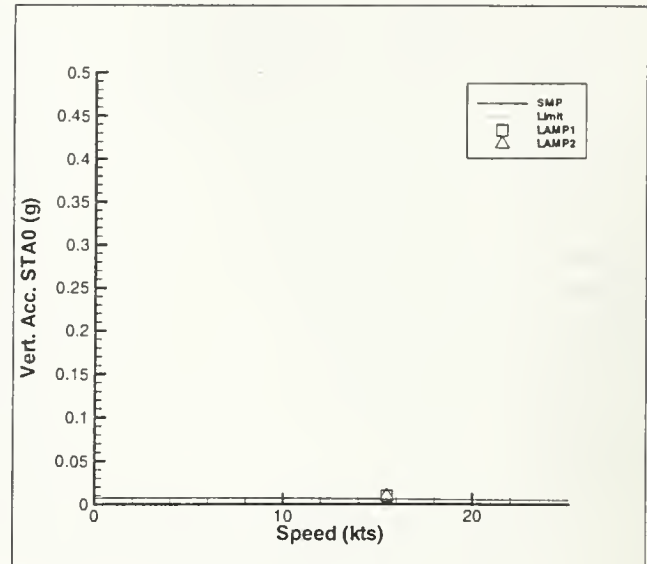
b. SS 5

c. SS 6
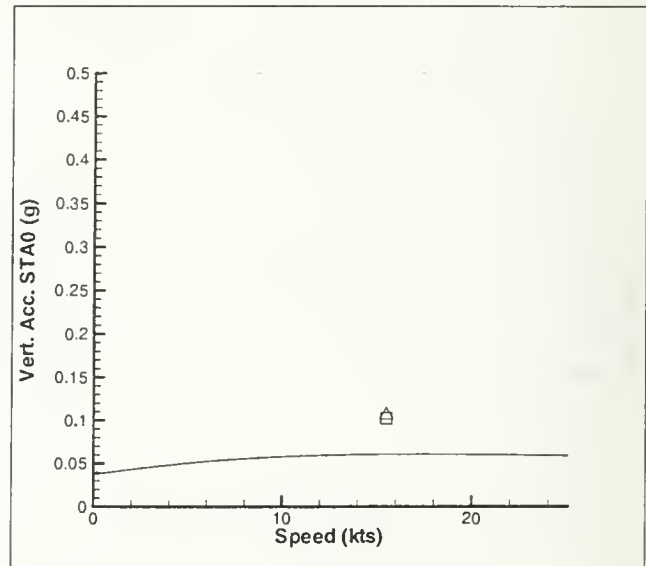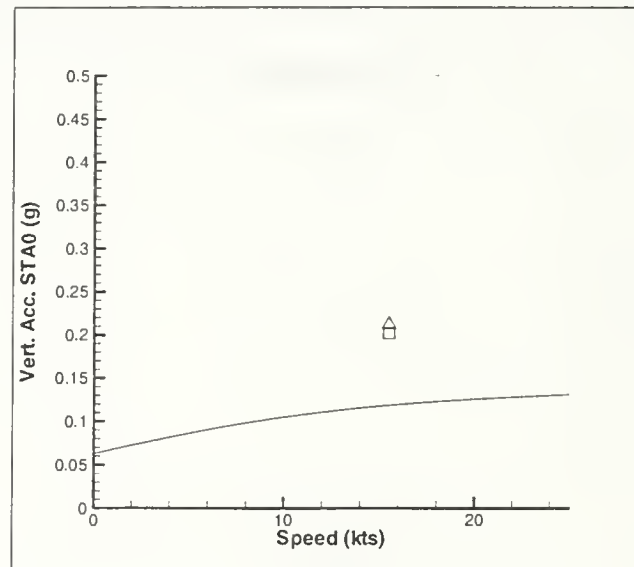
d. SS 7

e. SS 8

Figure 5-23: VLCC Vertical Acceleration STA0 (RMS SA)
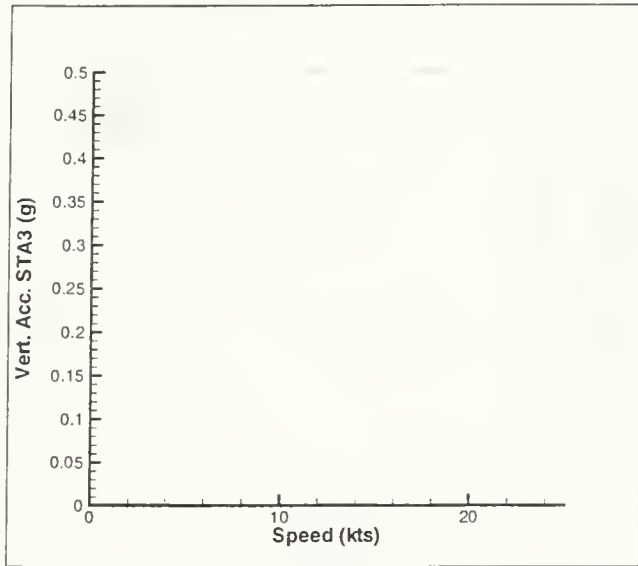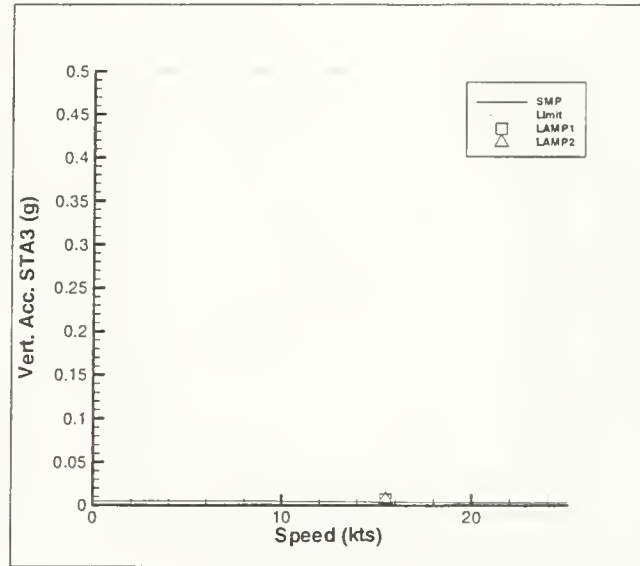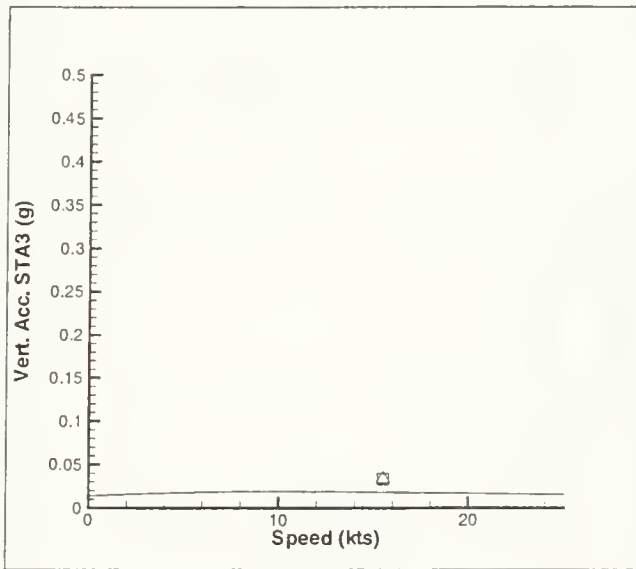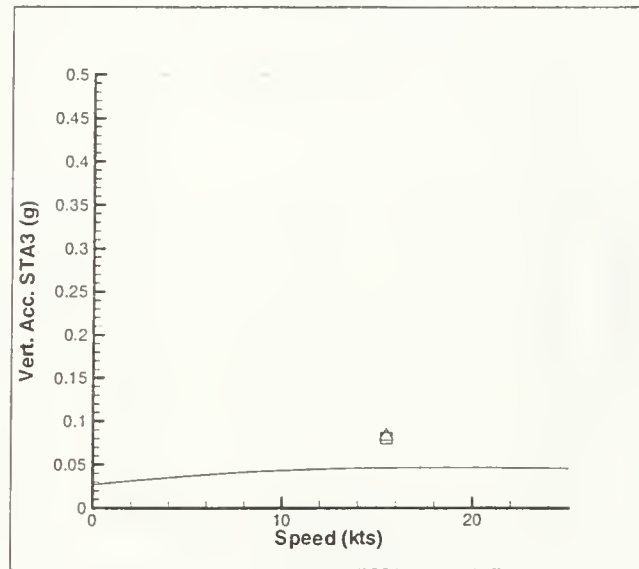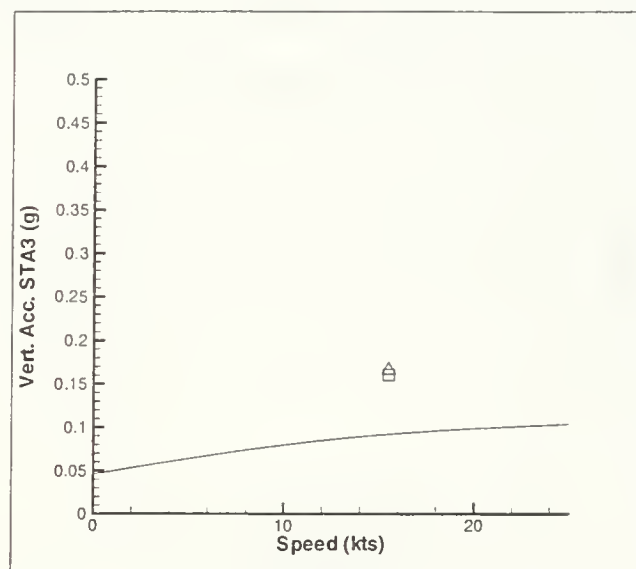
Figure 5-24: VLCC Vertical Acceleration STA3 (RMS SA), Limit ≡ Commercial Transit Limit
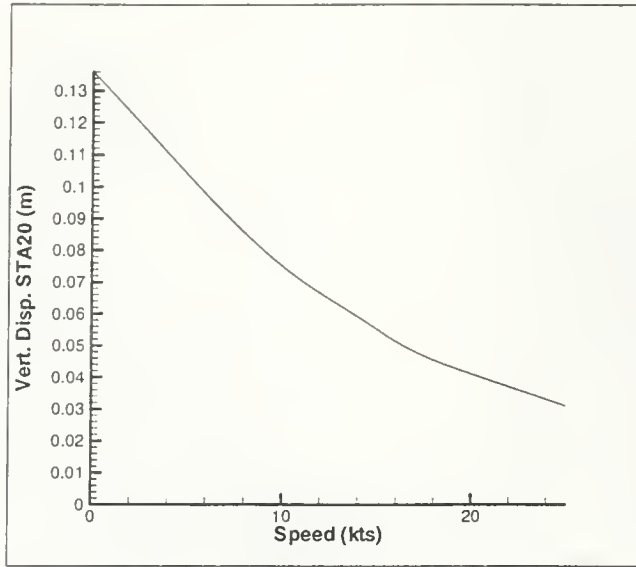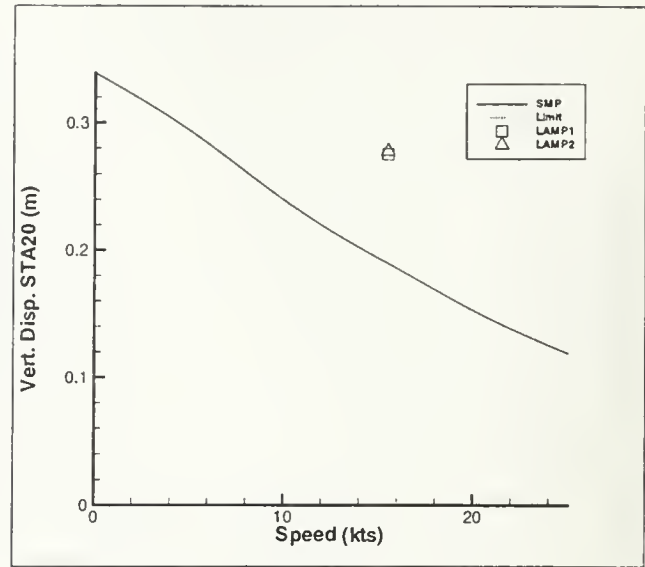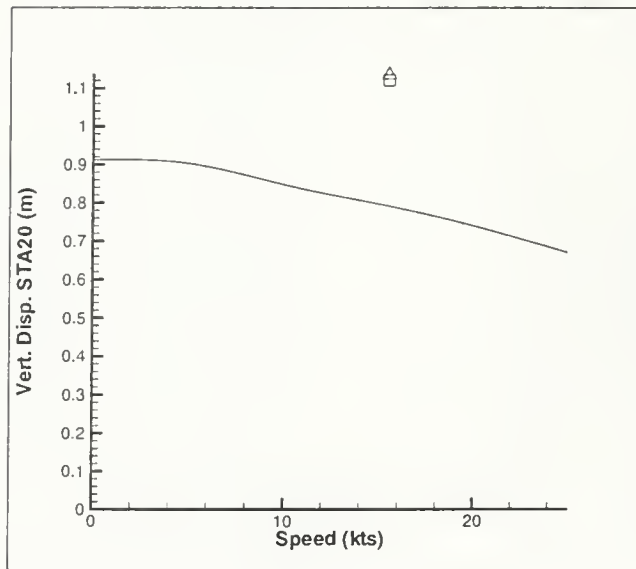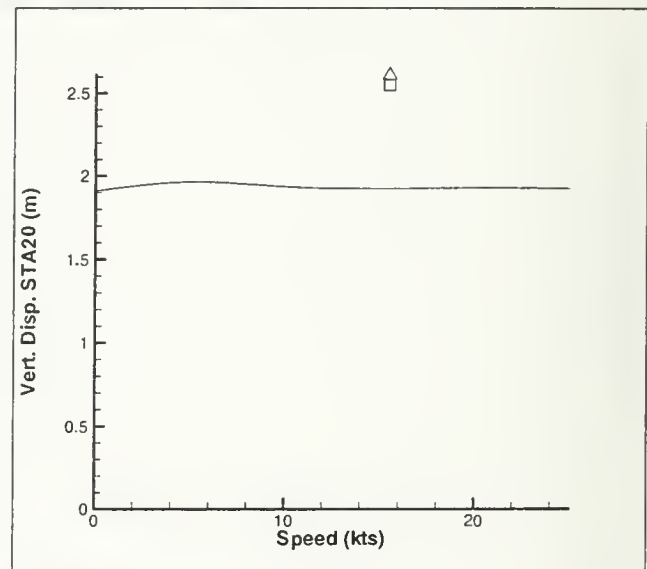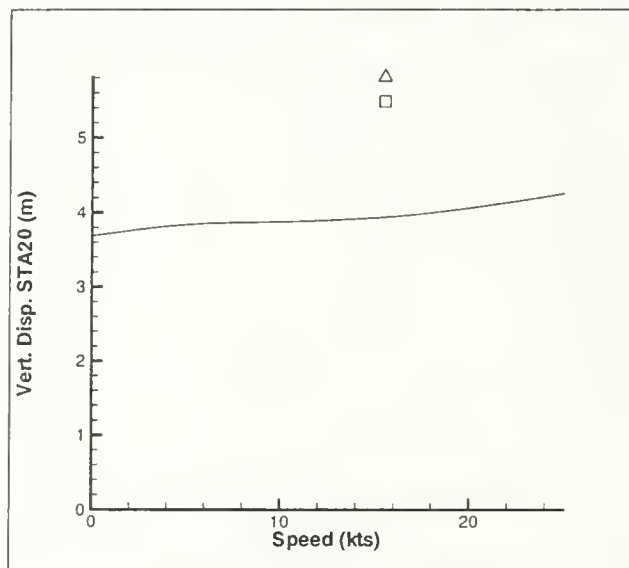
a. SS 4

b. SS 5

c. SS 6

d. SS 7

e. SS 8

Figure 5-25: VLCC Vertical Displacement STA20 (RMS SA)
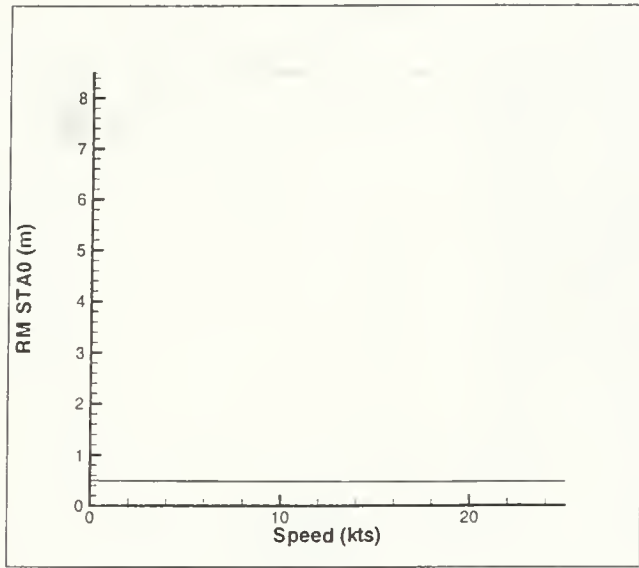
a. SS 4
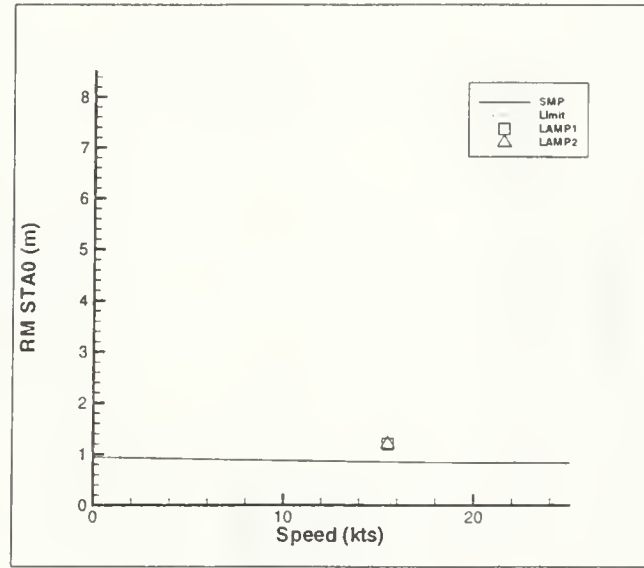
b. SS 5
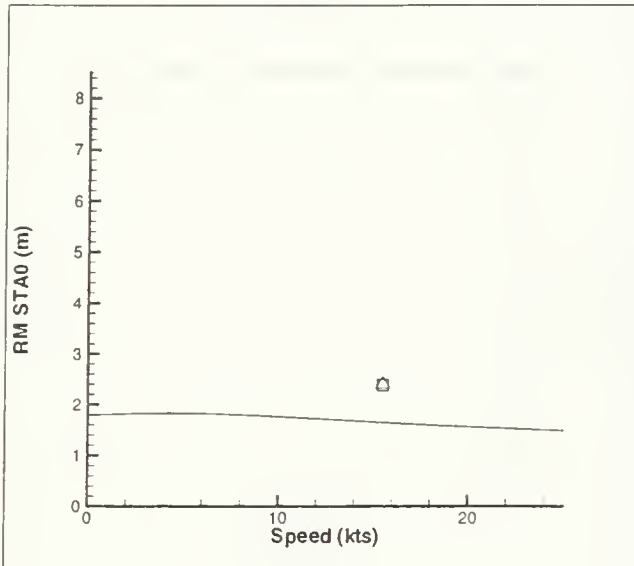
c. SS 6
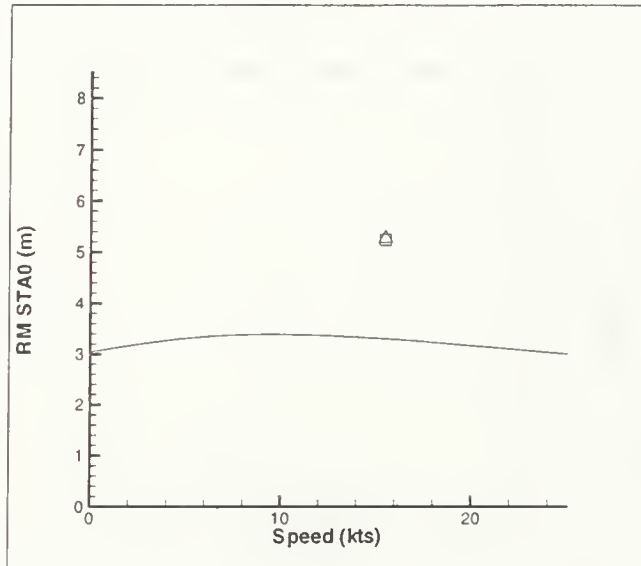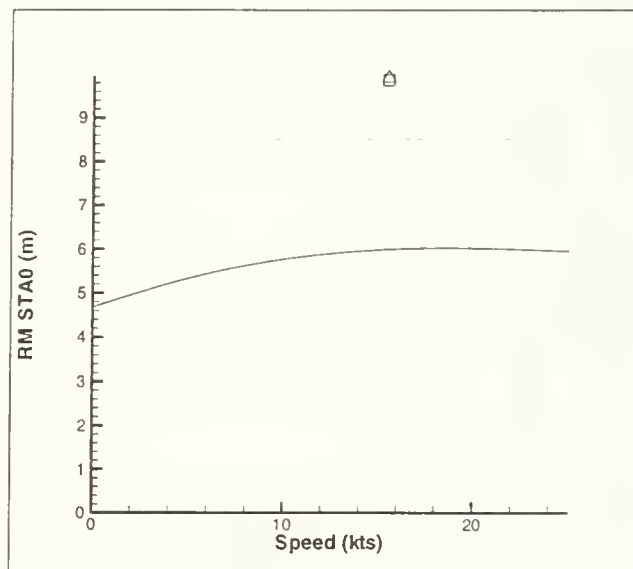
d. SS 7

e. SS 8

Figure 5-26: VLCC Relative Motion STA0 (RMS SA), Limit ≡ Freeboard (Deck Wetness Factor)
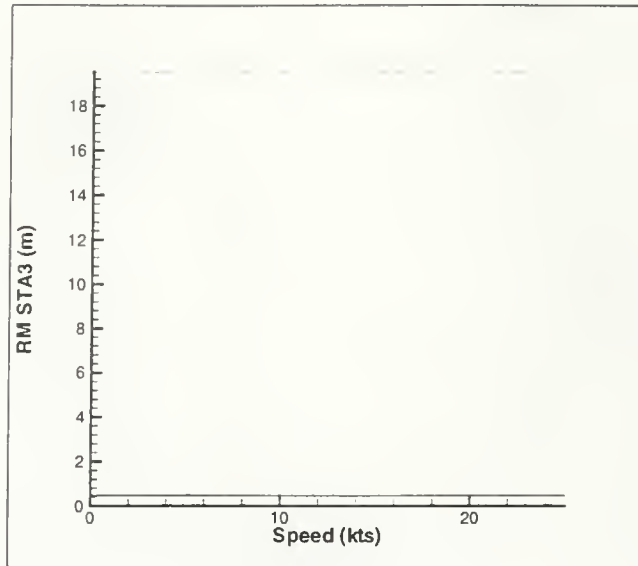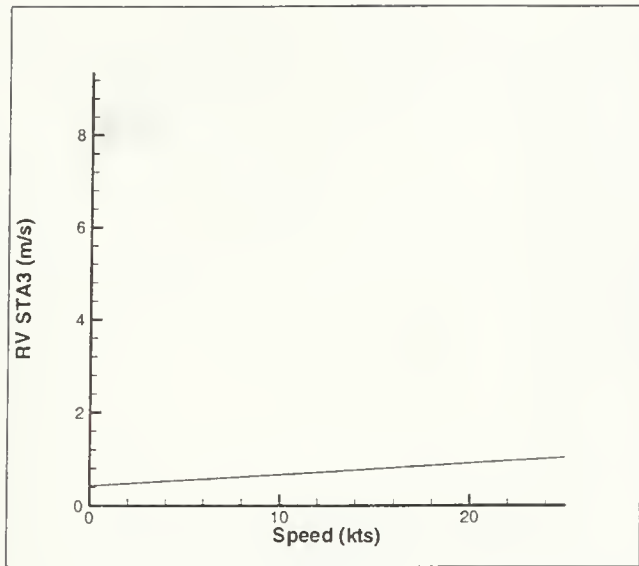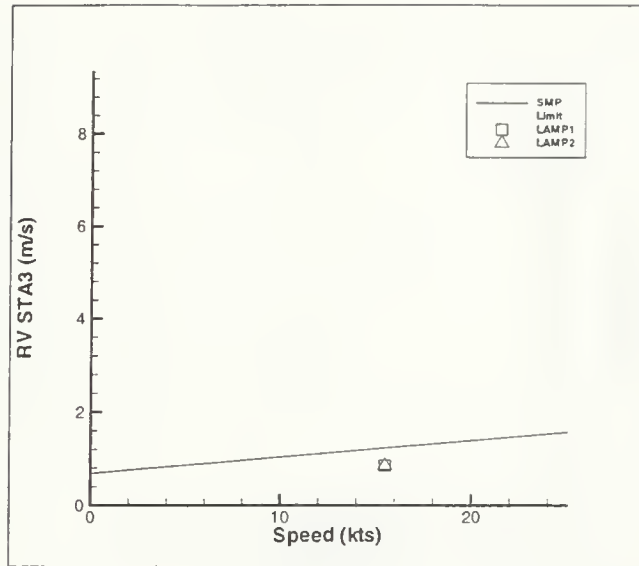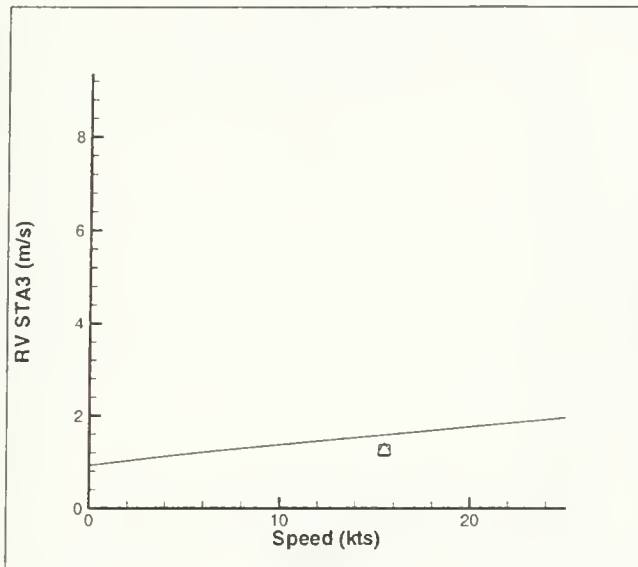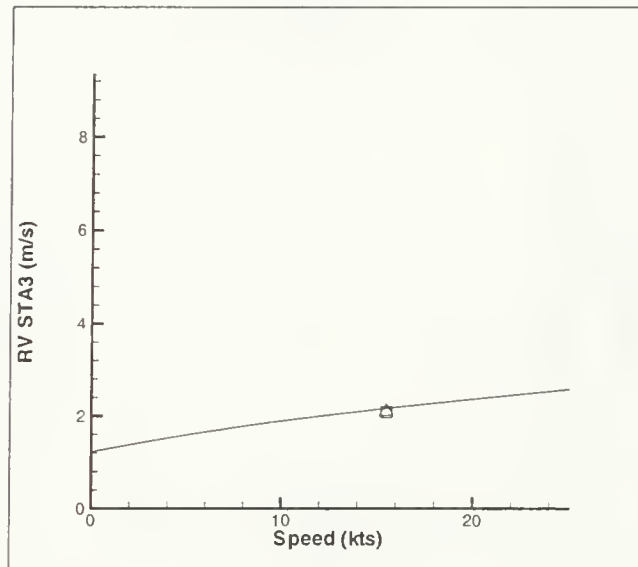
a. SS 4
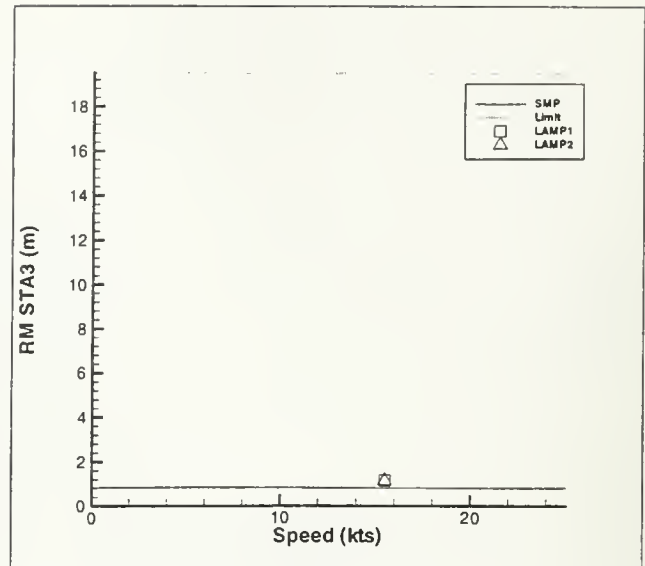
b. SS 5
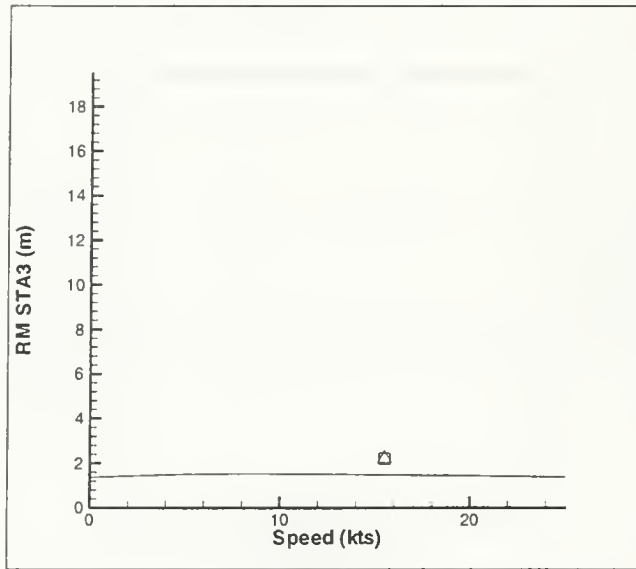
c. SS 6

d. SS 7

e. SS 8

Figure 5-27: VLCC Relative Motion STA3 (RMS SA), Limit $\equiv$ Keel Emergence (Slamming Factor)

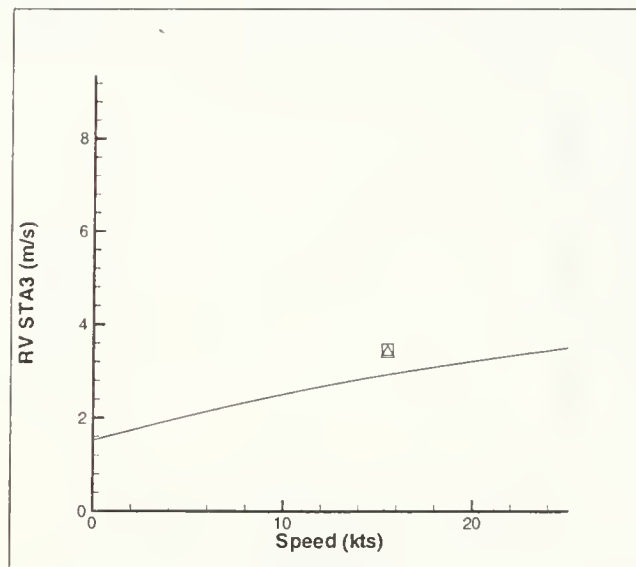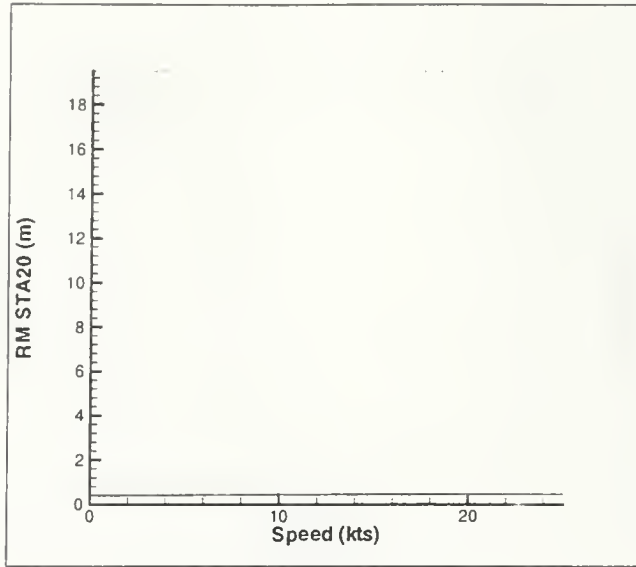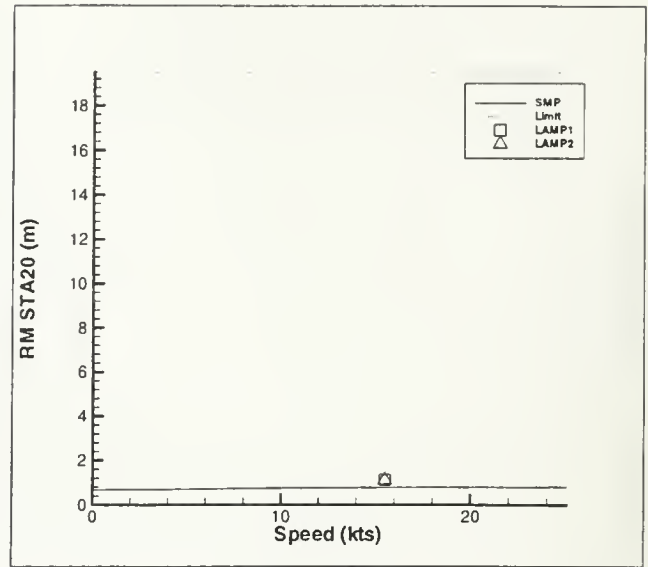Figure 5-28: VLCC Relative Velocity STA3 (RMS SA), Limit ≡ Slamming Threshold Velocity

a. SS 4

b. SS 5

c. SS 6

d. SS 7
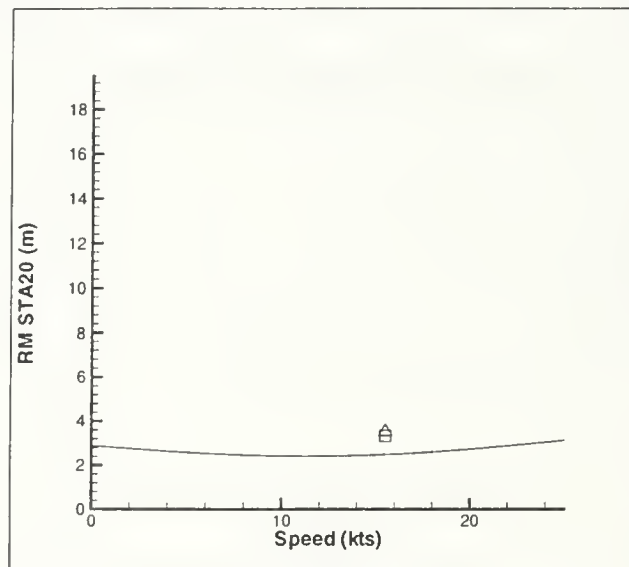
e. SS 8

Figure 5-29: VLCC Relative Motion STA20 (RMS SA), Limit $\equiv$ Keel/Propeller Emmersion
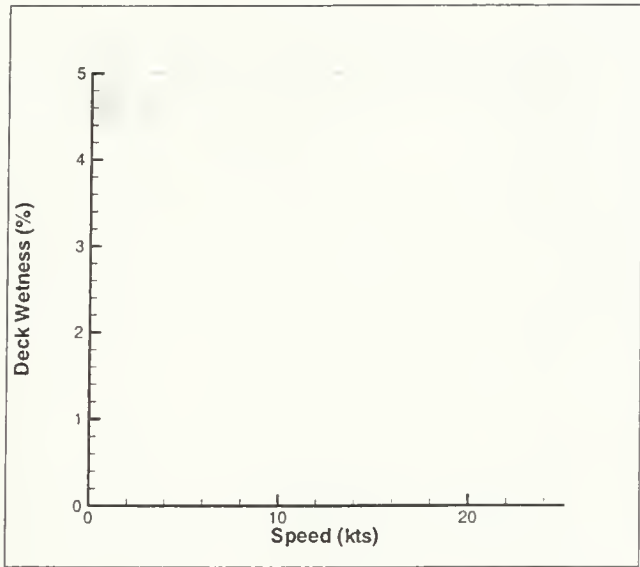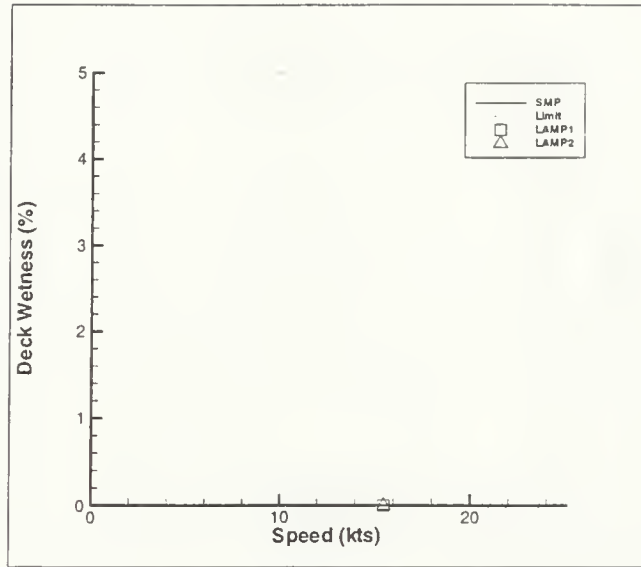
a. SS 4

b. SS 5

c. SS 6

d. SS 7

e. SS 8

Figure 5-30: VLCC Deck Wetness STA0 (RMS SA), Limit $\equiv$ Commercial Transit Limit
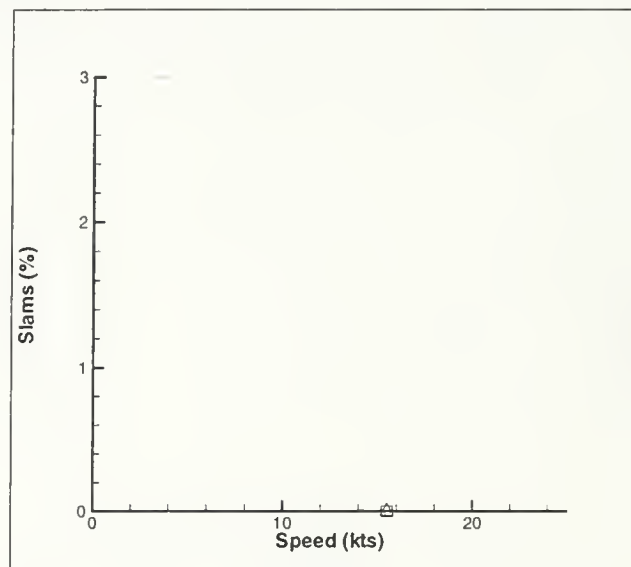
a. SS 4

b. SS 5

c. SS 6

d. SS 7

e. SS 8
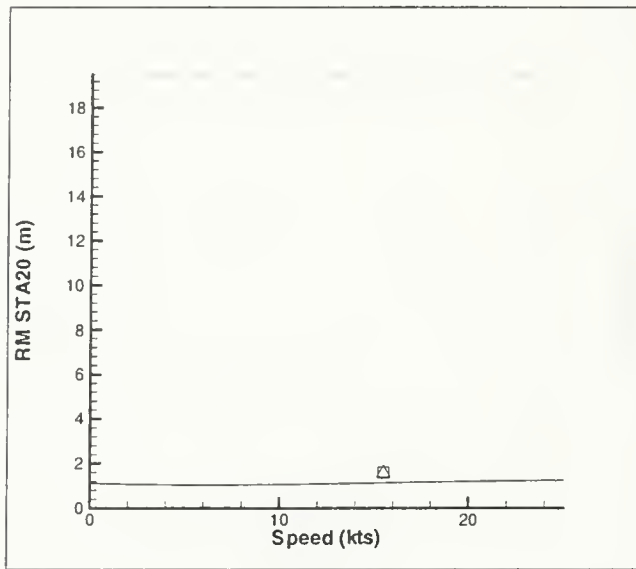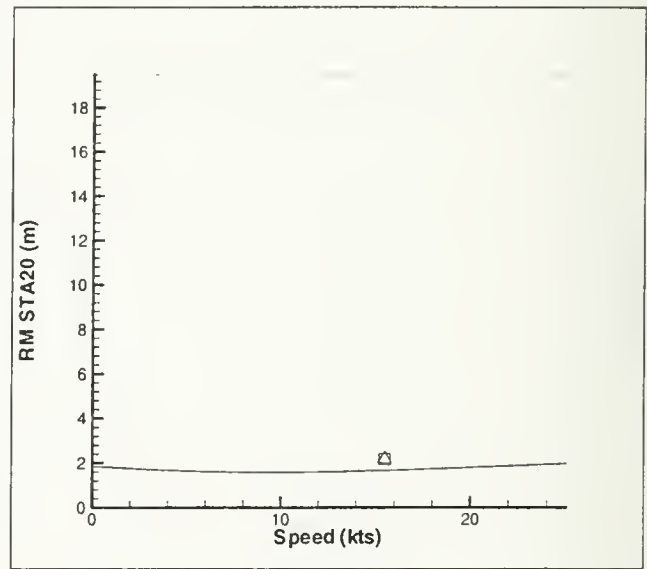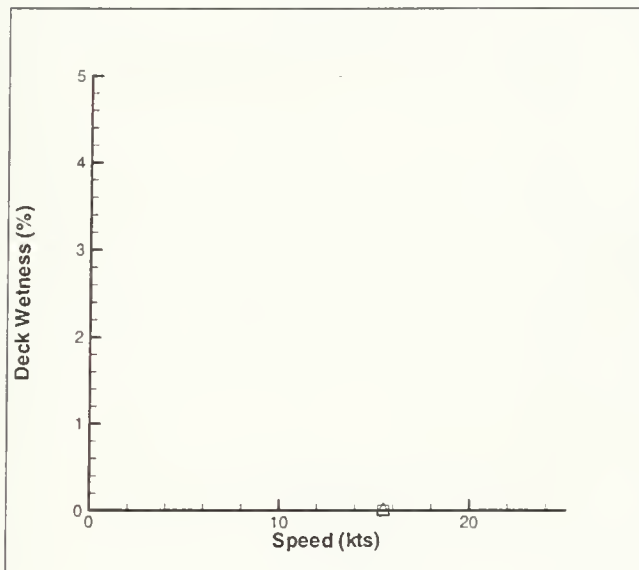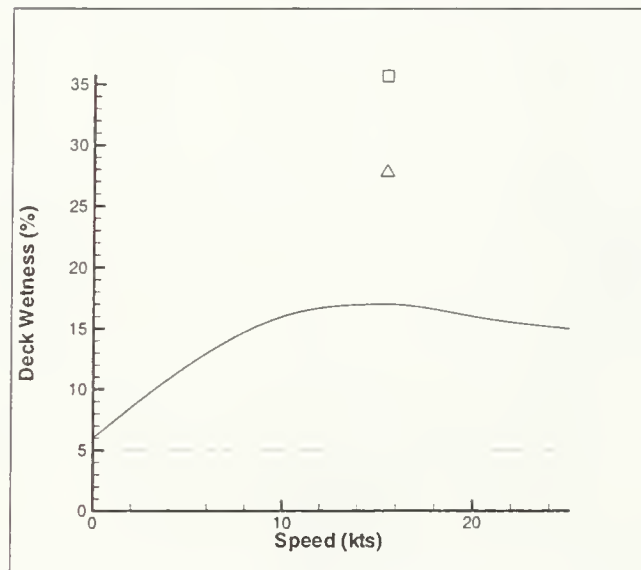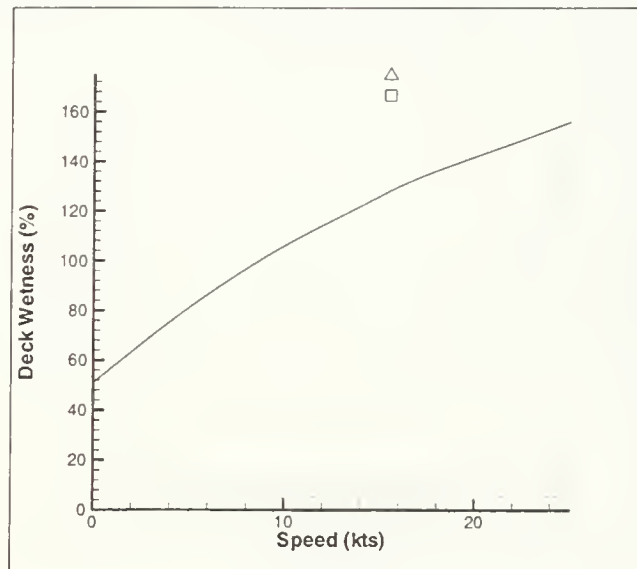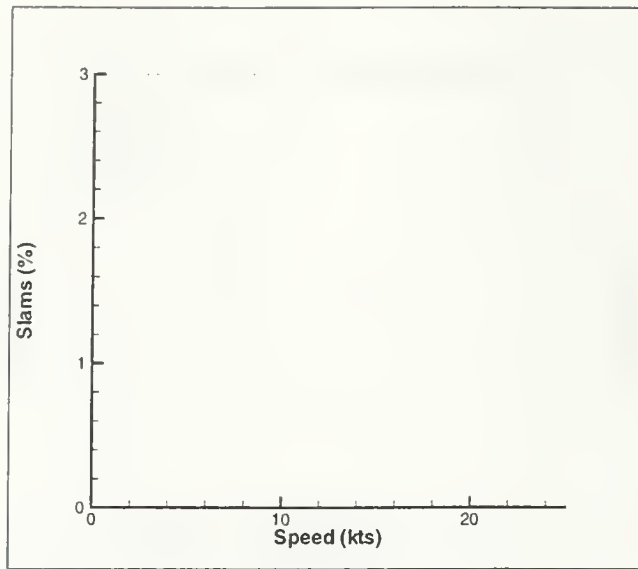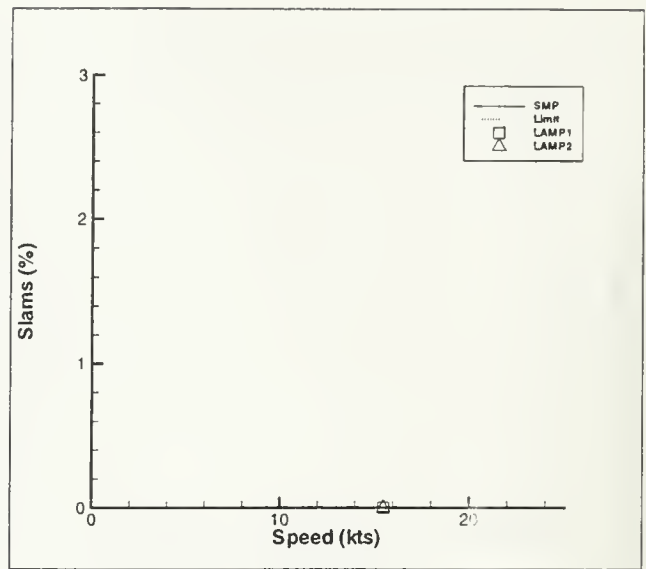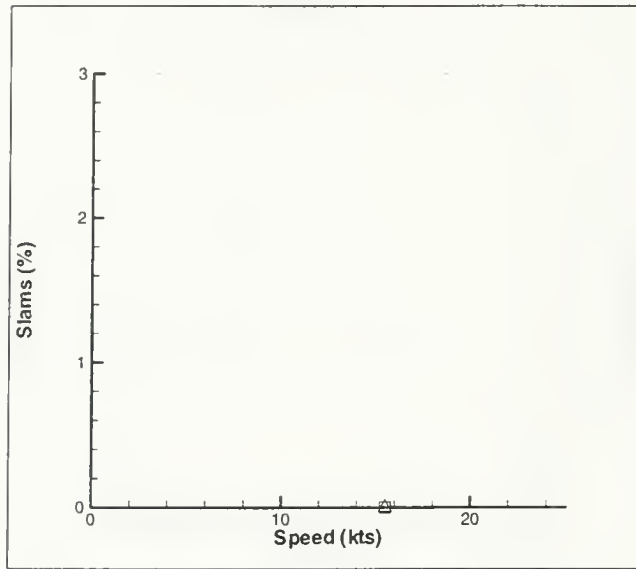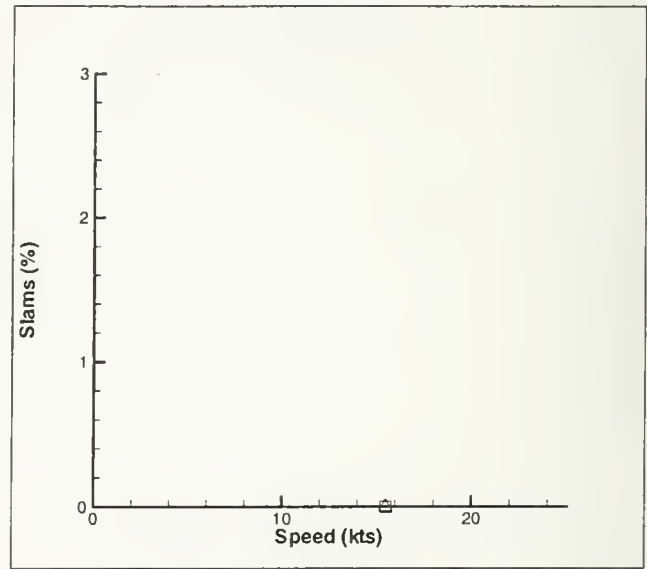
Figure 5-31: VLCC Slamming STA3 (RMS SA), Limit $\equiv$ Commercial Transit Limit
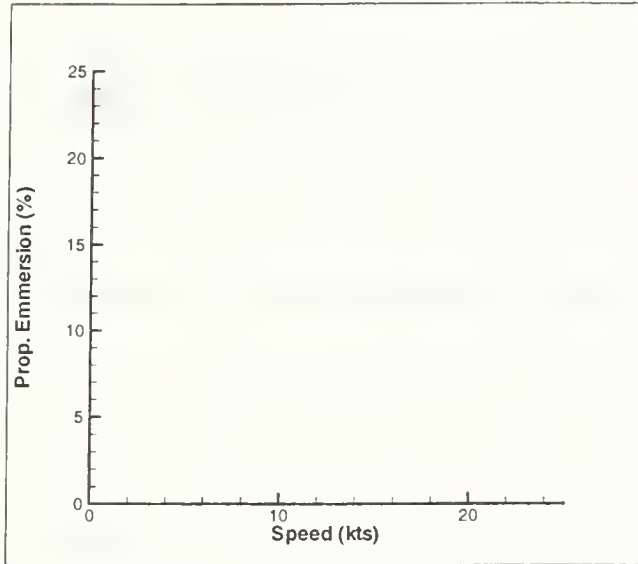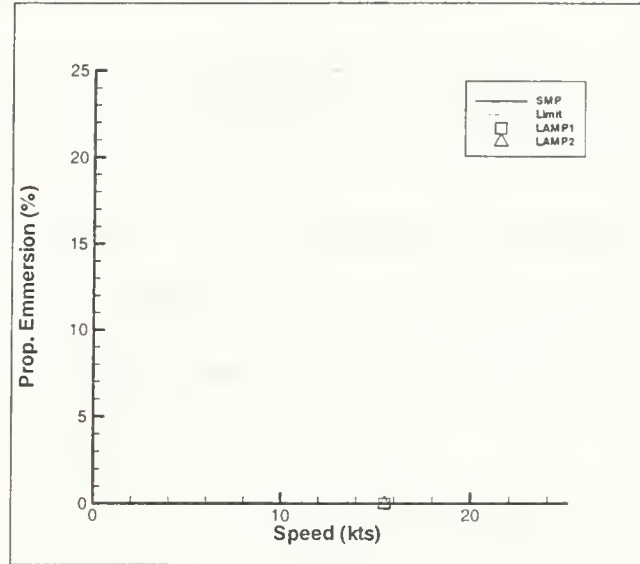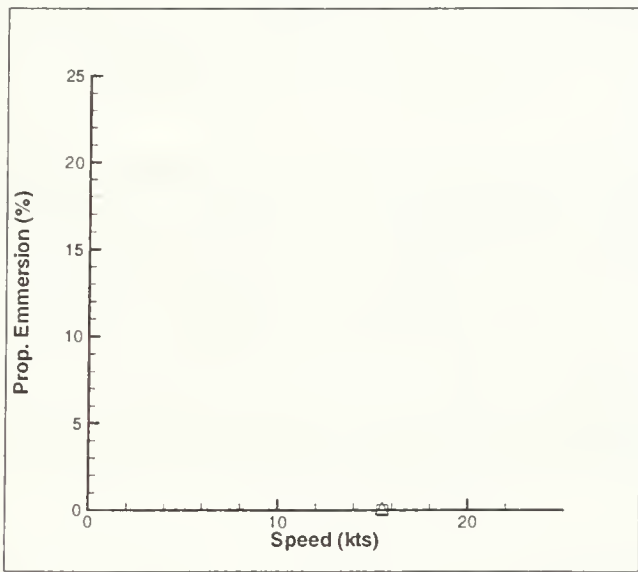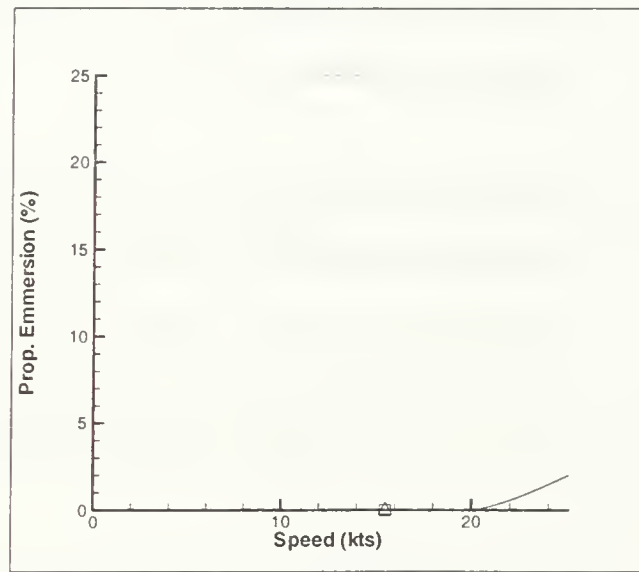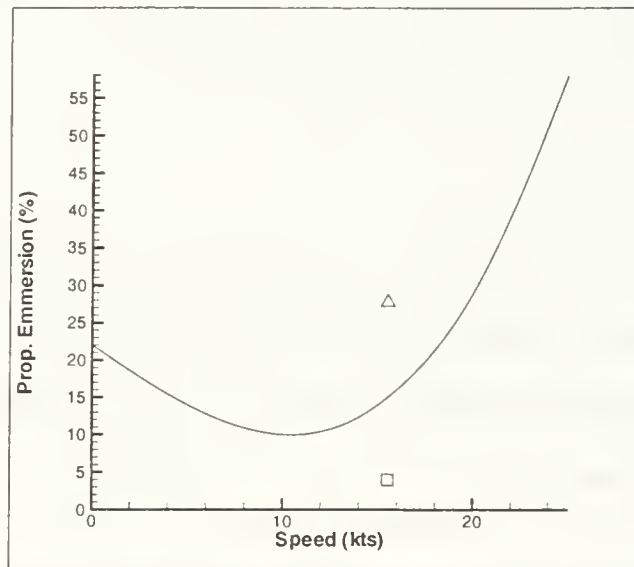
Figure 5-32: VLCC Propeller Emmersion STA20 (RMS SA), Limit $\equiv$ Commercial Transit Limit

5.4 Irregular Waves Tests Conclusions

The irregular seas tests are very useful and viable way of incorporating time domain codes in the design process, particularly since the statistical limitations of analyzing nonlinear responses may be overcome by simply recording and sorting all the peak responses. Using this processing method, the following important conclusions may be drawn from the mathematical hull and VLCC tests:

- SPI verification is an appropriate use of time domain codes, not withstanding the difficulties is forecasting discrete event probabilities. LAMP predicts that the motion criteria are met before the SMP threshold speeds. The opposite is true with loads.

- Simply switching to the time domain (whether LAMP-1 or 2) results in noticeable prediction differences from frequency domain codes. These differences generally increase as speed and/or sea state increases. The effect is seen for both the mathematical and VLCC hulls. This important conclusion is that linear superposition is not a valid procedure for large amplitude response cases.

- For motions, the LAMP prediction differences (LAMP-1 vs. LAMP-2) were typically not significant until the high speed case in sea state 6 for the mathematical hulls. For the VLCC, the differences were not large until sea state 8 at 15.5 knots.

- Vertical loads are more sensitive to speed and sea state than motions, with large differences between LAMP and SMP above sea state 4 for the mathematical hulls. The differences between LAMP-1 and 2 also grow sharply as response amplitudes increase.

- A "better" method does not necessarily mean a "worse" response. In several cases LAMP-2 predicted lower responses than LAMP-1, including pitch, . All LAMP responses for VSF5 and VBM10 are less than the SMP predictions.

152

- SMP and LAMP-1 do not predict any performance differences between hulls BL, V4, and V5. However, LAMP-2 does indicate differences for both variants. The effect of above water flare is particularly significant as response amplitudes increase.

- Entrance angle addition, in hulls V2 and V3, clearly improves motions performance, but increases dynamic loads. The differences are well predicted with both parametric (motions only) and frequency domain methods.

- Flare addition, in hulls V1 and V4, reduces heave, but increases pitch at higher speeds. Flare sharply increases dynamic loads, especially as response amplitudes increase.

- Incorporating 10° of tumblehome, as in hull V5, modestly increases heave and decreases pitch. V5 performs the best of all hulls in VSF5 and VBM10, with loads slightly less than BL.

- Displacement is the best seakeeping improvement. The VLCC has very low motion and load responses.

Many of these results are quite significant, with definite implications for the seakeeping design process, which are further discussed in Chapter 7. However, while cataloging all peak values in the time domain run is suitable for continually oscillating responses, the method is poor for assessing the probability of discrete events, where a percent likelihood or number per hour is desired. For instance, if the probability of a discrete event (such as slamming, wetness, or propeller emmersion) is physically one per hour, and this event occurs during fifteen minutes of time domain data, the resulting code prediction is four per hour. This discrepancy could potentially be solved by a better application of statistics. Another solution, discussed earlier in Section 5.1, is conversion of the time domain data to the frequency domain via Fourier Transforms. This would be necessary for relative displacements (and velocities, for slamming) at the longitudinal locations of interest. The discrete event

probabilities could then be calculated using well-known methods requiring the response spectral areas and second moments. Such methods however, are only proper when the response values are Gaussian. Problems with this assumption are further discussed in Section 6.4 on page 184. Both the cataloging method and the frequency domain method are flawed for the purpose of calculating discrete event probabilities. The application of time domain codes to such long term statistical problems may be difficult, particularly since the time domain codes are most important in conditions where linear statistical methods lose validity.

While the irregular seas method of using time domain codes is very appropriate to design, the results – significant or RMS amplitudes, or event probabilities – can be more difficult to physically understand. In addition, the computation times required for irregular waves runs, especially to achieve an acceptable sample size, can be quite daunting even when frequency domain tests are used to narrow the scope of testing.

To both further examine the nature of the mathematical and VLCC hull responses, and to test an alternative for using time domain codes for response predictions, a series of regular wave tests were completed, and are discussed in the next chapter.

Chapter 6

Time Domain Methods: Regular Waves

6.1 Regular Waves Methods in Design

6.1.1 Introduction

Regular wave testing is an excellent way of considering in detail the nature of a ship's motion and load responses, though their usefulness as a design tool is reduced when linear assumptions are violated. The studies in this chapter address both aspects of this statement. First, regular wave analysis is completed for a mathematical variant, and then for the VLCC. A comparison of the regular wave responses with the results of the irregular waves tests is particularly useful. In the last section of the chapter, several methods for considering regular wave results in engineering design and scientific analysis are discussed. In particular, a simplified approach for simulating time domain responses with regular wave harmonics is demonstrated, along with a discussion of the merits and considerable disadvantages of such a method. Additional implications of higher order responses in the design process are considered.

Conducting thorough regular waves tests for all of the mathematical variants would require an excessive amount of computer time, which is one of the reasons irregular waves tests are more practical for comparing the merits of several design

alternatives. Instead, a single hull is tested. Considering the results of the irregular seas tests in the previous chapter, Variant 4 is the most scientifically interesting hull. The underwater V4 hull is identical to the baseline hull, BL, but incorporates substantial flare above the waterline (20° at Station 3). As a result, parametric, frequency domain, and the linear LAMP-1 formulation all predict no difference between the responses for BL and V4 (or V5, the tumblehome hull). LAMP-2, however, predicted that V4 would have lower heave motions, but higher pitch and vertical loads, especially as response amplitudes increased. The V5 predictions in LAMP-2 also differed from the BL, but not as markedly. V2 and V3 were clearly superior (except in loads) for all responses in all methods, and so, while good design choices (resistance performance not withstanding), they are too "boring" for regular wave analysis. The V4 hull is used for all regular wave tests, since the differences between prediction methods should be significant.[1] Only one speed is tested, 20 knots, since (1) the high speed irregular seas runs showed greater differences between LAMP and SMP predictions, and (2) the resulting response characteristics may be compared with irregular seas runs in sea states 4 through 7.

The VLCC is also analyzed in regular waves at its service speed of 15.5 knots. Chronologically, the VLCC regular waves tests were conducted before any other LAMP tests, at the request of National Taiwan University, the hull's developer. Further detailed information on these tests is available [33].

6.1.2   Regular Waves Data Processing

Nature of Nonlinear Responses to Waves

Nonlinear responses to regular waves manifest themselves in harmonics, which occur at integer multiples of the exciting force frequency (the wave encounter frequency). Higher *order* nonlinear responses contribute to one or more harmonics. In particular, higher even order responses (2nd, 4th order, etc) also contribute to the mean response. In analyzing the harmonics of a ship's wave responses, the nature of the higher order

---

[1]Once again, however, the SMP and LAMP-1 regular wave results also apply to BL and V5.

contributions is important to understand, and is discussed in more detail below.

Higher harmonic responses will include components of different orders of nonlinear response. For example, the total wave exciting forces consist of harmonic components at the frequency of encounter, ω_e, and higher integer multiples of ω_e. For a given hull in regular seas, these wave forces are dependent on both wave amplitude and encounter frequency. The first component of the wave exciting force (or moment) may be considered in the form

$$\zeta(t) = A cos(\omega_e t)$$

The ship will then have some response function (ratio of response amplitude to wave amplitude), which for ease of discussion, is assumed to equal unity. Then the ship's first order response, $y_1(t)$, is simply:

$$y_1(t) = A cos(\omega_e t)$$

The first order response includes components in the first *harmonic* of the total response. The second order (or quadratic) response, $y_2(t)$, is of the form:

$$y_2(t) = A^2 cos^2(\omega_e t) = \frac{1}{2}A^2(cos(2\omega_e t) + 1)$$

from simple trigonometric identities. This second order response contributes to both the second harmonic *and* the mean response.

The third order (cubic) response, $y_3(t)$, is of the form

$$y_3(t) = A^3 cos^3(\omega_e t) = \frac{1}{4}A^3(3cos(\omega_e t) + cos(3\omega_e t))$$

and contributes to both the first and third harmonic responses. Likewise, the fourth order response contributes to the fourth and second harmonics, plus the mean; the fifth contributes to the fifth, third, and first harmonics; etc. For most ships (including the V4 and VLCC hulls), responses above the third harmonic are present, but

157

negligible compared to the first, second, and third harmonics. As such, these regular wave analyses concentrate on the first three harmonics. Additionally, all of the ship response analysis is discussed in terms of response harmonic vice response order since the harmonics are more easily measured.

The first, second, and third harmonic responses are divided by the first, second, and third power of the wave amplitude, respectively, to provide a type of "nonlinear RAO". These harmonic RAO's may then be used to simulate time domain responses in irregular seas. Such methods, which further consider the nature of the higher order responses, are presented in Section 6.4.1.

Post-Processing Methods

In regular wave tests, the time history traces for each run are first truncated to eliminate initial transient responses. An appropriate data window is then applied to perform Fourier analysis on the response. The first and higher harmonics are extracted from the resulting frequency domain representation of the response.

Linear frequency domain programs like SMP calculate only a first order, and thus first harmonic, response. Even in traditional experimental tests, only the first harmonic is calculated, since the statistical methods used in design use the first harmonic RAO's to generate response spectra. Higher harmonics information is available but generally not extracted, particularly since such harmonics are typically small for motions. Harmonics data are also available from the LAMP time domain simulations. Even in LAMP-1 predictions, which use a fully linear formulation, higher order responses are present simply as a result of calculating in the time domain.

For this study, the first through sixth harmonics are calculated by post-processing time domain data for the wave elevation at the center of gravity (CG) (encountered wave), heave, pitch, vertical shear forces, and vertical bending moments at station 10. The additional derived absolute and relative motions are not considered, since they are functions of the primary motions. In addition, harmonic data for hydrodynamic forces in the Z direction and moments about the Y axis are calculated. These forces and moments were primarily used to confirm a steady-state solution for truncating

158

the data for spectral analysis. However, the utility of solving for these forces in the time domain is also significant, since similar results from model tests may be difficult to measure.

For Fourier analysis, all time steps for all motions, loads, and hydrodynamic forces and moments are first plotted. By examination of the graphical results, the initial transients are truncated from the time history data. A window of data is then defined from the first wave crest in the steady state response to the last crest of the run. From the truncated data, the mean values are extracted and stored. Each time series is then detrended to remove the mean so that only the oscillatory harmonics are present before spectral analysis. Fast Fourier Transforms (FFT) are performed on the truncated, detrended time series data. The amplitude and phase of each response are calculated from the FFT output. Since the time series data were truncated from wave crest to wave crest, phase data for all motions and loads are with respect to the wave at CG.

6.1.3 LAMP Test Plan

As with irregular seas, frequency domain methods should be used to reduce the scope of required time domain tests. Tests can then be conducted only where the responses are significant. In particular, SMP can be used to define the first order response curve, determining the resonant frequencies for all motions and loads of interest. If only a few time domain runs are practical, the response is only investigated near resonance.

Once the frequencies of interest are determined, the test wave amplitudes are chosen. When linearity of responses is assumed, the first order responses are directly proportional to wave amplitude, so that any suitable amplitude may be used. However, significant higher order responses violate this assumption, since they are proportional to higher powers of the wave amplitude. The choice of amplitude for time domain testing is then quite important. An appropriate solution is to maintain a constant wave slope for all regular wave runs.

Many ship responses are actually more sensitive to wave slope than amplitude, including pitch, heave acceleration, and roll. Additionally, when wave energy spectra

159

are converted to wave slope spectra, the slope remains fairly constant at frequencies higher than the modal frequency [11]. If only one wave slope is practical for testing, the "modal wave slope" of the wave energy spectrum of interest is a good choice, since all waves at or above modal frequency should be near this slope. The modal wave slope may be directly calculated with the significant wave height and modal period, assuming a deep water wave dispersion relation, as $H_w/L_w = (2\pi H_{\frac{1}{3}})/(T_0^2 g)$. For sea state 8 ($H_{\frac{1}{3}} = 11.5m$, $T_0 = 17sec$), the modal wave slope is $(1/39.2)$. For SS7 (7.5 m, 14 sec), the slope is $(1/40.8)$, and for SS6 (5 m, 12 sec), $(1/45.0)$.

Since the differences for the mathematical hulls between SMP, LAMP-1, and LAMP-2 became significant in SS6, the slopes calculated above are of primary interest. A wave slope of 1/40 seems an appropriate value, since this is nearly the worst condition that should be encountered. All wave amplitudes for the V4 tests are calculated assuming this wave slope. For the VLCC, two wave slopes are tested: 1/40 and 1/60.[2] Differences between the wave slope results are discussed. Ideally, several wave slopes should be tested, since results for multiple wave amplitudes at a single frequency allow better definition of the lower harmonic contributions of higher order responses.

For the V4 tests, the LAMP regular wave runs are summarized in Table 6.1 on the next page. All runs were attempted in LAMP-1, 2, and 4. The frequencies were chosen based on the SMP motion and load RAO predictions. After a first set of tests, additional frequencies were added to better define the responses near resonance. LAMP setup for the runs was discussed in Section 3.1.5 on page 61.

For the VLCC, a set of wave conditions requested by NTU (as L_w/LOA and H_w/L_w) were first tested, and then the resonant peaks better defined. A summary of the completed LAMP tests is in Table 6.2 on page 162. Several LAMP-4 runs were completed for the VLCC. All LAMP runs were stable.

Additionally, at the request of the NTU designers, an analysis of total surface pressure over a specified area of the ship was completed. Although the results are themselves not significant for the conclusions of this study, the ease with which the

---

[2]Data at the 1/60 wave slope were calculated at the request of NTU.

Wave Frequency, ω (rad/sec)	V4 Runs
0.30	$1^\star,2,4^\ddagger$
0.40	1,2,4
0.45	1,2,4
0.50	1,2,4
0.55	$1,2,4^\ddagger$
0.575	$1,2,4^\ddagger$
0.60	$1,2,4^\ddagger$
0.65	$1,2,4^\ddagger$
0.70	1,2,4
0.75	1,2,4
0.85	1,2,4
0.90	1,2,4
0.95	1,2,4
1.10	1,2,4
1.30	1,2,4
Notes: "1", "2", and "4" refer to LAMP run type. All runs in head seas at 20 kts. Wave height determined by constant slope, $H_w/L_w = 1/40$ $\star$: LAMP-1 runs are linear. Apply to BL, V4, V5 $\ddagger$: Run failed; no data used.	

Table 6.1: Mathematical Hull LAMP Regular Waves Run Summary

Wave Frequency, ω (rad/sec)	L_w/LOA	Method
0.3534	1.50	1,2,4
0.3700[†]	1.37	1,2
0.3800[‡]	1.30	1,2
0.3949	1.20	1,2,4
0.4328	1.00	1,2
0.4565	0.90	1,2
0.4838	0.80	1,2
0.5170	0.70	1,2
0.6118	0.50	1,2
0.9681	0.20	1,2
Notes: "1", "2", and "4" refer to LAMP run type. All runs in head seas at 15.5 kts. Wave heights determined by constant slopes, $H_w/L_w = 1/40$ and $1/60$, for all frequencies. †Heave resonance. ‡Pitch resonance.		

Table 6.2: VLCC LAMP Regular Waves Run Summary

pressure may be calculated from the hydrodynamic solution has important implications for later design stages. Information such as this pressure analysis or fluid flow patterns around the hull are quite difficult to measure experimentally. Once a time domain method is validated for a candidate hull form, detailed calculations of pressure and flow velocity may be easily obtained and applied to design problems.

6.2 Mathematical Hull Predictions

All of the regular wave runs listed in Table 6.1 were completed except for the noted LAMP-4 runs. These runs failed for the same reasons as the irregular seas LAMP-4 runs, discussed in Section 5.2.3. As a result, the motions and loads responses near resonance could not be defined with LAMP-4.

For all motions and loads, harmonic response amplitudes above the third harmonic were negligible and not processed. The amplitudes and phases for the first through third harmonics are plotted in Figure 6-3 on page 170, through Figure 6-7 on page 174 for LAMP-1, 2, and 4. The SMP predictions for the first harmonic responses are also

plotted. As discussed above, the first harmonic amplitudes are normalized by wave amplitude, the second harmonics by wave amplitude squared, and the third harmonics by wave amplitude cubed. Mean responses are not plotted, although these vary with wave conditions due to the contribution of the 2nd order responses.

The following conclusions may be made from the response plots for the V4 hull:

- For heave:

  - The first harmonic response dominates the motions at all tested frequencies. The 2nd and 3rd harmonics are quite small, and exhibit substantial scatter in their amplitudes and phases. This is expected for motions.

  - For the first harmonic, the LAMP results converge to the SMP predictions at low and high wave lengths. Near resonance, both LAMP methods predict substantially higher heave. LAMP-2 predicts a higher heave response than LAMP-1.

  - The regular wave results correlate well with the irregular seas responses at 20 knots, particularly in SS6 and above. Both methods predict higher amplitudes in the time domain, and an increase in heave upon switching to LAMP-2.[3] In irregular seas, the LAMP-2 prediction for BL was also quite higher than the LAMP-1 predictions, and greater than the LAMP-2 predictions for V4.

- For pitch:

  - As with heave, the first harmonic in pitch dominates the response. Second and third harmonics are negligible, with some scatter. The phases of the higher harmonics are better behaved than with heave, but LAMP-1 and 2 approach substantially different values as wave lengths increase.

  - LAMP-1, 2, and 4 all converge to the SMP solution as first harmonic response amplitudes decrease. At resonance, LAMP-1 and 2 predict higher

---

[3]Conclusions about the effect of flare on responses should *not* be made, since the BL was not tested with LAMP-2 in regular waves.

responses, though not as substantial as with heave. This correlates well with the irregular wave findings.

– The LAMP-2 first harmonic peak is slightly lower and shifts to a lower frequency than LAMP-1. This corroborates the irregular seas results, where LAMP-2 predicts a lower response than LAMP-1 for V4.

• For VSF5:

– For the first harmonic responses, LAMP-1 predictions are lower than SMP, except at higher wave frequencies. The resonance peak is lower, and, unlike the motions, LAMP-1 approaches dynamic loads which are still lower than SMP at long wave lengths. The reduction in LAMP-2 loads is significant, with a peak almost 50% less than SMP. At both low and high wave frequencies, LAMP-2 predicts lower loads. The results correlate with the observed behavior in irregular waves, where the time domain predictions were lower than SMP, and the LAMP-2 predictions decreased relative to SMP markedly as speed and sea state increased. The LAMP-1 phase predictions also correlate with SMP. The LAMP-2 predictions are quite different.

– Disturbingly, the LAMP-4 predictions correlate closely with the LAMP-1 results, which is very unexpected. Assuming that LAMP-4 is the most physically accurate model, the LAMP-2 results should be closer than the LAMP-1 results. Confirmation that the LAMP-2 setup was identical to the LAMP-1 runs only increases the dilemma. The study time limitations did not permit a detailed examination of the differences observed in these cases, but such research is necessary. Additional work in particular should continue examining potential problems with the weight distribution, discussed in Section 5.2.3.

– Unlike the motion responses, the second harmonics are not insubstantial compared to the first harmonics. LAMP-1 predicts a sharp harmonic peak,

while LAMP-2's is only one-fifth as large as the first harmonic. The LAMP-4 results are inconclusive, since the peak is not defined. Because the harmonic amplitudes are higher, the phases are easier to measure, and behave similarly to the first harmonic phases, with rapid oscillations as frequency decreases while approaching a constant angle at high frequencies.

– The third harmonics, though comparatively larger than the motion values, are still quite low. The LAMP-1 and LAMP-2 predictions are similar.

• For VBM10:

  – The first harmonic LAMP predictions are closer to SMP than for VSF5, but still lower in magnitude. At high frequencies, all LAMP methods approach SMP. At low frequencies, LAMP is lower than SMP, but all formulations converge to the same limit. This is significant because the behavior for this load response (and for VSF15) lends credence to the behavior observed in VSF5. If an error in LAMP setup or processing affected VSF5, the error should also affect VBM10.

  – The LAMP-2 first harmonics are less than the LAMP-1 values, though not as markedly as with VSF5. This correlates with the observed behavior in irregular waves. However, in irregular waves, the LAMP-2 VBM10 response diverged from the SMP values much more quickly than with LAMP-1 in severe sea states. This may be due to the influence of second harmonics, which, at large wave amplitudes would be a significant component of the total response.

  – The second harmonic amplitudes and phases follow similar trends as VSF5. The LAMP-1 magnitudes are substantially higher than the LAMP-2 predictions. Phase angles functions are more reasonable, although for all higher harmonic responses the LAMP-1 and LAMP-2 phases do not correlate well.

  – The third harmonics follow similar trends as VSF5. LAMP-1 and 2 mag-

165

nitudes are close. The overall third harmonic magnitudes, though considerably more than for motions, are small portions of the total response.

- An interesting behavior is noted for LAMP-4 in the higher harmonic amplitudes. At high wave frequencies, the LAMP-4 predictions increase in magnitude, rather than converging to zero as with LAMP-1 and 2. The cause of this behavior, whether physical or numerical, is unknown.

- For VSF15:

  - The LAMP-1 and 2 predictions for the first harmonic amplitudes converge to the SMP values at higher frequencies, but, unlike VSF5 and VBM10, are substantially higher than SMP at resonance and lower frequencies. The magnitude of the resonance peak is nearly the same for both formulations, but the LAMP-2 response is more narrow banded, resulting in overall lower loads. These observations correlate well with the irregular seas results.

  - The SMP first harmonics are very narrow banded for VSF15, and for loads in general compared to motion predictions. LAMP results confirm this, although for VSF15 the effect is not nearly as substantial as predicted by SMP.

  - The VSF15 trends for second and third harmonics are very similar to the VSF5 and VBM10 results.

Overall, the regular wave results for the V4 hull correlate with the irregular seas observations quite well. Similar trends for LAMP-1, LAMP-2, and SMP predictions are observed in the high sea state high speed test cases. The motions and loads behave as expected, except for the differences in LAMP-2 results for VSF5. Considering the less perplexing behavior for VBM10 and VSF15, the VSF5 load responses should be credible. The differences in load predictions between LAMP-1 and LAMP-2 do seem more sensitive for VSF5 and VBM10 - this too correlates with the irregular seas data.

The observed second and third harmonics are small for the motions, but the second harmonics in particular are not insignificant for the loads. In severe seas, this

harmonic component should not be neglected, especially since the primary component is proportional to the square of the wave amplitude. Figures 6-1 on the following page, and 6-2 on page 169 clearly demonstrate this at one wave frequency ($\omega = 0.575 rad/sec$) for the V4 hull, near the first harmonic resonant response peaks. These plots are the frequency domain spectrum for the loads and motions with the response frequencies normalized by encountered wave frequency. The entire response spectra is also normalized by wave amplitude, so that harmonic magnitudes may be easily compared. In this representative case, the higher harmonic motions are clearly negligible. However, the load higher harmonics – the second in particular – are clearly *not* negligible. SMP does not predict any higher harmonics, and for loads this is an important limitation. Of note, the LAMP-1 second harmonic predictions are much higher than the LAMP-2 predictions for most tested cases. This is somewhat unexpected and should be studied further.

Finally, the phase angle predictions are well behaved for the first harmonic, but not so for the higher harmonics. For these responses, the LAMP-1 and LAMP-2 values differ considerably. For low magnitude harmonics including second and third motion harmonics and third load harmonics, the phase angles have excessive scatter and are hard to accurately measure. While phase angles are not used in linear frequency domain methods to predict statistical response amplitudes, they are important if accurate simulation of time domain motions and loads is desired. To potentially use regular waves tests for this purpose would require accurate definition of the phase angle response curve. However, unlike the amplitudes, the phase angles oscillate considerably as wave length increases until approaching a large wave length limit. A significantly higher number of regular wave runs may be required.
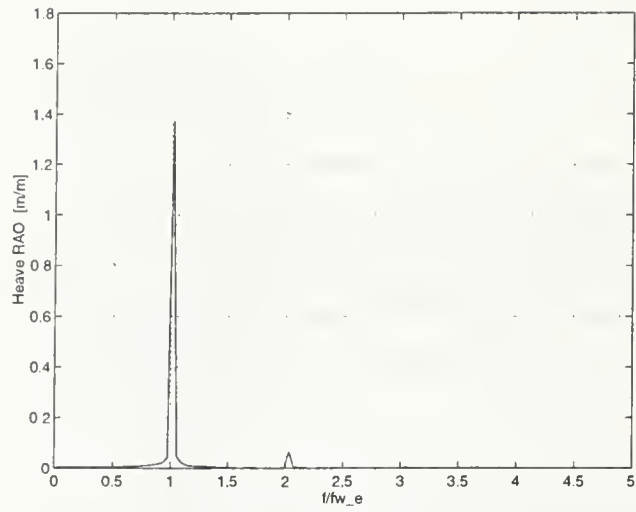
a. Heave, LAMP-1
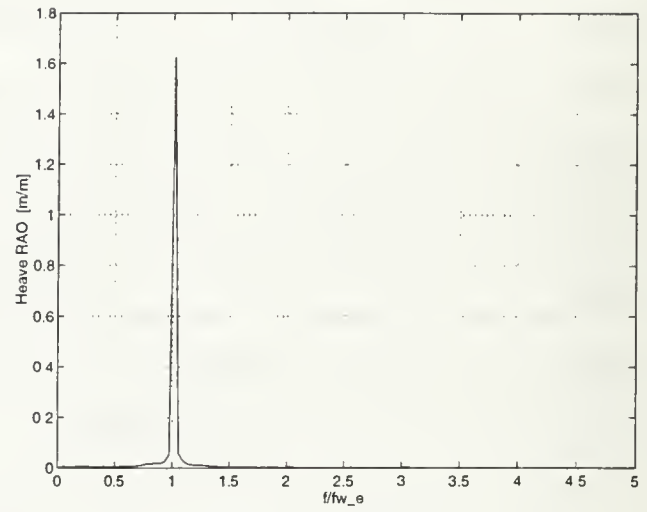
b. Heave, LAMP-2
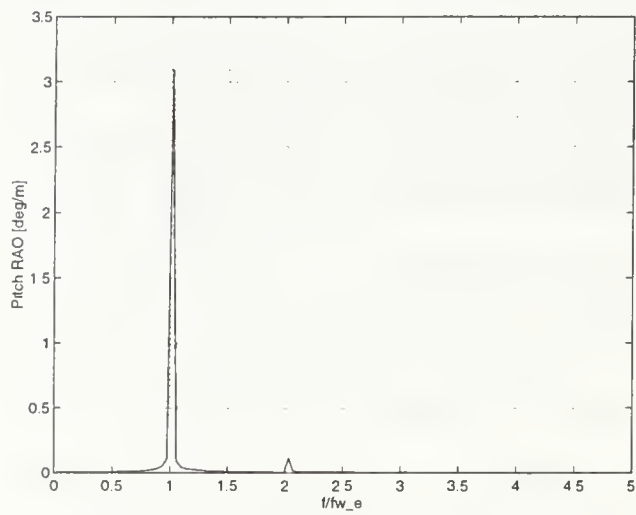
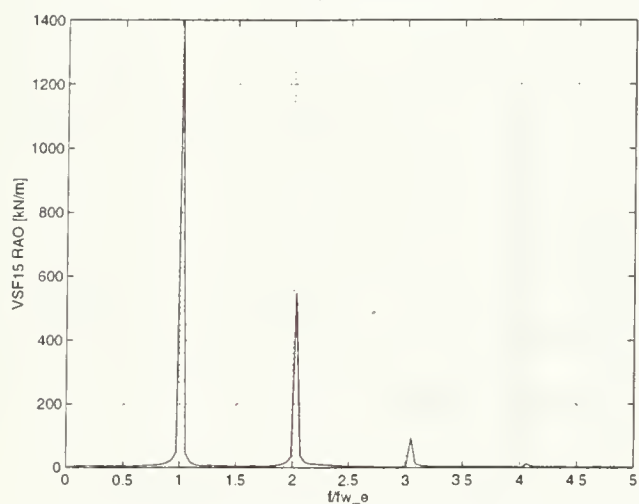c. Pitch, LAMP-1
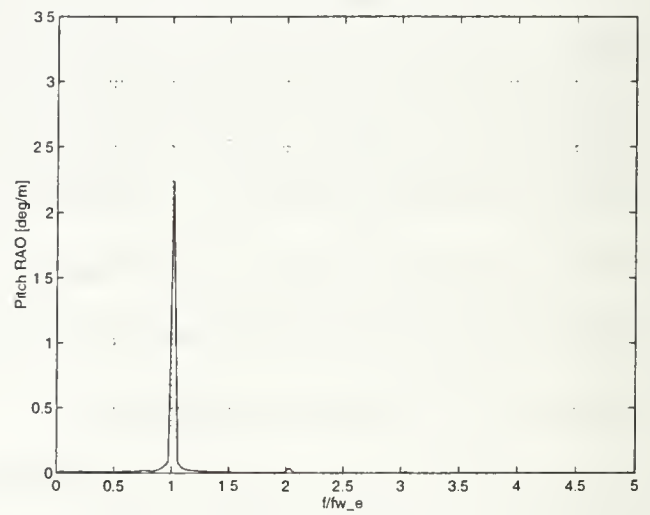
d. Pitch, LAMP-2

Figure 6-1: V4 Harmonics Comparison (Motions), $\omega = 0.575$, 20 knots, Head Seas

168
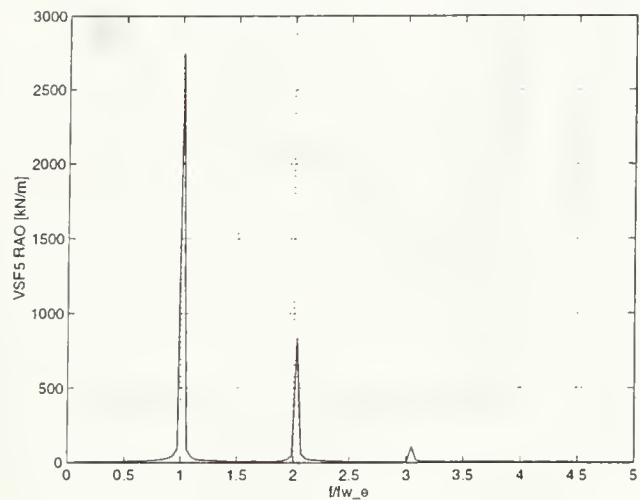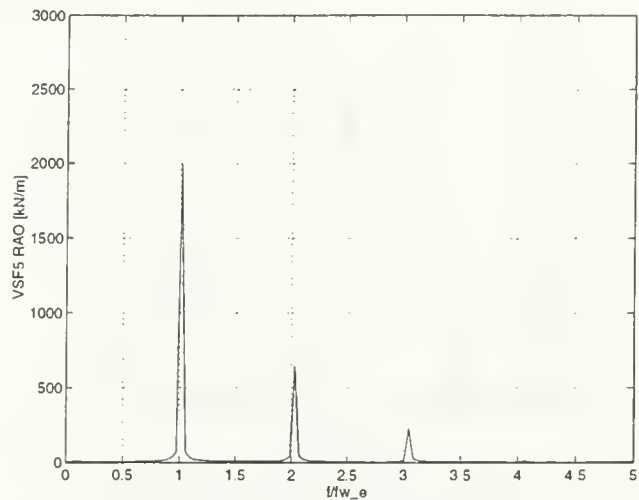
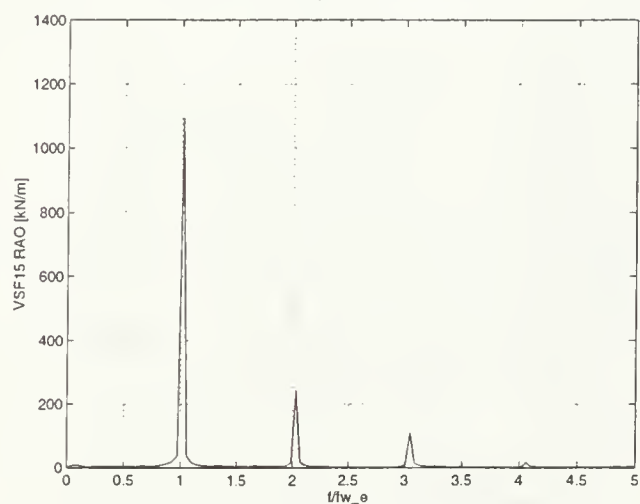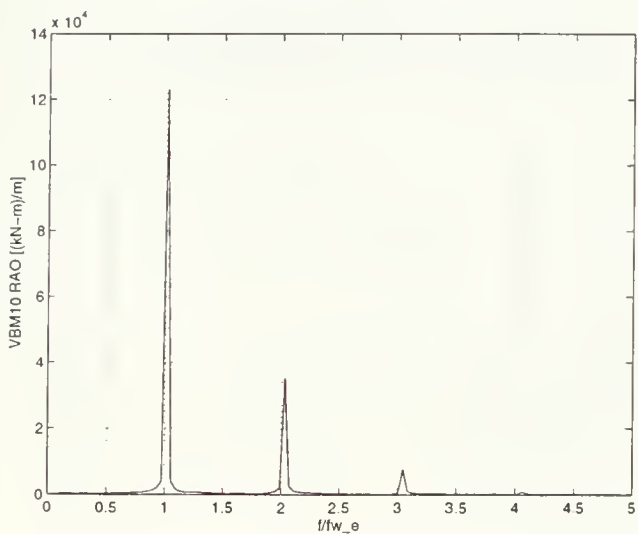a. VSF5, LAMP-1 b. VSF5, LAMP-2
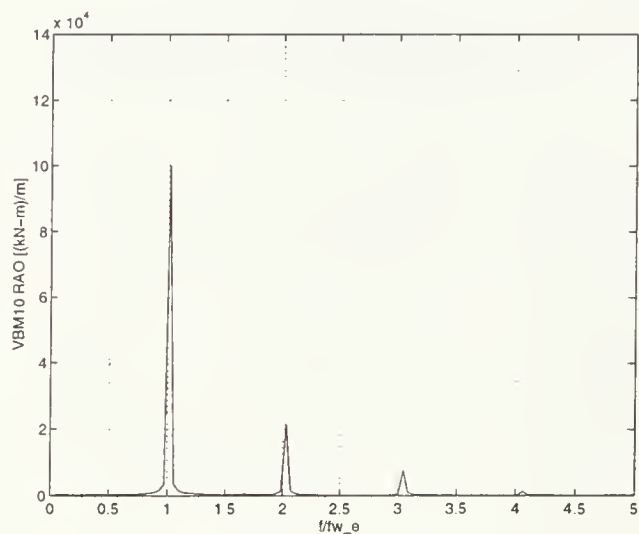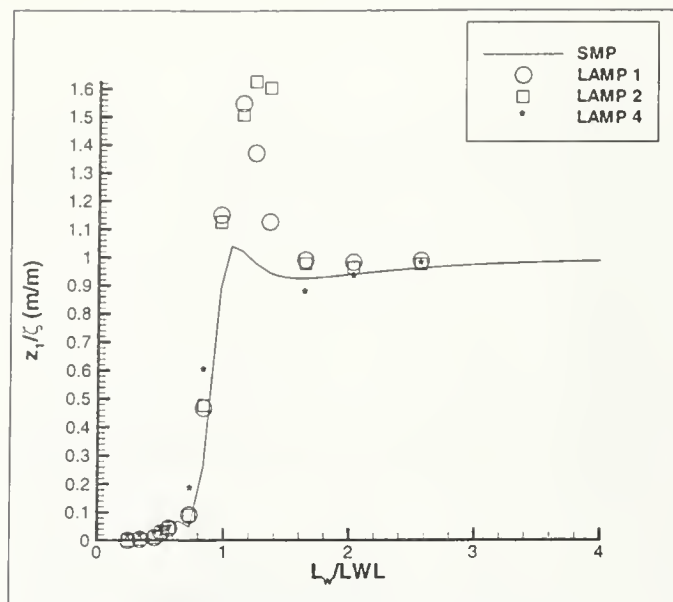
c. VSF15, LAMP-1 d. VSF15, LAMP-2
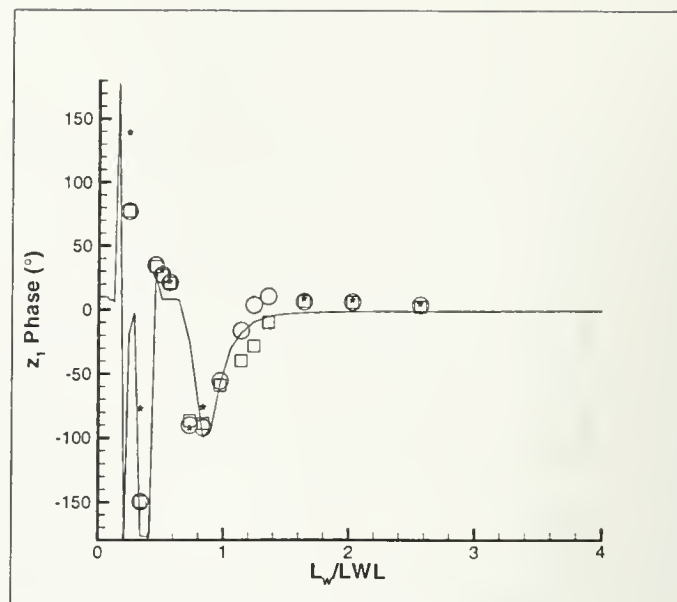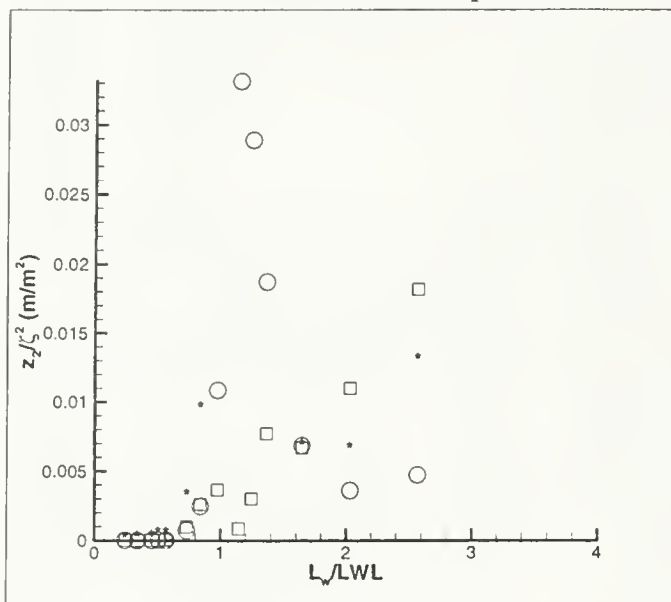
e. VBM10, LAMP-1 f. VBM10, LAMP-2

Figure 6-2: V4 Harmonics Comparison (Loads), $\omega = 0.575$, 20 knots, Head Seas
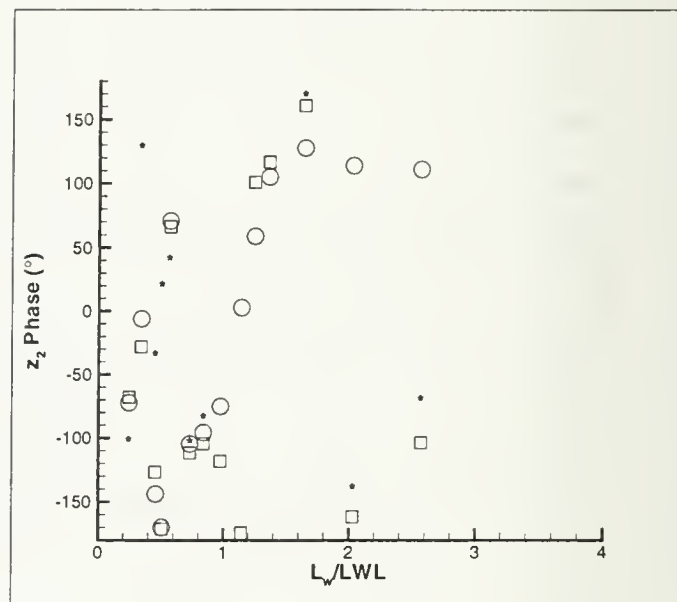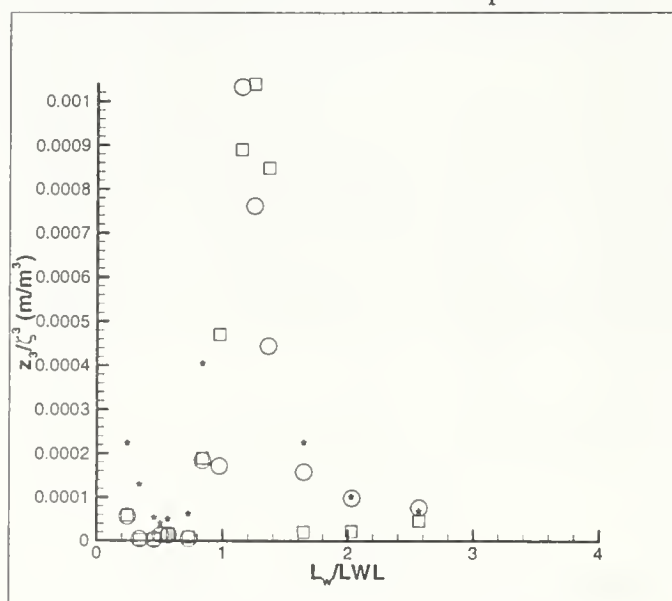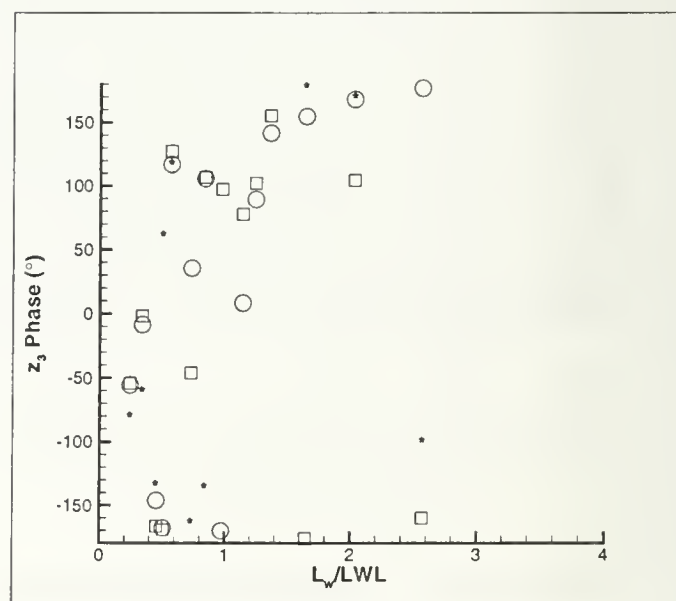
169

a. First Harmonic Amplitude

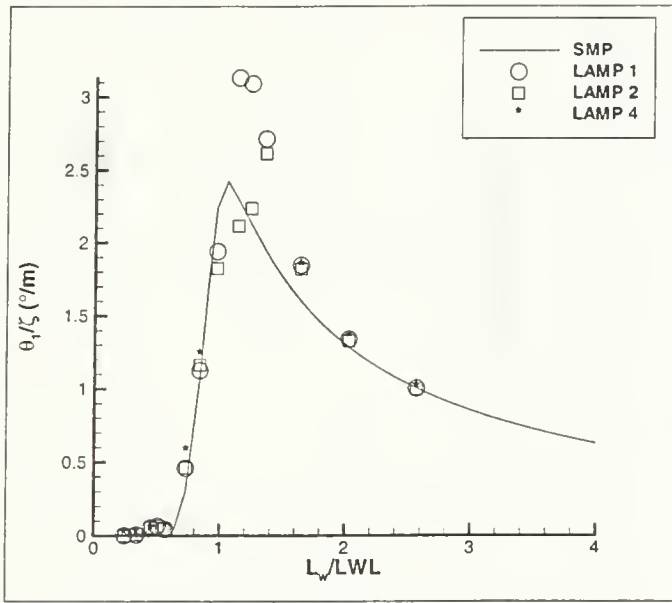b. Phase

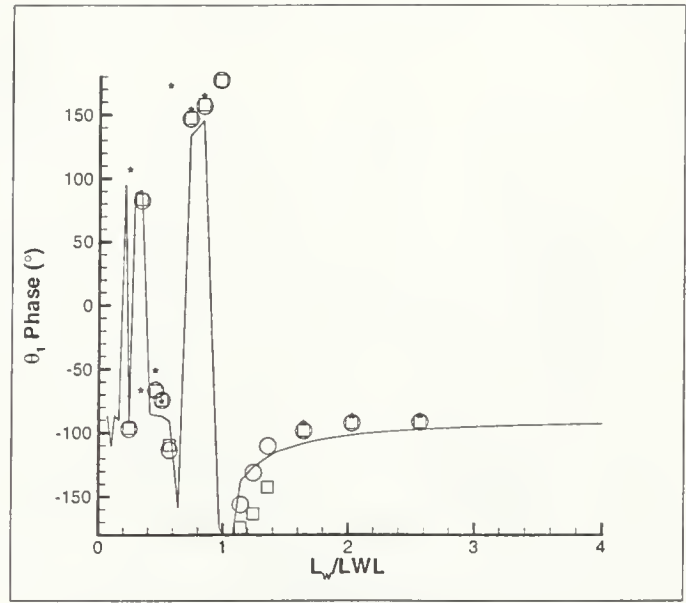c. Second Harmonic Amplitude
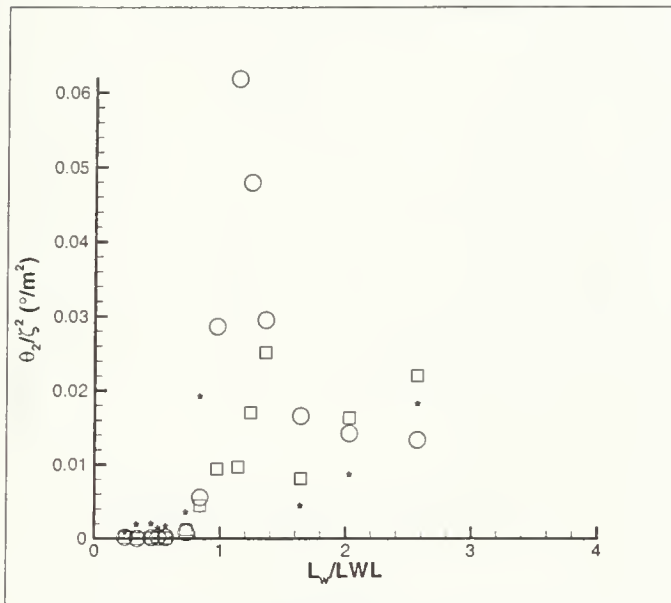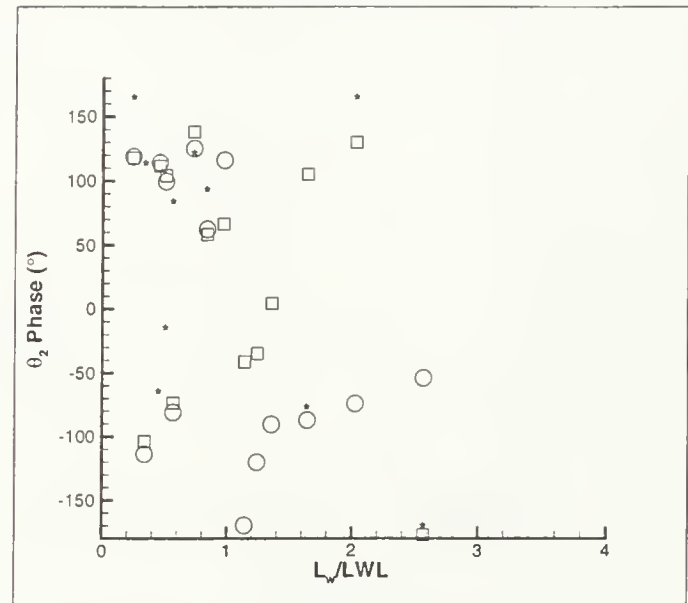
d. Phase

e. Third Harmonic Amplitude

f. Phase

Figure 6-3: V4 Heave RAO's, 20 knots, Head Seas

a. First Harmonic Amplitude

b. Phase

c. Second Harmonic Amplitude

d. Phase

e. Third Harmonic Amplitude

f. Phase

Figure 6-4: V4 Pitch RAO's, 20 knots, Head Seas
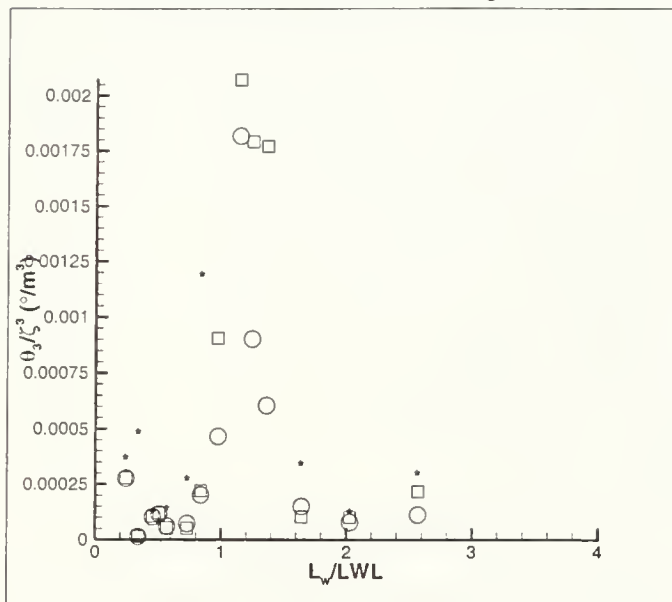
171
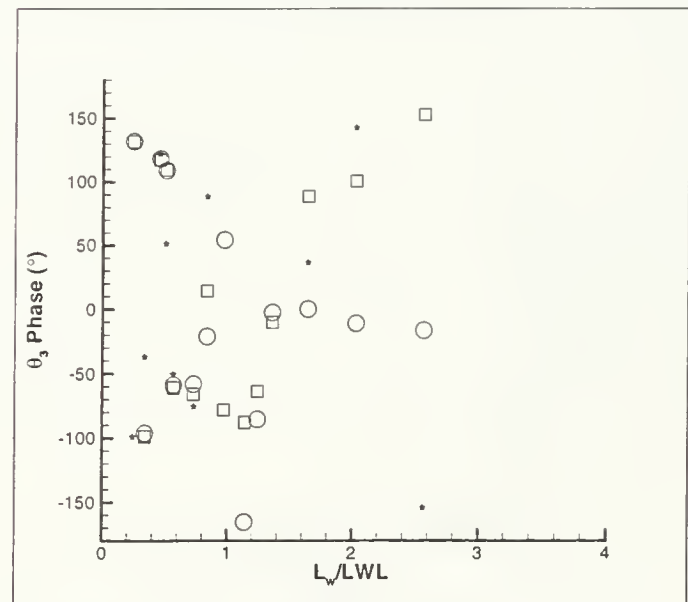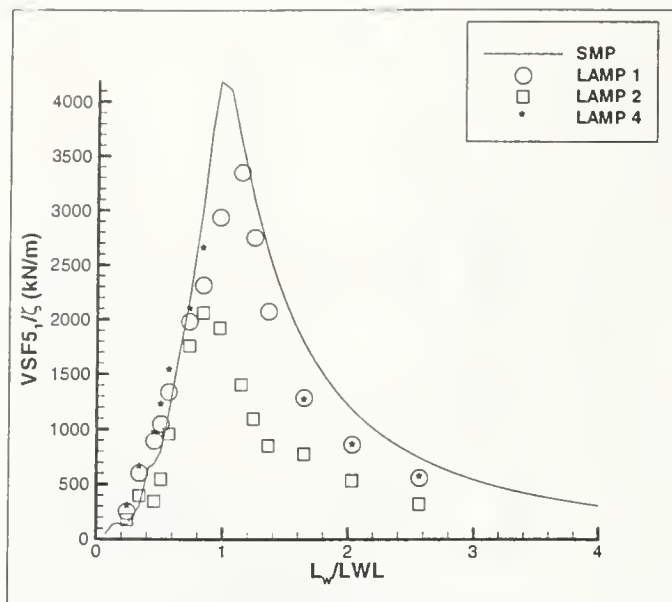
a. First Harmonic Amplitude

b. Phase

c. Second Harmonic Amplitude

d. Phase

e. Third Harmonic Amplitude

f. Phase

Figure 6-5: V4 VSF5 RAO's, 20 knots, Head Seas

172

a. First Harmonic Amplitude

b. Phase

c. Second Harmonic Amplitude

d. Phase

e. Third Harmonic Amplitude

f. Phase

Figure 6-6: V4 VBM10 RAO's, 20 knots, Head Seas

173

a. First Harmonic Amplitude

b. Phase

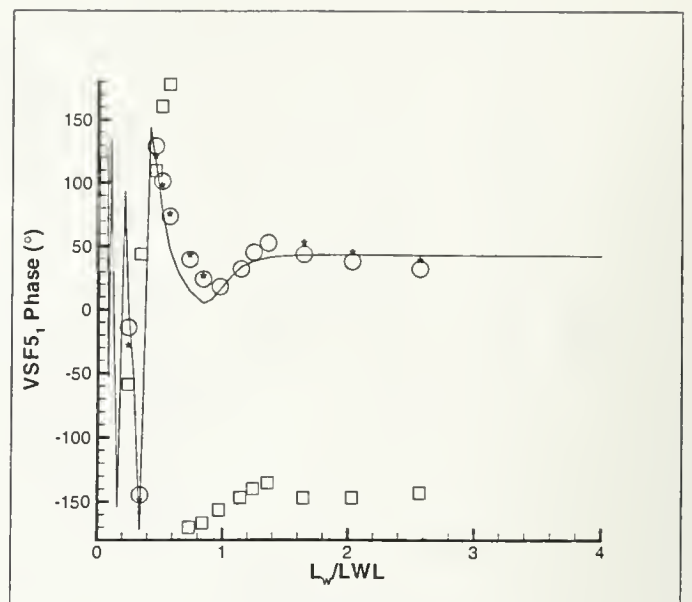c. Second Harmonic Amplitude
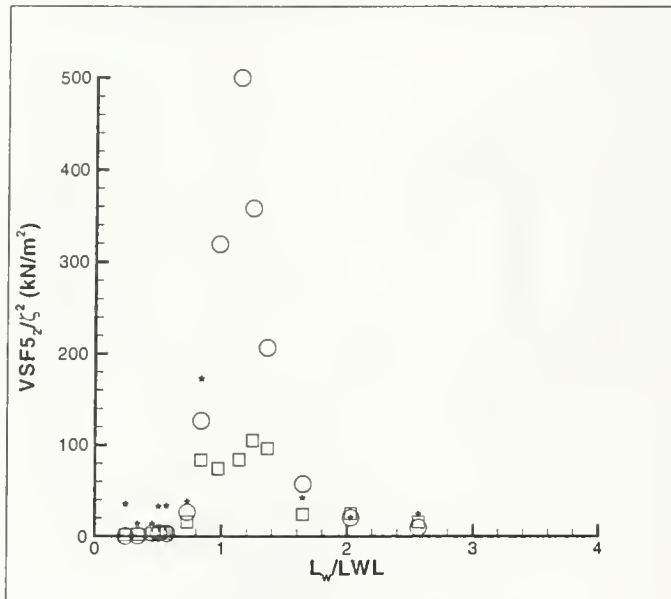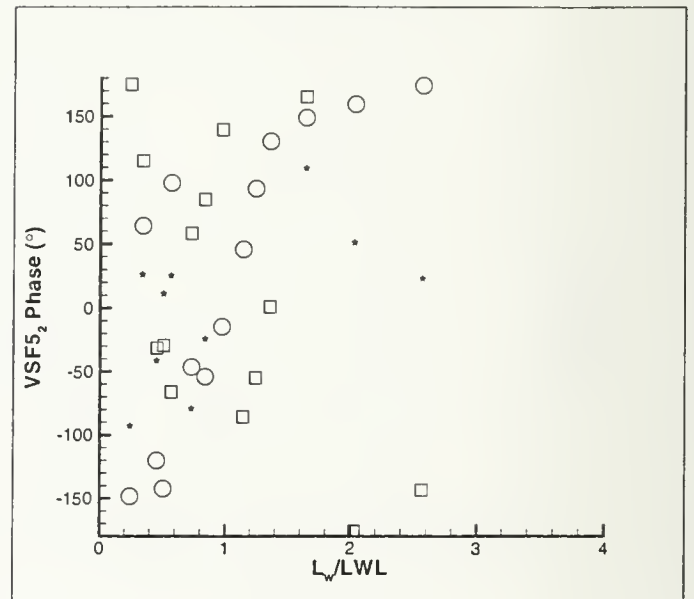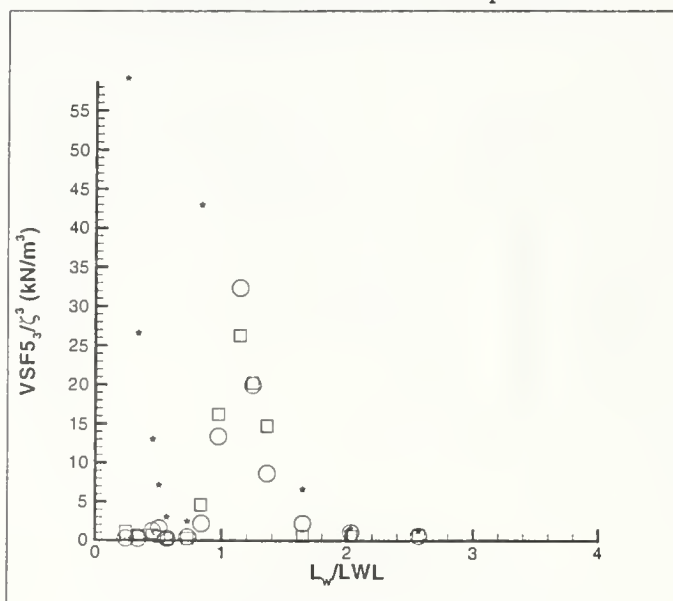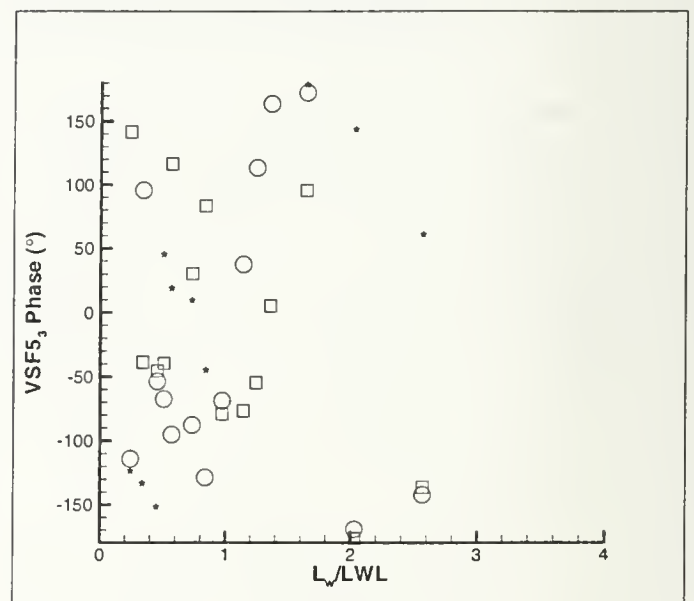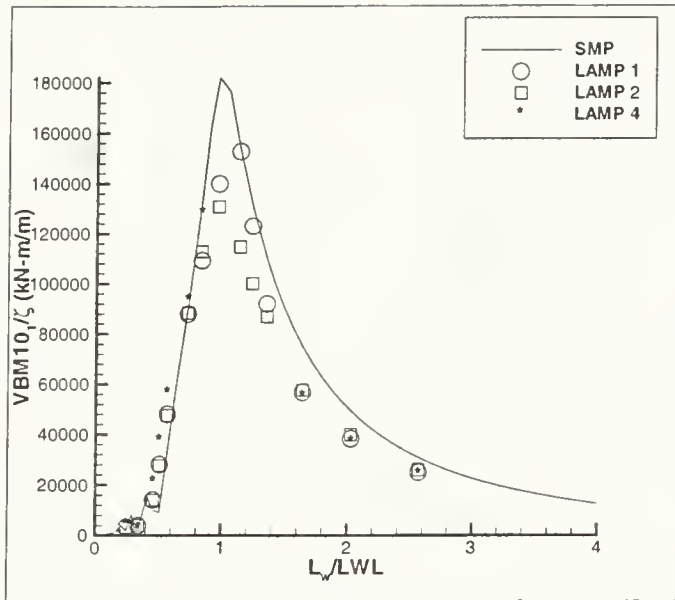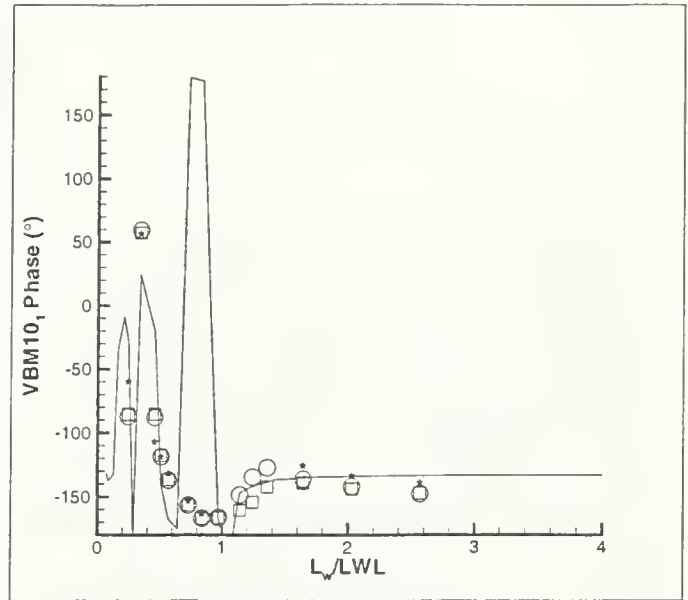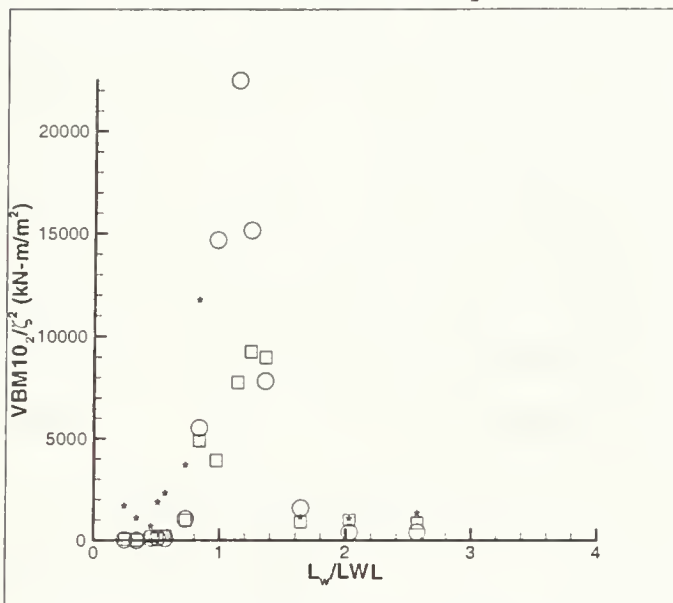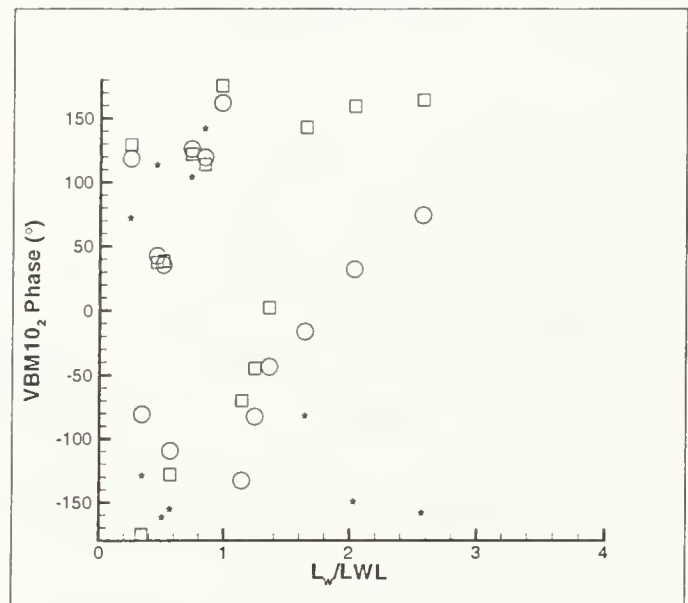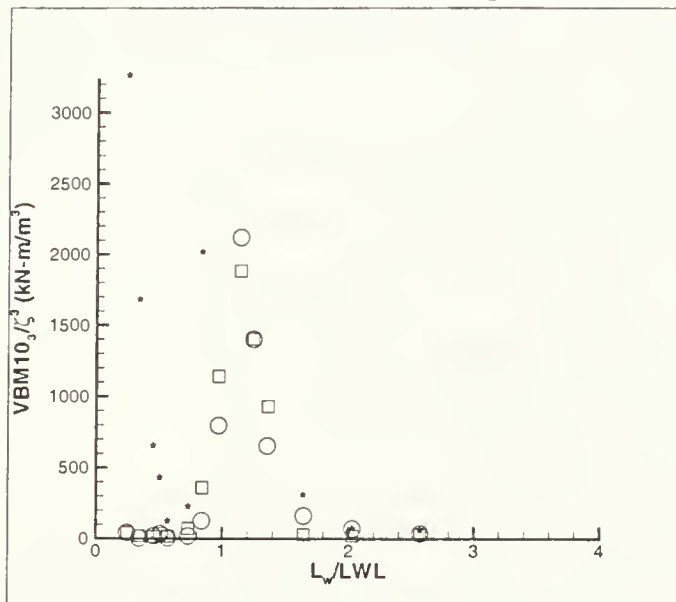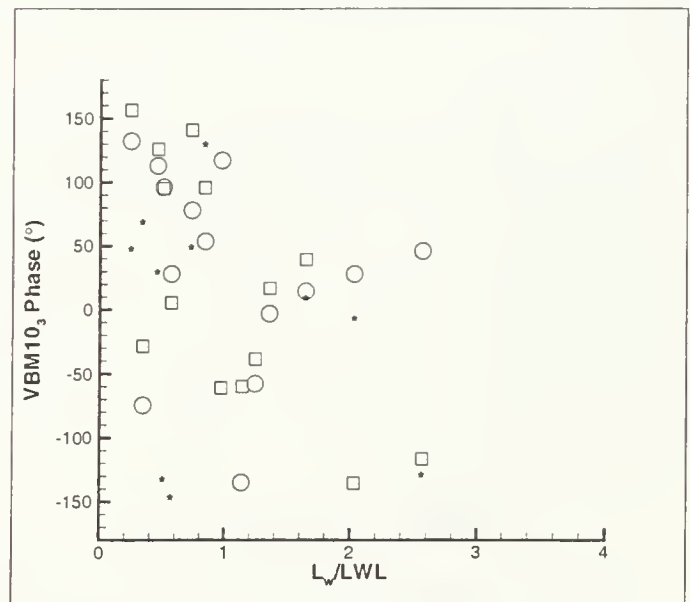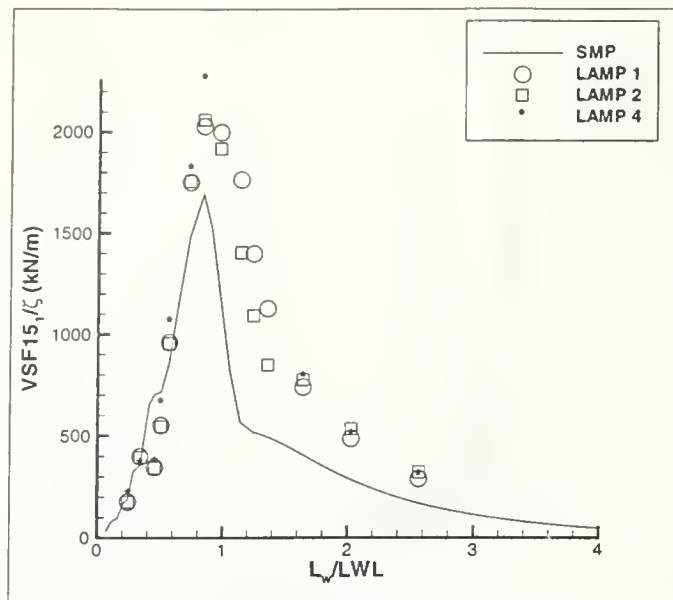
d. Phase

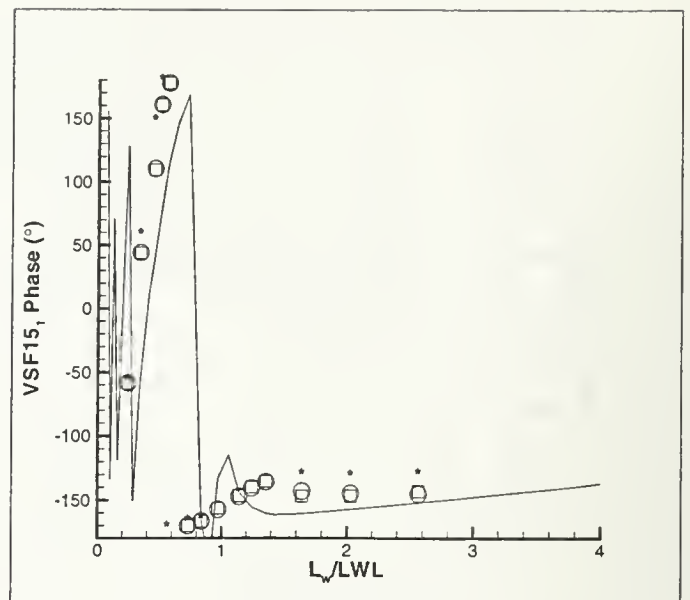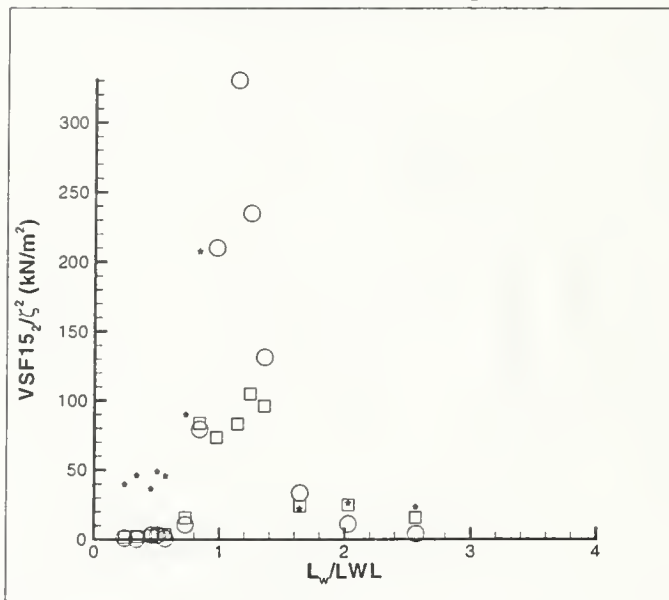e. Third Harmonic Amplitude

f. Phase

Figure 6-7: V4 VSF15 RAO's, 20 knots, Head Seas

174

6.3 VLCC Predictions

6.3.1 Motion and Loads Analysis

All of the runs listed in Table 6.2 on page 162 were completed successfully for both desired wave slopes, 1/40 and 1/60. The results are plotted in Figures 6-8 on page 178 through 6-12 on page 182, first without differentiation by wave slope. SMP predictions for the first harmonics of heave and pitch are plotted as solid lines for comparison. As mentioned earlier, load prediction methods are not correctly implemented in SMP91, which was used for the VLCC regular wave tests. Load RAO's have not yet been extracted from SMP95 for the VLCC. Normalized[4] mean responses, which consist of primarily 2nd order responses, are plotted in Figure 6-13.

In addition to the LAMP-4 runs listed, two additional LAMP-4 tests were conducted using component cutting (ICUTWL=0), so that panelization was resplined under the instantaneous waterline at each time step with a constant number of points, to examine the differences for this large displacement hull.[5] Comparison of the ICUTWL variation results showed that the differences were minor for the VLCC.

The following conclusions may be drawn from these plots, though not yet separated by wave slope:

- For heave and pitch motions:

    - For the first harmonics, the LAMP predictions match the SMP results well, except near response resonance, where both LAMP-1 and 2 predict higher motions. The LAMP-2 and 4 results actually predict lower heave responses than LAMP-1 at resonance. In pitch, however, LAMP-2 and 4 predict slightly higher responses than LAMP-1. Both of these results correlate with the LAMP observations in irregular seas, at high sea states.

---

[4]The difference between the mean responses and responses calculated in calm water is divided by the square of the wave amplitude.

[5]All other LAMP-4 tests were conducted with master geometry cutting (ICUTWL=1), so that the panelization is trimmed off at the instantaneous waterline, as with the V4 LAMP-4.

- As with the V4 hull, the differences are due possibly to a shift in response natural frequency in LAMP-2/4. The phase predictions support this, showing a reduction in phase lag near resonance for LAMP-2 and 4 compared to SMP and LAMP-1. Still, the LAMP phase predictions follow the SMP curve quite well for the first harmonic.

- In the second harmonic results, LAMP-2 predicts a lower response than LAMP-1, while LAMP-4 predicts a much larger response (though still very insignificant compared to the first harmonic). The LAMP-1 and 2 trends are very similar to those observed for the V4. Phase angles correlate well, but the LAMP-2/4 results again decrease in phase lag.

- Third harmonics are extremely negligible, and the scatter in phase predictions is a result of these very small amplitudes.

- Although the heave and pitch resonant peaks predicted by LAMP are both larger than the SMP predictions, the differences seem small compared to the response amplitude differences from the irregular seas tests. This effect may indicate that even for the large hull, linear superposition in heavy seas is not appropriate.

- For VSF4, the differences between LAMP methods are very small for the first harmonics, but much more significant in the higher harmonics. In the second harmonic, LAMP-2 generally underpredicts the LAMP-1 response except that LAMP-2 predicts a separate smaller peak not shown at all by LAMP-1. In all cases the phases correspond well for each LAMP method where the response amplitudes are also significant.

- For VSF16, the results are very close except near resonance, where LAMP-2 predicts a higher response than LAMP-1, and LAMP-4 higher than LAMP-2. The phase angles are quite close, although at resonance they are near 180°, making the plot look worse than the actual differences are. The trend of increasing responses from LAMP-1 to 2 to 4 continues in the second and third harmonics. Similar trends are identified in the VBM10 plots.

- For the normalized mean responses, Figure 6-13 shows that the trends observed in the second harmonics also apply to the second order mean contribution, as expected. LAMP-2/4 generally predict higher amplitudes than LAMP-1. For the motions, the absolute 2nd order mean responses are larger than the 2nd harmonic amplitudes, though still small. However, the load 2nd order mean responses are the same order as the 2nd harmonics. These mean responses, particularly the loads, can be significant in fatigue design by altering the constant structural stress which is then subjected to additional fluctuating stresses.

The differences between results of varying computational methods, panelizations, or LAMP parameters may seem significant for both the mathematical hulls and the VLCC case, primarily for the second and higher harmonics. However, the magnitude of these differences should be put in perspective by examining the absolute (non-normalized by varying orders of wave amplitude) responses. For example, a detailed comparison of the absolute harmonic responses for the VLCC shows that:

- For heave, the 2nd harmonic is generally less than 3% of the first harmonic, even near resonance. All higher harmonics were less than 1%.

- For pitch, the 2nd harmonics are less than 5% of the first harmonics, and higher harmonics are less than 1%.

- For VSF4, 2nd harmonics were up to 30% of the first harmonic, which is by no means insignificant. Even the third harmonic is in some cases greater than 10%.

- For VSF16, 2nd harmonics are again significant, up to 25%. 3rd harmonics were smaller but not negligible, and higher harmonics were very low.

- For VBM10, the 2nd harmonics were up to 20%, particularly for the larger wave slope. As mentioned below, the effect of wave slope was largest in the bending moment predictions. Third harmonics were low, generally below 5%, and higher harmonics were generally below 1%.
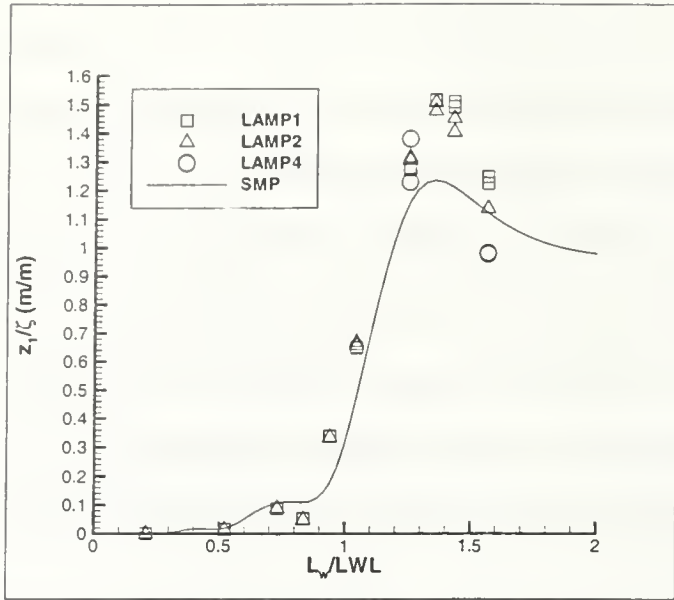
a. First Harmonic Amplitude
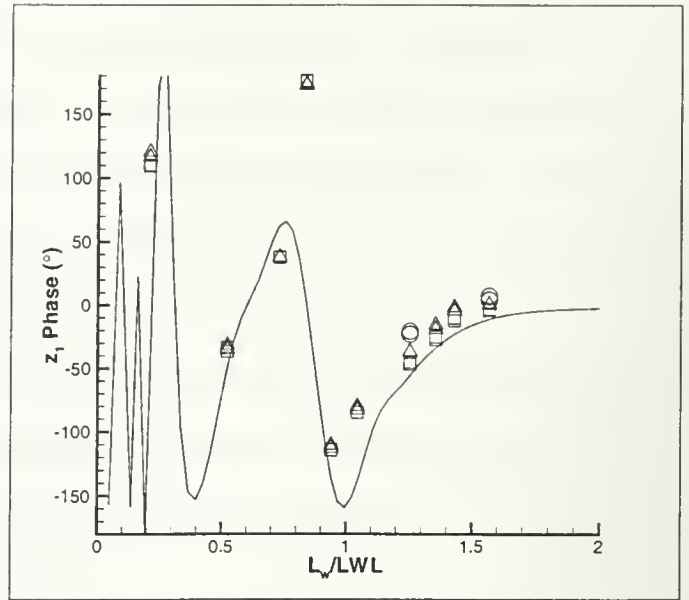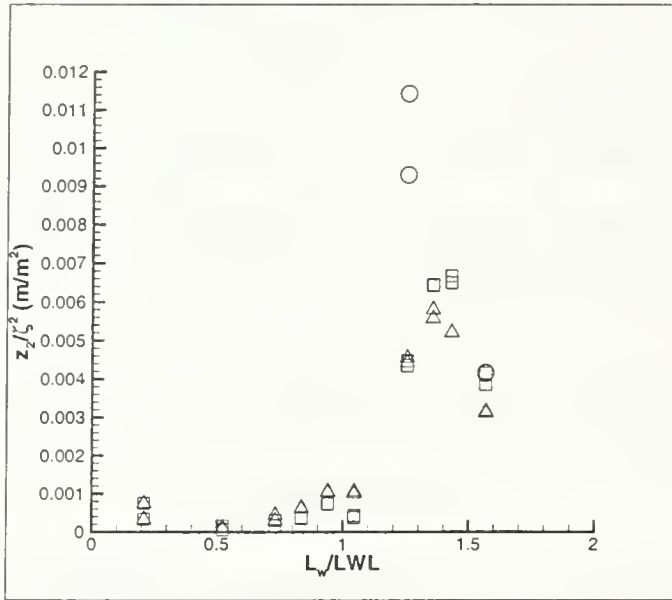
b. Phase

c. Second Harmonic Amplitude
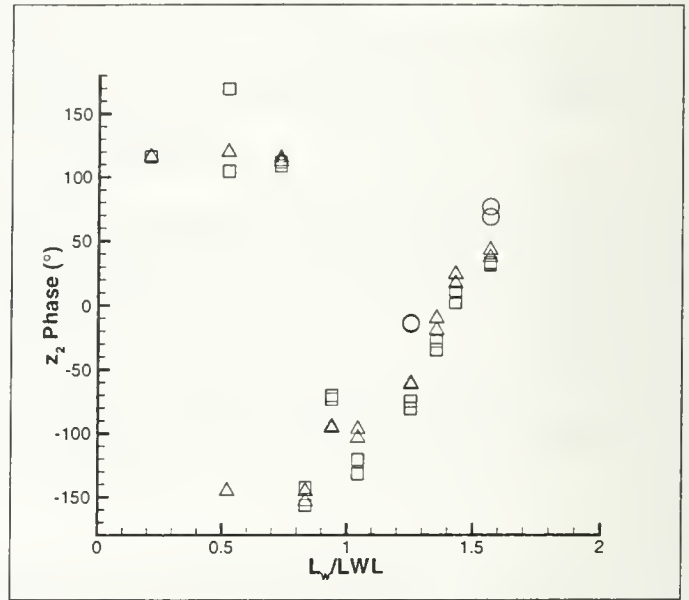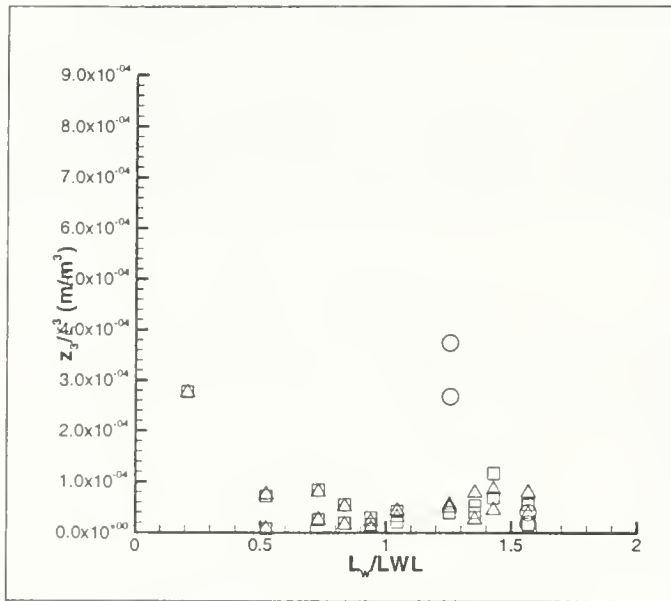
d. Phase

e. Third Harmonic Amplitude
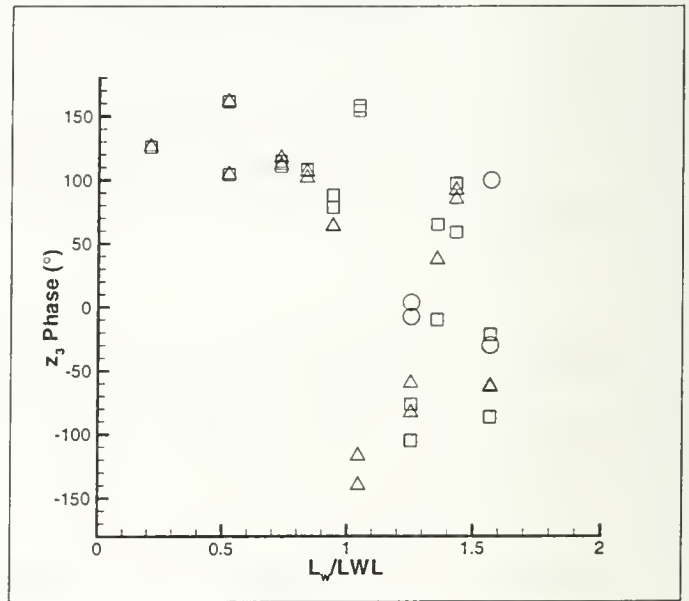
f. Phase

Figure 6-8: VLCC Heave RAO's
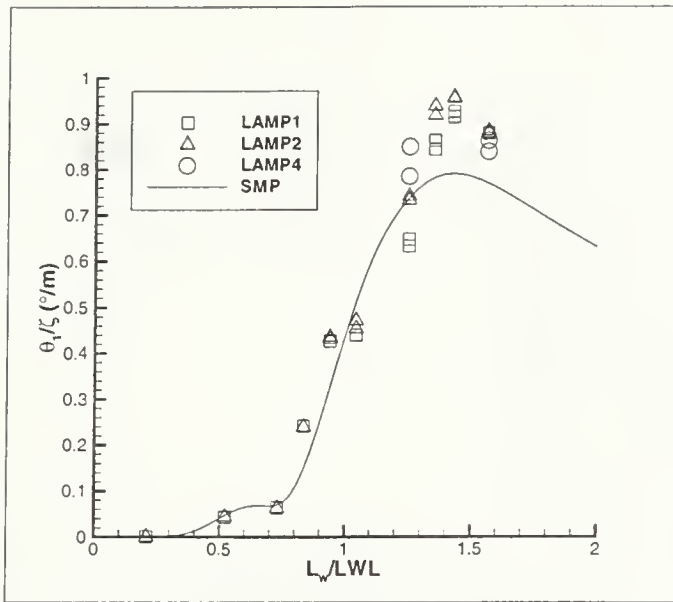
a. First Harmonic Amplitude
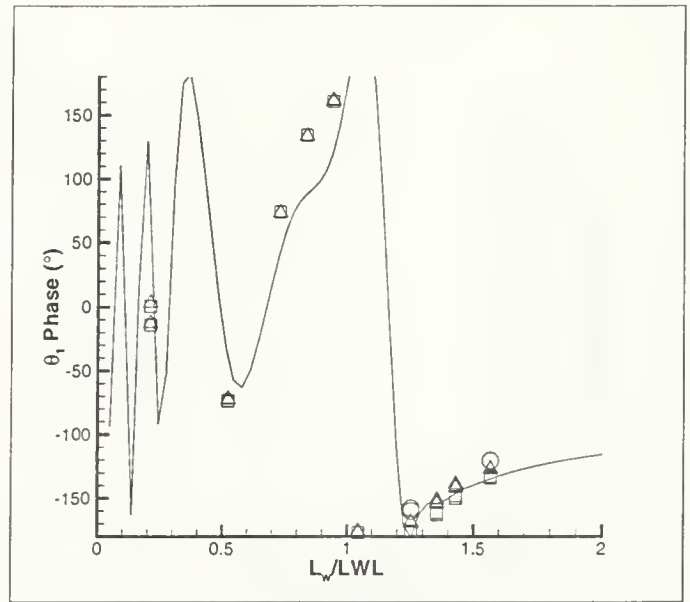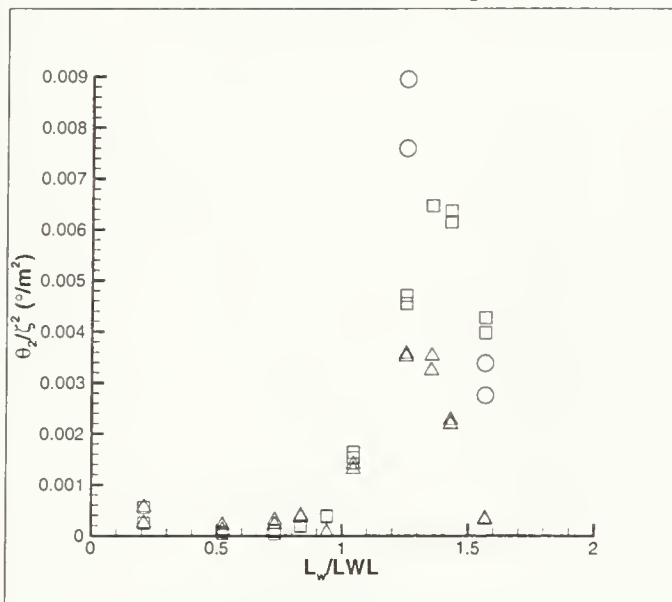
b. Phase

c. Second Harmonic Amplitude
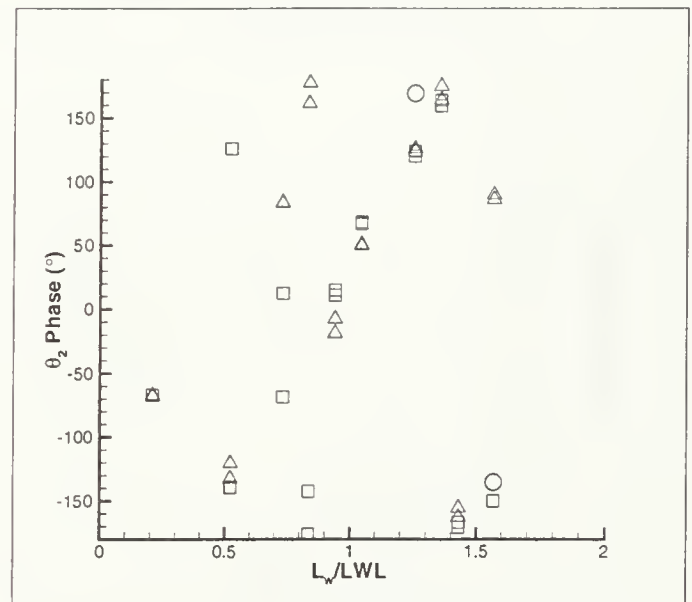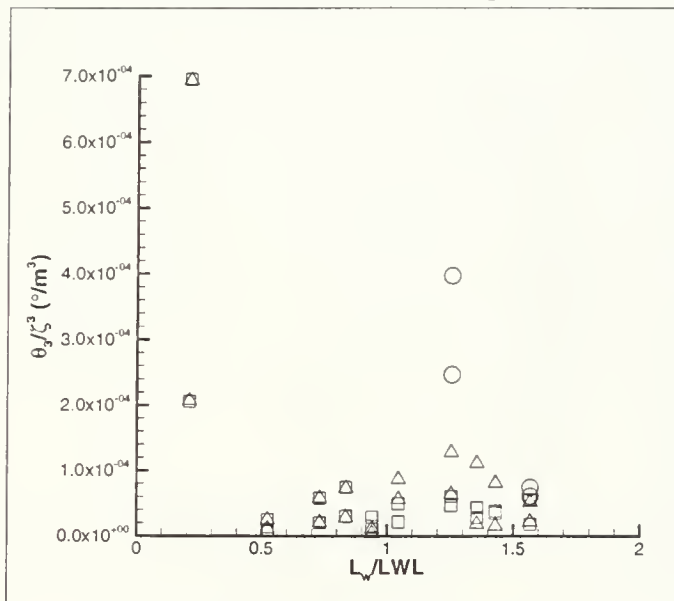
d. Phase

e. Third Harmonic Amplitude
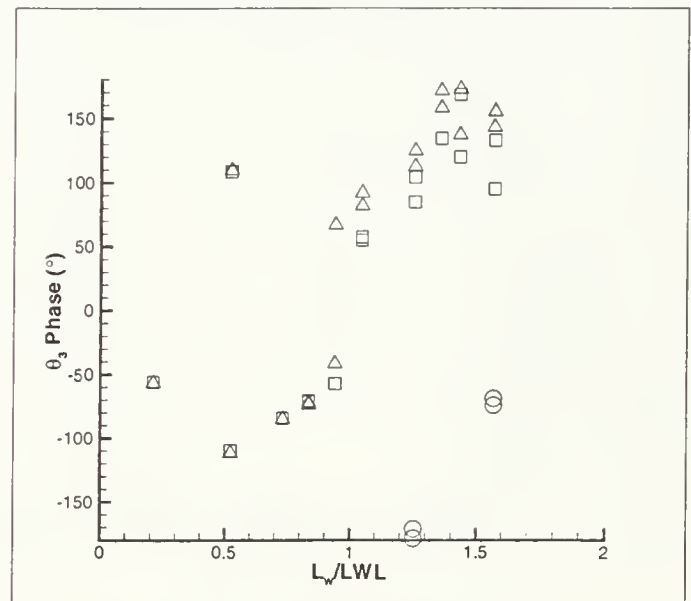
f. Phase

Figure 6-9: VLCC Pitch RAO's
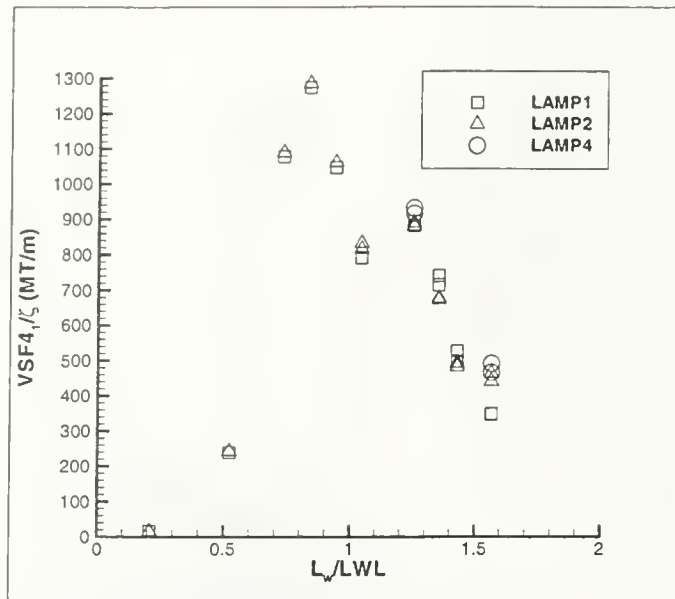
179

a. First Harmonic Amplitude
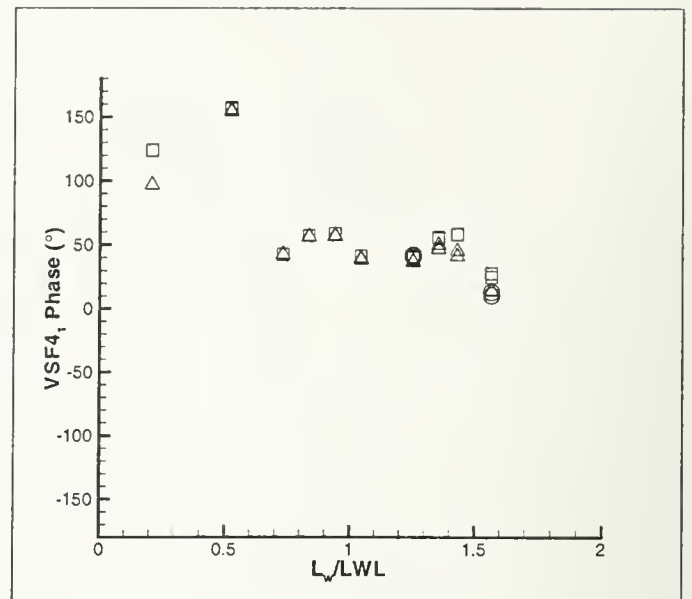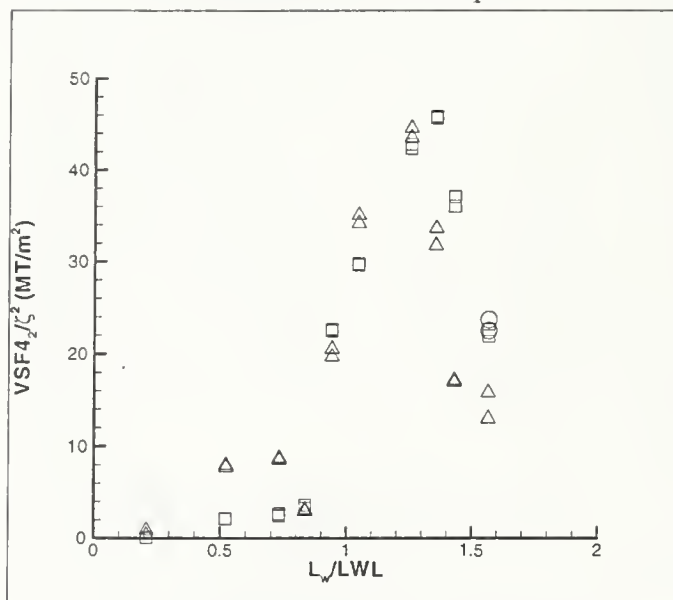
b. Phase

c. Second Harmonic Amplitude
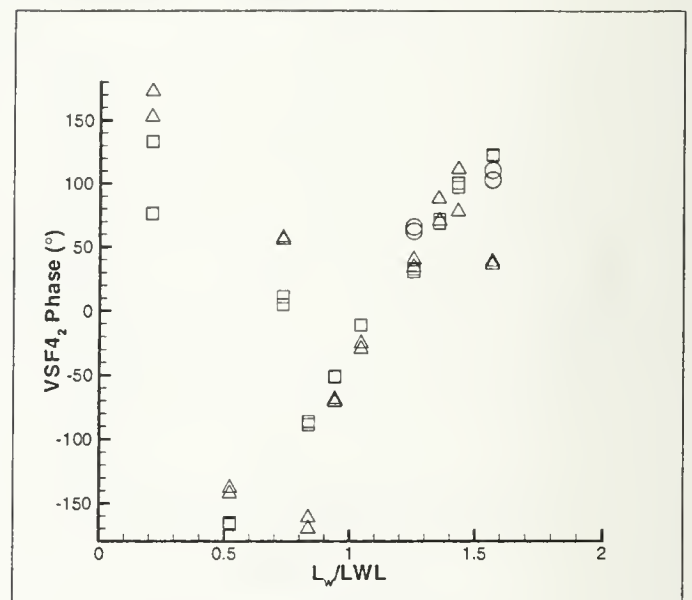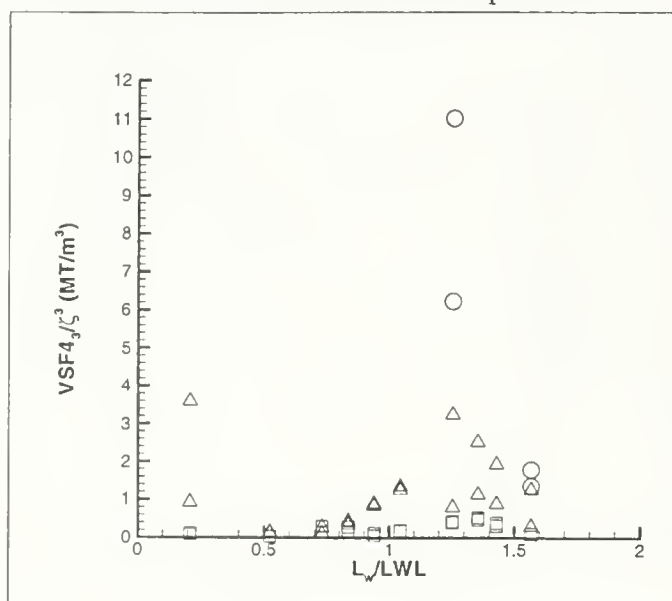
d. Phase

e. Third Harmonic Amplitude
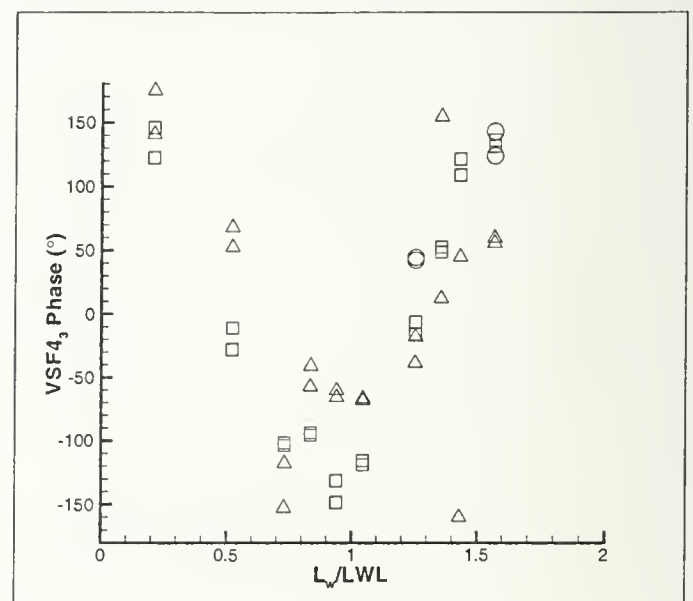
f. Phase

Figure 6-10: VLCC VSF4 RAO's
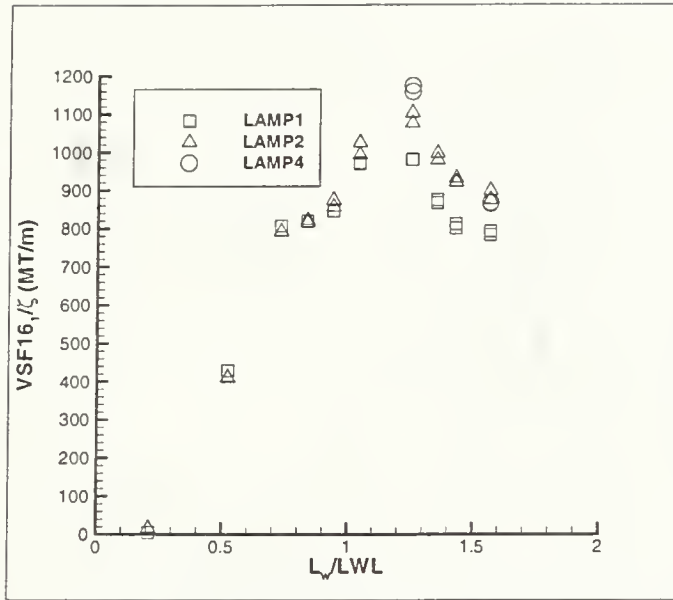
a. First Harmonic Amplitude
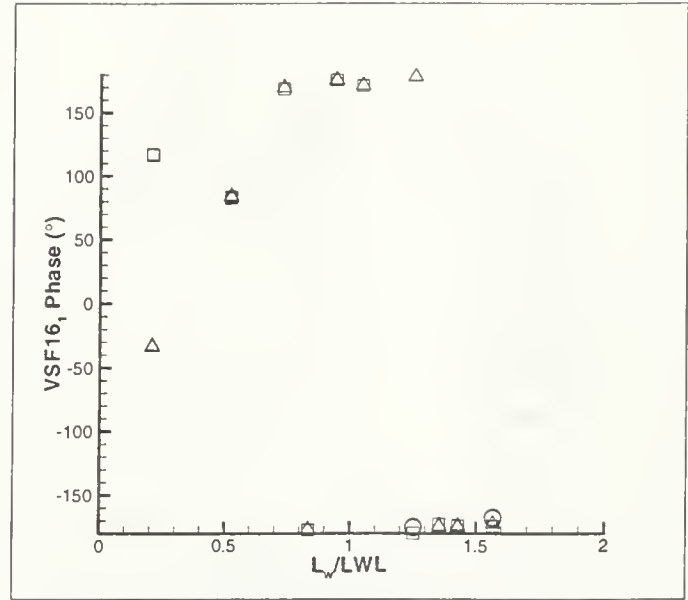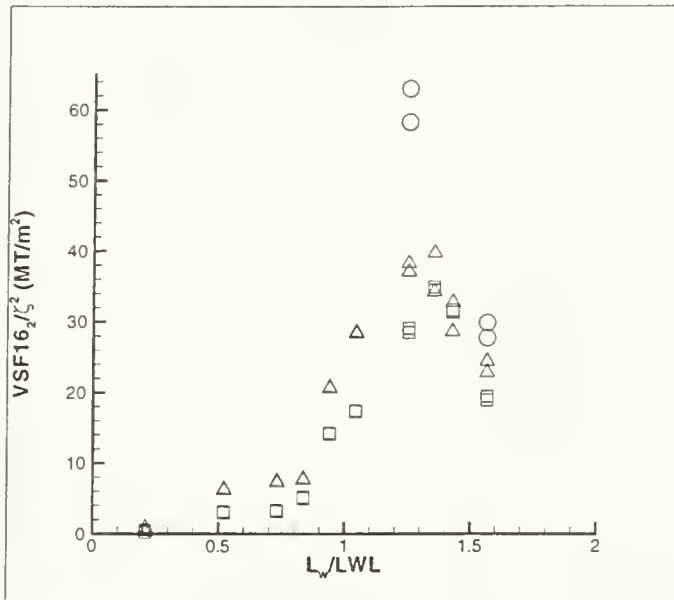
b. Phase

c. Second Harmonic Amplitude
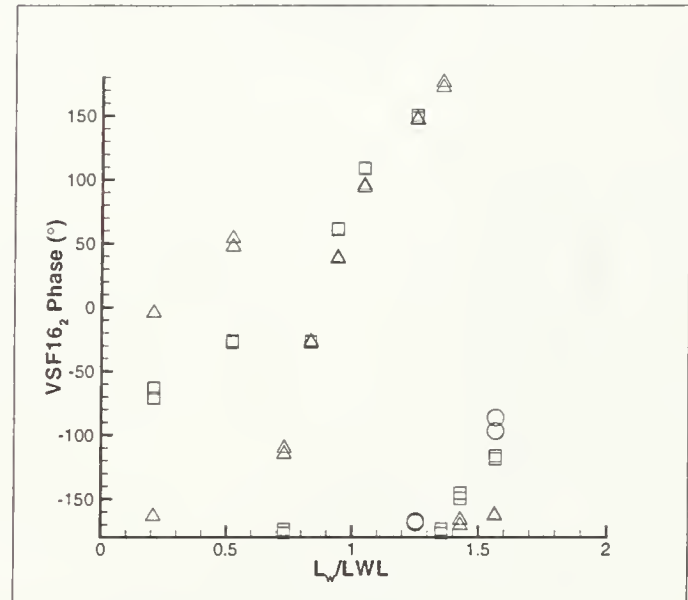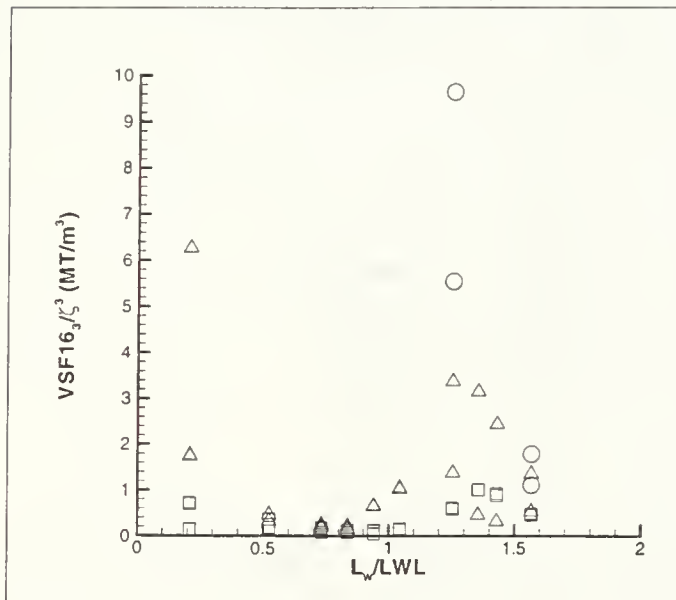
d. Phase

e. Third Harmonic Amplitude
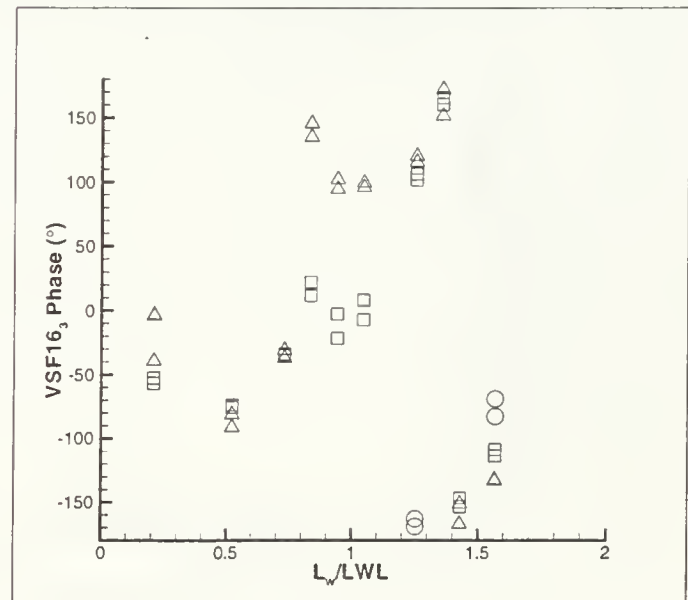
f. Phase

Figure 6-11: VLCC VSF16 RAO's
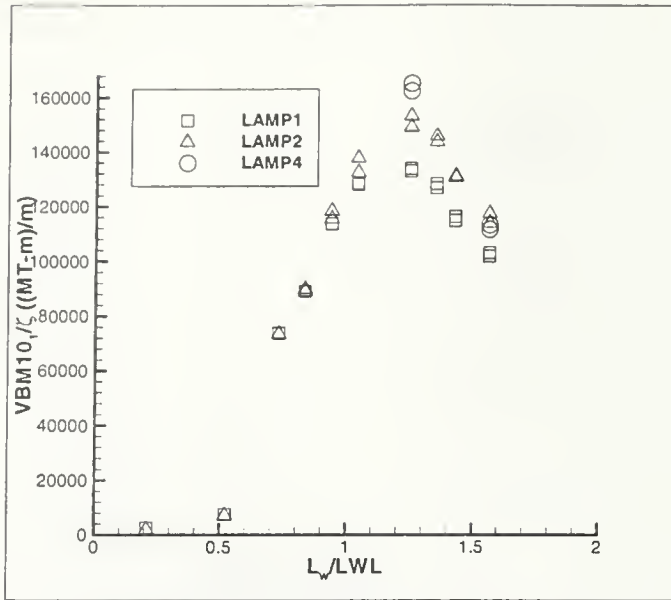
a. First Harmonic Amplitude
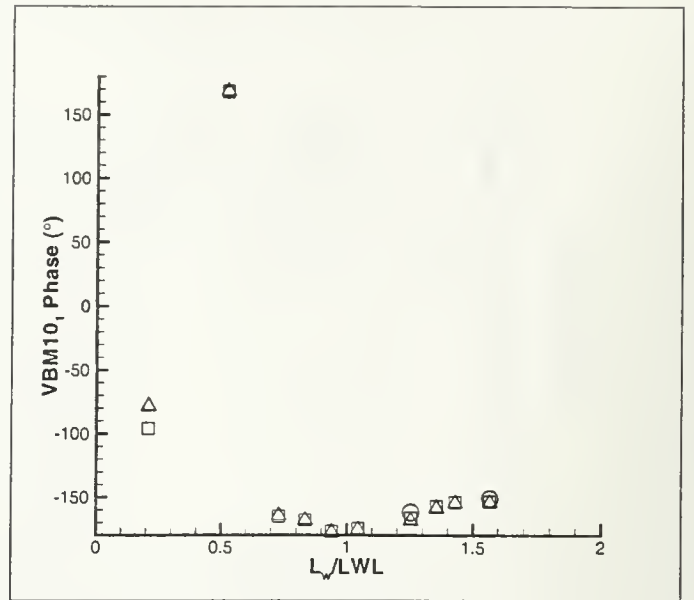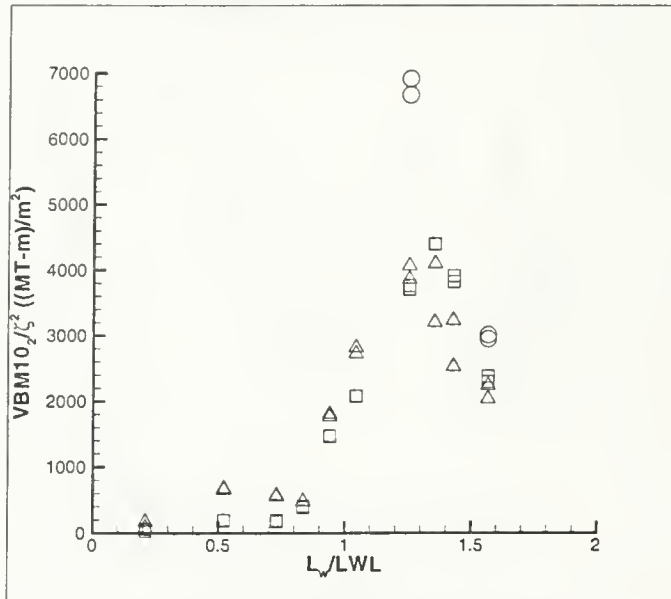
b. Phase

c. Second Harmonic Amplitude
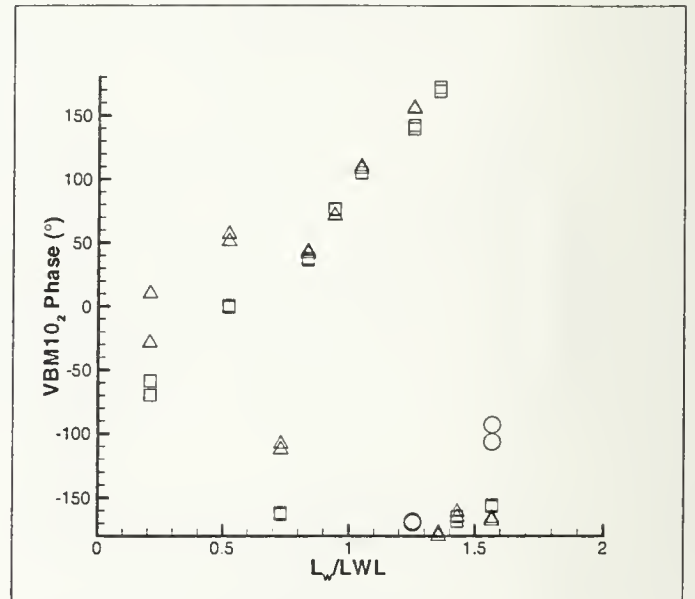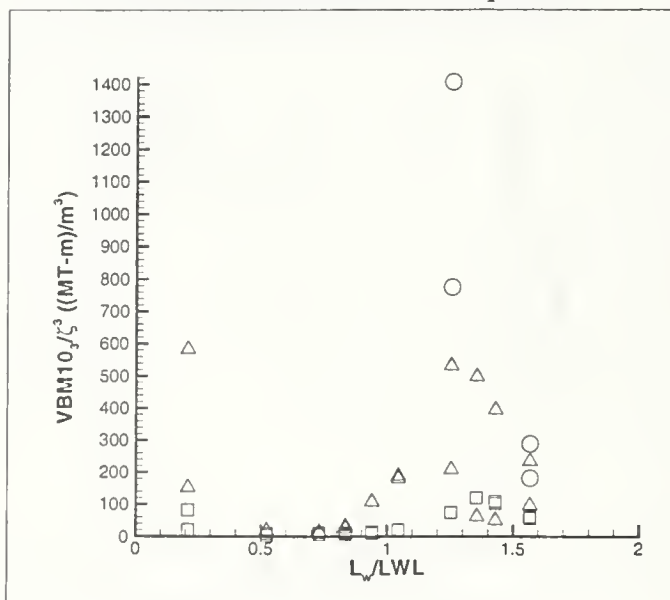
d. Phase

e. Third Harmonic Amplitude
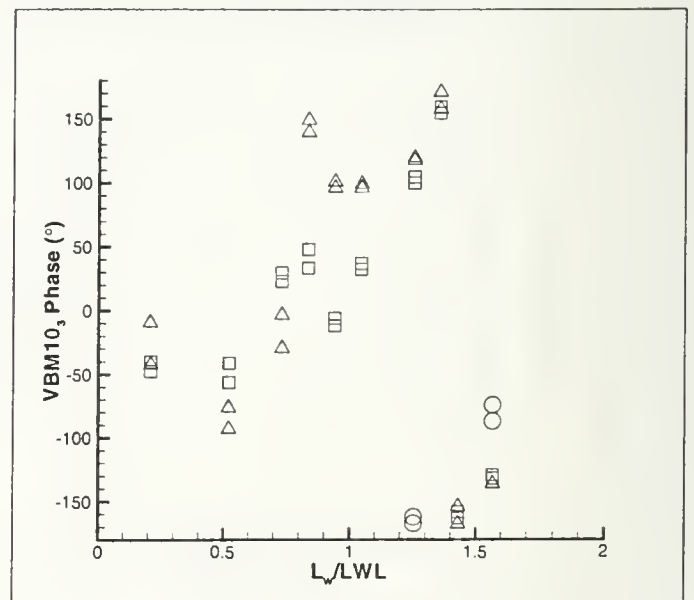
f. Phase

Figure 6-12: VLCC VBM10 RAO's

182
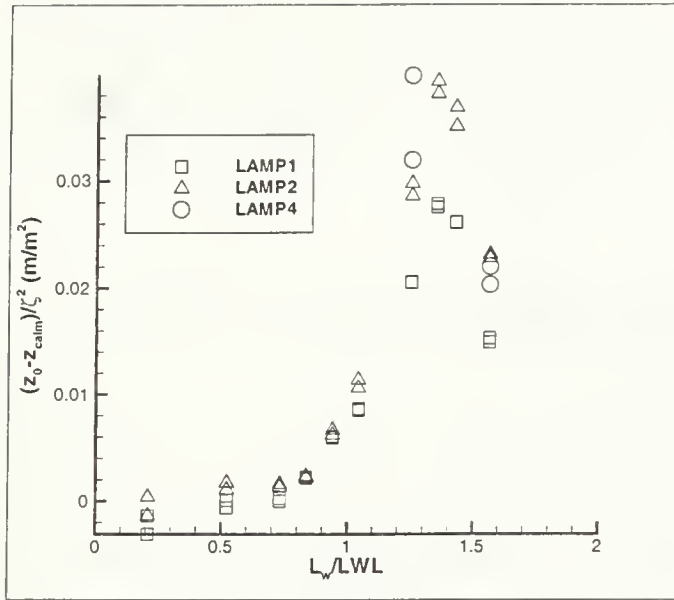
a. Heave
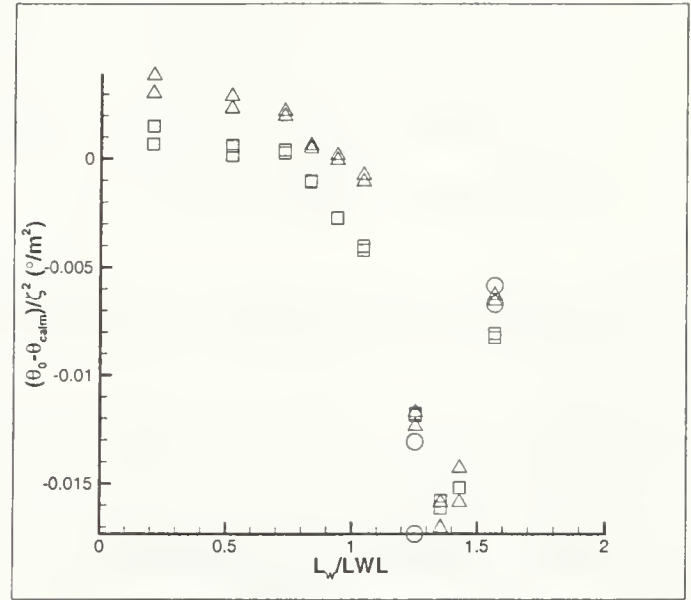
b. Pitch
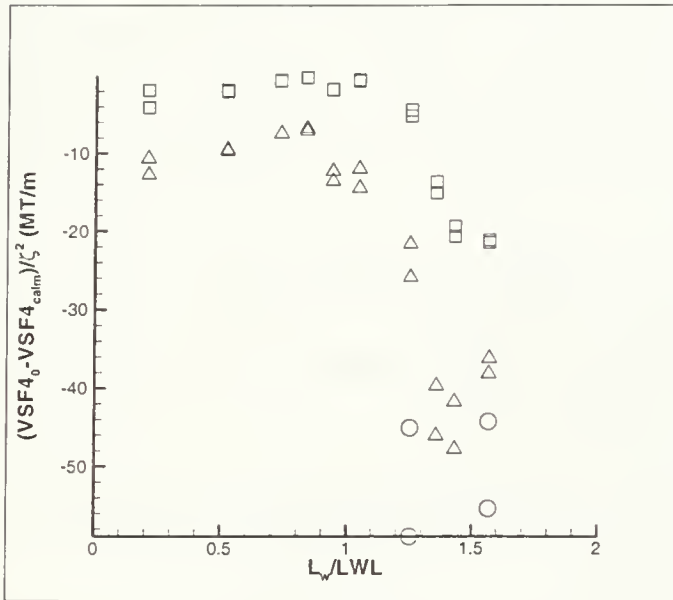
c. VSF4
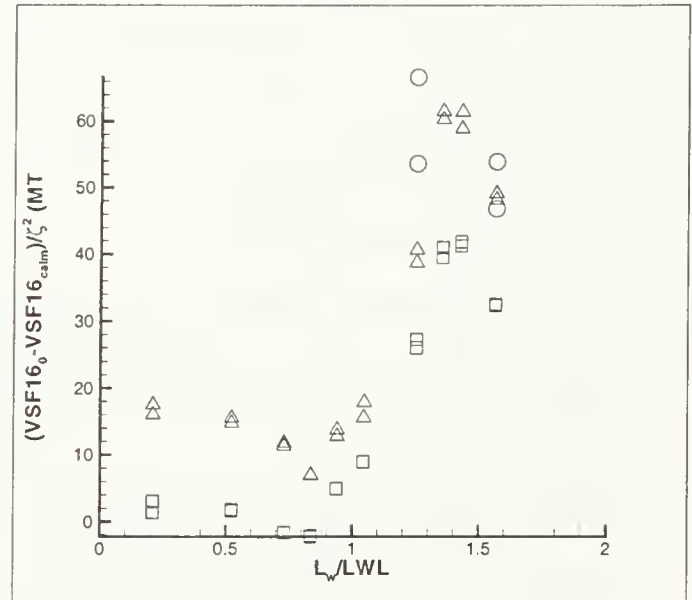
d. VSF16
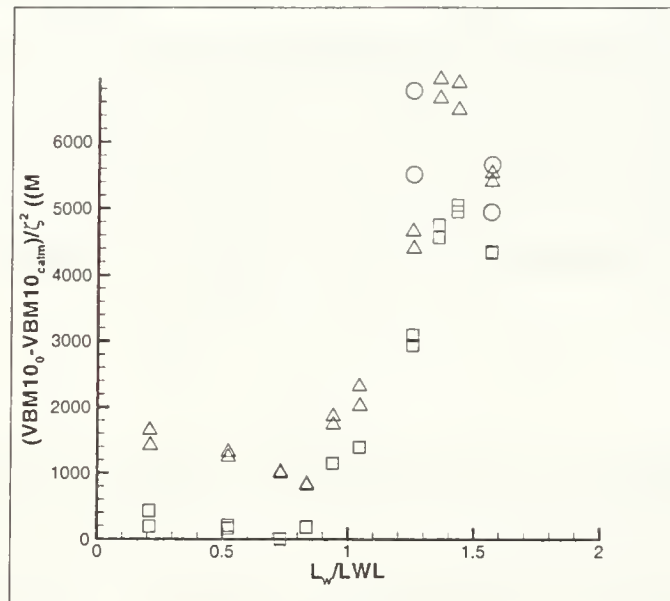
e. VBM10

Figure 6-13: VLCC Mean RAO's, $(R_0 - R_{calm})/\zeta^2$

The harmonics for the V4 hull follow the same basic trends – motion higher harmonics are quite small and may be neglected. Load higher harmonics, however, are not insignificant, and should play an important part in design, particularly at high speeds in large to severe seas.

### 6.3.2 Dependence of VLCC Responses on Wave Slope

Results were not differentiated by wave slope in the first set of plots. Multiple data points at a single L_w/LWL for each prediction method correspond to the two wave slopes, $H_w/L_w = 1/60$ and $1/40$. The wave slopes appeared not to have a large effect on the response transfer functions. To further confirm this, response amplitudes only are plotted for the first and second harmonics in Figures 6-14 on the next page through 6-18 on page 189. The responses are plotted against prediction method and wave slope. Each harmonic is plotted on the same vertical scale for ease of comparison between prediction tools.

For the motions, wave slope made very little difference in the LAMP-1 tests, and only a slight difference in the LAMP-2/4 results near resonance for both the first and second harmonics. For loads, wave slope surprisingly made little difference in response predictions for all methods. The only significant exception was the LAMP-2 predictions for VBM10 in the second harmonic.

The lack of strong dependence on wave slope for the VLCC should not be assumed for most hulls. As with all the VLCC responses, the motions and loads are dominated by the large displacement of the vessel. In general, motions and loads should be sensitive to wave slope, particularly when large-amplitude responses are expected. However, if motions are small, for ships such as the VLCC, the 1/40 wave slope tests should suffice.

6.4 Applications of Regular Wave Data

Besides their utility in better understanding the nature of motion and load responses, how can regular wave results be used to provide useful engineering data when linear
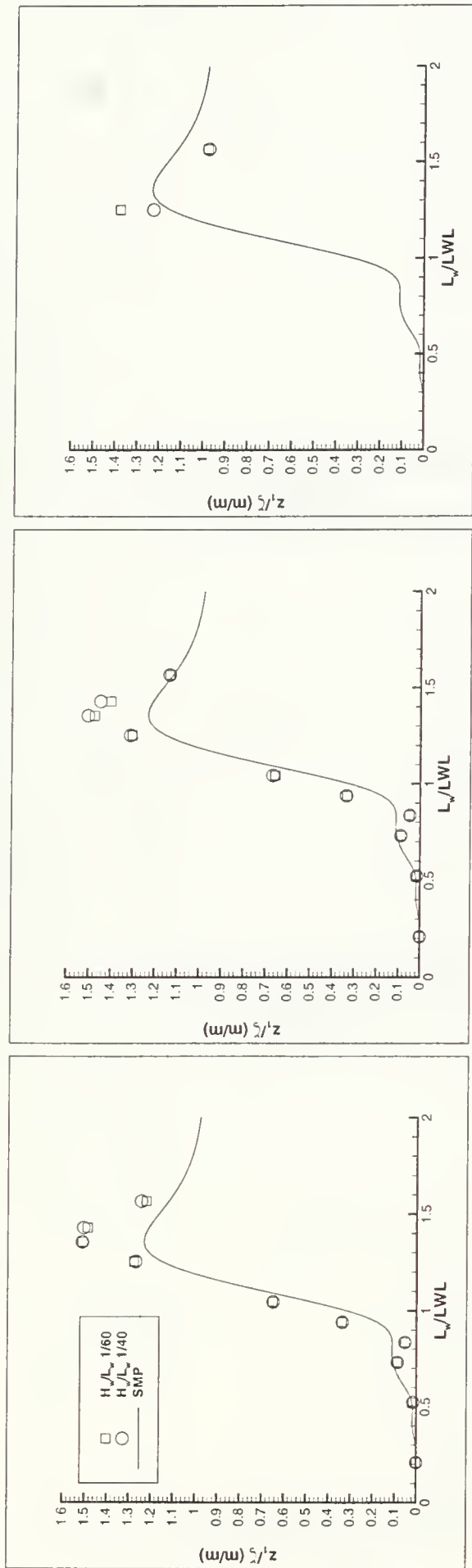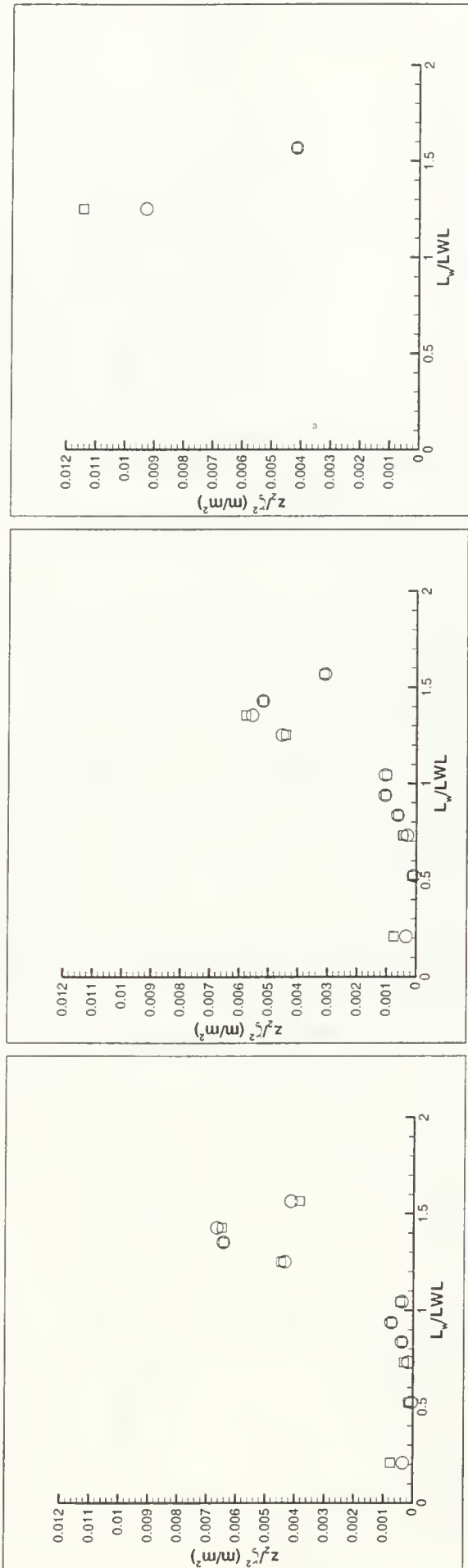
Figure 6-14: VLCC Heave RAO's by Wave Slope

185
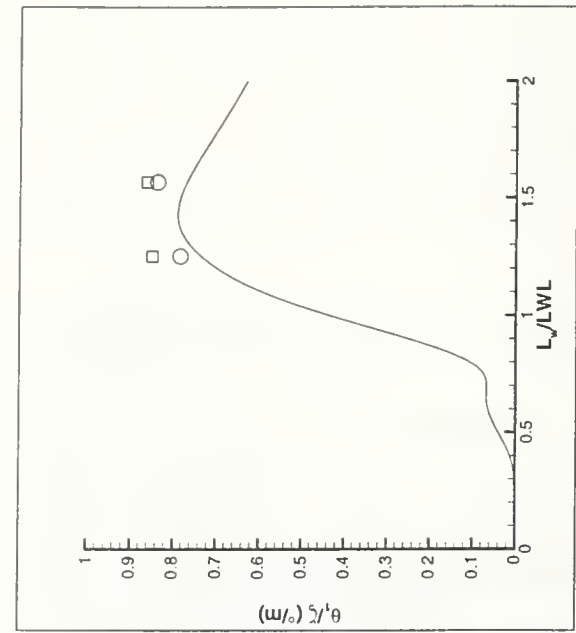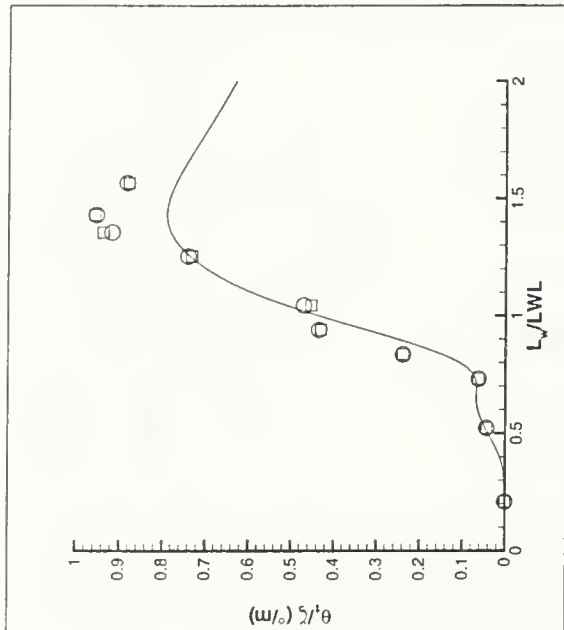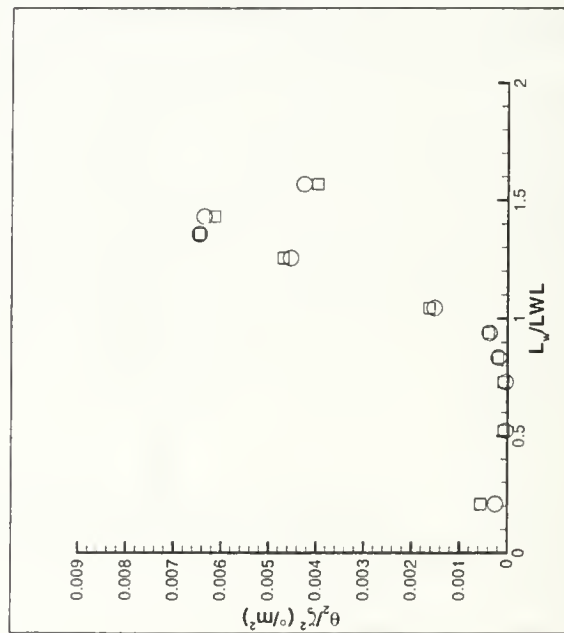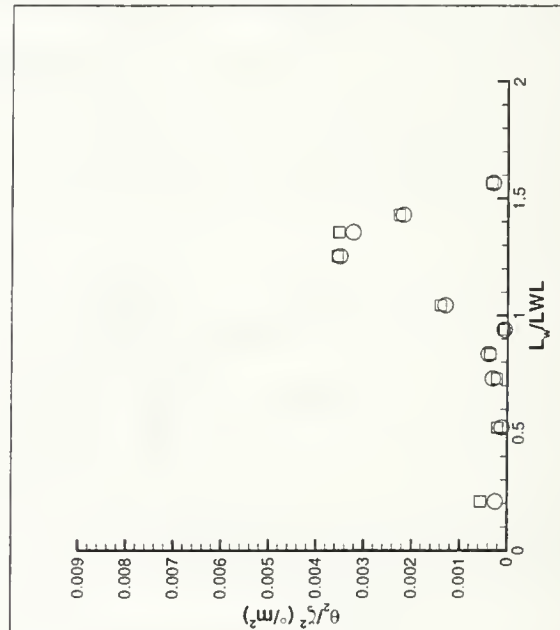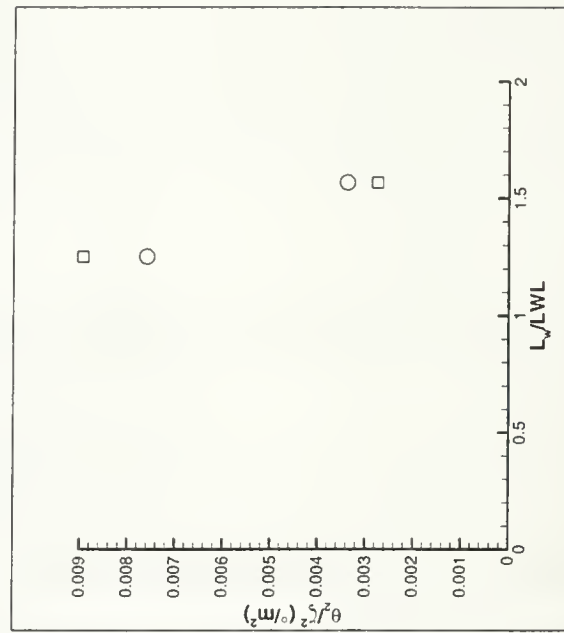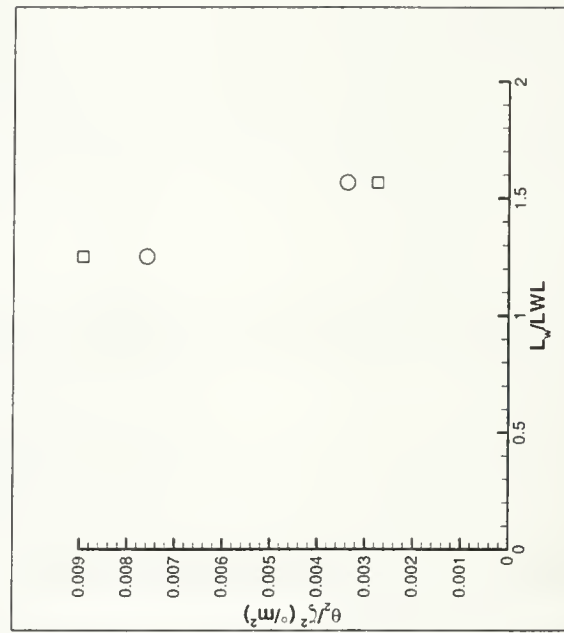
Figure 6-15: VLCC Pitch RAO's by Wave Slope
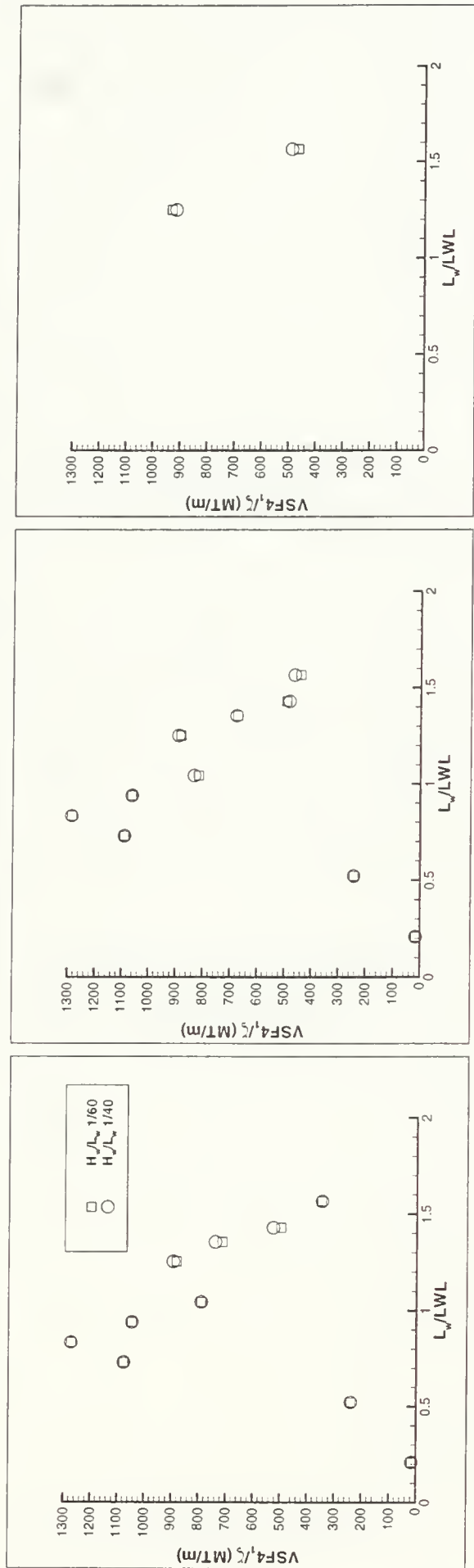
Figure 6-16: VLCC VSF4 RAO's by Wave Slope
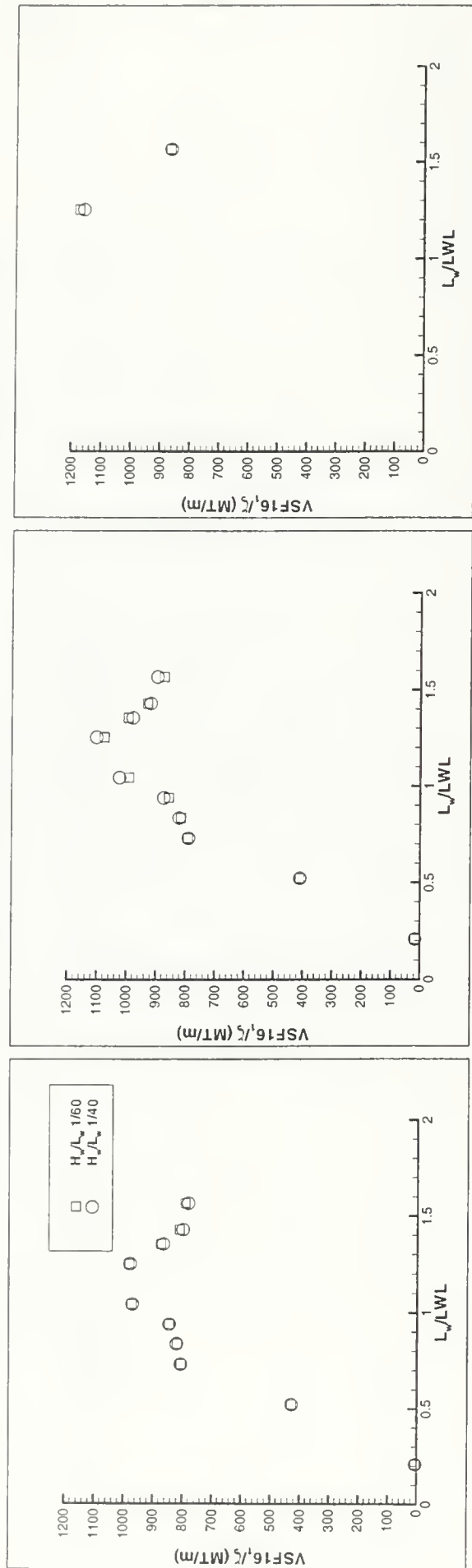
187

Figure 6-17: VLCC VSF16 RAO's by Wave Slope
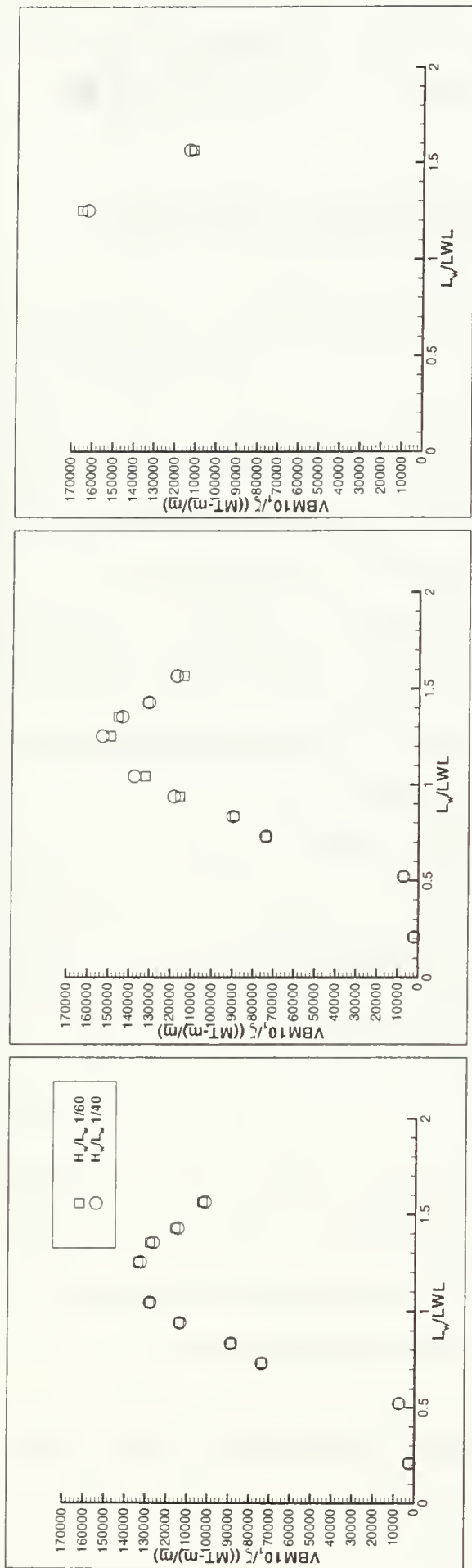
188
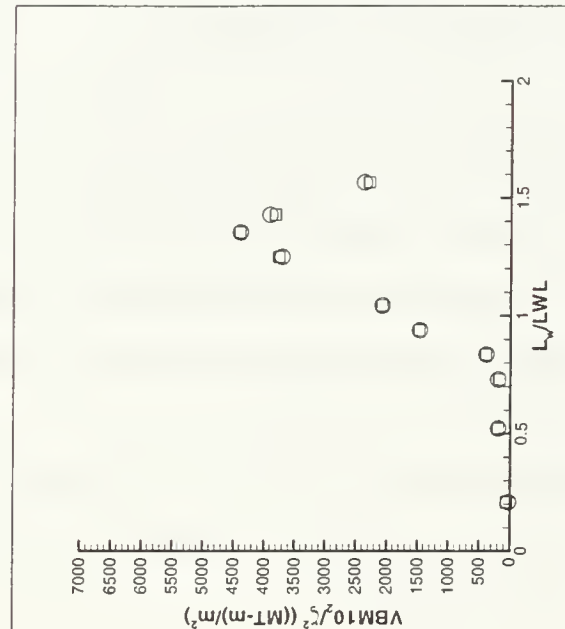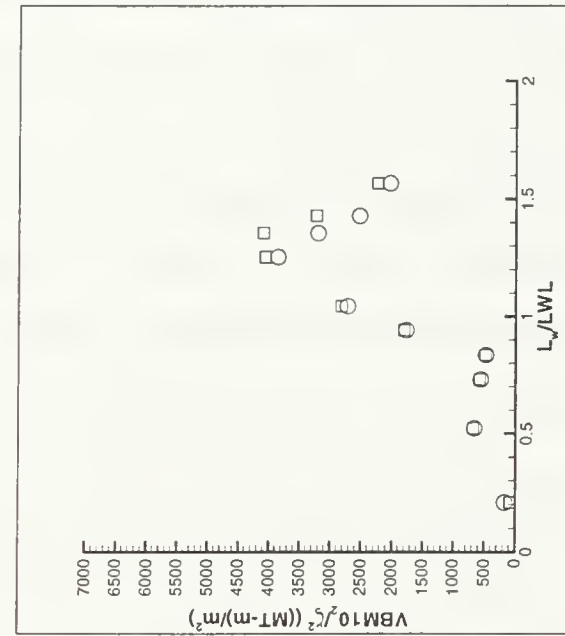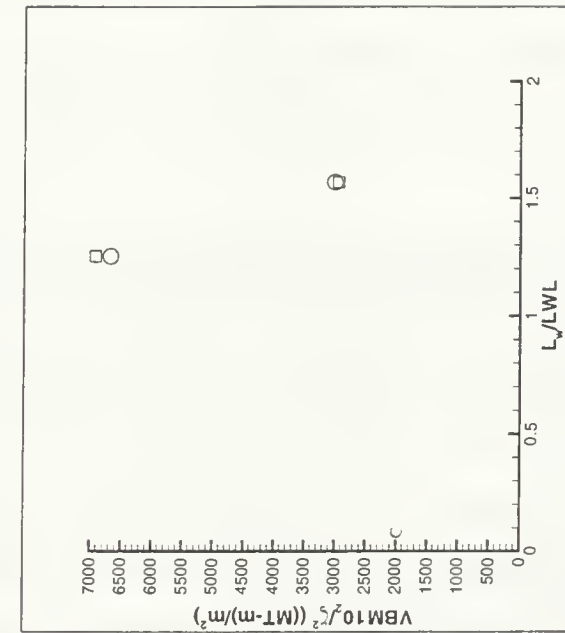
Figure 6-18: VLCC VBM10 RAO's by Wave Slope

assumptions are not valid? Additionally, can regular wave tests be used as a substitute for irregular wave tests in the time domain? This section analyzes the simplest such way that regular wave data can be applied to predict irregular seas responses.

6.4.1 Harmonic Methods for Time Domain Simulation

As discussed in Section 5.1, first harmonic regular waves results are typically used to calculate a response spectrum in the frequency domain, from which statistical characteristics are calculated. However, higher harmonics of motions and loads may be important components of the total response when amplitudes are large. Both this testing and similar previous research have suggested that even in severe seas, motion higher harmonics are small, but for loads they may not be insignificant.

Whether for computational tests in the time domain or experimental results, the information available on higher harmonic amplitudes may be used to more accurately simulate irregular wave responses. An application of the most simplistic such method is presented here. More accurate models are also discussed.

A "semi-linear" harmonic superposition method is used to simulate the irregular seas response of the V4 hull at 20 knots in sea states 4 through 7. The method is similar to current frequency domain methods which use first harmonic responses only, but the additional data on higher harmonics are incorporated in the predictions. The method is briefly outlined below.

1. Regular wave tests are completed to well define the first, second, and third harmonic response curves, in both amplitude and phase. Accurate phase angle measurements are essential when response amplitudes are not small. This may require more runs than necessary to describe the amplitude curve.

2. The absolute harmonic amplitudes and phases are combined to form complex response operators in the frequency domain, $\hat{R}_1(\omega_e)$, $\hat{R}_2(\omega_e)$, $\hat{R}_3(\omega_e)$. While the mean response components may also be normalized to consider higher order components, this is not done here.

3. The complex response operators are normalized by the appropriate power of the wave amplitude, such that: $\hat{H}_1(\omega_e) = \hat{R}_1(\omega_e)/\zeta$, $\hat{H}_2(\omega_e) = \hat{R}_2(\omega_e)/\zeta^2$, $\hat{H}_3(\omega_e) = \hat{R}_3(\omega_e)/\zeta^3$.

4. The *encountered* irregular wave system in the time domain is converted to the frequency domain via discrete Fourier transforms, yielding a series of discrete regular wave components, $\hat{Z}_n(\omega_n)$, where ω is now redefined as the encounter frequency, ω_e.

5. The total time domain response is then calculated with the assumption that the harmonic responses to each discrete wave component may be superposed. This the "semi-linear" description – nonlinear harmonics are used to generate responses which are assumed independent of each other and are combined through linear superposition. The calculations must ensure that the second harmonic responses are applied at twice the encounter frequency, and the third harmonics at three times the encounter frequency. The time domain approximation is then, *for oscillations about the mean response only*:

$$y(t) = \sum_{n=1}^{N}[\hat{H}_1 \cdot \hat{Z}_n e^{i\omega_n t} + \hat{H}_2 \cdot |Z_n|\hat{Z}_n e^{i2\omega_n t} + \hat{H}_3 \cdot |Z_n|^2 \hat{Z}_n e^{i3\omega_n t}]$$

This solution has several disadvantages. While considering higher order components, several assumptions are applied in implementing them. Since this is a "third harmonic" method vice a "third order" method, an accurate solution requires that (1) the third order (and higher) components of the first harmonic response are small, and (2) responses above the third order are insignificant and do not contribute to the first, second, or third harmonics. These assumptions are required because the contributions of the higher order components are proportional to higher powers of the encountered wave amplitude. For example, if the third order component of the first harmonic response is significant, the response will be too low since the entire harmonic is assumed to be first order.

Additionally, as with current frequency domain methods, linear superposition is

Method	Sea State			
	4	5	6	7
SMP (Irregular Waves)	0.449	0.983	1.902	3.166
SMP (RAO's)	0.419	0.923	1.818	3.025
	(-6.6%)	(-6.1%)	(-4.4%)	(-4.5%)
LAMP-1 (RAO's)	0.572	1.224	2.229	3.456
	(27.5%)	(24.5%)	(17.2%)	(9.2%)
LAMP-1 (Irregular Waves)	0.583	1.253	2.282	3.719
	(29.9%)	(27.5%)	(20.0%)	(17.5%)
LAMP-2 (RAO's)	0.616	1.313	2.424	3.702
	(37.1%)	(33.6%)	(27.4%)	(16.9%)
LAMP-2 (Irregular Waves)	0.577	1.236	2.345	3.955
	(28.6%)	(25.7%)	(23.3%)	(24.9%)

Table 6.3: V4 Method Comparison – Heave (SIG SA), 20 kts, Head Seas

assumed. This requires that the responses to the discrete regular wave components of the encountered spectrum are independent of one another.

For the V4 hull, a comparative summary of the Significant single amplitude response predictions using both regular and irregular seas methods is presented in Tables 6.3, through 6.7 on page 194.

The tables are separated by response type. Six response predictions are listed: the SMP, LAMP-1, and LAMP-2 irregular wave predictions, and the irregular wave simulations using RAO's from SMP, LAMP-1, and LAMP-2 regular waves tests. Since the SMP irregular seas predictions may be considered the current early design "standard", all percent differences are with respect to these values. The following conclusions may be made about the accuracy of the simple harmonic superposition method for the V4 hull. Because irregular wave results have already been compared in Sections 5.2, this discussion focuses on differences between the two predictions made with each method.

- The differences between the SMP irregular wave calculations and the magnitudes calculated using the SMP RAO's are small for all cases, all less than 8% different. The difference most likely results from the actual time domain wave spectrum, generated by LAMP.

Method	Sea State			
	4	5	6	7
SMP (Irregular Waves)	1.063	2.205	3.781	5.461
SMP (RAO's)	1.000 (-5.9%)	2.058 (-6.7%)	3.529 (-6.7%)	5.074 (-7.1%)
LAMP-1 (RAO's)	1.176 (10.6%)	2.479 (12.4%)	4.341 (14.8%)	6.118 (12.0%)
LAMP-1 (Irregular Waves)	1.217 (14.5%)	2.604 (18.1%)	4.443 (17.5%)	6.268 (14.8%)
LAMP-2 (RAO's)	0.991 (-6.8%)	2.068 (-6.2%)	3.767 (-0.4%)	5.506 (0.8%)
LAMP-2 (Irregular Waves)	1.223 (15.1%)	2.607 (18.2%)	4.328 (14.5%)	5.868 (7.5%)

Table 6.4: V4 Method Comparison – Pitch (SIG SA), 20 kts, Head Seas

Method	Sea State			
	4	5	6	7
SMP (Irregular Waves)	2105	4008	6109	8092
SMP (RAO's)	2009 (-4.6%)	3797 (-5.3%)	5748 (-5.9%)	7565 (-6.5%)
LAMP-1 (RAO's)	1690 (-19.7%)	3184 (-20.6%)	4772 (-21.9%)	6468 (-20.1%)
LAMP-1 (Irregular Waves)	1814 (-13.8%)	3350 (-16.4%)	5063 (-17.1%)	7160 (-11.5%)
LAMP-2 (RAO's)	1529 (-27.4%)	2797 (-30.2%)	4196 (-31.3%)	5501 (-32.0%)
LAMP-2 (Irregular Waves)	1837 (-12.7%)	3387 (-15.5%)	4826 (-21.0%)	6316 (-21.9%)

Table 6.5: V4 Method Comparison – VSF5 (SIG SA), 20 kts, Head Seas

Method	Sea State			
	4	5	6	7
SMP (Irregular Waves)	88730	169900	259600	343690
SMP (RAO's)	84796 (-4.4%)	161148 (-5.2%)	242952 (-6.4%)	319192 (-7.1%)
LAMP-1 (RAO's)	74858 (-15.6%)	143700 (-15.4%)	213500 (-17.8%)	292109 (-15.0%)
LAMP-1 (Irregular Waves)	81773 (-7.8%)	151641 (-10.7%)	226374 (-12.8%)	322002 (-6.3%)
LAMP-2 (RAO's)	69687 (-21.5%)	130374 (-23.3%)	196486 (-24.3%)	255391 (-25.7%)
LAMP-2 (Irregular Waves)	82595 (-6.9%)	152471 (-10.3%)	215660 (-16.9%)	281657 (-18.0%)

Table 6.6: V4 Method Comparison – VBM10 (SIG SA), 20 kts, Head Seas

Method	Sea State			
	4	5	6	7
SMP (Irregular Waves)	915	1565	2104	2612
SMP (RAO's)	881 (-3.7%)	1493 (-4.6%)	1980 (-5.9%)	2411 (-7.7%)
LAMP-1 (RAO's)	1198 (30.9%)	2170 (38.7%)	3119 (48.2%)	4088 (56.5%)
LAMP-1 (Irregular Waves)	1255 (37.2%)	2263 (44.6%)	3225 (53.3%)	4440 (70.0%)
LAMP-2 (RAO's)	1151 (25.8%)	2061 (31.7%)	2906 (38.1%)	3676 (40.7%)
LAMP-2 (Irregular Waves)	1255 (37.2%)	2266 (44.8%)	3186 (51.4%)	2817 (7.8%)

Table 6.7: V4 Method Comparison – VSF15 (SIG SA), 20 kts, Head Seas

- For heave:

  - The differences between the two calculations made with LAMP-1 are generally small, about 3%.

  - The LAMP-2 RAO predictions are lower than in irregular waves at moderate sea states (6 to 7%). In SS7, the RAO result is slightly higher.

- For pitch:

  - With LAMP-1, the differences between the two predictions are larger than for heave, but still small, about 3 to 5%.

  - The LAMP-2 RAO values are substantially lower than the irregular seas values, but the percent difference decreases as sea state increases. The LAMP-2 RAO responses are lower than the SMP irregular wave predictions. The opposite is true when comparing LAMP-2 irregular seas predictions.

- For VSF5:

  - All of the LAMP predictions are substantially less than SMP, as expected.

  - The LAMP RAO predictions are lower than the irregular seas predictions, about 4 to 10% for LAMP-1, and 10 to 15% for LAMP-2. The differences between the two LAMP regular wave predictions are much larger than the differences between the irregular wave values.

- For VBM10, similar trends are observed as for VSF5. Interestingly, the differences between the LAMP RAO and irregular seas values do not differ considerably with speed.

- For VSF15, similar trends are observed. The differences between the LAMP RAO and irregular wave values are, as with the other loads, much worse for LAMP-2 than LAMP-1.

195

Overall, the LAMP RAO predictions consistently underpredict the irregular wave time domain responses, except for a few LAMP-2 cases, notably in heave. The differences are generally much higher for LAMP-2 than for LAMP-1.

For two cases, 20 knots in SS5 and 7, the time domain predictions (without mean values) for pitch and VBM10 are compared graphically, in Figures 6-19 on the next page, through 6-22. These predictions were chosen for plotting to demonstrate the accuracy (or lack thereof) of the harmonic method between (1) motions and loads, (2) sea conditions, and (3) prediction method. The discussion is necessarily qualitative, since only a small portion of the harmonic method predictions can reasonably be included. For each sea state, the entire time domain runs were examined, and a short window picked to compare predictions during the most severe responses. Each plot includes the wave trace, the time domain prediction made with SMP RAO's, and the LAMP-1 and LAMP-2 predictions. For LAMP, the dashed lines are the time domain responses from the irregular waves runs.

In sea state 5, the severe events occur near 590 and 740 seconds. For pitch, the LAMP-1 predictions are quite close, but the RAO prediction peaks are smaller. The differences are most noticeable when the pitch responses are low, and higher frequency components are not dominated by the response at the "modal" pitch frequency. In LAMP-2 the RAO predictions are much worse. All peaks are consistently underpredicted by the RAO method. While the phases are quite close in LAMP-1, the LAMP-2 traces show that phase is also not as accurate for the RAO method. Similar trends are noted for VBM10 at the low sea state.

In sea state 7, severe events are noted at about 355, 425, and 505 seconds. Similar trends are noted as for pitch at SS5. The two LAMP-1 methods are quite close, in fact better than at SS-5, because the modal pitch response is more dominating. Again in LAMP-2, the RAO method is a worse simulation. Peaks are consistently underestimated, and the phase is again slightly off. However, the quality of the simulation seems similar to the lower sea state. For VBM10, the RAO methods seem equally poor for both LAMP-1 and 2. At the high state, the loads simulations are noticeably worse than the pitch simulations. This is probably a result of a higher
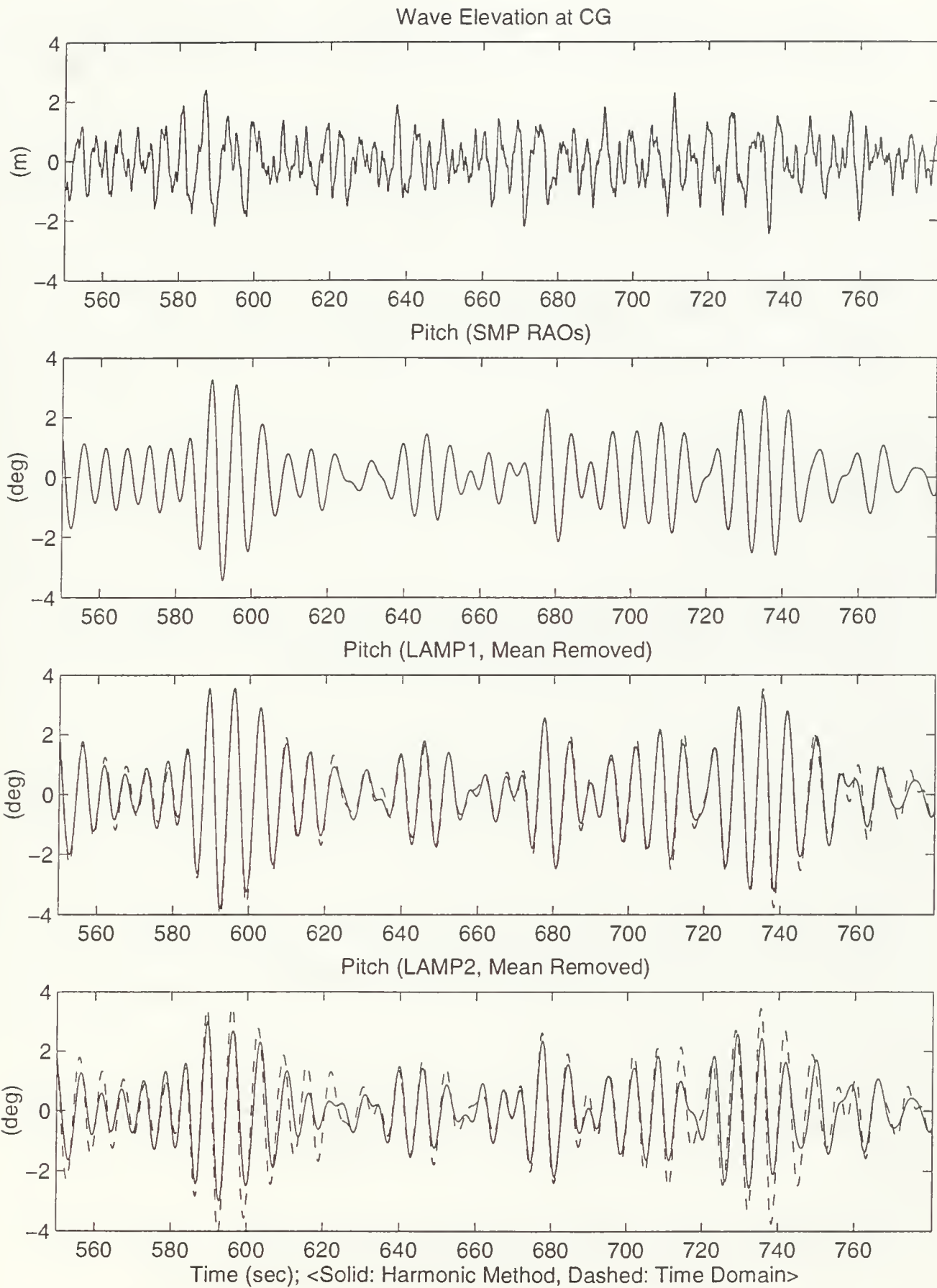
Figure 6-19: Variant 4 Harmonics Method Time Domain Comparison: Pitch (SS5, 20 kt, Head Seas)

197
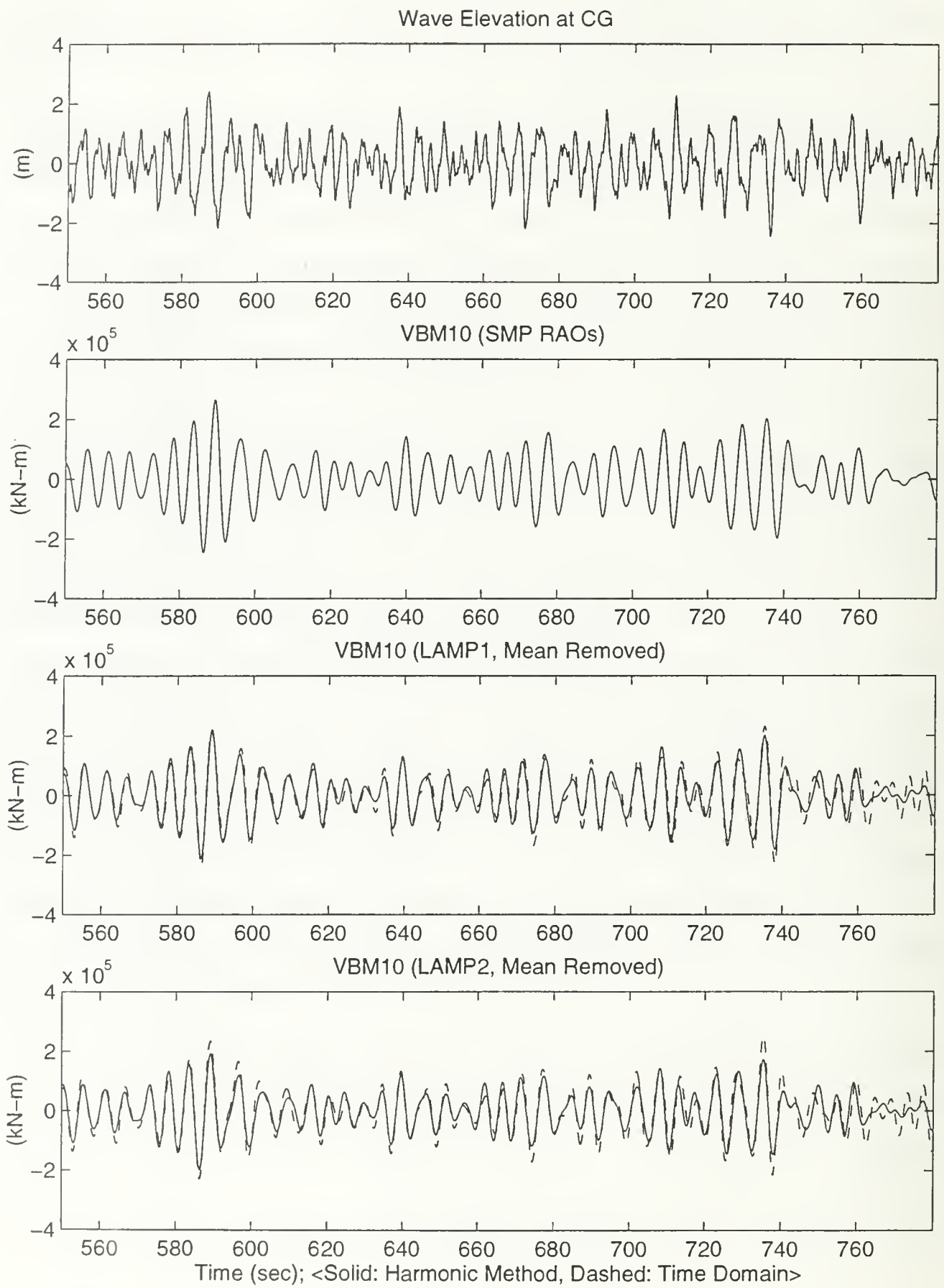
Figure 6-20: Variant 4 Harmonics Method Time Domain Comparison: VBM10 (SS5, 20 kt, Head Seas)
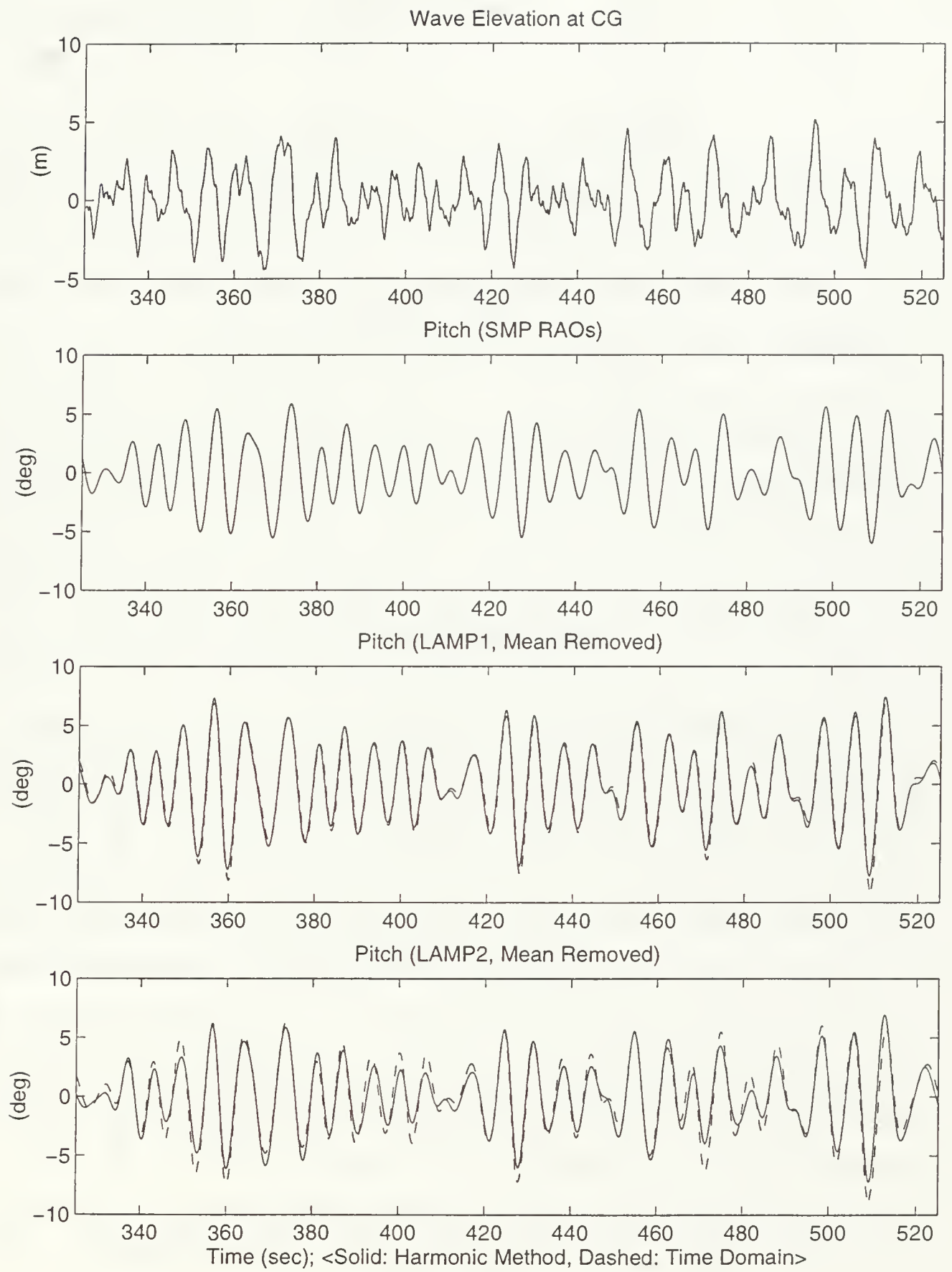
Figure 6-21: Variant 4 Harmonics Method Time Domain Comparison: Pitch (SS7, 20 kt, Head Seas)
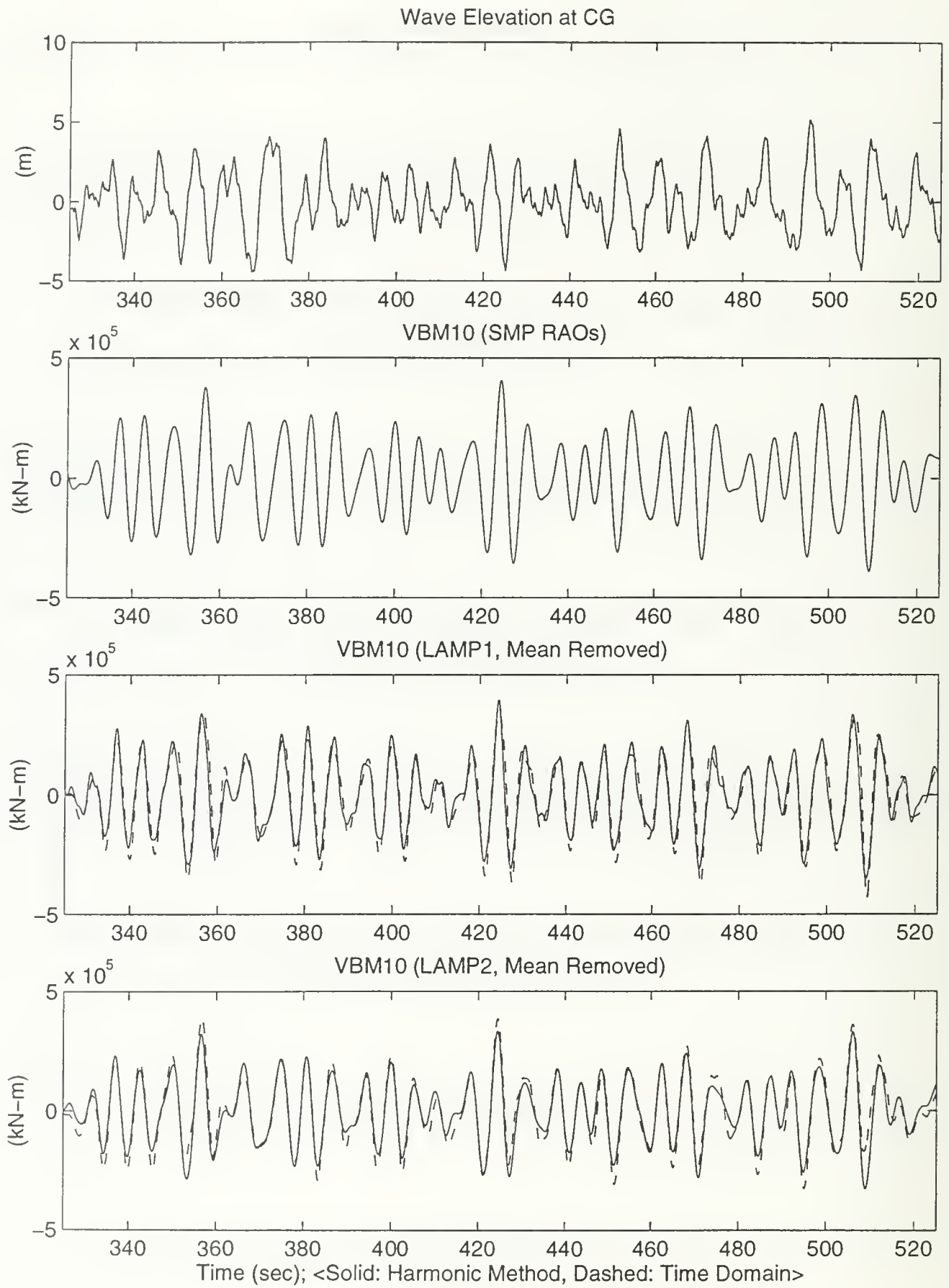
Figure 6-22: Variant 4 Harmonics Method Time Domain Comparison: VBM10 (SS7, 20 kt, Head Seas)

second order response, which affects the second harmonic components proportionally as the square of the wave amplitude.

6.4.2 Suitability of Regular Wave Methods

Simple linear superpositions of regular wave harmonics to simulate irregular wave time domain solutions, as performed in this chapter, do not accurately match the irregular wave runs predictions. The differences are smaller for motions than for loads, where higher order responses are not negligible. The two LAMP-1 methods are fairly close, but the agreement between the two LAMP-2 methods is poor. In particular, because the RAO method peaks generally underestimated the irregular seas peaks, the Significant response magnitudes, which are so commonly used in seakeeping design, are quite lower. If the amount of computer time required to gather the regular wave data was much less than required for the irregular seas runs, the method would still be of some use. However, to properly define the harmonic amplitude and phase (particularly) curves may require a substantial number of runs.

Insight into why linear superposition fails, even when utilizing higher harmonic data is gained by examining the degree of nonlinearity present in the irregular seas responses. One of the most effective methods of doing so is by plotting the probability distribution function of the instantaneous response elevations. For a linear process, this distribution should be Gaussian, which was derived to study such systems.[6] Determining whether a process is Gaussian may be easily done using a technique called the "normal probability plot." Normal probability plots for the V4 irregular seas simulations of pitch and VBM10 for sea states 5 and 7 at 20 knots (the same conditions simulated with harmonic superposition) are shown in Figures 6-23 on page 203 and 6-24 on page 204, along with the wave elevation probabilities. In a normal probability plot, the response values are on the x-axis, and the cumulative distribution function (CDF), determined directly from the time domain data, is plotted on the y-axis. The y-axis spacing is then adjusted so that a Gaussian CDF plots as a straight line. For

---

[6]Not the single or double amplitude peaks. For a linear process with a narrow band spectrum, these should follow a Rayleigh distribution.

a zero mean process[7], the line should pass through zero elevation at 0.50 probability. The slope of the line is equal to $1/s$, where s is the sample standard deviation, used to estimate the population standard deviation, σ.

The actual sample CDF is then added to the normal probability plot. If the sample is linear (Gaussian), it should not deviate from the straight line. Mathematically, the key statistical properties of the sample are the mean,

$$\bar{x} = \frac{1}{N} \sum_{j=1}^{N} y_j$$

the standard variance (where the standard deviation is the square root of the variance),

$$s^2 = \frac{1}{N-1} \sum_{j=1}^{N} (y_j - \bar{x})^2$$

the skew,

$$\kappa_3 = \frac{1}{N} \sum_{j=1}^{N} (\frac{y_j - \bar{x}}{s})^3$$

and the kurtosis,

$$\kappa_4 = \frac{1}{N} \sum_{j=1}^{N} (\frac{y_j - \bar{x}}{s})^4 - 3$$

where N is the sample size, and y_j are the sample values.

The skew, third moment of the probability density function, quantifies the amount of asymmetry about the mean. The kurtosis, the fourth moment, quantifies the height of the sample density function as compared to the Gaussian equivalent. For a Gaussian distribution, the skew and kurtosis, as defined, should both equal zero. The sample skew and kurtosis for each response are included in the heading above each normal probability plot. The use of these plots as applied here is slightly flawed because the sample standard deviation is used to approximate the population standard deviation. For a nonlinear sample, the standard deviation itself will also be affected by the nonlinearities. However, graphical analysis is still very helpful. To more easily see the nonlinearities in the plotted response CDF's, the reader may wish to hold the

---

[7]As in the harmonic simulation plots, all responses have been normalized to zero mean.
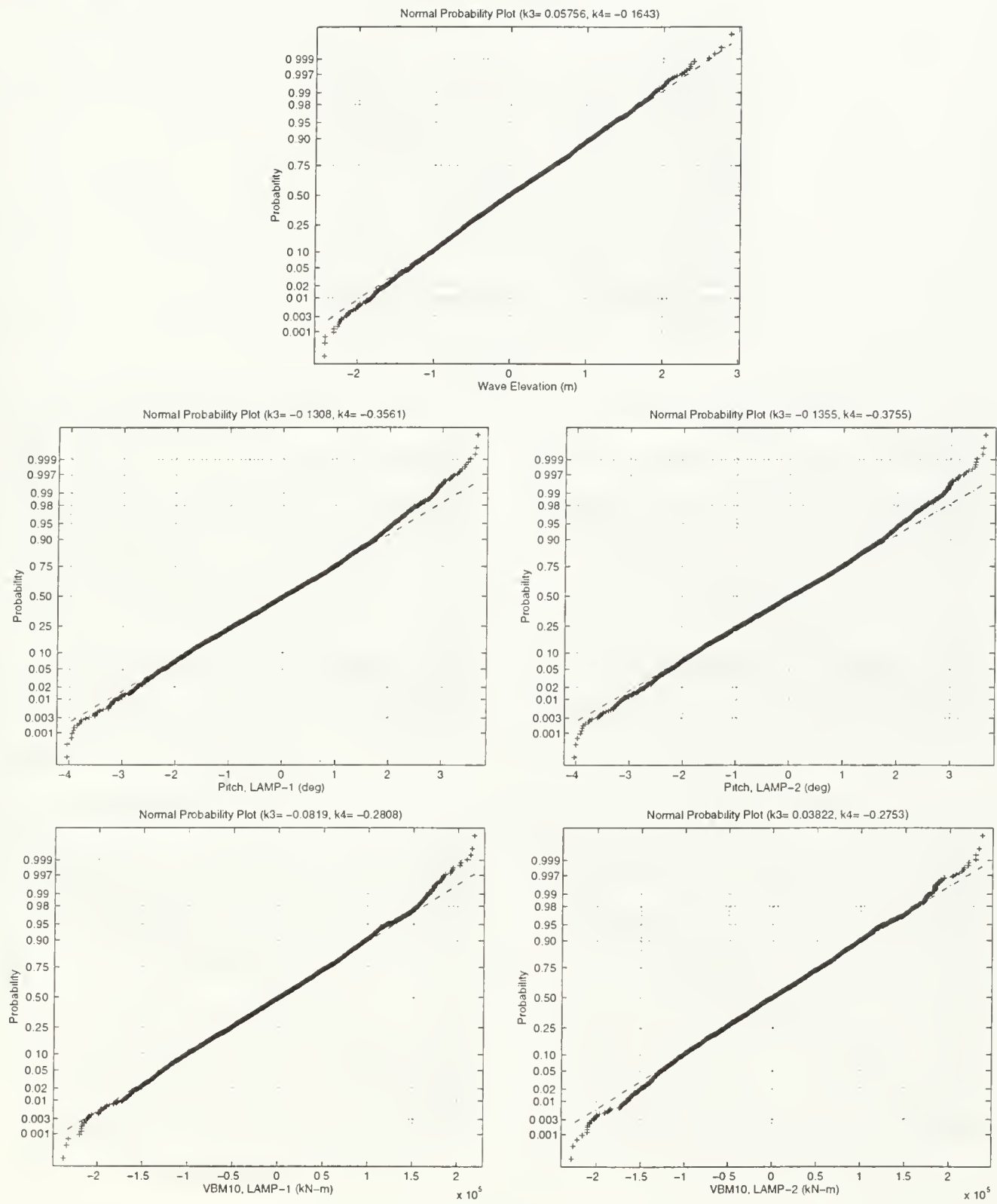
Figure 6-23: Normal Distribution Analysis, V4, Pitch & VBM10, SS5 20kts
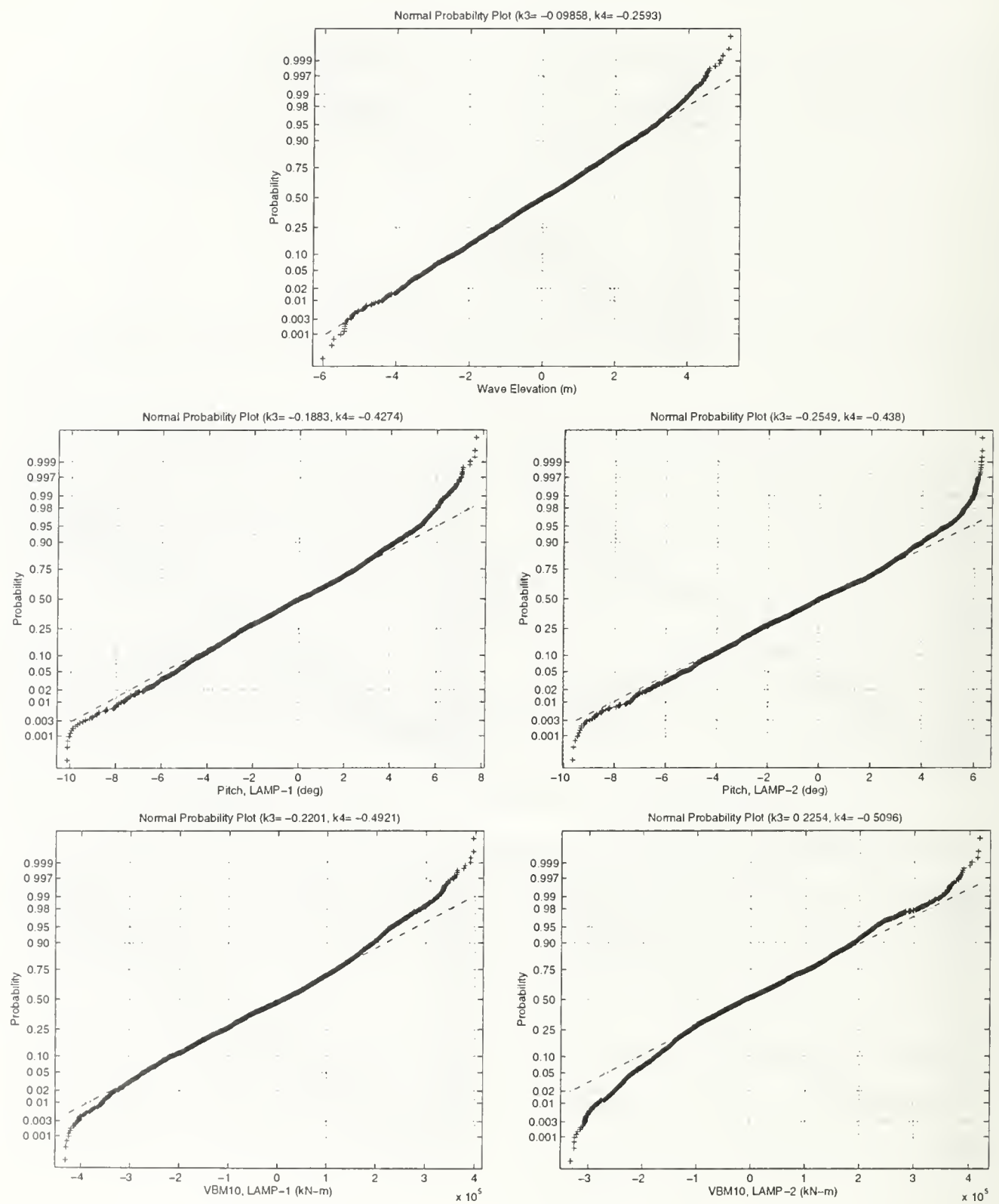
Figure 6-24: Normal Distribution Analysis, V4, Pitch & VBM10, SS7 20kts

paper nearly edge on to examine line curvature.

From the normal probability plots for the sea state 5 case, nonlinearities are present, but are not extremely significant for pitch or VBM10. For pitch, there is very little difference between the LAMP-1 and LAMP-2 plots. For VBM10, the difference is also small, but more curvature is present in the LAMP-2 response. The change in sea state 7 is substantial. For both pitch and VBM10, significantly more nonlinearities are present than in SS5. The pitch nonlinearities and the differences between LAMP methods are again fairly small. The VBM10 response includes large nonlinear components. These nonlinearities are also greater in LAMP-2 than LAMP-1. The wave system generated by LAMP in SS7 also contains more nonlinearity than at SS5, and this bears further investigating. While some of the nonlinear response may be contributed to nonlinear input forces, the analysis beginning on page 192 of the responses calculated by harmonic superposition showed that the SMP RAO predictions were consistently much closer to the frequency domain results than the LAMP time domain predictions.

The plots graphically explain partially why linear superposition, even if higher harmonics are included, is inadequate. The other important implication is to the method of processing irregular seas. As discussed in Section 5.1.2, statistical response amplitudes from irregular seas data may be obtained by cataloging the peak responses, or by applying discrete Fourier Transforms to the time history. RMS or Significant response amplitudes may then be calculated by applying long-term statistics to the resulting response spectra. However, such methods typically assume a Gaussian distribution for the response, so the cataloging peaks method may be more appropriate. Further tests are needed to confirm this.

Although this simplistic method is not adequate, other more sophisticated methods are available. Adegeest, in particular, has tested an approximate Volterra model for simulating third order nonlinear hull girder loads [26, 34]. The Volterra model also uses harmonic response operators obtained from head seas regular waves tests. Unlike the method presented here, the harmonics are used to approximate the actual second and third order contributions. For the third order particularly, the accuracy

205

of the solution may be improved by increasing the number of tested wave amplitudes at each frequency. This allows the contributions of the first and third order responses to the first harmonic to be separated. The Adegeest study compared predictions (for Wigley hulls with $L/B = 7$, and $B/T = 2.6$) in irregular seas corresponding to a significant wave height of 4.8 m (in the SS6 range) at speeds corresponding to 22.4 knots, higher than those successfully tested with LAMP. These results looks quite promising and may allow successful use of regular wave results to simulate ship responses in arbitrary seas. However, the amount of model or computational testing required for an accurate solution may still near or exceed the time or cost required for irregular seas tests. Additionally, the performance of such models should be further examined in more severe response conditions.

Chapter 7

Design Implications

7.1 Summary of Observations

The use of time domain hydrodynamic codes for seakeeping predictions in early ship design studies has been successfully demonstrated. A series of hull alternatives meeting specified main dimensions (the mathematical hulls) have been studied in moderate to severe seas, at several speeds. A commercial hull, typical of current large displacement tankers, has also been evaluated at service speed in a range of sea states. A procedure which uses linear frequency domain methods to reduce the scope of required time domain testing for design tradeoffs has been proposed and partially completed. Two methods for analyzing ship seakeeping characteristics, irregular and regular waves testing, have been applied. Conclusions are now proposed comparing the merits of the prediction methods as a function of hull characteristics and operating conditions. In addition, the utility of the irregular versus regular waves methods is also compared.

To assist in the discussion, the results of both the mathematical[1] and VLCC hull tests are summarized:

- The McCreight method (parametric index) ranks the BL, V1, V4, and V5 hulls

---

[1]BL – Wigley Seakeeping Hull; V1 – Flare 20°, underwater hull changed; V2 – Zero flare, waterline entrance increased from 11.9° to 17°; V3 – Combination of V1 and V3 changes; V4 – Identical to BL underwater, 20° flare above water; V5 – Identical to BL underwater, 10° tumblehome above water.

equally. Flare and tumblehome above the waterline do not impact the index value. The underwater flare in V1 and V3 is not sufficient to affect the ranks. Increase in underwater waterline entrance angle improves motions performance, and is adequately predicted by the McCreight method.

- A frequency domain program (SMP) was used to rapidly predict irregular seas responses for all hulls in sea states 4-8, for all heading and speed combinations. All mathematical hulls perform poorly in roll. In head seas, the limiting motion criteria is pitch (3° Significant single amplitude limit). The VLCC fails deck wetness criteria at all speeds in SS7 and 8, but no other commercial criteria are ever surpassed.

- The Transit Speed SPI predicted by SMP indicates V1 is a slightly worse choice than BL. The results for BL, V4, and V5 are identical due to the linear body boundary condition. V3 is the superior design choice, considering only motions. V2 is only slightly worse.

- SMP indicates that the chosen dynamic structural load limits are not surpassed until relatively high speeds in severe seas, SS7 and 8, for the mathematical hulls. The VLCC limits (ABS derived) are never approached.

- Using LAMP-1 for SPI verification, the motion limits in SS6 and SS7 are exceeded well before predicted by SMP. The load limits are not exceeded until higher speeds than shown by SMP. SPI verification using time domain codes is feasible and recommended, since critical conditions may not occur until cases where the limitations of frequency domain programs are exceeded.

- As speed and sea state increase, simply switching to time domain calculations from frequency domain methods results in higher motions and lower loads for the cases analyzed here, even with the linear LAMP-1 formulation. The effect is observed for all of the mathematical hulls and the VLCC. The linear superposition assumption seems to fail earlier than the small response assumption.

208

- The LAMP-1 and LAMP-2 prediction differences are also sensitive to speed and sea state. For motions, large differences occur for the mathematical hulls in SS6 at 20 knots, and not for the VLCC until SS8. Dynamic loads are more sensitive than motions in this respect, as with the differences between frequency and time domain methods.

- Linear methods (SMP and LAMP-1) do not predict response differences between hulls BL, V4, and V5. LAMP-2 does predict differences, particularly with the addition of flare in V4. The superior performance of hulls V2 and V3 (and worse performance in loads) is well predicted by SMP, LAMP-1, and LAMP-2.

- Regular wave results for V4 and the VLCC correlate with the irregular seas trends. Higher harmonics are insignificant for motions, even in heavy seas, but not for loads. Higher harmonics are predicted with the switch to time domain methods. SMP does not predict responses above first order.

- Regular wave methods are enlightening for further understanding hull responses, but are not as valuable as irregular seas in early design tradeoffs. When motions and loads are nonlinear, and time domain analysis is required, using regular wave methods to generate accurate response predictions is difficult. The harmonic superposition technique demonstrated here is inadequate. Other models, such as the approximate Volterra model implemented by Adegeest, may be acceptable.

- Based on the methods applied here[2], entrance angle should improve motions and degrade dynamic loads. The tested flare angle reduces heave, increases pitch (at higher speeds), and sharply increases dynamic loads in heavy seas. The moderate tumblehome modestly increases heave, decreases pitch, and decreases structural loads (VSF5 and VBM10).

---

[2]The reader is reminded that no experimental or full scale data has yet been compared to the computational predictions.

- Motions and loads for the VLCC are reduced because of the large displacement (No matter the prediction method, $\sum \vec{F} = m\vec{a}$.)

7.2 Discussion and Recommendations

With useful results obtained, the ultimate goal of the research is now assessed – Can time domain hydrodynamic, and particularly seakeeping computational methods be applied to the early stages of ship hull design?

The answer is definitely "Yes." However, though 3-D time domain codes should be incorporated earlier in the design procedure, they do have disadvantages that make their use difficult. The three most significant problems are (1) difficult program and hull geometry setup, (2) extensive computational time, and (3) requirement for experimental validation. None of these problems are specific to the LAMP code. In fact, other than some problems which are common to many CFD codes, LAMP is well-documented and easy to operate for a qualified user. A qualified user implies an operator with a background (not necessarily an expertise) in both naval architecture and marine hydrodynamics.

The program setup problem is addressed first. Details of the problems encountered with LAMP in this study have already been discussed in Section 5.2.3 on page 94. As mentioned, most of the problems were the fault of the author, and, time permitting, could have been corrected, especially with the help of the code's authors, SAIC. However, the fact that an engineer with a reasonably solid background in naval architecture and hydrodynamics required extensive technical assistance to apply the code is a valid observation. While providing results based on more physically accurate models than linear strip theory, the 3-D time domain methods are more difficult to use. In particular, the author was unable to use LAMP-1 and 2 at very high speeds, and had problems with gradually unstable runs at lower sea states. LAMP-4 was successfully implemented only at a low speed in SS6, and for regular waves where response amplitudes were moderate. Unfortunately, the failed conditions also correspond to critical cases, where the accuracy of nonlinear time domain simulations is

most important. Of note, once problems with the VLCC panelization were solved, no such LAMP difficulties occurred. Again, displacement helps. However, in head seas the performance of the mathematical hulls is not unreasonable – particularly for relative motions and their derived responses, slamming, wetness, and propeller emmersion.

For the failed LAMP-1 and 2 runs, and possibly the LAMP-4 runs, the encountered problems could most likely be solved with time step reductions and adjustments to the hull and matching surface panelizations. Ideally, though, such considerations should not be the concern of the designer. Accurate results are what matter, particularly in a design process. Codes such as LAMP become much more useful to designers in the *early* stages, if the process of hull panelization and formulation setup could be even somewhat handled automatically by the code. Because of the complexities of the fluid-hull interaction, such automation may never be possible. Still, taking a set of proposed offsets (especially unpanelized ones), importing them into a CFD code, and immediately beginning to generate volumes of useful engineering data may not be possible, but, regardless, it should be the goal. Despite the difficulties of setup, however, the time domain codes do have an important place in ship design.

The second major problem with running 3-D nonlinear codes in the time domain is computation time. Because computational clock times vary significantly with computer capability and LAMP setup, quoting absolute times here is not helpful. However, a relative comparison is appropriate. Table 7.1 on the next page shows relative clock times required for the irregular and regular wave analyses of the V4 at 20 knots and the VLCC at 15.5 knots, using LAMP-1 and 2. Compared to the total LAMP computer times, the time required for SMP analyses may be considered zero. Because clock times vary substantially, the only appropriate conclusions are first that the 3-D time domain codes take considerably longer than frequency domain codes. Although not quoted here, the LAMP-4 clock times are substantially higher than for LAMP-1 and 2. Engle, et al. (1997) state that LAMP-4, with nonlinear pressure calculations implemented, is about thirty times slower than LAMP-1 and 2 [10].

The second conclusion is that the "efficiency" of the regular versus irregular wave

Parameter	V4 (20 kt)		VLCC (15.5 kt)	
	Irregular	Regular	Irregular	Regular
Total # Runs	4	15	5	20
# Body Panels	351		230	
Time Step Size	$0.04^{\dagger}$ (0.156 sec)		0.04 (0.227 sec)	
Time Steps/Run	6000	1400	4000	1000
Clock Time/Time Step[‡]	1.86	1.0	1.37	1.62
Total Time per Run	11,160	1,400	5,480	1,620
Total Time per Method	44,640	21,000	27,400	32,000
Notes: Times apply to LAMP-1 and LAMP-2. LAMP-4 times are much larger. All runs on same computer in equivalent conditions. †Nondimensionalized by $\sqrt{L/g}$. ‡All times normalized to V4 clock time per time step.				

Table 7.1: Relative Clock Time Comparison – V4 and VLCC Analyses

methods, as applied here, depends very much on: the number of time steps needed for convergent or statistically significant sample sizes, and the number of runs required to adequately define the regular wave amplitude and phase curves.

For head seas cases, where hydrostatic and Froude-Krylov forces are expected to dominate hydrodynamic forces, the LAMP-2 modified-nonlinear formulation may be sufficient for accurate results. When the hydrodynamic forces are significant, fully nonlinear methods such as LAMP-4 are required. If so, the issue of computer time is even more critical. However, with a proper use of frequency domain codes to reduce the scope of LAMP-1 and 2 tests, which are in turn used to further limit LAMP-4 runs, the test program is feasible. In the most severe response cases, LAMP-4 can even be used to examine only specific critical events in the time domain record.

The total computing time may be reduced even further by eliminating the use of LAMP-1. Although simply switching to time domain from the frequency domain resulted in substantial response differences, the nonlinear calculation of hydrostatic and Froude-Krylov forces in LAMP-2 does not increase computing time over LAMP-1. Assuming that the LAMP-2 implementation is the more physically accurate model, then there is no need to apply computer time to the 3-D linear solution.

Although the number of computer runs may be reduced to a feasible level by

applying a hierarchal process of prediction methods, one potential class of tools, not analyzed in this research, may prove quite useful. These tools are nonlinear implementations of 2-D strip theory in the time domain. One such method, the program FREDYN, has been developed and initially tested, with computing times between SMP and LAMP [6]. If successful, such a code could fill the gap between 2-D frequency domain and 3-D time domain.

Incorporation of all of these different prediction methods into one design package would be useful. Such a design package could test ship performance in desired operating conditions, beginning with linear strip theory. Use of the next higher level code could be automatically recommended based on the magnitude of responses, or on the comparative magnitude of the components of the total forces and moments. In such a way, the total computing time required to accurately define ship response operating envelopes could be minimized. In particular, time domain methods could be combined so that the simulation begins at the lowest level of accuracy, such as time simulation with strip theory RAO's. The code could dynamically assess the magnitude of calculated forces, motions, and loads, and switch solution methods to the next better system when warranted. Thus, high computation time methods like LAMP-4 would only be implemented during peak responses.

A third disadvantage of the time domain simulation codes is the need for thorough experimental validation. However, this requirement is no different for these codes than for any other programs designed to predict real world events. Whenever any hull or operating condition (speed, heading and sea state) fall outside the range of existing code validation, experimental tests should be required to confirm the computer solution accuracy. Codes like LAMP should not totally replace experimental testing, just as experimental testing must be validated by full scale observations. However, as more and more hull types and conditions are examined, the validated database of such programs will increase.

Even with the need for experimental validation, time domain codes can significantly reduce the scope of such testing, just as frequency domain codes are used to reduce the scope of time domain tests. The use of time domain codes to reduce the

213

number of required experiments[3] is extremely important to allow examination of new hull concepts early in the ship design process. Problems with hulls are then discovered earlier in the design, drastically reducing the time and money required to fix them. In fact, a study of the naval ship design process showed that if computer simulation were extensively incorporated in early design, typical total design times might be cut by almost 15% [35].

Additionally, once validation is complete, the time domain codes can quite easily provide extensive information that is much harder to obtain experimentally. Hull girder loads, which were analyzed here, require a substantial increase in both model and facility cost to obtain experimentally. Additionally horizontal and torsional loads may also be obtained in cases other than head seas. Flow visualization, which may be difficult to record in model tests, may calculated by the CFD codes.

Structural fatigue design may be improved by the analysis of hull surface pressure, also difficult to obtain experimentally. Fatigue is increased by the effect of higher harmonic hull girder loads. These loads, shown here to be significant, occur at twice or three times the frequency of the first harmonics. Over the life of the ship, these harmonics will increase the number of stress cycles, reducing fatigue life. Because these fluctuations occur combined with the overall mean state of stress resulting from the first harmonic, the impact may be even more critical. These important aspects of design, which typically occur quite late in the process, may be considered earlier, and in greater detail using computer simulations.

In some cases, the early application of time domain predictions may bring good news, rather than bad. As stated earlier, a more accurate prediction does not necessarily mean a worse response. For the mathematical hulls for instance, LAMP generally predicted more severe motions than SMP, especially as speed and sea state increased. However, the trend in two critical loads, VSF5 and VBM10, was reversed. LAMP predicted that dynamic loads would not be as severe as SMP, and again, the difference between the methods increased as responses grew. Overdesign of a ship system may be just as economically costly as underdesign is in the price of ship and

---

[3]As discussed in detail in Section 2.3.2 on page 41.

crew effectiveness or survival.

Considering the potential advantages and disadvantages of 3-D nonlinear time domain codes, the following recommendations are made to improve the seakeeping process:

- Parametric methods remain an excellent and extremely quick tool for very early design. Particularly, they are quite useful in choosing main hull parameters that are likely to result in good seakeeping. If any aspect of the hull is outside the range of parameters considered in the method, extreme caution is required.

- Frequency domain codes should continue to be a vital part of the early seakeeping process. The codes provide very rapid results, which are quite good when their assumptions are not violated. Although the prediction of ship performance in heavy seas is critical and should drive the design, low to moderate sea states are still the most probable.

- The frequency domain codes must then be used to narrow down the required time domain conditions if these codes are to be feasible for design. This can be done based on SPI criteria or a systematic analysis of responses, similar to typical seakeeping experimental investigation. Nonlinear strip theory codes may prove to be a useful intermediate step.

- The choice of when to use nonlinear time domain codes to verify linear frequency domain results should consider the hull and operating conditions being tested. If rapid changes in the ship's waterplane characteristics occur either *above or below* the calm waterline, linear theory will not predict a change in performance. When motions become large, performance for these ships will be different than predicted by linear theory.

- Time domain codes, despite the difficulties discussed above, should be used to verify critical points in the frequency domain predicted response envelopes. 3-D linear implementations, such as LAMP-1, need not be used since the LAMP-2

nonlinear hydrostatic and Froude-Krylov force method does not increase computation time.

- As with frequency domain methods, if any aspect of the hull or operating condition is outside the range of validation for the time domain codes, experimental tests should be conducted. Once validation is complete, variations on a baseline hull – whether slightly modified hull forms (as with the mathematical hull series), additions of appendages, or changes in weight distribution – may be confidently assessed with the CFD code.

- In addition to verifying design measures of performance, time domain codes should be use to conduct thorough studies of motions and loads effects on the ship system, but much earlier in the design than is current practice. The conclusions may significantly reduce the scope of later design changes.

- In cases where responses are large enough to warrant time domain analysis, the irregular seas method demonstrated here should be used to develop predictions for statistical response magnitudes. Regular wave methods are still very helpful in understanding the nature of the ship's response. However, adequate definition of amplitude and phase curves to successfully implement methods such as the discussed approximate Volterra model may require more computer time than irregular seas methods.

The bottom line is that incorporating advanced time domain methods in ship design does not require a change in the methods which are currently used to describe and understand a ship's response to ocean waves. Despite the frustration sometimes encountered in preparing the codes for use, the benefits are worth it. If validation is properly conducted, the codes will save money and time by reducing the requirements for physical model tests. The experiments that are required may be conducted far earlier in the design process, and used to investigate innovative hull concepts, rather than ensuring the suitability of a final hull form after the fact.

7.3 Recommendations for Future Research

Although this research has demonstrated the feasibility and importance of incorporating advance seakeeping methods in typical design processes, much more should be done to investigate the matter. Recommendations include:

- Validate the conclusions obtained here with additional codes, including possibly the MIT RAO5D program for strip theory, and available alternatives to LAMP.

- Apply a nonlinear strip theory code to the same hulls and conditions tested here to compare results and design utility.

- Conduct validation experiments on one or more of the hulls tested here (possibly the V4), including measurements of motions and hull girder loads. Although the dimensions of other experimentally tested Wigley hulls were considered out of the range of naval applicability, these hulls should be computationally tested in a similar manner as conducted here.

- Increase the scope of the testing. Analyze non-head seas cases at more speeds. Investigate variations on more realistic hulls. Develop a better understanding of what hull characteristics and operating conditions most affect the accuracy of linear frequency domain methods.

- Analyze the reasons for the LAMP-4 failures experienced, and increase the scope of LAMP-4 tests.

- Further study the use of regular wave results to model irregular seas responses when significant nonlinearities are present. The approximate Volterra model is one such method. Analyze the effect of varying wave slope and/or wave height on the suitability of the harmonic response operators.

- Conduct further study on statistical modeling of nonlinear systems, to improve the predictions of long term response magnitudes. In particular, investigate how to best calculate discrete event probabilities using nonlinear time domain simulations.

- Investigate further the observed sensitivity of dynamic loads to prediction method and operating condition. In particular, study the effect of changes in weight distribution on dynamic load magnitudes. Additionally, study loads associated with slamming. Incorporate load calculations directly into fatigue models.

- Other than SPI verification techniques, develop a more quantitative method of cuing successively more advanced prediction methods. At the highest level, such dynamic methods could adaptively switch to the fully nonlinear formulation at points in the time domain trace where hydrodynamic forces become significant.

Finally, while the advanced time domain codes fit easily into current hydrodynamic design procedures, they also offer the opportunity for a potentially revolutionary new framework. Computation time will decrease and design utility will increase with methods such as the dynamic prediction formulation discussed above. Multiple hull variations in a wide range of operating conditions can then be assessed quickly and accurately. The results can be used in better design decision-making methods, such as the recently examined genetic algorithm techniques, to optimize hull forms and ensure that any potential problems are solved in simulation, not while actually performing a mission.

Bibliography

[1] NAVSEA Research and Technology Directorate Report. *"Seakeeping in the Ship Design Process," Report of the Seakeeping Workshop at the U.S. Naval Academy,* July 1975.

[2] Nathan K. Bales. Optimizing the Seakeeping Performance of Destroyer-Type Hulls. In *13th ONR Symposium on Naval Hydrodynamics*, pages 479–503, Tokyo, Japan, 1980. Office of Naval Research.

[3] W.R. McCreight. Estimating the Seakeeping Qualities of Destroyer Type Hulls. Technical Report DTNSRDC/SPD-1074-01, David W. Taylor Naval Ship Research and Development Center, January 1984.

[4] Theodore A. Loukakis and Chryssostomos Chryssostomidis. Seakeeping Standard Series for Cruiser-Stern Ships. In *Transactions*, volume 83, pages 67–114. Society of Naval Architects and Marine Engineers, 1975.

[5] Nils Salvesen, E.O. Tuck, and Odd Faltinsen. Ship Motions and Sea Loads. In *Transactions*, volume 78, pages 250–287. Society of Naval Architects and Marine Engineers, 1970.

[6] D. Burton, J. deKat, R. Sheinberg, and P. Minnick. Extreme Motion Analysis and Simulation for Ship Design and Operations. *Naval Engineers Journal*, 110(2):73–91, March 1998.

[7] Woei-Min Lin and Dick K.P. Yue. Numerical Solutions for Large-Amplitude Ship Motions in the Time Domain. In *Proc. Eighteenth Symposium on Naval Hydrodynamics*, 1990.

[8] Woei-Min Lin, Michael J. Meinhold, Nils Salveson, and Dick K.P. Yue. Large-Amplitude Motions and Wave Loads for Ship Design. In *Proc. Twentieth Symposium on Naval Hydrodynamics*, 1994.

[9] Y.S. Shin, J.S. Chung, W.M. Lin, S. Zhang, and A. Engle. Dynamic Loadings for Structural Analysis of Fine Form Container Ship Based on A Non-Linear Large Amplitude Motions and Loads Method. In *Proc. SNAME Annual Meeting*, pages 4.1 – 4.24, Ottawa, Canada, October 1997. SNAME.

[10] A. Engle, W. Lin, N. Salveson, and Y. Shin. Application of 3-D Nonlinear Wave Load and Structural-Response Simulations in Naval Ship Design. *Naval Engineers Journal*, pages 253–268, May 1997.

[11] Edward V. Lewis, editor. *Principles of Naval Architecture - Motions in Waves and Controllability*, volume 3. The Society of Naval Architects and Marine Engineers, Jersey City, New Jersey, second edition, 1989.

[12] Rameswar Bhattacharyya. *Dynamics of Marine Vehicles*. John Wiley and Sons, New York City, New York, 1978.

[13] E.N. Comstock and R.G. Keane. Seakeeping by Design. *Naval Engineers Journal*, 92(2), 1980.

[14] Naval Sea Systems Command (SEA 55W3). *Manual for Seakeeping Performance Analysis in Ship Design*.

[15] G. Aertssen. Laboring of Ships in Rough Seas with Special Emphasis on the Fast Ship. SNAME Diamond Jubilee International Meeting, 1968.

[16] G. Aertssen and M.F. van Sluijs. Service Performance and Seakeeping Trials on a Large Container Ship. In *Transactions*, volume 114. RINA, 1972.

[17] DOD-STD-1399 (Navy). *Interface Standard for Shipboard Systems, Ship Motion and Attitude*, 21 July 1986.

[18] Naval Sea Systems Command. *Manual for Naval Surface Ship Design Technical Practices*. T-9070-AA-MAN-010/(C).

[19] American Bureau of Shipping, New York, NY. *Rules for Building and Classing Steel Vessels*, 1994. Part 3, Hull Construction and Equipment.

[20] Edward N. Comstock, Susan L. Bales, and Dana M. Gentile. Seakeeping Performance Comparison of Air Capable Ships. *Naval Engineers Journal*, pages 101–117, April 1982.

[21] Naval Sea Systems Command. *Hull Form Design System v6.5 User's Manual*, 18 October 1994. Seakeeping: SMP91 chapter.

[22] Woei-Min Lin, Michael J. Meinhold, Kenneth M. Weems, Sheguang Zhang, and Marian H.C. Weems. *User's Guide to the LAMP System*. Science Applications International Corporation, Ship Technology Division, 134 Holiday Court, Suite 318, Annapolis, MD 21401, USA, current edition, September 1997. SAIC Report 96/1040.

[23] Woei-Min Lin, Kenneth Weems, Sheguang Zhang, and Nils Salveson. LAMP (Large-Amplitude Motions Program) for Ship Motion Simulations and Wave Load Predictions. David Taylor Model Basin, Carderock, MD, 2-3 June 1997. ONR Workshop on 'Computational Ship Hydrodynamics', Ship Technology Division, Science Applications International Corporation. Presentation Material.

[24] J. Gerritsma. Motions, Wave Loads and Added Resistance in Waves of Two Wigley Hull Forms. Technical Report 804, Technische University Delft, Delft, Netherlands, November 1988.

[25] J.M.J. Journée. Experiments and Calculations on Four Wigley Hullforms. Technical Report MEMT 21, Technische University Delft, Delft, Netherlands, 1992.

[26] Leon Adegeest. Experimental Investigation of the Influence of Bow Flare and Forward Speed on the Non Linear Vertical Motions, Bending Moments and Shear Forces in Extreme Regular Wave Conditions. Technical Report 993, Delft University of Technology, February 1994.

[27] Naval Sea Systems Command. *Minimum Required Freeboard for U.S. Naval Surface Ships*, 1 March 1982.

[28] Nathan K. Bales. Minimum Freeboard Requirements for Dry ForeDecks: A Design Procedure. In *STAR Symposium*, Houston, Texas, 25-29 April 1979. SNAME.

[29] Casey J. Moton. Systematic Variation of Mathematically Generated Ship Hulls for Hydrodynamic Analysis. 13.710 Special Project Final Report, MIT, 23 August 1996.

[30] Edward V. Lewis, editor. *Principles of Naval Architecture, Stability and Strength*, volume 1. The Society of Naval Architects and Marine Engineers, Jersey City, New Jersey, second edition, 1989.

[31] Carderock Division, Naval Surface Warfare Center. *Advanced Surface Ship Evaluation Tool - Monohull Surface Combatant (ASSET-MONOSC)*, 4.2.0 edition, 29 October 1997. Online and written help manuals.

[32] Harold E. Saunders. *Hydrodynamics in Ship Design*, volume I,II. SNAME, New York, NY, 1957.

[33] Casey J. Moton and Dick K.P. Yue. Regular Wave Testing of the VLCC26. Technical report, Department of Ocean Engineering, Massachusetts Institute of Technology, 20 February 1998.

[34] Leon Adegeest. Third-Order Volterra Modeling of Ship Responses Based on Regular Wave Results. In *Proc. 1996 ONR Conference on Naval Hydrodynamics*, pages 141–155, Norway, 1996.

[35] Thomas Laverghetta. Dynamics of Naval Ship Design: A Systems Approach. Master's thesis, Department of Ocean Engineering, Massachusetts Institute of Technology, May 1998.